Production of Fungal Biomass (*Aspergillus awamori*) from Almond Hulls for Food Applications

By

LIN CAO

DISSERTATION

Submitted in partial satisfaction of the requirements for the degree of

DOCTOR OF PHILOSPHY

in

Biological Systems Engineering

in the

OFFICE OF GRADUATE STUDIES

of the

UNIVERSITY OF CALIFORNIA

DAVIS

Approved:

Dr. Ruihong Zhang, Chair

Dr. Zhongli Pan

Dr. Zhiliang Fan

Committee in Charge

2023

ABSTRACT

There are over 1.1 million tons of almond produced in California resulting in over two million tons of almond hulls generated each year. Currently, those hulls are mostly used for dairy feed and bedding at low value. However, the almond industry is growing faster than the dairy industry, producing large amounts of excess hulls. Finding alternative uses for almond hulls while increasing their value is essential for the almond industry to achieve its zero-waste goal and improve sustainability. Due to their high sugar and fiber contents, almond hulls have the potential to be utilized for producing edible filamentous fungal biomass for food applications. Fungal biomass can serve as an important source of protein and other nutrients for feeding the increasing population. The overall goal of this research was to develop an efficient system for producing edible fungal biomass from almond hulls by integrating sugar extraction, enzymatic hydrolysis, and submerged cultivation.

In the first study, almond hulls of three varieties collected from almond processors were characterized for chemical and physical properties, such as total solids, fiber, protein and fat contents. The three varieties were Independence, Nonpareil, and Monterey. Sugars were extracted from hulls and used for the production of edible fungi. Two different grinding methods, continuous and successive grinding, were compared to get desired particle size for sugar extraction using water as an extraction medium. A kinetic model was developed, based on Fick's law, for sugar extraction from Independence almond hulls using three different liquid-solid ratios. The model was validated with data collected from extraction experiments conducted at different temperatures. Results showed that successive grinding was chosen to prepare almond hulls with particle sizes in the range of 2.36 to 3.38 mm. The established model was applied to predict sugar extraction from Nonpareil and Monterey almond hulls. The model provided a theoretical framework to understand

the extraction process, which is helpful in designing sugar extraction processes for different purposes.

Experiments were also conducted to optimize sugar extraction from Independence almond hulls. Response Surface Methodology (RSM) based on Box-Behnken Design was utilized to determine the optimal combination of time, temperature, and liquid-solid ratio for achieving the maximum total reducing sugar yield. The optimum extraction conditions were determined to be as follows: extraction time of 86.6 minutes, temperature of 77.4°C, and a liquid-solid ratio of 14. Under these conditions, the experimental sugar yield was 38.1%, which was well matched with the predicted yield 39.3%.

The almond hull extract was used for fungal biomass production of *Aspergillus awamori* (*A. awamori*). In 250 mL glass bottles or flasks, *A. awamori*'s growth in pellet form, was investigated under different conditions including inoculum level, aeration, nitrogen source and carbon to nitrogen ratio (C/N ratio). Subsequently, the fungal cultivation was scaled up to a 2 L bioreactor, where configurations that could favor pellet formation were studied. The structure and morphology of fungal pellets at various growth stages were observed and compared using an environmental scanning electron microscope. Results indicated that yeast extract and NH_4Cl worked better than peptone and $NaNO_3$, respectively, as supplemental nitrogen sources. To reduce the cost of raw materials, a combination of yeast extract and NH_4Cl was chosen to adjust the initial C/N ratio. The highest concentration and yield of *A. awamori* biomass were observed when the fungus was cultivated at a C/N ratio of 15, compared to ratios of 30 and 45. At a C/N ratio of 15, the crude protein content in pellets was at its highest at 18.10% (dry basis, d.b.). While the fat content was at its lowest at 2.28% (d.b.). The effects of pH control and agitation on *A. awamori* growth were investigated in the bioreactor. Ultimately, the optimal conditions for *A. awamori*

growth in almond hull extract were determined to be a C/N ratio of 15, an inoculum level of 10^3 spores/mL, without pH control, and an agitation rate of 150 rpm over a period of five days in a bioreactor with aeration at 1 air volume per working volume per minute to control dissolved oxygen above 25% of the saturation. Under these conditions, the biomass yield was around 0.85 g VSS/g sugar, with an average pellet size of 3.75 mm.

In addition to using the water-soluble extracts from almond hulls for fungal biomass cultivation, the potential of the residual almond hull solids (RASH) after sugar extraction for fungal cultivation was studied by using enzymatical hydrolysis. The effect of three different enzymes (Cellic CTec2, Viscozyme L and Pectinex Ultra SPL) and their combinations on hydrolysis performance were investigated and compared. The optimum loadings of enzymes were determined. The ability of *A. awamori* to grow on the resulting hydrolysate was evaluated. The most effective hydrolysis in terms of liquefaction and sugar yield was achieved through the combination of Cellic CTec2 and Viscozyme L. Using 200 uL/g RASH of Cellic CTec2 and 60 uL/g RASH of Viscozyme L resulted in a total sugar yield, total fiber conversion, and liquefaction efficiency of 41.36%, 86.01%, and 51.61%, respectively. Applying these optimal conditions at a larger scale resulted in improved liquefaction efficiency, reaching 72.53%. While the sugar yield was similar to small scale hydrolysis. After cultivating *A. awamori* in hydrolysate for five days, uniform yellow fungal pellets were observed, resulting in a biomass yield of 0.8 g VSS/g sugar. This study suggests that RASH could be a promising source for fungal-based food production, thus optimizing almond hull utilization and increasing the yield of fungal biomass from almond hulls.

A techno-economic analysis was conducted for an industrial-scale system for the production of *A. awamori* fungal biomass. Almond hulls were utilized as the feedstocks, with an

input of 50 MT/batch (wet basis, w.b.). SuperPro Designer software was used for process simulation and economic assessment. Two different scenarios were evaluated: the first system was using sugar extract alone as a source of nutrients needed for fungi cultivation and the second was similar to the first system plus the nutrients produced from the enzymatically hydrolyzed residual almond hull solids after sugar extraction. A sensitivity analysis was carried out for studying different parameters, affecting the breakeven price of fungal biomass, such as almond hull price and facility processing capacity. Using the same amount of hulls, the simulated systems produced approximately 2,971 MT/year fungal biomass using the sugars extracted from the hulls using hot water; and around 4,653 MT/year fungal biomass using the sugars extracted from the hulls using hot water plus the sugars produced from the enzymatic hydrolysis of the hulls with the same amount of almond hulls. The breakeven price of the fungal biomass from both systems ranged from $6 to $7 per kg of fungal biomass (d.b.). In both scenarios, the breakeven price of fungal biomass is more sensitive to the capacity at small scale (lower than 50 MT/batch) and more sensitive to almond hull price at larger scale. The results of this study indicate that almond hulls are very good feedstock for the production of myco-foods that can be competitive in the markets of proteins, probiotics, and other food categories, benefiting both the almond and food industries.

Finally, the potential of using *A. awamori* pellets for developing different products (myco-foods) was explored. The color and characteristic of the pellets were studied using both artificial food dyes and natural colored media derived from agricultural and industrial byproducts. Pellets' colors obtained from natural colored media were more stable after one-month storage. A method to create multilayered color pellets was developed successfully by deactivating pre-cultured pellets and then growing new spores on them. The texture of pellets was improved by coating with potato dextrose agar (PDA) and re-growing to form condensed mycelium inside fungal pellets. The

potential for developing *A. awamori* biomass into dried products was also evaluated. A mice study was conducted to determine the health benefits of the developed products. It was found that the biomass could potentially be processed into protein/fiber powder-based products through freeze drying or transformed into crispy, snack-like myco-chips through hot air drying. Lighter color was obtained after freeze drying, while hot air drying led to darker color of the fungal biomass. No mycotoxins were detected in the *A. awamori*-based foods, and the foods showed significant health benefits in the mice study. The spent media collected after pellet production contained enzymes, suggesting the potential for its utilization in the development of beverages. The findings from this study provided important information of the potential of developing *A. awamori* biomass into novel functional food.

In summary, based on the findings from this study, California's two million tons of almond hulls can be potentially transformed into 0.6 million tons of fungal biomass. This conversion could increase the revenue generated from almond hulls, from a previous 0.4 billion dollars (when sold as dairy feed) to 4.2 billion dollars in fungal products. This research demonstrated converting almond hulls into fungi-based food could significantly add economic value to the almond hulls. Further investigations can be undertaken to scale up the production of fungal biomass from almond hulls to large scale. Additionally, exploring the viability of utilizing almond hulls for cultivating various fungal strains could be a promising way forward for future research.

ACKNOWLEGEMENTS

I would like to sincerely thank my major professor Dr. Ruihong Zhang for her constant guidance, encouragement, patience and inspiration through my PhD studies. I couldn't reach this milestone without her. She is my real-life role model both in life and academia. Hope I can be someone like her in the future. I also want to thank Drs. Zhiliang (Julia) Fan and Zhongli Pan, for serving on my dissertation committee and providing their critical review and guidance as well as offering their laboratory facilities for my research. I am also extremely thankful to Drs. Bryan Jenkins, David Slaughter, Zhiliang (Julia) Fan, Christopher Simmons and Edward Spang who served on my qualifying exam committee.

In addition, I want to thank Dr. Jean-Jacques Lambert, who generously offered me opportunities to gain teaching experience. I am grateful for the many students and researchers from Dr. Zhang's lab group for their support and friendship. I especially acknowledge Dr. Hamed El-Mashad, who has been ever-ready to assist and offer invaluable professional advice; Dr. Tyler Barzee, who helped me get started with fungal research and kept teaching me professional knowledge and offering me guidance. I can always learn something new and interesting from him, which improved my skills as both a scientist and an engineer; Dr. Yike Chen, who has taught me how to balance life and academics, and the skills of self-discipline, which are essential in alleviating the pressure of my PhD studies; Dr. Ke Wang, whose influence has helped me develop my confidence; Allan Chio, who has always been willing to help and never said no to me; Jiayong (Kary) Liang, who accompanied and supported me during my initial years at UC Davis, which were the hardest time for me. I also want to thank Dr. Cai Shu, Hossein Edalati, Emily Sechrist; Cody Yothers; Alex Hobby; Kelly Mackenzie Graff, Ian Nielsen, Dr. Chang Chen, Ruoyi Liang, Dr. Steve Zicari, Dr. Mianfeng Zhang, Dr. Xindan Qi; Dr. Yunliang Zhang; Dr. Xinjun Lin; Dr.

Jiafu Zhang. I am grateful to the friendly and collaborative environment created by all the colleagues and staff in the Biological and Agricultural Engineering Department: Dr.Ragab Gebreil, Dr. Yuting Tang, Dr. Yi Wang, Dr. Chang Chen, Dr. Yingying Zheng, Dr. Xingzhu Wu, Irving Francisco Rabasa; Jiajie Wang, Vu Quach, Peter Russell, Kameron Chun, and Victor Duraj, thank you so much for all your help. There are numerous people who I would like to list here and all of them have provided me with assistance and education, both great and small.

I acknowledge the financial support from Almond Board of California, and California Department of Food and Agricultural, for enabling this research. I am also thankful to Jastro-Shields Awards, Walter Rosenburg Research Fund, UCD Graduate Program Fellowship Award and UCD Graduate student Travel Award for generously supporting my work and my development as a researcher.

Last but not the least, I am extremely grateful to my fiancé, Zhaokun Ning and his family, for their constant love, support, and encouragement. I am indebted to my family for their unconditional love and support; particularly my grandmother, dad, mom, sister, brother-in-law and nieces, who are my foundation. I also wish to express my deep gratitude towards my late grandfather, Xiaolong Cao. I love and miss you forever!

TABLE OF CONTENTS

LIST OF FIGURES

LIST OF TABLES

Chapter 1 Research Overview and Literature Review

1.1 Introduction

The world population is growing rapidly and is expected to reach 9-10 billion by 2050. The United Nations projects that food production will need to increase more than 50% by 2050 to feed an extra 2.5 billion people. Demand for resource-intensive foods like meat and dairy products is projected to rise by 70%. There is a need of 593 million hectares more agricultural land area, which is nearly twice the area of India, to meet the demand of food production by 2050. However, agriculture already uses 37% of the world's vegetated land. Besides land use, around one quarter to one third of global emissions come from food production system (Searchinger et al., 2014). Based on these facts, the challenge is to feed the future population without using more land while lowering emissions. One possible solution to this issue is to produce food products using high nutrition value microorganisms cultivated in bioreactors that could have less environmental impacts, and require low footprints (Onyeaka et al., 2022).

The potential edible microbes include bacteria, microalgae, and fungi. Among them, filamentous fungi possess unique pellet morphology under controlled conditions that simplifies the harvesting process (Anuradha et al., 2014) and may be economically advantageous as compared to microalgae, bacteria, and yeast. The unique fibrous hyphal structure allows filamentous fungi to be easily processed and shaped into various forms and provide better textural properties (K. Kim et al., 2011). Filamentous fungi also have high nutritional values, offering a variety of essential nutrients and bioactive compounds that contribute to healthy diets including protein, carbohydrates, fatty acid, minerals, vitamins, and antioxidants. Some of the most used and well-studies filamentous fungal strains for food applications belong to the general *Aspergillus*,

Penicillium, *Rhizopus* and *Fusarium*. The fungal strain used in this study is *Aspergillus awamori* (*A. awamori*), which is named after the alcoholic beverage "awamori" and has been widely used in food processing industry. The products of *A. awamori* are given Generally Recognized as Safe (GRAS) status from Food and Drug Administration (FDA) (Saleh et al., 2014). Much research has been done on feeding *A. awamori* to animals with demonstrated health benefits, including improved growth performance, modified lipid metabolism, meat quality, and immune responses etc.(Abdelhady et al., 2017; El-Deep et al., 2021; Lee et al., 2017; C. Li et al., 2019; Saleh et al., 2014).

Fungal biomass, specifically in the form of fungal pellets, has a great potential for the development of innovative food products, by utilizing fungal intrinsic characteristics. One potential product can be a healthy, sustainable alternative to traditional boba (tapioca pearls), which can be named as "mycoBoba". In 2022, the global bubble tea market was estimated at $2.8 billion dollars, with an estimated compound annual growth rate of 8.9% from 2023 to 2030 (Grand View Research, 2023). North America dominates the market, constituting 36% of the total market share. The key hurdle to even more widespread bubble tea consumption is due to the low shelf-stability of tapioca pearls, which degrade rapidly in liquid. This constraint forces boba tea to only be produced in the brick and motor stores, as they need to be produced on demand as cafes combine the beverage liquid and pearls immediately prior to delivery to the customer. Traditional tapioca boba is produced from cassava starch and as a result is composed almost entirely of carbohydrates. A single small serving of tapioca pearls in a milk tea beverage consists of 17-26% of the recommended maximum daily intake of sugar for men and women (NHS, 2019; USDA, 2023c). Growth in the bubble tea market is expected to be partially driven by the growing health awareness of young consumers, the main customer base, with a predicted increase in demand for healthier

and more sustainable bubble tea components. The introduction of mycoBoba can revolutionize this space by offering a healthier, more stable, and sustainable alternative to traditional boba. Furthermore, the appeal of mycoBoba can be enhanced by producing it from various agricultural byproducts, which results in a range of different colors. This not only makes the product more visually appealing to consumers, but also broadens the potential for different byproducts to be effectively repurposed.

Fungi possess a unique ability to utilize a wide range of substrates due to their complex enzyme systems (Chan et al., 2018). Generally, sucrose and glucose are two main carbon sources that have been utilized for fungal cultivation (American Type Culture Collection, 2023). However, the high feedstock cost is a limiting factor for industrial production (G. Liu et al., 2020). Utilizing agricultural byproducts or waste for fungal cultivation can reduce the environmental impact while lowering the production cost (T. J. Barzee et al., 2022).

Almond hulls are the most abundant byproduct of almond processing, comprising about 52% of the fruit fresh (Garcia, 2021). The hulls can be a potential substrate for fungal biomass production because of its high sugar content (>25%) and abundance in almond-producing regions (Holtman et al., 2015). Soluble sugars and nutrients can be extracted by water and serve as nutrient sources for fungal biomass cultivation. Almond hull also contain over 20% of fibers (Offeman et al., 2015), which can be hydrolyzed into simpler sugars and be further utilized for fungal cultivation. Traditionally, almond hulls are sold as a supplement feed for dairy cows. However, the almond industry is growing faster than the dairy industry, producing large amounts of excess hulls. Finding alternative uses for almond hulls while increasing their value is essential for the almond industry. Using almond hulls for fungal biomass production will not only reduce the costs

of raw materials for fungi production but can also help the almond industry achieve its zero-waste goal and improve sustainability.

1.2 Background and literature review

1.2.1 Almond hull production and characteristics

Almond (*Prunus dulcis*) belongs to the family Rosaceae and is placed under the genus *Prunus*, the same as peach (*Prunus persica*) (DePeters et al., 2020a). Similar to the fleshy fruit of peaches, almond hulls are the outer casing of the almond fruit and encloses the shell. The almond kernel is enclosed in the shell covered by a thin skin (Figure 1.1). Over 80% of global almond are produced by the United States, especially in California due to its Mediterranean climate (Huang and Lapsley, 2019). In 2022, approximately 2.9 billion pounds of almond kernels were produced by California. At the same time about 4.6 billion pounds of almond hulls and 1.9 billion pounds of shells were produced (Almond Board of California, 2022). Although the ratios vary with varieties, each pound of kernels produces approximately 2 pounds of hulls and 0.7 pounds of shells (Harris and Ferguson, 2013).

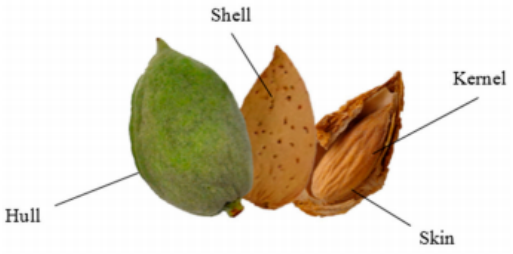

Figure 1.1. Parts of almond fruit (Prgomet et al., 2017)

California is known for cultivating over 30 varieties of almond. However, over 95% of the state's almond production is attributed to 10 major varieties. The top three producing varieties in 2022 were Nonpareil, Monterey and Independence, which accounted for 39%, 18% and 12% of

the total almond yield, respectively. Those three varieties alone were responsible for approximately 70% of the entire almond yield in 2022 (Almond Board of California, 2022). Nonpareil almonds, which are more than 120 years old, are highly prized for their medium size, uniform shape, smooth and light-colored skin, and sweet, buttery flavor. They also have thin shells, making them easily to process (Danyluk et al., 2008). Monterey almonds also have a high consumer demand, which are good for slicing or silvering process due to their large kernel sizes. Independence almonds, which is a new variety and was available to growers since 2008, increased fast in the past years. What makes this variety popular is its self-pollinating characteristic, reducing reliance on been pollination and the almonds are similar in size and flavor to Nonpareil (Sideli et al., 2020).

The characteristics of almond hulls can vary significantly depending on factors such as almond variety, environmental conditions, and agronomic practices, such as irrigation, fertilizing and harvesting. Some hulls may be thin and dry, while others are thick and fleshy (Prgomet et al., 2017). As these hulls mature on trees, they tend to harden, transitioning into a dry, woody texture and becoming less porous. In addition to physical characteristics, the composition of almond hulls can also vary. Various almond hull compositions are summarized in the Table 1.1. As can be seen from Table 1.1, up to 64.8% (on a dry basis, d.b.) of the hulls is water extractable. Soluble sugars like glucose, fructose, xylose, and sucrose represent a significant portion of these water extractable compounds (Table 1.2). Because Independence variety is a new variety, limited information could be found on its individual sugar content. The total sugar content in almond hulls varies between 24.4 to 46.3%, with the Independence variety containing the highest sugar content. Saura-Calixto et al. (1983) reported that soluble ash accounted for around 3.4% of the total water-soluble compounds in almond hulls. Table 1.3 shows the micronutrients detected in almond hull for three

popular varieties. The highest ash content reported in the literature is up to 17% from Nonpareil almond hulls, with potassium being the most abundant micronutrient detected in the almond hull, which is essential for cell wall development, improving resistance to environmental stress and participating in the activation of several enzymes involved in biochemical pathways (Andrews et al., 2021). The protein content in almond hulls ranges from 3.8% to 10%, and between 33.3% and 44.5% of this protein is soluble protein, as reported by Asmus (2016). The rest of the soluble compounds partly comprise fats, tannins, polyphenols, and other polysaccharides.

Besides water soluble compounds, almond hulls consist of approximately 35.2% to 45.4% water insoluble components. These mainly include structural and fibrous materials such as cellulose, hemicellulose, lignin, and pectin, which give the form and rigidity of hulls. Among those structural components, the total hemicellulose and cellulose accounted for up to 33% of the total hulls. Another portion is the lignin, a complex organic polymer highly resistant to degradation, accounting for up to 12.3% of almond hulls. Saura-Calixto et al (1983) and Almond Board of California (2019) reported the pectin content in almond hull samples containing mixed varieties was in the range of 4%-6%.

Table 1. 1 Compositions of almond hulls of three popular varieties (units: %, d.b.)

Component	Nonpareil	Monterey	Independence
Sugar	24.4 - 37.9	26.5 - 34.5	38.1 - 46.3
NDF	19.6 - 36	37.0 - 43.0	23.8 - 27.4
ADF	14 - 23.5	25.1 - 32.9	17.6 - 34.1
Crude protein	3.8 - 6.7	6.1 - 6.8	6.3 - 10
Fat	2.1 - 3.5	2.7 - 3.3	4.4 - 5.0
Lignin	3.5 - 12.3	7.5	-
Cellulose	6.6 - 9.6	20.8	-
Hemicellulose	5.2 - 12.5	10.1 - 11.9	6.6 - 16.2
Ash	3.5 - 17.0	5.9 - 11.9	13.3 - 16.9
Water soluble	61.5 - 64.8	54.6 - 62.4	
Water insoluble	35.2 - 39.8	37.6 - 45.4	
Reference	Holtman et al.2015; Offeman et al.,2014; DePeters et al., 2020; Palma et al., 2020; Sechrist, 2022	Offeman et al., 2014; Palma et al., 2020; Sechrist, 2022	Sechrist, 2022

Table 1. 2. Individual sugar in Nonpareil and Monterey almond hulls (units: %, d.b.)

	Glucose	Fructose	Sucrose	Xylose	Total sugar	Reference
Nonpareil	15.8- 16.3	13.0 - 15.9	3.9 - 5.2	0.6 – 0.7	33.3 - 37.9	Holtman et al., 2015; Offeman et al., 2014
Monterey	12.4	9.9	3.1	1.1	26.5	Offeman et al.,2014

Table 1. 3. Micronutrients in almond hulls of three popular varieties

Component	Unit (d.b.)	Nonpareil	Monterey	Independence
Potassium	%	2.5 - 3.3	3.5 - 3.9	4.0 - 5.2
Calcium	%	0.1 - 0.2	0.2 - 0.3	0.4 - 0.5
Phosphorus	%	0.10 - 0.16	0.1	0.1
Magnesium	%	0.07 - 0.1	0.1	0.2
Sulfur	%	-	0	0 - 0.1
Sodium	%	0.01 - 0.02	0	0 - 0.1
Iron	ppm	136 - 282	263 - 1068	401 - 585
Manganese	ppm	12 - 15	21 - 27	19 - 27
Zinc	ppm	7 - 16	11 - 16	17- 26
Copper	ppm	1 - 4	2 - 7	8 - 11
Reference		DePeters et al., 2020	Sechrist, 2022	Sechrist, 2022

The presence of pesticides in almond hulls might be a potential concern when considering their use in feed or food applications. However, several studies have been done to directly assess pesticide levels in almond hulls or evaluate their impact on animals or insects that consume them. In a study conducted by DePeters et al. (2020), concentrations of 20 different pesticides were investigated in Nonpareil almond hulls, and two other varieties. The study discovered that the most abundant pesticides present in the hulls were bifenthrin (0.3-0.8 mg/kg) and methoxyfenozide (1-1.5 mg/kg). All tested almond hull samples, except bifenthrin, were at least 16 times below the legal limit. The bifenthrin was still 2.5 times below the legal limit. Li and Bischel, (2022) also investigated the pesticide composition of almond hulls. They discovered that esfenvalerate (381.6 ± 47.7 ng/g), cyhalothrin (148.2 ± 64.4 ng/g), and bifenthrin (81.7 ± 33.3 ng/g) were the most abundant pesticides. They fed these hulls to black soldier fly larvae (BSFL) and observed a survival rate greater than 90%, indicating a low toxicity level of hulls to BSFL. Schnell et al. (1997) studied pesticide residues in the muscle, adipose, liver, and kidney samples from cattle that fed almond hulls, finding no pesticide presence in those tissues. All those findings indicate that almond hulls are safe for feed or food applications.

1.2.2 Almond hull current applications

Almond hulls are a rich source of many valuable nutrients that can be extracted or reutilized rather than being discarded in landfills. The current applications of almond hulls are summarized in Table 1.4. A lot of studies have demonstrated the effectiveness of almond hulls as feed supplement for livestock, especially for dairy cows. This effectiveness can be attributed to their high sugar and fiber content, which provide energy (Norollahi et al.,2005; Alibes et al.,1983), aid digestion and improve feed intake (Swanson et al., 2021; J. Wang et al., 2021). It's important to maintain a balanced diet in animal's feed by properly mixing almond hulls with other nutritional

sources. Currently, almond hulls make up about 5%-9% of a dairy cow's diet and could potentially be increased to 20% (Almond Board of California, 2022). In addition to their direct use in feed, almond hulls have proven to be a suitable substrate for insect farming, such as the cultivation of Black Soldier Fly Larvae (BSFL). BSFL is a rich source of protein, making them an attractive option for animal feed. Studies have successfully reared BSFL on a diet of almond hulls under controlled conditions within one month, resulting in a protein content of up to 51%, including essential amino acids such as methionine and cystine (Palma et al. 2018; Palma et al., 2019; Miner et al., 2022). These almond hulls can also be utilized for bioenergy production, such as biofuels and biogas. As reported by Holtman et al. (2015), each ton of almond hulls could generate 185 L bioethanol and 75 m^3 methane by utilizing the extracted sugar syrup from almond hulls.

Almond hulls can also be applied back into almond orchards by mixing ground almond hulls back into the soil to promote soil health and increase water-holding capacity (Tomishima et al., 2022). Moreover, almond hulls can be used as materials for biosolarization, which is a soil treatment process that utilizes organic waste materials together with solar energy, to manage soil-borne pests, diseases, and weeds. During biosolarization, almond hulls can serve as a significant source of carbon, which is necessary for microbial activity and can retain significant amount of water, which help maintain the moisture level during biosolarization. A study by Fernandez-Bayo et al. (2020) demonstrated the suitability of almond hulls as a soil amendment to control *Pratylenchus vulnus* and potentially other soil agricultural pests during biosolarization. More recent research conducted by Pastrana et al. (2022) found also that soil, when solarized and amended with almond residues (including hulls), had a greater reduction in pathogen presence compared to untreated and unamended controls.

Almond hulls are also abundant in natural antioxidants, especially phenolic compounds, which have a content around 3%-8% in almond hulls (Sechrist, 2022). Those antioxidants have several health benefits including reducing the risk of heart diseases, cancer, and other inflammatory conditions (Safarian et al., 2016; Sfahlan et al., 2009). There are numerous studies investigating the extraction of antioxidants from almond hulls, by different solvents (water, ethanol and methanol and different method (solvent and ultrasound-assisted methods) (Kahlaoui et al., 2019; Pinelo et al., 2004; Isfahlan et al., 2010; Rubilar et al., 2007). The antioxidants extracted through these processes can be employed as functional ingredients in food, pharmaceuticals, or cosmetics.

Table 1. 4. Current applications of almond hulls

Application	Description	Reference
Livestock feed	Supplement to feed due to high sugar and fiber contents as an energy source and aid digestion	Norollahi et al., 2005; Alibes et al., 1983; Swanson et al., 2021; Wang et al.,2021
Insect farming	Used as substrate for rearing insects such as black soldier fly larvae for feed	Palma et al. 2018; Palma et al., 2019; Miner et al.,2022
Bioenergy production	Feedstock for fermentation for production of biofuels or for anaerobic digestion for biogas production	Holtman et al., 2015
Soil amendment or biosolarization materials	Improve soil structure and provide essential nutrients to soil directly; or provide benefits through biosolarization, such as pest control	Pastrana et al., 2022; Fernandez-Bayo et al., 2020
Source of valuable compounds	Source of extracting value-added compounds, especially antioxidants, to be employed as functional ingredient in food, pharmaceuticals, or cosmetics.	Kahlaoui et al., 2019; Pinelo et al., 2004; Isfahlan et al., 2010; Rubilar et al., 2007

1.2.3 Sugar extraction from almond hulls

Solid-liquid extraction process has long been used for extracting valuable products from different biomass. Depending on the structure of the biomass, the solute to be extracted may exist on the surface of the solid, may be chemically bound or exist inside plant cells (Schweitzer, 1979). In most plant, sugars (sucrose, glucose, and fructose) exist interior plant cells (Desnoues et al., 2018). An example schematic diagram indicating the transfer of sugar from interior plant cell into the bulk solution is shown in Figure 1.2. Due to the fact that sugars are surrounded by cell membrane and cell wall, sugar diffusion inside the solid may be the rate limiting step. In this case, size reduction is important by increasing the surface area exposed to the solvent and reducing the internal diffusion path (Adapa et al., 2011). However, too fine particle will consume more energy for milling and will make it more difficult for solid-liquid separation after extraction. Temperature is another important factor influencing the extraction rate: increased temperature can lead to high extraction rate. However, then energy consumption could be a concern and there might be more undesired materials extracted and affect the product quality. Water is often used as the solvent for sugar extraction due to the high solubility of sugar in water and the safety of extracted sugar for food applications. Solvent ratio is also an important factor, which could influence both sugar yield and final sugar concertation. As the applications of almond hulls introduced in previous section, most of the research has focused on utilizing the whole almond hull solids for different application in order to utilize the sugars or fibers in the hulls. However, there has been limited research that focuses on extracting sugar from almond hulls first and then utilizing the sugars. To the best of our knowledge, only three literatures (Patterson et al., 2022; Holtman et al., 2015; Offeman et al., 2014) have included sugar extraction from almond hulls.

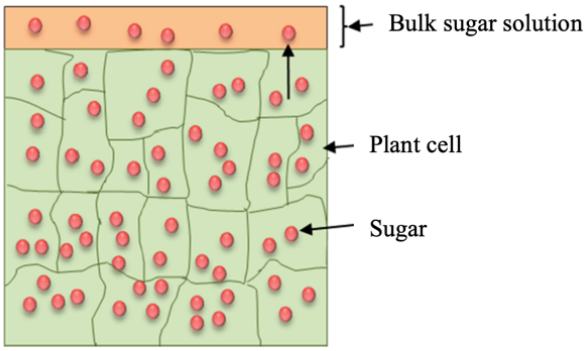

Figure 1. 2. Transfer of sugar from interior plant cell into the bulk solution (Baah et al., 2019)

Offeman et al. (2015) investigated the leaching behavior of water-soluble carbohydrates, including sugars, from nonpareil almond hulls by firstly studying the batch extraction rate and then studying the equilibration runs to use a standard leaching model for the calculation of stage-to-stage concentrations and flows in a countercurrent extractor. The major objective of that study was to produce concentrated extract. From the equilibrium countercurrent runs (70℃ for 2.5h at liquid-solid ratio of 9), they found that the probable maximum product solute concentration was in the range of 18% – 20%. The extraction rate experiments investigated the extraction of water-soluble carbohydrates from whole or milled almond hulls with different sizes (0.7-2 mm, 2-2.36 mm, 2.36-3.35 mm, and 3.35-6.24 mm) at three temperatures (40, 55 and 70℃) with a liquid-solid ratio (L/S ratio) of 19. The findings indicated that milling exerted a stronger impact on extraction than the temperature variations studied. The slowest extraction process was observed with whole almond hulls at 40 ℃, requiring about 196 minutes to reach 90% of the equilibrium concentration. Conversely, the quickest extraction process was the smallest particles at 70℃, with the time to reach 90% of equilibrium concentration being approximately 30 minutes. Similar extraction times were needed with particle sizes of 1.7-2, 2-2.36, and 2.36-3.35 mm, particularly at higher temperatures. The final sugar centration from this batch extraction process was around 21 g/L, contributing to about 63% of the total extracts. Notably, the total sugar in this literature included

both free sugars (sucrose, glucose, fructose, and xylose) and sugar alcohols (inositol and sorbitol). Free sugars accounted for 80.4% of the total sugars.

Holtman et al. (2015) focused on the recoverable sugar efficiency from the free water during the extraction process due to the absorption of water by almond hulls. Batch extraction experiments were carried out at 50°C and varying total solids (TS) loadings ranging from 5% to 20%, for either 1 hour or overnight, at 50°C. Before extraction, unground almond hulls were blended with hot water at the specified TS loading and milled for a minute to reduce particle size. At a TS loading of 5%, the sugar recovery efficiency was approximately 74%, with a low sugar concentration of 17.6 g/L. The study determined that the maximum TS loading for sugar extraction was 20% to have free water in the extraction system. They also conducted countercurrent extractions to achieve high concentrations of sugar for bioethanol production. High sugar concentration is important in commercial ethanol production to achieve sufficient alcohol content, making distillation economically. The countercurrent extraction was performed with a one-hour steep, followed by three wash stages, using the wash water for the subsequent steep process. During the extraction process, 0.05% (w/v) pectinase was added to enhance water recovery efficiency. After five rounds of extraction, a high concentration syrup was produced, containing 131 g/L of fermentable sugar (sucrose, glucose, and fructose). This countercurrent process resulted in an overall sugar recovery efficiency of 88%.

Patterson et al. (2022) extracted sugar from almond hull under a single set of conditions, as their research was mainly focused on the production of cellulose nanofibrils from the residual solids after sugar extraction. In their study, sugars were extracted from Carmel almond hulls at a temperature of 70℃ for 30 minutes, using a particle size of 0.25 mm. However, the L/S ratio was

not specified in their experiment. After extraction, 48.6% of the water-soluble compounds was removed from the almond hulls, without specifying the sugar content.

From these studies, it is apparent that the countercurrent extraction process, which involves multiple steps, is necessary to produce an extract with a high sugar concentration for applications requiring high sugar concentrations. Conversely, a batch extraction process can yield relatively low sugar concentrations which can also be applied for different applications. These studies provide information on the ranges of particle size, temperature, L/S ratio, and time for the extraction. More research is needed for investigating extraction kinetics and modelling to predict the sugar extraction process and apply to different almond hull varieties. Since the sugar concentration is related to the L/S ratio, sugar extraction at different ratios to yield different sugar concentrations for different applications need to be studied. However, it is important to maintain the L/S ratio above 4, as recommended by Holtman et al. (2015). Optimizing the sugar extraction process to achieve the highest sugar yield could also be a valuable area of research.

1.2.4 Fungal cultivation on agricultural and food processing byproducts

Fungi are heterotrophic and require organic carbon source, such as simple sugars (e.g., glucose and sucrose) which can be rapidly and directly utilized by fungi. However, they are not limited to these sugars and can utilize more complex substrates, including lignocellulosic biomass, for their growth. Complex biomass substrates are first broken down into simple sugars using extracellular enzymes, which are then transported inside the cell for further use. Many byproducts and waste from agriculture or the food industry contain a high load of organic carbon. Using these byproducts as a resource to cultivate fungi provides a sustainable strategy to capture and convert these low value organic carbons into valuable products. This approach can potentially reduce the

feedstock cost for fungal cultivation, which proving an environmentally friendly and economically solution for managing byproducts and producing fungal-based products.

Recently, there have been growing research focus on utilizing agricultural byproducts/wastes as substrates for fungal cultivation to reduce the cost of fungal product production and alleviate industrial pressure for waste treatment or upgrade byproducts values. An overview of utilizing byproducts for fungal biomass production is summarized in Table.1.5. The fungal performance can vary depending on the fungal species and cultivations. Therefore, it is important to develop efficient strategies for using different byproducts for different purposes.

Table 1. 5. Fungal cultivation on agricultural/food processing byproducts/waste

Species	Byproducts	Method	Bioproduct	Bioproduct content /productivity	Time (d)	Reference
Aspergillus oryzae	Wastewater from wheat starch processing	SmF*	Protein	0.36 g/g	3	Souza Filho et al.,2019
	Pea-industry byproduct	SmF	Protein	0.43 g/g	1.5	Souza et al., 2018
	Potato-processing byproducts		Oil	0.4 g/g	5	Muniraj et al., 2013
Rhizopus oryzae	Wastewater from wheat starch	SmF	Protein	0.37 g/g	3	Souza et al., 2019
	Potato-protein liquor		Protein	0.50 g/g	2.3	Souza et al., 2017
Aspergillus niger	Bagasse sugarcane	SSF*	Citric acid	2.51 mg/g/h	7	Bastos and Ribeiro, 2020
	Potato-chip-industry wastewater		Protein	0.39 g.g	3	Mishra and Arora, 2014
Aspergillus awamori	Jack fruit rind	SSF	Pectinase	412 U/gm	4	Padma et al., 2012
	Mango peel	SSF	Pectinase	217 U/gm	4	Padma et al., 2012
	Rice straw	SmF	Cellulase	15.19 U/mg	5	Naher et al., 2021
	Bread waste	SSF	Glucoamylase	114 U/g	7	Melikoglu et al., 2015
			Protease	83.2 U/g	7	Melikoglu et al., 2015

*SmF: Submerged fermentation; *SSF: solid state fermentation

1.2.5 Fungal biomass for food applications

The use of fungal biomass in food applications has been the focus of many studies due to its potential to produce high-value, sustainable and nutritious food products, based on their physical and chemical characteristics. Fungal biomass can be a valuable source of single cell

protein (or mycoprotein), which can reach high levels of protein (30-50%) that includes essential amino acids required for human nutrition (Souza Filho et al., 2019). Due to the increased demand for protein and a global push toward lowering greenhouse gas emissions, mycoprotein has been adopted as a meat substitute, which could be produced quickly than traditional meat production with a lower carbon footprint (Barzee et al., 2022). The firstly successfully commercialized fungal based mycoprotein on the market is Quorn, which was launched in 1985 by Marlow Food in the UK after over ten years rigorous safety testing. Derived from the filamentous fungus *Fusarium venenatum* (*F. venenatum*) through aerobic cultivation using corn starch, Quorn has different products made from the fungal mycelium, such as meatless and soy free nugget, patties and grounds etc. (Whittaker et al., 2020). Due to the mycelium structure, these products have similar texture as meat. In terms of the protein quality, Quorn has better protein-digestibility-corrected amino acid score than beef, which are 0.99 and 0.92 respectively (Chan et al., 2018). The expiry of numerous Quorn patents, coupled with a significant venture capital interest in animal-free proteins, has spurred the emergence of several start-ups keen to utilize similar technologies to generate meat alternatives. This involves the production of fungal biomass through both solid-state fermentation and submerged fermentation (Strong et al., 2022). Meati Food, which is a food technology startup started in 2016, also focused on developing meat alternatives through mycelium fermentation to generate various meat-like products (Meati Foods, 2023). Ecovative Design, a company uses mycelium to develop material alternatives, including food products from mycelium. They spun off a new independent company called My™Forest Foods with their first retail product My™Bacon launched in 2020 (ecovative, 2023). Prime Roots, another startup, uses koji fungal strain to produce meat alternatives. According to claims on their website, the production of 1 kg of Prime Roots' bacon contributes to significant environmental savings: it prevents the emission

of 9 kg of CO_2 compared to conventional pork bacon, decreases water usage by 92%, and reduces water eutrophication by 89% in contrast to animal meat (Prime Roots, 2023). With many new companies choosing to make meat substitutes from filamentous fungi, it's clear that these kinds of fungi have a lot of promise. They could really change the way we eat in the future, offering a solution that's good for both our health and the planet.

In addition to high protein content, some filamentous fungi can produce a significant amount of single cell oils (Athenaki et al., 2018). *Mucor circinelloides* was the first filamentous fungi to be used commercially to produce polyunsaturated fatty acids (Čertík et al., 2012). Fungal strains like *Mortierella isabellina*, *Mortierella vinacea*, *Aspergillus oryzae*, and *Humicola lanuginosa* can build up oil contents of 86%, 66%, 57%, and 75% respectively when grown in media rich in sugar (Subramaniam et al., 2010). The oil produced by these filamentous fungi could potentially serve as a substitute for vegetable oil, due to the similarity in their oil compositions, with the main lipids being triacylglycerols (Rivaldi et al., 2017). Oleic acid, palmitic acid, and linoleic acid are the major fatty acids found in fungal oil (Akpinar-Bayizit, 2014). Moreover, they are rich in polyunsaturated fatty acids like arachidonic acid (ARA; 20:4) and γ-linolenic acid (GLA; C18:3). For instance, *Mortierella alpina* (*M.alpina*) was found to contain over 60% of ARA in its total lipid content (Eroshin et al., 2000). *Cunningamella echinulata* was found to able to produce 49% lipid which had a GLA content of 16.4% (Gema et al., 2002). A product known as Fungal Oil SUN-TGA40S, branded as ARASCO, is a fungal oil rich in ARA obtained by fermentation from *M.alpina*. In 2001, this product was granted GRAS (Generally Recognized as Safe) status by the FDA, making it an approved supplement for infant formula products (Archer et al., 2008).

Fungal biomass with its unique nutritional and physical characteristics, can be innovatively employed as an ingredient in food products. An example, Stoffel et al. (2021) used fungal biomass flour from *Pleurotus albidus* as a substitute for wheat flour in cookie production. The research indicated that incorporating fungal biomass significantly enhanced the nutritional profile of the cookies and increased the protein, dietary fiber, and phenolic compounds content. Moreover, the addition of fungal biomass also changed the color and increased the hardness of the cookies.

1.2.6 *Aspergillus awamori* for food or feed applications

Aspergillus awamori can also be named as *A. niger var. awamori*, which is a specific variety of *A. niger* (Saleh et al., 2011). The *A. awamori* species was granted GRAS status by the FDA for its role in the production of rennet and chymosin, used in the coagulation of milk for the creation of cheese and other dairy products (under the regulation code 184.1685) (U.S. Food & Drug, 2018). *A. awamori*, which is named from the alcoholic beverage “awamori” and has been widely used in food fermentation, especially in Asian countries. According to research in 2013, *A. awamori* can also be referred to by the scientific name *Aspergillus luchuensis*, along with other koji strains (Hong et al., 2013).Traditionally, *A. awamori* is used in the fermentation of "Shochu," a popular distilled beverage in Japan (Hayashi et al., 2021). *A. awamori* is also known for its ability to produce a variety of enzymes, including proteases, amylases, and lipases, which contribute to the breakdown of proteins, carbohydrates, and fats in food substrates, enhancing flavor and nutritional profiles (Kiran et al., 2015; X. Liu & Kokare, 2023; Negi & Banerjee, 2009).

The safety and effects of *A. awamori* as feed supplements for animals have been studied by many researchers. For instance, El-Deep et al. (2021) investigated the effects on rabbits when fed *A. awamori* biomass powders. They found that supplementing the diet with *A. awamori* (0.01%-0.015%) improved nutrient digestibility, increased body weight, and increased immune

responses and antioxidant activity. Similarly, Saleh et al. (2011) found that broilers fed a diet containing 0.05% *A. awamori* experienced an increase in body weight, breast muscle, and feed intake. In another separate study, Saleh et al. (2013) fed *A. awamori* to rats and noted a reduction in abdominal and plasma lipid levels, effectively modifying the plasma lipid profile without any adverse effects. They also observed an increase in body weight and feed efficiency. These studies on different animals suggest that *A. awamori* may play a potential probiotic role in animal feed, and potentially in human food as well.

1.2.7 Fungal cultivation

Filamentous have been cultivated through both Submerged Fermentation (SmF) and Solid-State Fermentation (SSF) for many years for different applications as shown in Table 1.5. SSF involves the fugal growth on a solid substrate with a minimal free water. The moisture required for fungal growth is provided within the solid substrate. Compared with SmF, SSF has several advantages, including lower energy and water consumption, higher product concentration, less wastewater generation, and a more natural habitat simulation for the fungi. However, it has challenges like the difficulty in controlling environmental parameters like temperature, higher contamination risk, and difficulty in biomass recovery (López-Pérez & Viniegra-González, 2016). On the other hand, SmF is a traditional method which involves the growth of fungi in a liquid medium. The advantages of SmF include easier control of cultivation parameters, such as pH, temperature and oxygen levels, and easily to separate fungal biomass (Huq et al., 2022). But it requires well-designed bioreactors and high energy input for aeration and agitation. Both SmF and SSF have unique advantages and limitations, and the choice between them depends on the specific fungal strain, desired product, and available resources. In terms of food product production by

utilizing filamentous fungal biomass, SmF is preferred due to its capacity clean biomass recovery (Rousta et al., 2021).

In SmF, the morphology of filamentous fungi plays an important role in the productivity and efficiency of the process. Typically, fungi exhibit a complex, filamentous structure comprising hyphae (long, thread-like cells) which can intertwine and form a network known as a mycelium. This structure facilitates the absorption of nutrients from the surrounding medium. During SmF, filamentous fungi can exist in different morphological forms, ranging from freely dispersed hyphae, clumped hyphal fragments (pellets or clumps), to dense spherical growth forms (pellets) (Patel et al., 2023). The specific morphology that a filamentous fungus takes can greatly impact the fermentation process. For instance, freely dispersed hyphae can lead to higher product yields due to increased exposure to the nutrient-rich medium but can also result in higher viscosity and mass transfer limitations (Antecka et al., 2016). On the other hand, pellet formation can reduce broth viscosity, improving oxygen and nutrient transfer (Lu et al., 2015). However, too large size pellets can lead to diffusional limitations, potentially creating zones of nutrient deprivation within the pellets. It's important to note that fungal morphology during SmF can be influenced by numerous factors, including fungal strain, medium composition, and fermentation conditions (such as agitation and aeration) (Patel et al., 2023). Therefore, controlling and optimizing the morphology of filamentous fungi in SmF is a key strategy to enhance productivity in fungal fermentation processes.

1.2.7.1. Inoculum

Generally, fungal morphology in submerged culture depends on the species and the environmental parameters of cultivation. Not all fungal species or strains form pellets under the same conditions. Even the pellet formation species have different mechanisms to form pellets.

These mechanisms of pellet formation have been studied by literatures (Veiter et al., 2018; J. Zhang & Zhang, 2016). Depending on the formation process, fungal pellets are divided into two types (Figure 1.3). The first type is coagulative type which starts from the aggregation of spores within 6-8 h of cultivation, and then germinating and finally forming pellets. Metz & Kossen (1977) reported that one fungal pellet could be formed from up to 500 spores. The second type is non-coagulative type, in which spores germinate and grow as hypha and then form pellets without spores' aggregation (J. Zhang & Zhang, 2016). Among these two types, several researchers consider pellets formed by *Aspergillus* are coagulative type (Lin et al., 2008). The level of spores' concentration can influence the morphological characteristics of fungal mycelium. It has been reported that at low inoculum level of fungal spores ($< 10^8$ spores/ml), the formation of pellets is induced. Whereas too high concentrations of fungal spores will lead to dispersed mycelia (Papagianni & Moo-Young, 2002). Many literatures have analyzed and reported the relationship between amount of inoculum used and pellet size. Normally, the higher inoculum levels lead to smaller pellet size.

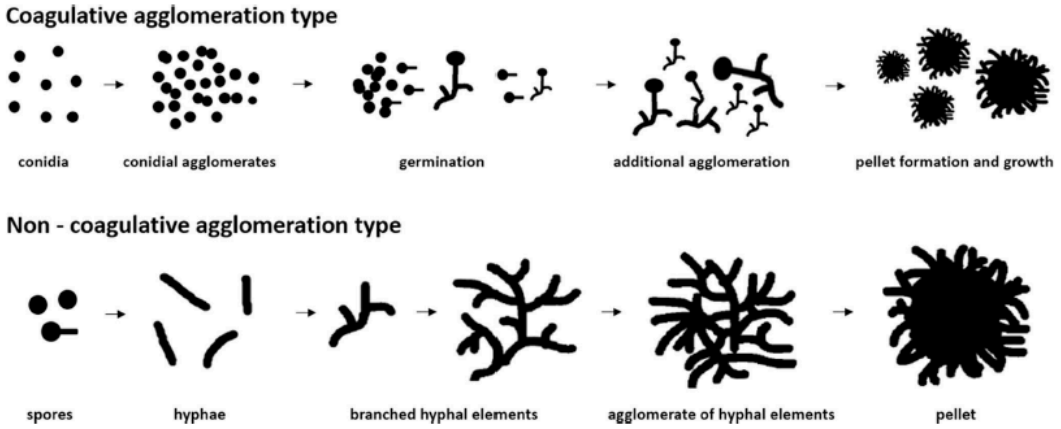

Figure 1. 3. Coagulative and non-coagulative models for pellet formation (Veiter et al., 2018)

1.2.7.2. Agitation

Agitation plays a very important role in fungal cultivation. Various studies over the years have investigated its impact on fungal morphology, pellet size, and overall productivity. One of the earliest works in this area by Metz & Kossen (1977) who reported that mixing in submerged cultures is crucial for promoting fungal growth and metabolite production. They demonstrated that an increase in the agitation speed can reduce the fungal pellet size, leading to a larger surface area exposed to the medium, thereby enhancing nutrient uptake and improving productivity. However, a study conducted by Purwanto et al. (2009) suggested that high agitation rates caused a mechanical damage to the *A. niger* mycelium (over 130 rpm) and finally leading to reduced enzyme productivity. They concluded that moderate agitation speeds were beneficial for maintaining fungal structure and improving metabolite production. Ibrahim et al. (2015) found highest biomass was achieved at agitation speed of 200 rpm for *A. niger*. Similarly, Seth & Chand (2000) examined the impact of agitation speed on the performance of *A. awamori*. They noticed a significant decline in the specific enzyme activity when agitation speed exceeded 400 rpm due to the shearing effects on the mycelium. Meanwhile, an agitation speed below 300 rpm led to inadequate mixing of the broth during the later growth stages. Beniwal & Chhokar (2010) found that an agitation speed of 125 rpm was the optimal speed for tannase production by *A. awamori*, showing better results compared to both 50 and 200 rpm. Normally, both free mycelium and pellets can exist in bioreactor, while the ratio between them are depended on the cultivation conditions, the resilience of the hyphae to mechanical stress and their physiological state (Papagianni, 2004). Examples of changes in pellet size, morphology, and biomass at various agitation speeds reported in literature are summarized in Table 1.6. To summarize, the optimal agitation speed can vary

significantly depending on the target products. Even for the same strain, the performance can be different at the same agitation speed because of other conditions.

Table 1. 6. Effects of agitation speed on fungal morphology

Strain	Agitation* (rpm)	Morphology	Biomass (g/L)	Reference
A. niger	0	Mycelial mat on the surface of media with spores	0.9	Ibrahim et al., 2015
	50	Slimy small (2.8 cm) mycelial clumps	1.4	
	100	Slimy medium (3.6 cm) mycelial clumps	1.6	
	150	Slimy big (4.7 cm) yellow mycelial clumps	1.8	
	200	Few spherical and elongated pellets with size between 0.6-1.0 mm	1.9	
	250	Mixture of small and bigger pellets	1.7	
A. niger	0	Slimy and mycelial	2.15	Purwanto et al., 2009
	100	Big, rounded pellets, diameter > 10 mm	4.35	
	130	Medium rounded pellets, 4-6 mm diameter	4.10	
	150	Pellets and mycelium, 2-2.5 mm diameter	3.55	
	200	Small pellets without free mycelia, diameter < 1.5 mm	2.50	

*Flask agitation speed

1.2.7.3. Reactor configuration

Bioreactor configuration can also influence the fungal performance during submerged cultivations. The most used bioreactors for fungal pellets cultivation are the stirred tank reactor (STR), airlift reactor (ALR), and bubble column reactor (BCR) (Espinosa-Ortiz et al., 2016). The STR, which consists of a cylindrical vessel with mechanical stirring, disperses air supplied at the reactor's bottom through mechanical agitation. It can generate high shear stress zones throughout the liquid volume and necessitates power for agitation. Due to these characteristics, STR is typically the preferred choice for culturing fungi in highly viscous broths. Moreover, operational parameters can be easily controlled and monitored in STRs (Espinosa-Ortiz et al., 2016). The ALR uses pneumatic agitation in an internal loop with a gas draft tube inside the reactor, causing an

upflow of liquid and fungal biomass within the tube. The gas then escapes from the top of the reactor while the fluid and fungal biomass move downward through the external loop (Zhu, 2007). Compared to an STR, an ALR provides a lower and more homogeneous shear stress. The BCR, a non-mechanically agitated reactor, uses a suitable gas distributor at the bottom. Gas moves upward in the column reactor in bubble form, inducing agitation of the liquid phase. The reactor configuration can affect fungal morphology mainly due to the differing shear force characteristics in each reactor configuration. Babič & Pavko (2012) observed a successful cultivation of *Dichomitus squalens* in pellet form in both STR and BCR. However, the cultures in BCR were fluffy, while round and smooth pellets were obtained in STR. More hairy fungal pellets of *Pycnoporus sanguineus* were found in ALR than in STR (Cao et al., 2014). In summary, the choice of reactor configuration for cultivating filamentous fungi in submerged conditions should be carefully made for different applications.

Based on those facts from literature, there is significant value to convert almond hull nutrients into *A. awamori* biomass which have a potential for use in food products. Therefore, the technology and processes for this conversion have to be investigated and designed to maximize the yield of *A. awamori* from almond hulls and evaluate this concept from both economical and nutritional perspectives.

1.3. Research goals and objectives

The overall goal of this research was to develop an efficient system for producing edible fungal biomass from almond hulls by integrating sugar extraction, enzymatic hydrolysis, and submerged cultivation. The main processes included in this study are shown in Figure 1.4. The specific objectives include:

1. Study extraction kinetics of sugars and optimize the sugar extraction process from almond hulls.
2. Determine the operational parameters affecting the production of *Aspergillus awamori* fungal biomass on almond hull extracts.
3. Conduct the enzymatic hydrolysis of almond hull residuals after water extraction to obtain more sugars and evaluate fungal performance on the hydrolysate.
4. Perform an economic analysis of the production of fungal biomass from almond hulls.
5. Develop fungal-based novel food products and evaluate their safety and health benefits.

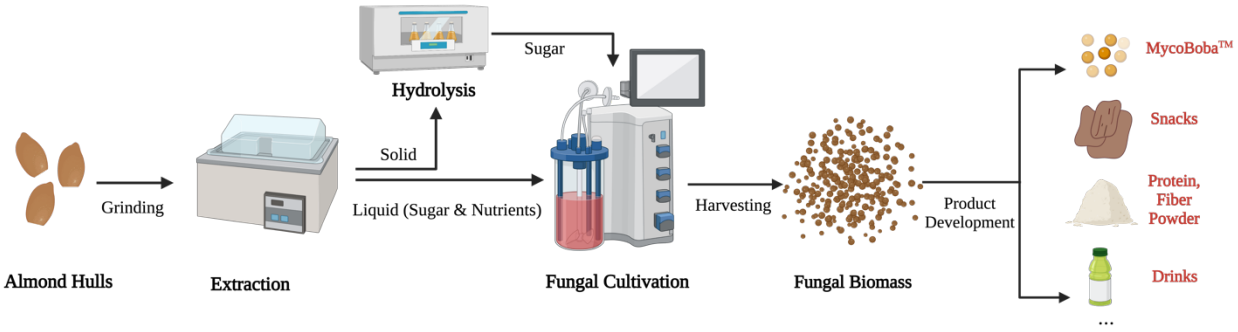

Figure 1. 4. General process flow of fungal biomass production from almond hulls

Chapter 2 Kinetic Modeling for Sugar Extraction from Almond Hulls

2.1 Abstract

The high sugar content in almond hulls makes them a valuable resource for producing high-value products. In this study, almond hulls collected from almond processors were examined to assess their characteristics for three popular varieties: Independence, Nonpareil, and Monterey. Two different grinding methods, continuous and successive grinding, were compared in order to get desired particle size for sugar extraction. A kinetic model was developed, based on Fick's law, for sugar extraction from Independence almond hulls using three different liquid-solid ratios. The model's accuracy was confirmed through validation at different temperature. Results showed that successive grinding was chosen to prepare almond hulls with a medium size range of 2.36 to 3.38 mm. The established model was also able to predict sugar extraction from Nonpareil and Monterey almond hulls. The model provided a theoretical framework to understand the extraction process, which is helpful to design sugar extraction experiment for different purpose.

2.2 Introduction

California is the world leading producer of almond, producing over 80% of the world's supply. Almond fruit consists of almond kernel covered by a thin layer of skin and surrounded by a hard shell. Outside the shell is almond hull. Almond hulls are the most abundant byproducts of almond processing, comprising about 52% of the fruit fresh wight (Almond Board of California, 2020). In 2022 alone, 4.6 billion pounds of almond hulls were generated in California (Almond Board of California, 2022). There are over 30 varieties of almonds produced in California, with more than 98% almonds produced from 13 varieties. The top three varieties in 2022 are Nonpareil, Monterey and Independence, which accounted for 39%, 18% and 12%, respectively. Those three

varieties alone were responsible for approximately 70% of the entire almond yield in 2022 (Almond Board of California, 2022). Nonpareil is over 120-year-old and the dominate variety, accounting for 39% almond production in 2022. Independence, the leading self-pollinate variety, was first introduced to California in 2008 and increased fast over the past few years (Sáez et al., 2020).

Traditionally, almonds are harvested by using mechanical tree shakers to get the almonds fall to the ground and letting the almonds dry on the ground for one to two weeks. After drying, almonds are swept into rows, vacuumed into trailer and transported to processors to remove hulls and shells. Some contaminants, such as sticks, soil and molded hulls, can be induced through those processes.

Almond hulls have high sugar content, mainly including glucose, fructose, xylose and sucrose (Holtman et al., 2015). The high sugar content in almond hulls offers a possibility to upgrade the value of almond hulls, which could be converted into microbial-based foods. In order to utilize the sugars in almond hulls, sugars can be extracted first. Solvent extraction is a solid-liquid separation process to extract soluble products. The extraction of sugar from almond hulls involves three steps: (1) water diffusion into almond hulls; (2) sugar diffusion to the surface of almond hull particles; and (3) sugar diffusion out of almond hull particles (C. W. Yu, 2012). The extraction process can be influenced by serval factors, such as temperature, solvent, liquid-solid ratio, time, particle size, etc. In order to design, control and predict the extraction process, studying the extraction kinetics and modeling are important.

Mathematical models are usually applied to obtain kinetic parameters, effective diffusivity and external mass transfer coefficient and to improve the extraction process. Mathematical models for solid-liquid extraction could be classified into two types: theoretical and empirical models. The

theoretical model is derived from the Fick's second law. The empirical models of extraction are established by fitting extraction concentration curves (Winitsorn et al., 2008). These models are simple and commonly used. However, no model was found for describing sugar extraction from almond hulls.

The goal of this study was to develop a sugar extraction model from almond hulls, which could be applied to different varieties. The objectives of this research were to: (1) collect, analyze and compare the physiochemical characteristics of three major varieties of almond hulls; (2) compare two different grinding methods for almond hulls; (3) study the sugar extraction kinetics from almond hulls, establish a kinetic model for sugar extraction and validate established model at different temperature and for different varieties of almond hulls.

2.3 Materials and Methods

2.3.1 Almond hull collection and characterization

Three different varieties of almond hulls, including Independence, Nonpareil and Monterey, were collected from West Valley Hulling Company (Firebaugh, CA, USA) in 2020 (Figure 2.1). All those three varieties were harvested and dried on-ground. Once those almonds were harvested, they were transported to West Valley Hulling Company and stored in stockpiles covered with plastic sheets before hulling. The first step for hulling and shelling was pre-cleaning, large sticks, fine soil, large soil clumps and small twigs were removed by screening and vibration. Hulling is accomplished by passing the in-hull almonds through initial vibration machines to loosen the hulls. All those processes could introduce contaminants such as sticks, shells, dust and shell fragments to the collected almond hulls. Hulls could be broken during those processes which led to different particle size distributions. Independence, Nonpareil, Monterey and Fritz hulls harvested in 2019

and a mixture of Carmel and Fritz hulls harvested in 2018 were also collected in order to analyze and compare the sugar content from different varieties harvested in different years.

Contaminants (sticks, shells, kernels, discolored hulls, etc.) were removed manually. The collected hulls, contaminants and clean hulls were weighted to calculate the fractions of contaminants and clean hulls in the collected samples. Clean almond hulls were stored in sealed buckets under dry and cool environment (around 24℃) before use. The physical and chemical properties of collected hulls, including moisture content (MC), total solids (TS), ash, neutral detergent fiber (NDF), acid detergent fiber (NDF), protein, fat and trace elements, were analyzed by Denele Analytical Inc. (Turlock, CA, USA).

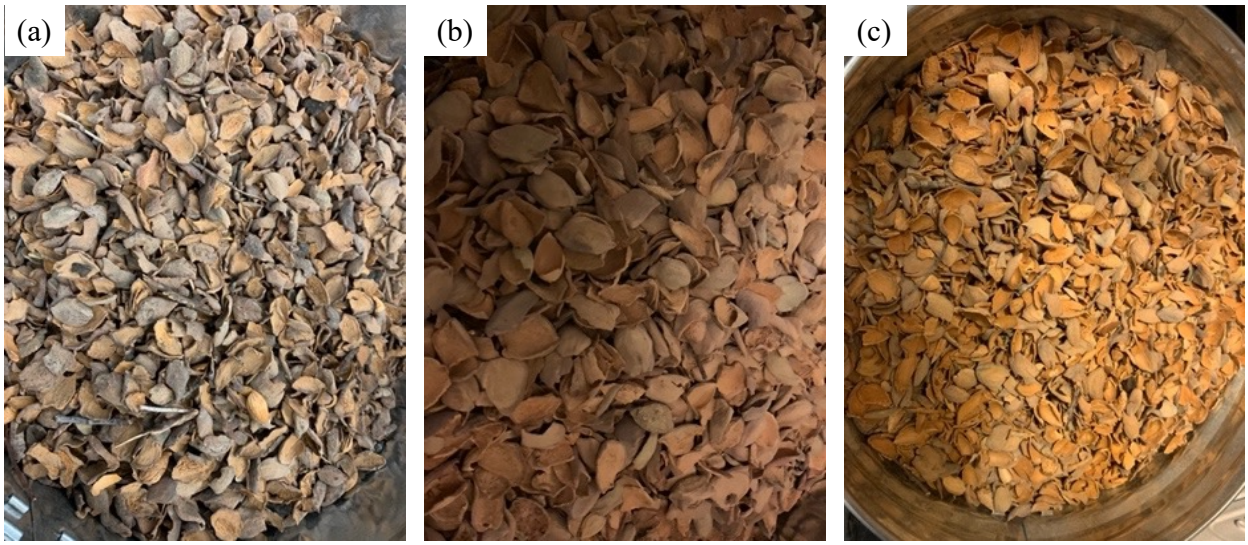

Figure 2. 1. Almond hulls: (a) Independence; (b): Nonpareil; (c): Monterey.

2.3.2 Almond hull grinding and fractionation

Grinding almond hulls could reduce the particle size and therefore influence the sugar extraction efficiency. Independence almond hull was selected as a model feedstock for the grinding and extraction experiments. Particle size distribution of unground clean almond hulls were analyzed by screening 300 g almond hulls sequentially through four sieves (15.9 mm, 12.5 mm,

7.9 mm and 4.7 mm) (Figure 2.2). The sieves were arranged on a sieve shaker (Retsch AS200) and vibrating until the accumulated hulls above each sieve appeared constant in size. The mass of almond hulls on each sieve were measured.

Two different grinding methods were studied: continuous and successive (Figure 2.3). Continuous grinding is a one-step grinding process, which involves feeding the large particles into a grinder or miller and then continuously grinding them to desired particle size. On the other hand, successive grinding involves multiple rounds of grinding and sieving processes to achieve the desired particle size. Continuous grinding was accomplished by grinding 300 g unground almond hulls for a certain time (1.5, 2.5, 3.5 or 4.5 min) using a food processor. After grinding, ground almond hulls were screened sequentially through two sieves (3.38 mm and 2.36 mm). Particles between 2.36-3.38 mm were collected and weighted. During successive grinding, 300 g unground almond hulls were grounded for 1.5 min and then passed through two sieves (3.38 mm and 2.36 mm). Particles with size larger than 3.38 mm were grounded again for one more minute. This step was repeated three times. Total grinding time were 0.5 min, 1.5 min, 2.5 min, 3.5 min and 4.5 min. Mass fractions of different particle size were calculated and compared with continuous grinding.

Figure 2. 2. Sieve shaker used to separate almond hulls with different size

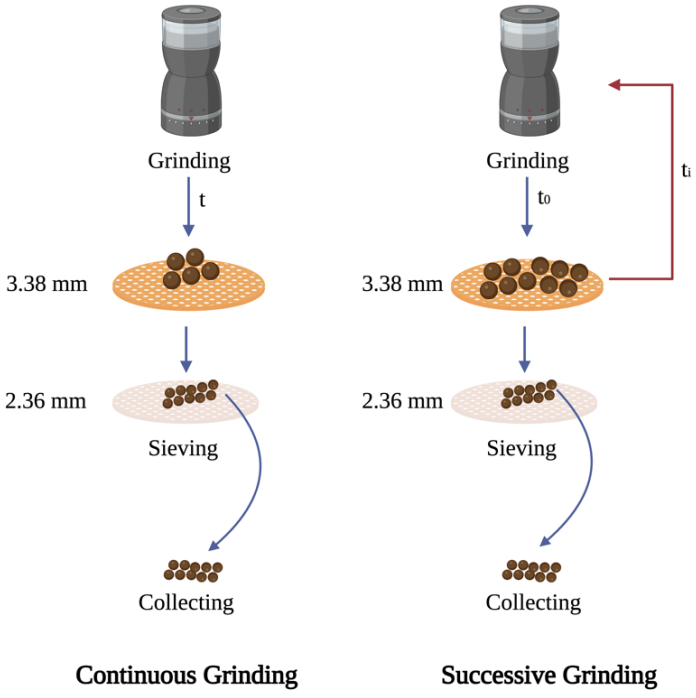

Figure 2. 3. Description of continuous and successive grinding processes

2.3.3 Sugar extraction process

Sugar extraction from Independence almond hull was studied. Three temperature levels (40, 60 and 80°C) and three liquid-solid ratios (L/S ratio) (10, 15 and 20 mL/g) were chosen in this research. Deionized (DI) water was utilized as extraction solvent. Before extraction process, hulls were grounded by a food blender into a particle size between 2.36-3.38 mm. The extraction was done by adding 200 mL DI water into 500 mL flasks and preheated in a water bath (Precision SWB 27, Thermos Fisher Scientific, USA) (Figure 2.4). After preheating, ground almond hulls were added to each flask at selected L/S ratios. During extraction, solvent and solid were mixed by the shaking water bath at a speed of 120 rpm. Each flask was capped by a plastic stopper (Jaece Industries Indenti-plug^{TM}) to avoid water evaporation. All treatments were conducted in triplicates.

About 1 mL of liquid sample was taken from each flask by a pipette at 12 selected sampling time points: 2, 5, 8, 10, 15, 20, 30, 40, 50, 60, 90, and 120 minutes. The liquid samples were filtered through 0.22 µm syringe filters (MilliporeSigma) immediately to remove fine particles and avoid continuous sugar extraction. The filtered liquid samples were frozen at -20°C before sugar analysis.

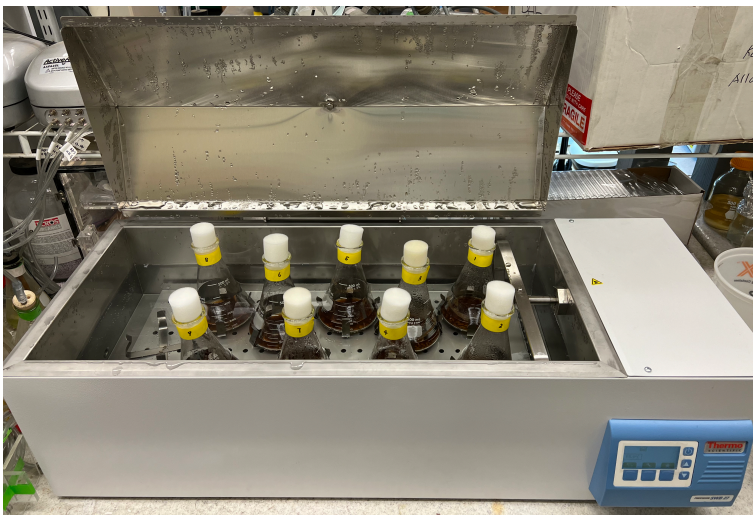

Figure 2. 4. Sugar extraction from almond hulls by shaking water bath

2.3.4 Sugar analysis

Total reducing sugar concentrations were determined calorimetrically by using 3,5-dinitrosalicylic acid (DNS) method (Miller, 1959). One mL of prepared DNS reagent and 0.1 mL of five times diluted samples were mixed well in disposable borosilicate glass tubes (10 mm outer diameter, Fisherbrand^{TM}). A mixture of water and DNS reagent was used as a blank. Glucose samples with different concentrations were used as standards. All tubes, including samples, blank and standards were covered by aluminum foil and boiled together for 10 min in a vigorously boiling water bath. After boiling, all tubes were transferred to a cold ice-water bath and cooled for 10 min. All tubes were then diluted by adding 1 mL DI water. The absorbance was measured at 540 nm using a Hach DR/2700 portable spectrophotometer (Hach company, Loveland, Colorado).

2.3.5 Modelling

A partial differential equation based on Fick's second law for one-dimensional diffusion was employed to investigate sugar extraction from almond hulls. In order to simply describe the sugar transfer during the extraction, some assumptions were made as follows:

(1) The geometry of ground almond hulls was considered as flat plates, which had a half thickness of L.

(2) Sugar was initially uniformly distributed in almond hulls.

(3) Transport of sugar inside the almond hulls was due to diffusion. The effective diffusion coefficient (D_e) was independent of time.

(4) The diffusion of each type of sugar was in parrel. There was no interaction between them or other compounds.

(5) External mass transfer resistance is negligible.

(6) At the solid liquid interface, sugar concentration between the internal liquid and external to almond hull particles was assumed to be equal.

(7) The extraction medium (i.e., water) was perfectly mixed in flasks. Sugar concentration in water only depends on time.

(8) Physical properties of almons hulls, including density, particle size and porosity were assumed to be stable during the extraction process.

Based on the above assumption, a basic 1-D diffusion model derived from Fick's second law for a plate geometry is presented as follows:

$$\frac{\partial C_s}{\partial t} = D_e \frac{\partial^2 C_s}{\partial x^2} \qquad \text{(Eqn. 2.1)}$$

where C_s is the sugar concentration in solid phase (g/L); t is time (s); D_e is the effective diffusivity (m^2/s) inside the solid; x is the axis perpendicular to the plate surface (m).

The initial concentration of sugar inside the almond hull was assumed to be uniform at a value equal to C_{S0} (g/L). Therefore, the initial condition is:

$$t = 0, C_s = C_{S0} \quad \forall x \qquad \text{(Eqn. 2.2)}$$

Assuming no external mass transfer resistance, the two boundary conditions are:

$$t > 0, C_s = C_0 \quad x = \pm L \qquad \text{(Eqn. 2.3)}$$

$$t > 0, \frac{\partial C_s}{\partial x} = 0 \quad x = 0 \qquad \text{(Eqn. 2.4)}$$

where C_{S0} is the initial sugar concentration inside the solid (g/L); C_0 is the constant sugar concentration at the interface the particle.

The solution of Eqn. 2.1 could be written as Eqn. 2.5 (Crank, 1979):

$$\frac{C_s - C_{S0}}{C_0 - C_{S0}} = 1 - \frac{4}{\pi}\sum_{n=0}^{\infty}\frac{(-1)^n}{(2n+1)}\exp\left(\frac{-D_e(2n+1)^2\pi^2 t}{4L^2}\right)cos\frac{(2n+1)\pi x}{2L} \qquad \text{(Eqn. 2.5)}$$

The mass of sugar transferred from the particles at any time (M_t, g) could be calculated by integrating the sugar concentration over the thickness of particles to obtain Eqn. 2.6 (Crank, 1979):

$$\frac{M_t}{M_\infty} = 1 - \frac{8}{\pi^2}\sum_{n=0}^{\infty}\frac{1}{(2n+1)^2}\exp\left(\frac{-D_e(2n+1)^2\pi^2 t}{4L^2}\right) \qquad \text{(Eqn. 2.6)}$$

where M_∞ is the total amount of sugar transferred after infinite time (g). M_t and M_∞ can be expressed as Eqn. 2.7 and 2.8, respectively.

$$M_t = C_{L,t}V_{aq} \qquad \text{(Eqn. 2.7)}$$

$$M_\infty = C_{L,\infty}V_{aq} \qquad \text{(Eqn. 2.8)}$$

where $C_{L,t}$ (g/L) is the sugar concentration in liquid phase at time t; $C_{L,\infty}$ (g/L) is sugar concentration in liquid phase after infinite time; V_{aq} (L) is total volume of water in extraction flask. Because the flasks were covered, V_{aq} was considered as constant during the extraction. By substituting Eqn. 2.7 and 2.8 into Eqn. 2.6, the following Eqn. 2.9 was obtained:

$$\frac{C_{L,\infty} - C_{L,t}}{C_{L,\infty}} = \frac{8}{\pi^2}\sum_{n=0}^{\infty}\frac{1}{(2n+1)^2}\exp\left(\frac{-D_e(2n+1)^2\pi^2 t}{4L^2}\right) \qquad \text{(Eqn. 2.9)}$$

The effective diffusion coefficient D_e in Eqn. 2.9 is a function of temperature, which could be described by Arrhenius equation shown in Eqn. 2.10 (Yu, 2012):

$$D_e = A\exp\left(\frac{-E_a}{RT}\right) \qquad \text{(Eqn. 2.10)}$$

where A is the pre-exponential factor (m^2/s); E_a is the activation energy (kJ/mol); R is the universal constant; T is temperature (K).

By substituting Eqn. 2.10 into Eqn. 2.9, the sugar concentration at time t and any temperature T could be expressed by Eqn. 2.11.

$$C_{L,t} = C_{L,\infty} * \left[1 - \frac{8}{\pi^2}\sum_{n=0}^{\infty}\frac{1}{(2n+1)^2}\exp\left(\frac{-A\exp\left(\frac{-E_a}{RT}\right)(2n+1)^2\pi^2 t}{4L^2}\right)\right] \qquad \text{(Eqn. 2.11)}$$

Nomenclature	
A	pre-exponential factor (m^2/s)
C_0	sugar concentration at the interface the particle (g/L)
$C_{L,t}$	sugar concentration in liquid phase at time t (g/L)
$C_{L,\infty}$	sugar concentration in liquid phase after infinite time (g/L)
C_{S0}	Initial sugar concentration inside the solid (g/L)
C_s	sugar concentration in solid phase (g/L)
D_e	effective diffusion coefficient of sugar inside almond hull
E_a	activation energy (kJ/mol)
L	half thickness of ground almond hulls
M_t	mass of sugar transferred from the particles at any time (g)
M_∞	total amount of sugar transferred after infinite time (g)
R	universal constant
t	time (min)
T	temperature (K)
V_{aq}	total volume of water in extraction flask (L)

2.3.6 Model validation and application

The established model was validated at different temperatures and applied for different varieties of almond hulls. Validating the model at different temperature was accomplished by generating the sugar concentration profiles at a different temperature (50℃) and three L/S ratios (10, 15 and 20) using Independence almond hulls. Sugar extractions from Nonpareil and Monterey almond hulls were also conducted at 60℃ and three L/S ratios (10, 15 and 20). The established model was evaluated by comparing the experimental and predicted data.

2.3.7 Statistical analysis

All data were organized, processed and subjected to statistical analysis using Microsoft Excel (Redmond, WA), GraphPad Prism software (San Diego, CA) and MATLAB (Natick, MA). The difference between treatments were statistically analyzed using Analysis of Variance (ANOVA) and Tukey's range test, with a significance level set at 5%.

2.4 Results and Discussion

2.4.1 Sugar content of different almond hulls

The sugar contents in almond hulls harvested from different years with different verities are listed in Table 2.1. The total sugar contents ranged from 31.84% to 42.23%, which were consistent with the reported values from the literature (Holtman et al., 2015; Offeman et al., 2014; Sechrist, 2022). The sugar content in almond hulls varied between different varieties and years. One reason could be intrinsic genetic differences of almond varieties. The processing could be another reason, such as the production, harvesting and storage. Environmental conditions during the growing season, such as temperature and humidity, could also affect the sugar content by affecting the growth, maturation, and metabolism of almond orchards. The cultivation practices, such as fertilization, irrigation and harvesting are also possible reasons led to the sugar variations in almond hulls.

Table 2. 1. Total sugar content in different almond hulls (dry basis, d.b.)

Variety	Harvested year	Sugar content (%)
Independence	2019	42.23
	2020	38.72
Nonpareil	2019	31.84
	2020	41.47
Monterey	2019	33.11
	2020	39.60
Fritz	2019	41.65
Carmel and fritz mixture	2018	33.66

2.4.2 Contaminants and compositions

As shown in Figure 2.5, the collected almond hulls contained some contaminates, which mainly included shell, sticks, twigs, kernels, and molded hulls. Those contaminants were evenly distributed in both Independence and Nonpareil almond hulls, which accounted for 5.57% and 4.02% respectively. No significant difference was found between those two varieties ($p < 0.05$). Monterey hulls contained 23.02% contaminants, while the majority were shells (17.19%) (Table 2.2). Both Independence and Nonpareil varieties have soft and thin shells. Monterey has thicker shell (Saa, 2020), which may make them more difficult to be separated with hulls during hulling and shelling processes. It was reported by Offeman et al. (2014) that hard- shelled almond varieties tended to have a portion of the shell adhering to the hulls leading to more debris mixed with the almond hulls. Similar findings were observed by (DePeters et al., 2020b). Our data agree with literature findings, since Monterey almond had harder shell compared with Nonpareil and Independence varieties.

Figure 2. 5. Clean Independence almond hull (left) and contaminants and discolored hulls (right)

Table 2. 2. Fractions of clean hulls and contaminants (unit, %)

Variety	Clean Hulls	Contaminants	Total
Independence	94.15 (0.47)	5.57 (0.53)	99.72 (0.06)
Nonpareil	96.01 (1.97)	4.02 (2.00)	99.68 (0.32)
Monterey	76.64 (0.30)	23.02 (0.19)	99.66 (0.32)

Approximately 30 g of Independence, Nonpareil and Monterey almond hulls were sampled for compositional analysis. The detailed compositions are shown in Table 2.3. Among those three varieties, Monterey almond hulls had the lowest moisture content. Most of the compositions were similar among those three varieties. As expected, almond hulls had around 21.3-23.6% acid detergent fiber (ADF, mainly include cellulose, hemicellulose and lignin) or 25.5-27.3% natural detergent fiber (NDF, including cellules and lignin). Protein and fat content were relatively low compared to fiber content, which were 4.69-4.82% and 2.4-3.7%, respectively.

Ash content in Independence almond hulls was slightly higher than Nonpareil and Monterey, which was attributed to the higher calcium, chloride, phosphate, and iron present in Independence almond hulls. Potassium is the most abundant cation in plant cells, which is essential for cell wall developments, improving resistance to environmental stress and participating in the activation of several enzymes involved in biochemical pathways (Andrews et al., 2021). The

potassium content in almond hulls was 2.03-2.38% which was the greater nutrient. Similar potassium content in almond hulls (2.15%) was reported by Calixto & Cañellas (1982).

Table 2. 3. Characteristics of Independence, Nonpareil and Monterey almond hulls

Compound	unit	Independence	Nonpareil	Monterey
Moisture [a]	%	11.83	13.46	9.87
Total solid[a]	%	88.17	86.54	90.13
Ash[b]	%	13.76	13.10	13.50
ADF[b]	%	23.60	21.3	21.3
NDF[b]	%	27.3	25.5	25.5
Crude protein[b]	%	4.72	4.82	4.69
Crude fat[b]	%	2.80	3.7	2.40
K[b]	%	2.38	2.32	2.03
Ca[b]	%	0.30	0.18	0.20
Cl[b]	%	0.17	0.10	0.12
Mg[b]	%	0.16	0.10	0.10
P[b]	%	0.20	0.09	0.08
Na[b]	%	0.01	0.01	0.01
S[b]	%	0.05	0.05	0.04
Fe[b]	ppm	409.79	152.60	191.15
Mn[b]	ppm	6.81	3.42	8.13
Zn[b]	ppm	4.15	2.29	0.98

[a] As total weight of sample; [b] As TS of sample.

2.4.3 Grinding and particle size distribution

Particle size distributions of collected independence almond hulls were analyzed. Over 97% of collected Independence almond hulls were larger than 7.9 mm. The most common particle size range was between 12.5-15.9 mm, which accounted for 40.7% of the total hulls. Conversely, only 2.04% almond hulls were smaller than 4.7 mm in size (Figure 2.6). Such a distribution of particle sizes in almond hulls is not efficient for sugar extraction. Therefore, grinding the hulls into smaller particles is necessary.

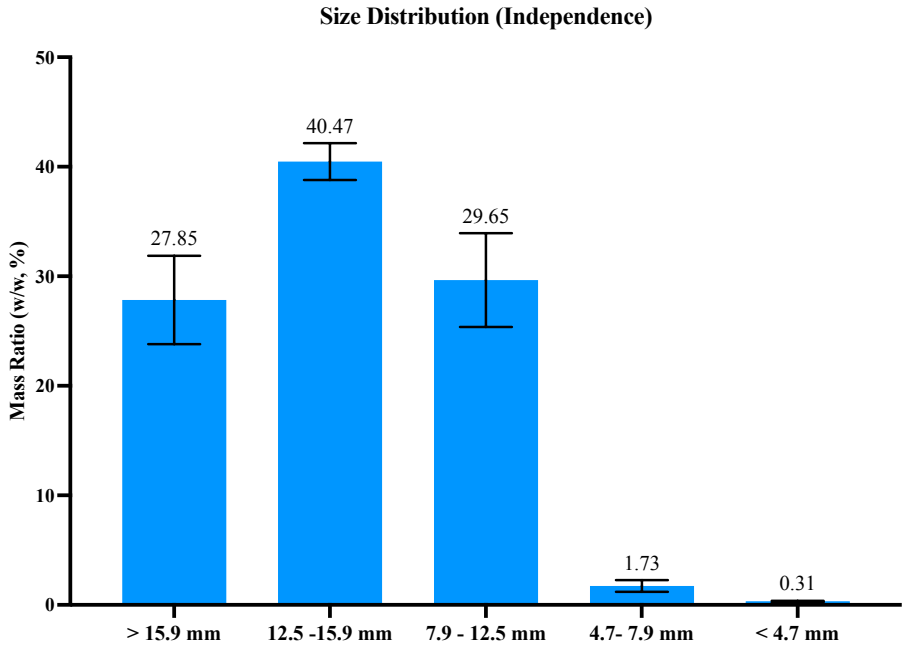

Figure 2. 6. Particle size distribution of unground Independence almond hulls

(Y error bars are standard deviations, n = 5)

According to our pre-liminary sugar extraction experiments, fine particles (< 2.36 mm) were hard to be separated after extraction, which could increase the separation cost or lower the separation efficiency. Offeman et al. (2015) compared the sugar extraction from almond hulls with different particle size, including 2-2.36 mm, 2.36-3.35 mm and 3.35- 6.24 mm. They found that similar time was needed to extract 90% of sugars from almond hulls with particle size of 2-2.36mm and 2.36-3.35mm. Therefore, the desired particles after grinding were medium size (2.36-3.38 mm). Fine particles which were considered as a "loss" had to be controlled as less as possible.

Particle size distributions of ground hulls using continuous and successive grinding methods are shown in Figures 2.7 and 2.8. By using continuous grinding, large particles (> 3.38 mm) were the most among all the studies. Medium particles didn't increase too much after 1.5 min. After 4.5 min, medium and large particles accounted for 28.83% and 38.97%, respectively. By successive grinding, medium particles were increasing, and large particles were decreasing over

time. After 6.5 min, increase of medium particles and decrease of large particle size slowed down because of the low almond hull loadings for grinding. Fine particles increased slowly after 3.5 min, indicating that most of the large particles were converted into medium particles instead of fine particles. Comparing those two grinding methods, successive grinding was more efficient than continuous grinding, and the amount of oversized or undersized particles could be controlled and minimized by successive grinding. Successive grinding is a more energy-efficient method compared to continuous grinding. This is because continuous grinding requires a constant energy input throughout the process, while successive grinding involves breaks between grinding stages and less sample loading into the grinder. These factors result in less energy consumption during successive grinding.

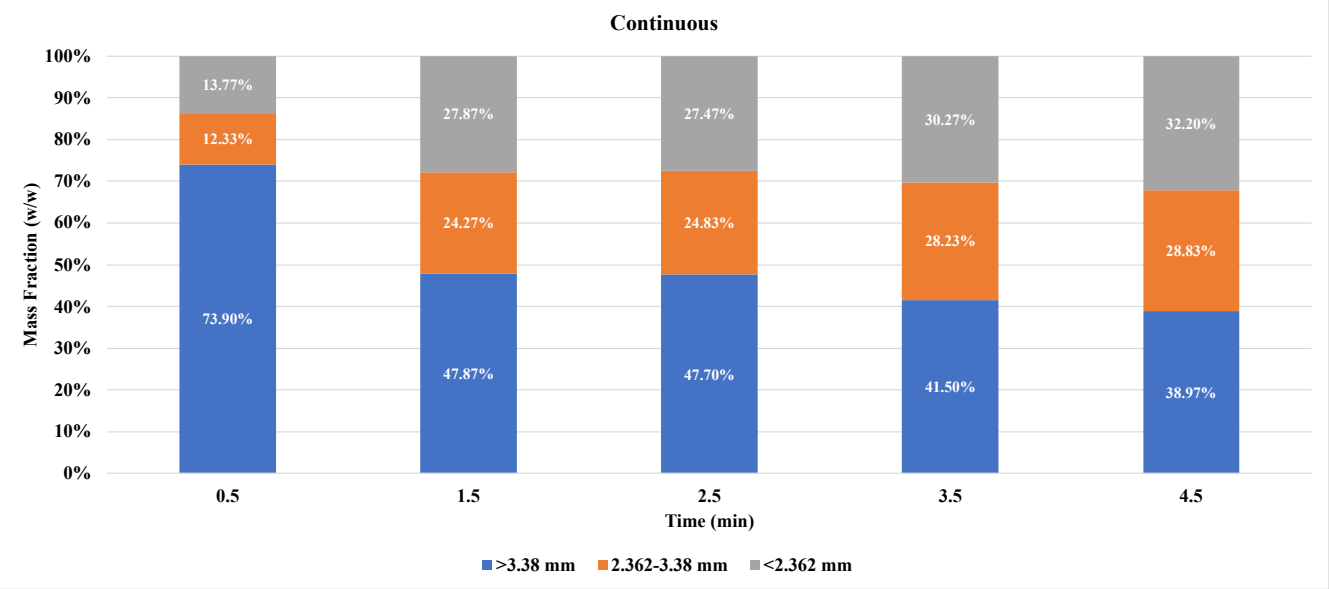

Figure 2. 7. Particle size distribution of almond hulls by continuous grinding

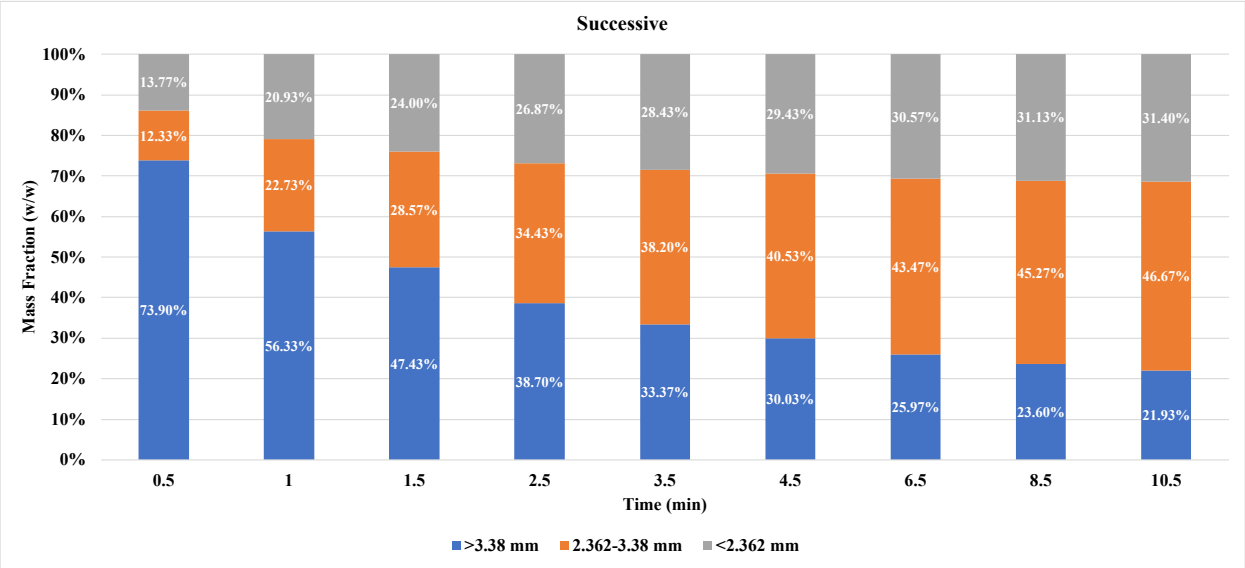

Figure 2. 8.Particle size distribution by successive grinding

The compositions of large, medium and fine particles were analyzed and is shown in Table 2.4. Fine particles had higher ash content (14.90%) than large and medium-sized almond hulls. The high ash content in fine particles could be attributed to the presence of dust from the original collected almond hulls, which had been sieved and screened into the fine particle portion. The higher calcium content in fine particles also supported that, as calcium is a primary component of dust and debris (Van der Hoven & Quade, 2002). Therefore, medium-sized almond hulls could be used for the extraction because they were cleaner and more efficient for extraction.

Table 2. 4. Characteristics of ground Independence almond hulls

Compound	unit	Whole	Large (>3.38 mm)	Medium (2.36 - 3.38mm)	Fine (<2.36 mm)
Moisture [a]	%	11.83	9.70	9.40	8.60
TS[a]	%	88.17	90.30	90.60	91.40
Ash[b]	%	13.76	12.41	12.43	14.90
K[b]	%	3.38	2.23	2.84	2.41
Ca[b]	%	0.30	0.23	0.29	0.34
Cl[b]	%	0.17	0.14	0.18	0.20
Mg[b]	%	0.16	0.12	0.15	0.15
P[b]	%	0.20	0.17	0.20	0.16
S[b]	%	0.05	0.04	0.04	0.05
Na[b]	%	0.01	0.02	0.02	0.02
Fe[b]	ppm	409.79	172.05	183.93	372.85
Mn[b]	ppm	6.81	5.52	7.51	9.64
Zn[b]	ppm	4.15	2.4	4.18	5.74

[a] As total weight of sample; [b] As TS of sample.

2.4.4 Effects of temperature and liquid-solid ratio on sugar extraction

The sugar concentration and yield profiles at different temperature and L/S ratios are shown in Figures 2.9, 2.10 and 2.11. Sugar concentrations and sugar yields increased quickly at the first 30 min and then gradually slowed down due to the decreasing concentration difference between the almond hulls and bulk solution during extraction. Around 90% of the sugars could be extracted within 60 minutes. As expected, lower L/S ratios resulted in higher sugar concentrations. Sugar yields increased with increasing L/S ratios at 40℃, while at 60℃ and 80℃, increasing the L/S ratio didn't significantly increase the sugar yield.

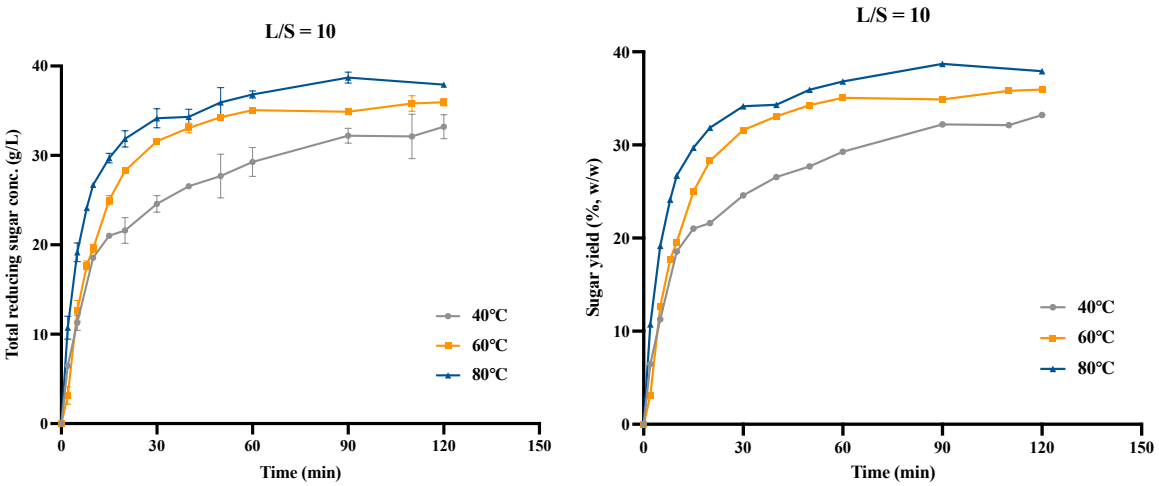

Figure 2. 9. Sugar concentrations (left) and yields (right) from almond hulls at L/S =10 and different temperatures

(Y error bars represent the standard deviations, n = 3)

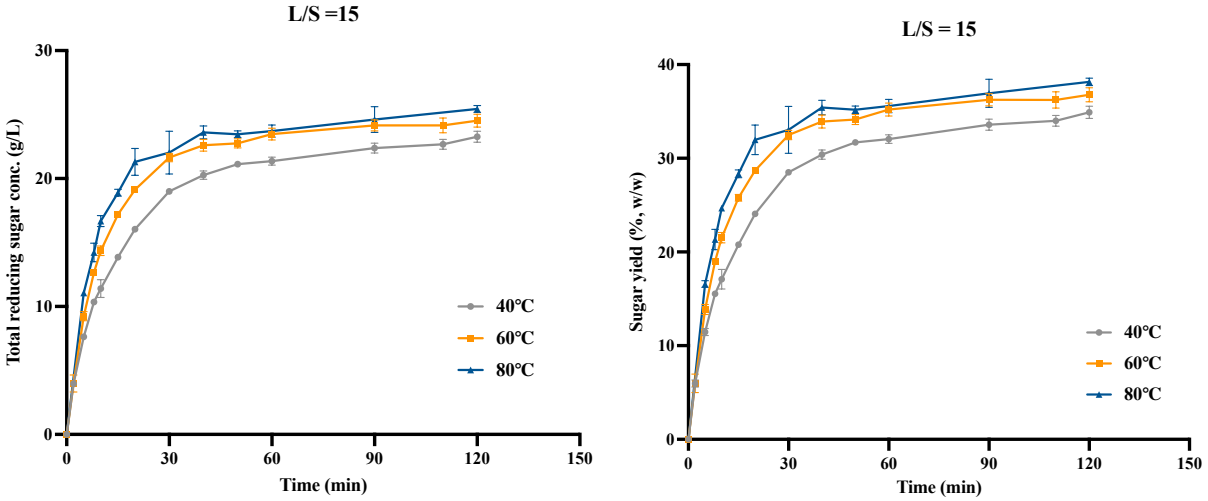

Figure 2. 10. Sugar concentrations (left) and yields (right) from almond hulls at L/S =15 and different temperatures

(Y error bars represent the standard deviations, n = 3)

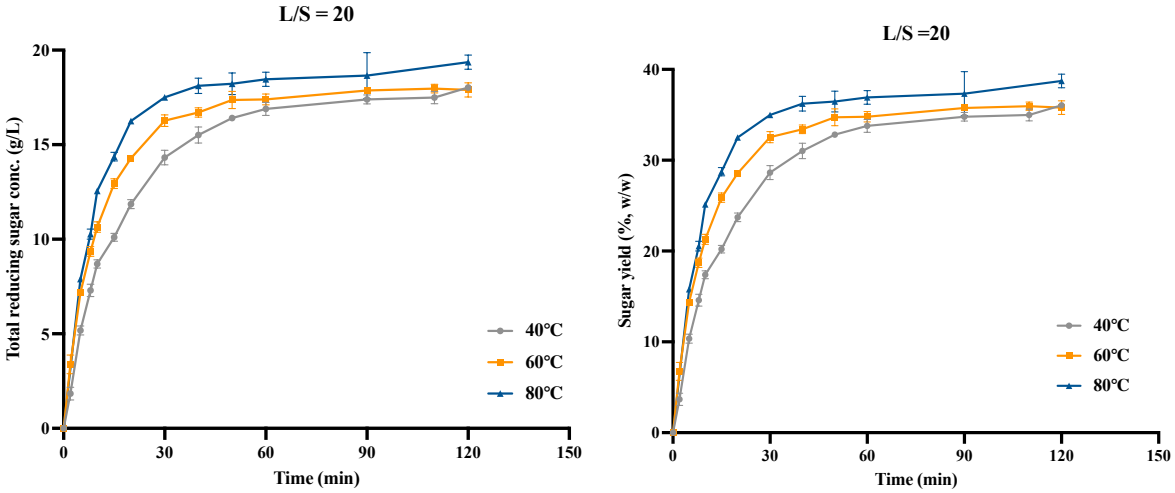

Figure 2. 11. Sugar concentrations (left) and yields (right) from almond hulls at L/S =20 and different temperatures

(Y error bars represent the standard deviations, n = 3)

2.4.5 Kinetic model

The estimated effective diffusion coefficients (D_e, Eqn. 2.9) under different conditions with different L/S ratios and temperature are listed in Table 2.5. It was observed that, with increasing temperature, the estimated values of D_e increased. This indicated that sugar could diffuse more easily from the almond hulls into the water at high temperatures. This is because high temperatures increase the kinetic energy of the sugars, making them more easily to diffuse across the concentration gradient. In addition, high temperatures could weaken the almond hull structure (Barakat et al., 2014), which can increase the contact area between water and almond hulls and facilitate the extraction process.

As L/S ratio increased from 10 to 15, D_e also increased due to the higher sugar concentration difference between the almond hull and solvent. While increasing L/S ratio from 15 to 20 didn't lead to significant increase of D_e. There might be limited surface aera of the almond hulls that could interact with the extracting solvent (i.e., water), which could affect the diffusion rate.

Table 2. 5. Estimated effective diffusion coefficients D_e of sugar from Independence almond hulls (Unit: 10^{-10} m^2/s)

	L/S =10	L/S =15	L/S =20
T = 40 ℃	0.65	0.91	0.90
T = 60 ℃	1.22	1.45	1.36
T = 80 ℃	2.15	1.95	1.94

After finding effective diffusion coefficients D_e, the pre-exponential factor A in Eqn. 2.10 could be estimated. By taking the natural logarithm of both side of Eqn. 2.10, the flowing linear equation was obtained:

$$\ln(D_e) = \ln(A) + \left(\frac{-E_a}{RT}\right)\left(\frac{1}{T}\right) \qquad \text{(Eqn. 2.12)}$$

Therefore, pre-exponential factor A and the activation energy E_a in Eqn. 2.12 could be determined by plotting $\ln(D)$ versus $1/T$ (Figure 2.12). The estimated parameters are shown in Table 2.6. The pre-exponential factor A represented the collision rate between sugar and almond hulls. The activation energy E_a represented the energy barrier that had to be overcome during the extraction process,

As the L/S ratio increased from 10 to 15, low values of A were obtained. Similarly, decreased when L/S ratio E_a increased. However, similar parameters were obtained between L/S ratios at 15 and 20. More intuitively conclusion could be drawn in Figure 2.12, where it can be observed that the two regression lines for L/S ratios of 15 and 20 were nearly parallel, indicating the activation energy E_a were similar at both conditions. Those E_a values were consistent with E_a values reported in literature.

Table 2. 6. Pre-exponential factor A and activation energy E_a of sugar extraction from Independence almond hulls at different L/S ratios

L/S ratio (mL/g)	A (10^{-8} m^2/s)	E_a (kJ/mol)	R^2
10	241.70	27.40	0.999
15	8.09	17.64	0.991
20	8.31	17.80	0.999

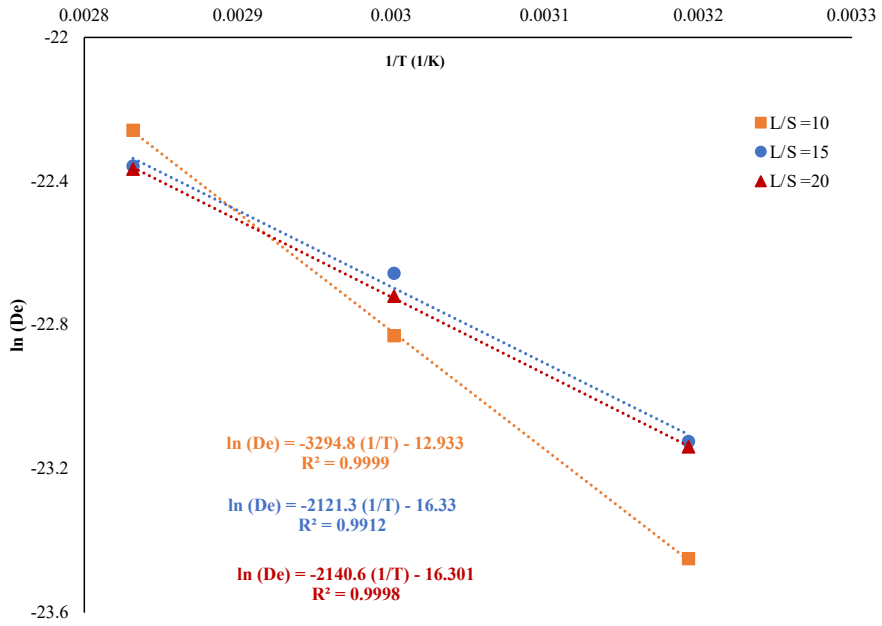

Figure 2. 12. Relationship between ln(D_e) and 1/T at different L/S ratios

2.4.6 Model validation-different temperature

In order to test the accuracy and reliability of the established models, nonlinear regression analysis between the experimental and predicted data was performed. Figure 2.13 are plots showing the comparison between experimental and predicted data from the previously established model. The agreement between the experimental data and model values was assessed by coefficient of determination (R^2) (listed in Table 2.7). High values of R^2 could be estimated,

indicating that the models well fitted experimental data. The model for L/S ratio of 10 lightly underestimated the sugar concentration at the beginning of the extraction process. This could because of the high solids loading in the flask, which increased the interactions between the particles. Such collisions could breakdown the particles and/or accelerate the extraction.

Table 2. 7. Coefficient of determination of experimental and modeled sugar yield at 50 ℃

L/S ratio	R^2
10	0.9311
15	0.9839
20	0.9912

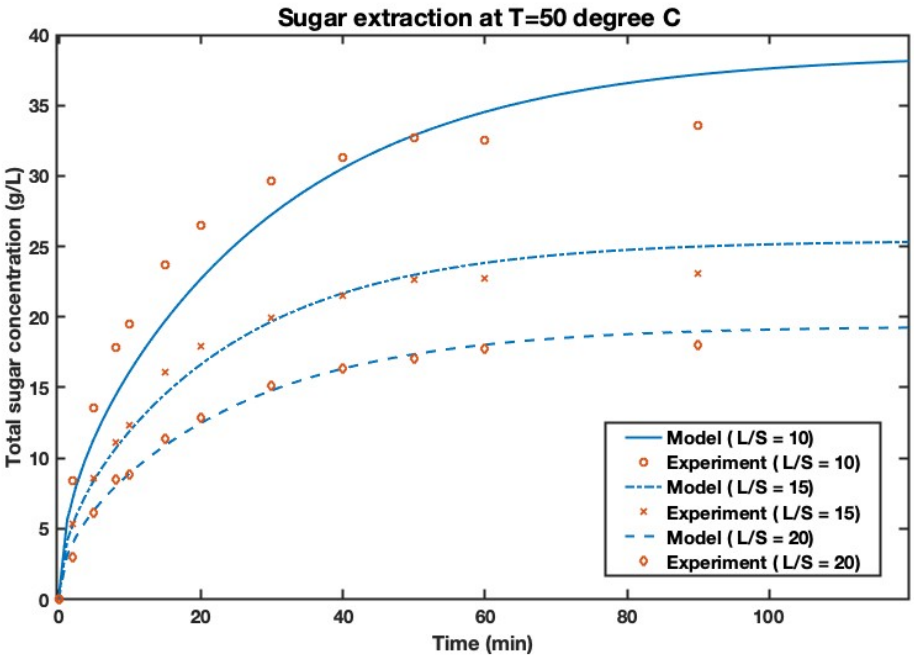

Figure 2. 13. Comparison of experimental data with predicted values of sugars extracted at 50℃.

2.4.7 Model application-predicting sugar extraction from different varieties

The abilities of the established models to predict sugar extraction from almond hulls with different varieties (Nonpareil and Monterey) were tested at 60℃. The experimental values versus

predicted values are shown in Figure 2.14 and R^2 values are shown in Table 2.8. The models fitted sugar extraction from Nonpareil almond hulls very well, with high R^2 values. The models could also predict sugar extraction from Monterey almond hulls, where R^2 values ranged from 0.95 to 0.86 when S/L ratios increased from 10 to 20. As shown in Figure 2.14, all three models were overestimated the sugar concentrations. This indicated that the real diffusion coefficients in Monterey almond hulls were smaller than that was estimated for Independence almond hulls due to the different characteristics of their physical structure, such as porosity, hardness, density etc.

Table 2. 8. Coefficient of determination of experimental and model predicted values for Nonpareil and Monterey almond hulls at 60 ℃

Variety	L/S	R^2
Nonpareil	10	0.9641
	15	0.9811
	20	0.9749
Monterey	10	0.9535
	15	0.9075
	20	0.8574

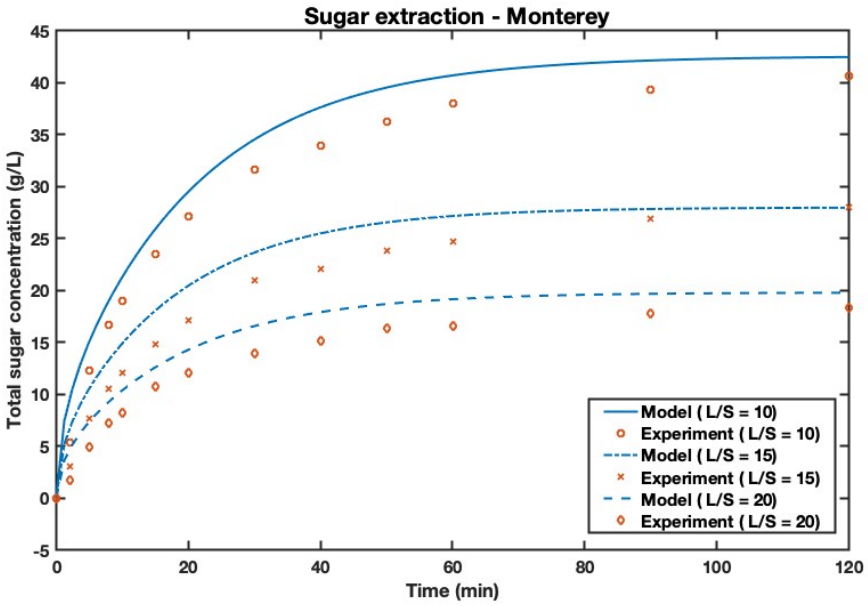

(a)

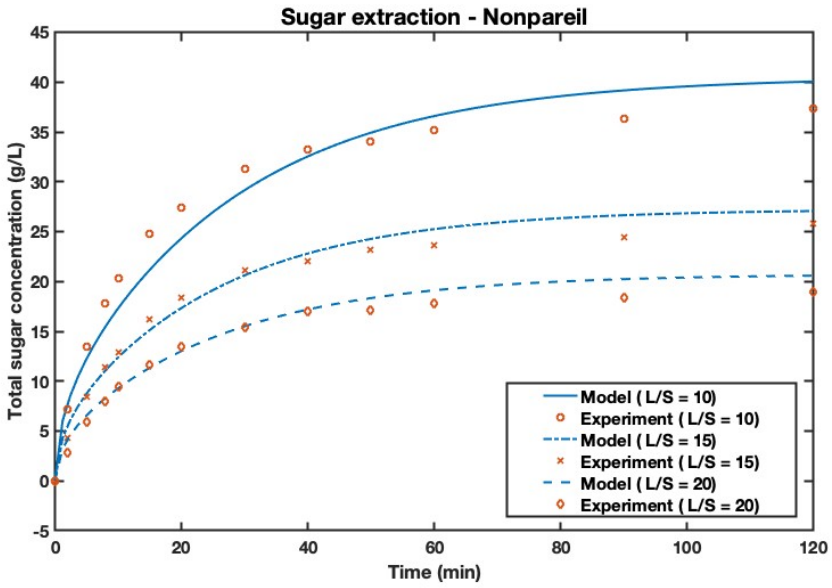

(b)

Figure 2. 14. Comparison of experimental data with predicted values of sugars extracted from Monterey (a) and Nonpareil (b) almond hulls at 60℃.

2.5 Conclusions

Monterey almond hull was found to have the highest foreign material content among the three varieties, reaching 23.02%. While Nonpareil and Independence hulls contained approximately 5% foreign materials. The sugar content of the almond hulls ranged from 31.84% to 42.23%, with variations depending on the variety and harvest year.

Continuous grinding resulted in minimal changes in the particle size distribution of fine, medium, and large particles after 3.5 min. Medium-sized particles (2.36-3.38 mm) accounted for approximately 28% of the total. On the other hand, successive grinding proved to be more efficient, achieving 38.20% medium-sized particles after 3.5 minutes, which further increased to 46.67% after 10.5 minutes. Given the preference for medium-sized particles for sugar extraction considering both solids separation and extraction efficiency, successive grinding was chosen as the preferred method. The developed theoretical model, based on Fick's law, could be used to accurately predict sugar yields from almond hulls at various temperature and liquid-solid (L/S)

ratios. The findings of this study contribute to a better understanding of the almond hulls' properties and offer insights for designing sugar extraction processes

Chapter 3 Optimization of Sugar Extraction from Almond Hulls

3.1 Abstract

Sugar extraction from almond hulls by hot water was optimized. Response Surface Methodology (RSM) based on Box-Behnken Design was utilized to determine the optimal combination of time, temperature, and liquid-solid ratio for achieving the maximum total reducing sugar yield. The resulting optimum extraction conditions were as follows: extraction time of 86.6 minutes, temperature of 77.4°C, and a liquid-solid ratio of 14. Under these conditions, the experimental yield was 38.1%, which was well matched with the predictive yield 39.3%.

3.2 Introduction

Utilization of almond hulls for different applications has gained a significant attention in recent years due to their potential as a valuable source for a high-value sugar production. The key issue for utilizing sugars from almond hulls is the extraction of sugars from it. Response Surface Methodology (RSM) is a powerful tool for optimizing the extraction process and to efficiently explore the effects of multiple factors and their interactions on sugar yield. This approach offers a strategic and an efficient approach to maximize sugar extraction from almond hulls, leading to enhanced productivity and economic viability. Understanding the effects of various factors and their interactions on sugar extraction is important for designing the extraction process effectively and efficiently, which allows for the selection of optimal factor levels to achieve the highest sugar yield. Therefore, the objective of this study was to investigate the effect of different extraction factors (time, temperature, and liquid to solid ratio) and their interactions on sugar extraction from almond hulls and to optimize the extraction process using RSM.

3.3. Materials and Methods

3.3.1 Sample preparation

Independence almond hulls were cleaned by removing the contaminants (sticks, shells, kernels, discolored hulls, etc.) manually. The clean hulls were grounded by a food processer into a particle size between 2.36-3.38 mm. Grounded hulls were stored in a plastic container at cool environment (around 24℃) before use.

3.3.2 Sugar extraction and analysis

The samples were subjected to sugar extraction by adding ground almond hulls into 500 mL flasks with 200 mL preheated deionized water (DI water). All the flasks were capped by plastic stoppers to prevent water evaporation during the extraction and fixed in a shaking water bath at a constant shaking speed of 120 rpm. Samples of 1 mL of liquid were collected during the extraction process. The liquid samples were filtered through 0.22 μm syringe filters and then frozen at -20℃ before sugar analysis.

Total reducing sugar concentrations in the collected samples were analyzed by using 3,5-dinitrosalicylic acid (DNS) method (Miller, 1959). The sugar yield during the extraction process was calculated by Eqn.3.1:

$$Sugar\ yield\ (\%) = \frac{C \times V}{M} \times 100\% \quad \text{(Eqn.3.1)}$$

Where C is the total sugar concentration at different time, (g/L); V is the working volume, (L); M is the mass (dry matter) of almond hulls, (g).

3.3.3 Experimental design

A Box-Behnke design employing response surface methodology was selected for optimization of the sugar extraction process and to test the effect of time (min, factor A), temperature (℃ , factor B) and liquid-solid ratio (mL/g, L/S, factor C) and their interactive effects. In the design, each factor was evaluated at three levels. Extraction time (t) values varied between 10 and 110 min, temperature (T) between 40℃ and 80℃ and liquid-solid ratio (L/S) between 10 and 20. Variables were codified in the range between +1 and -1, as calculated below:

$$t = (\mathbf{t}\text{-}60)/50 \qquad \text{(Eqn. 3.2)}$$

$$T = (\mathbf{T}\text{-}60)/20 \qquad \text{(Eqn. 3.3)}$$

$$L/S = (\mathbf{L/S}\text{ -}15)/5 \qquad \text{(Eqn.3.4)}$$

There were 16 experimental runs, including 4 center point replicates and 12 middle edge points of the cubical design region. All the experiments were performed in triplicates (n = 3). The geometry of this three-factor Box-Behnken design is depicted in Figure 3.1. All the experimental runs are marked by red circles.

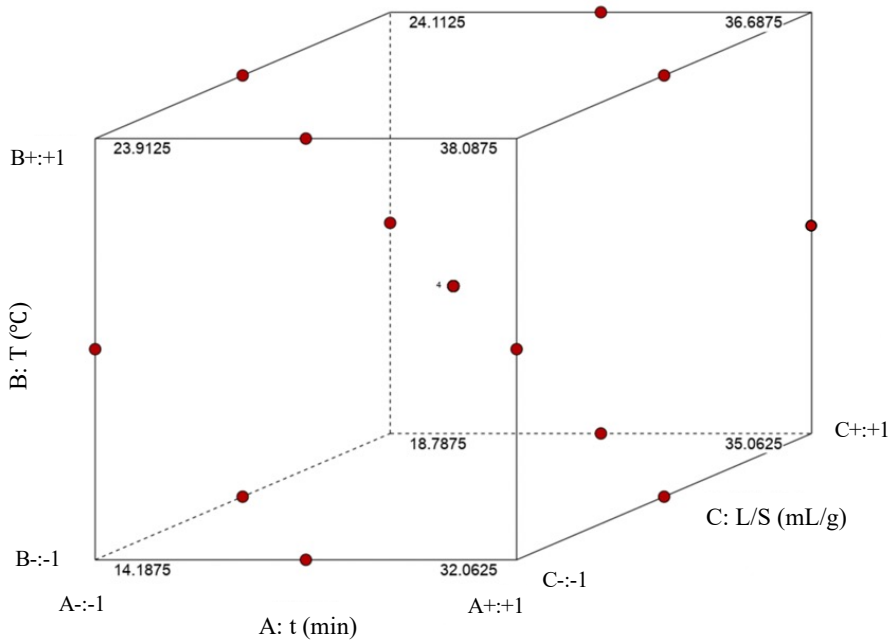

Figure 3. 1.The geometry of three factor Box-Behnken design

Experimental data were analyzed using Design-Expert software (State-Ease, InC., Minneapolis, MN, USA) with a second-order response surface regression model (Eqn. 3.5):

$$Sugar\ yield\ (\%) = b_0 + b_1A + b_2B + b_3C + b_{12}AB + b_{13}AC + b_{23}BC + b_{11}A^2 + b_{22}B^2 + b_{33}C^2 \qquad \text{(Eqn. 3.5)}$$

Where, A, B and C represented time, temperature and liquid to solid ratio, respectively. b_0 is a constant, b_1, b_2 and b_3 are the linear coefficients; b_{11}, b_{22} and b_{33} are the quartic coefficients; b_{12}, b_{13} and b_{23} are the interactive coefficient.

The significance of full or reduced regression was tested by analysis of variance (ANOVA). The significance of each coefficient and corresponding p values were determined by F-test. Optimized extraction conditions were determined based on the maximum sugar yield from almond hulls using a desirability function approach implemented in Design Expert software. Validation

was performed to evaluate the accuracy of the model. Sugars were extracted in triplicates using the optimum conditions determined above. The predicted sugar yield from the model was then compared with the experimental data.

3.4 Results and Discussion

Experimental design and results of sugar yield from almond hulls are summarized in Table 3.1. The collected experimental data were first analyzed in order to establish second-order equations including terms of interaction between the three experimental factors. Based on the statistical analysis, Eqn. 3.6 was obtained. The significance of the model coefficients along with other statistical parameter are shown in Table 3.2. The mathematical expression of relationship between reducing sugar yield from almond hulls with the coded factors A, B and C (time, temperature, and liquid solid ratio respectively) is presented in Eqn. 3.6:

$$Sugar\ yield = 35.2 + 7.61A + 2.84B + 0.8C - 0.925AB - 0.4AC - 1.1BC - 6.34A^2 - 0.2875B^2 - 0.7128BC^2 \quad \text{(Eqn. 3.6)}$$

Table 3. 1. Sugar extraction yield from Independence almond hulls from Box-Behnken design

Sample #	Run	True Level			Coded Level			Response
		Time (min)	T (℃)	L/S (mL/g)	Time (min)	T (℃)	L/S (mL/g)	Yield (%)
2	1	60	60	15	0	0	0	35.0
6	2	60	60	15	0	0	0	36.0
8	3	10	60	20	-1	0	1	21.3
4	4	110	80	15	1	1	0	38.2
11	5	110	40	15	1	-1	0	34.0
9	6	60	40	20	0	-1	1	33.8
15	7	110	60	10	1	0	-1	35.8
16	8	110	60	20	1	0	1	35.9
13	9	60	80	10	0	1	-1	36.8
14	10	60	80	20	0	1	1	36.9
10	11	60	60	15	0	0	0	34.6
12	12	10	60	10	-1	0	-1	19.6
1	13	60	60	15	0	0	0	35.2
7	14	60	40	10	0	-1	-1	29.3
5	15	10	80	15	-1	1	0	25.0
3	16	10	40	15	-1	-1	0	17.1

Table 3. 2. Analysis of variance of second-order models and corresponding F and P values for each obtained coefficient to express the extracted sugar yield from almond hulls.

Source	Sum of squares	Degrees of freedom	Mean square	F value	P value	
Model	705.05	9	78.34	198.96	< 0.0001	Significant
A (t)	463.6	1	463.6	1177.4	< 0.0001	
B (T)	64.41	1	64.41	163.58	< 0.0001	
C (L/S)	5.12	1	5.12	13	0.0113	
AB	3.42	1	3.42	8.69	0.0257	
AC	0.64	1	0.64	1.63	0.2495	
BC	4.84	1	4.84	12.29	0.0127	
A^2	160.66	1	160.66	408.01	< 0.0001	
B^2	0.3306	1	0.3306	0.8397	0.3948	
C^2	2.03	1	2.03	5.16	0.0636	
Residual	2.36	6	0.3937			
Lack of fit	1.32	3	0.4408	1.27	0.4241	Not significant
Pure error	1.04	3	0.3467			
Cor total	707.41	15				

The ANOVA (analysis of variance) test was performed to assess the significance of the full or reduced regression model. The results of the ANOVA test are presented in Table 3.2. The model F value, which was found to be 198.96, indicated that the model was highly significant. This high F value, coupled with a very low p value (< 0.0001), indicated that the selected variable ranges incorporated in the model were effective in accurately predicting the sugar yield. Furthermore, the lack of fit F value was 1.27, with a corresponding p value of 0.4241 (> 0.05). This implies that the lack of fit was not significant when compared to the pure error, confirming the adequacy of the model in accurately reflecting the experimental results.

Figure 3.2 depicts the correlation between the actual and predicted reducing sugar yield using the regression model. The data points closely cluster around the line representing the predicted values, indicating a strong fit of the model to the data. The coefficient of determination (R^2) was calculated to be 0.9675, meaning that 96.75% of the variation in the response (sugar yield) can be explained by the model. This high R^2 value indicates a high level of agreement between the predicted and actual values, further supporting the accuracy and reliability of the model. Additionally, the coefficient of variation was determined to be 1.99%, suggesting that the model is precise and reliable. A lower coefficient of variation indicates a lower degree of variability within the data, further affirming the model's accuracy and consistency.

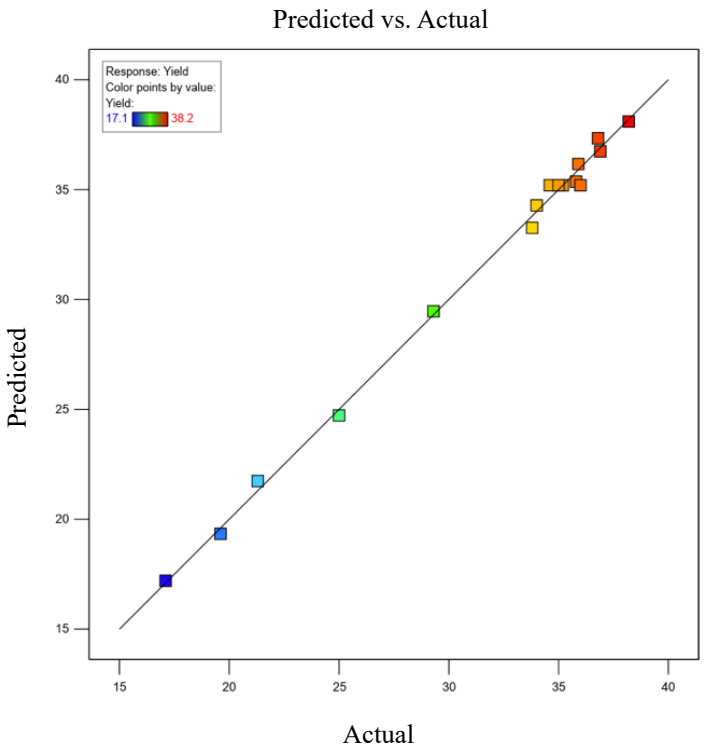

Figure 3. 2. Correlation between actual experimental values (sugar yield) and predicted values by the model. (R^2 = 0.9675)

Temperature and time demonstrated a high level of significance (p value < 0.0001) in their relationship with reducing sugar yield. On the other hand, the liquid-solid (L/S) ratio was found to have a significant effect on sugar yield, but to a lesser extent (p value = 0.0113). Only time exhibited a significant quadratic effect on sugar yield, while temperature and L/S ratio did not display any significant quadratic effects, as depicted in Figure 3.3.

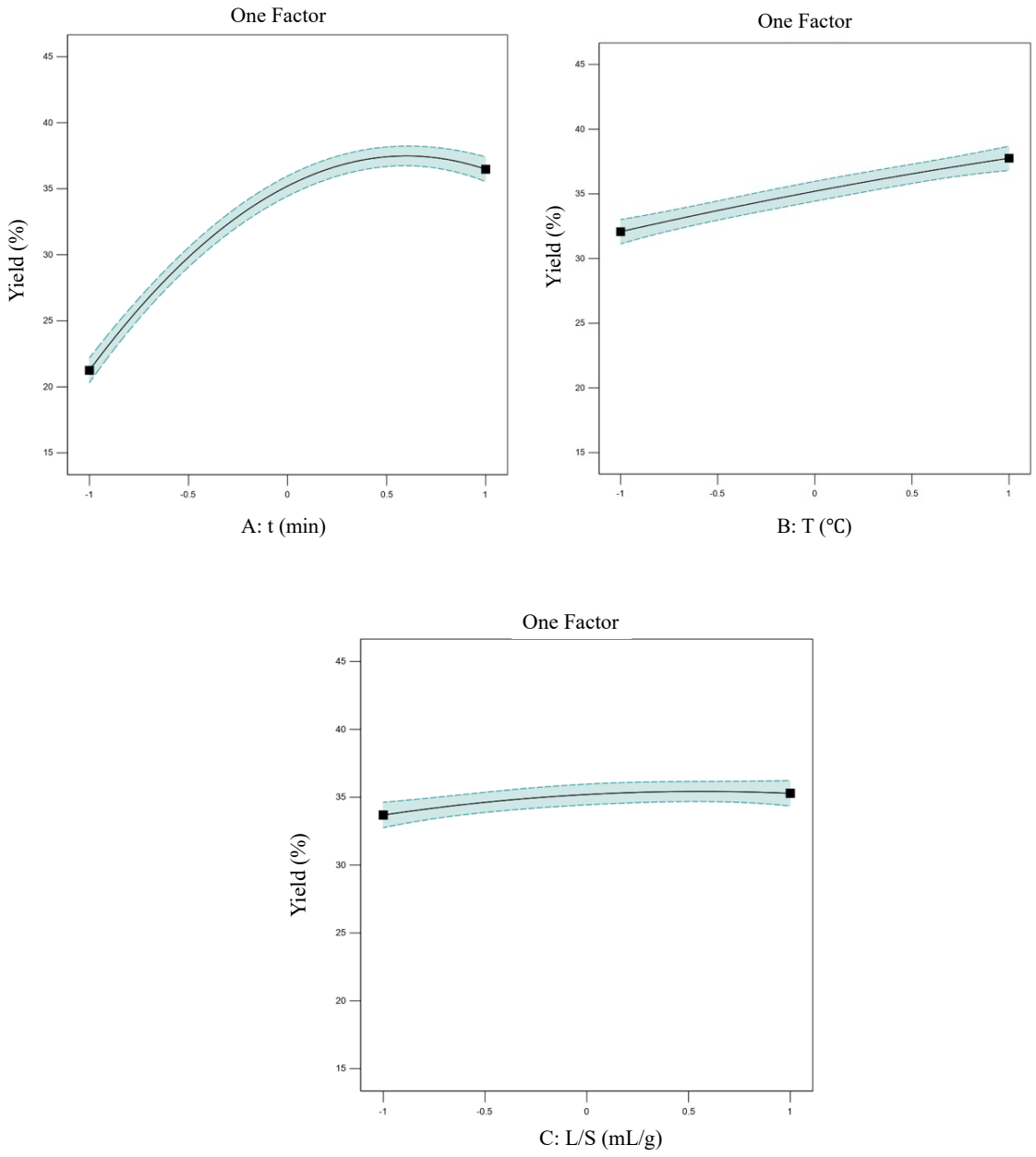

Figure 3. 3. Effects of individual variable on sugar yield. (A) Time; (B)Temperature; (C) L/S ratio. For each graph, the other two variables were fixed at the central value.

The significance of interactions between factors is evident in Table 3.2, except for the interaction between time and liquid-solid ratio (AC term). To visualize the pairwise interactions, three-dimensional (3-D) surface response plots were generated, as shown in Figure 3.4. Figure

3.4a shows the interaction between time and temperature. The total reducing sugar yield increased with extraction time, but beyond a certain level of L/S ratio, increasing the L/S ratio decreased the total reducing sugar yield. Additionally, increasing the temperature had a significant positive impact on the total reducing sugar yield. The combined effect of temperature and L/S ratio was found to be significant in reducing sugar yield. Figure 3.4b illustrates the combined effect of time and L/S ratio on reducing sugar yield. At a fixed extraction time, the sugar yield remained relatively constant at the studied L/S ratios. As mentioned earlier, the interaction between L/S ratio and time was not found to be significant (p value = 0.25).

Figure 3.4c shows the interaction between the L/S ratio and temperature at a fixed extraction time of 60 minutes. The graph shows that, due to the extraction time of 60 minutes, most of the data points indicated high total reducing sugar yields (represented by yellow to red colors). Consequently, there is a relatively slow increase in reducing sugar yield with an increase in L/S ratios. However, even though the increase is slow, it is still statistically significant (p value = 0.01). On the other hand, a more significantly increase in reducing sugar yield is observed when the temperature is raised. Overall, there is a significant interaction observed between the L/S ratio and temperature (p value = 0.01). This indicates that the combined effect of these two factors has a substantial impact on the resulting sugar yield from almond hulls.

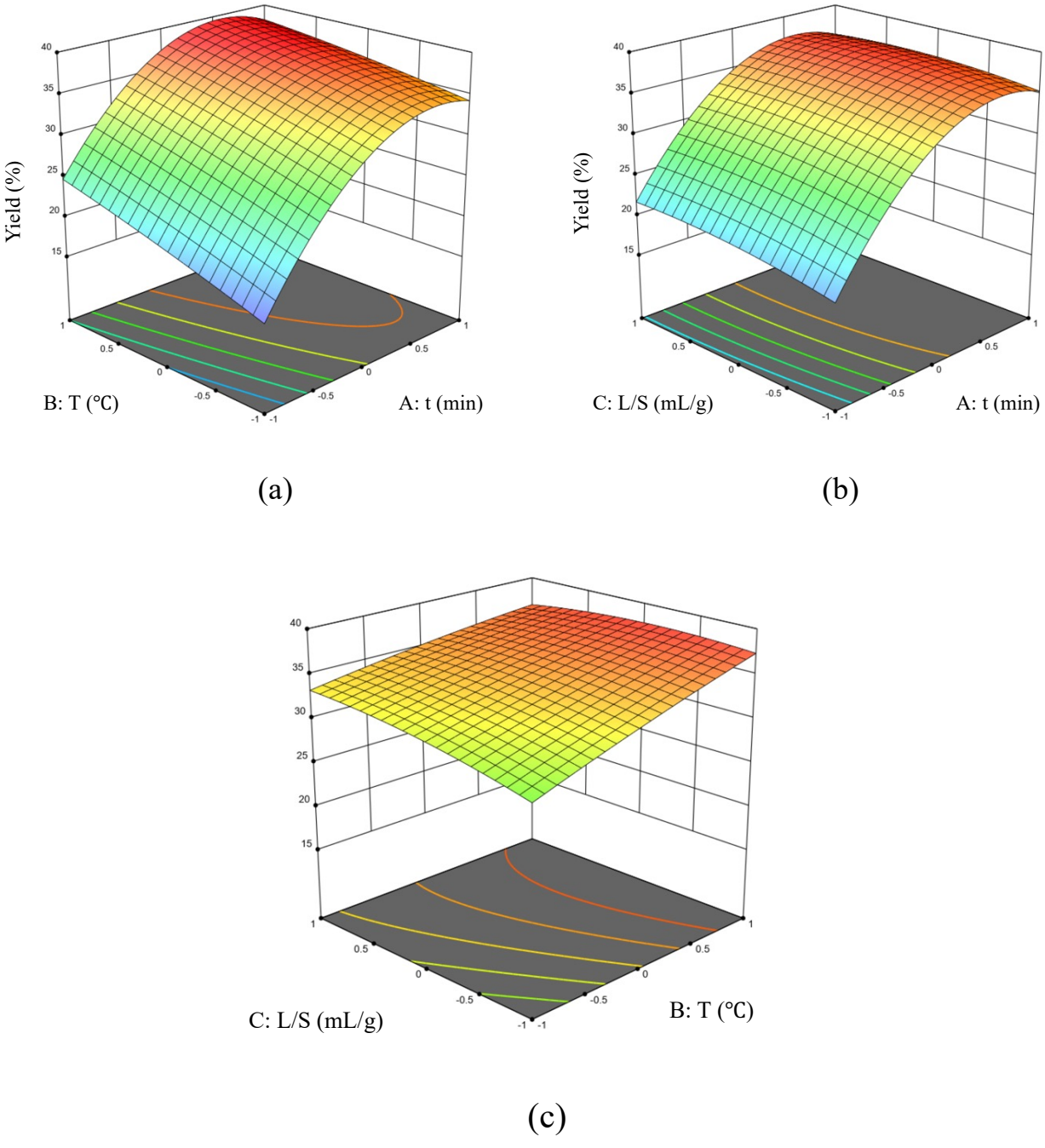

Figure 3. 4. 3-D response surface plots. (a) Effect of time and temperature on sugar yield at a L/S of 15; (b) Effect of L/S ratio and time on sugar yield at temperature of 60℃; (C) Effect of L/S ratio and temperature on sugar yield at time of 60 min. For each graph, the third variable was fixed at the central value.

The optimum combination of time, temperature, and liquid-solid (S/L) ratio for sugar extraction was determined using a desirability function approach implemented in Design Expert

software. The specific values for each variable were determined as follows: t = 86.6 min, T = 77.4℃, and L/S ratio = 14. Under these conditions, the predicted total reducing sugar yield was 39.3%.

To validate this prediction, experimental testing was conducted under the determined optimum conditions, resulting in a maximum reducing sugar production of 38.1%. This observed value is to the predicted response. These results confirmed the success of the optimization process for sugar extraction from almond hulls using response surface methodology.

3.5 Conclusions

Extraction time, temperature and L/S ratios had a significant effect on total reducing sugar yield. Among the three factors, only time exhibited a significant quadratic effect on sugar yield. The interactions between the factors were also investigated, with the exception of the interaction between time and L/S ratio, which was found to be not significant.

The resulting optimal extraction conditions were identified as an extraction time of 86.6 minutes, a temperature of 77.4°C, and a L/S ratio of 14. Under these optimized conditions, the experimental sugar yield was 38.1%, which closely matched the predicted sugar yield of 39.3%. This close agreement between the experimental and predicted yields demonstrated the effectiveness of the developed model to predict sugar yields at different extraction conditions.

Chapter 4 Production of *Aspergillus awamori* Pellets in Almond Hull Extract

4.1 Abstract

This study investigated *Aspergillus awamori*'s growth in pellet form under different conditions, including inoculum level, aeration, nitrogen source and carbon to nitrogen ratio (C/N ratio) in 250 mL glass bottles or flasks. Subsequently, the fungal cultivation was scaled up to a 2L bioreactor, where configurations which could favor pellet formation were tested. The structure and morphology of fungal pellets at various growth stages were observed and compared using an environmental scanning electron microscope. Results indicated that yeast extract and NH_4Cl worked better than peptone and $NaNO_3$, respectively. In order to reduce the cost of raw materials, a combination of yeast extract and NH_4Cl was chosen to adjust the initial C/N ratio. The highest concentration and yield of *A. awamori* biomass were observed when the fungus was cultivated at a C/N ratio of 15, compared to ratios of 30 and 45. At a C/N ratio of 15, the crude protein content in pellets was at its highest at 18.10% (d.b.), while the fat content was at its lowest, at 2.28% (d.b.). After scaling up from flask cultivation to bioreactor scale, the impacts of pH control and agitation on *A. awamori* growth were further investigated. Ultimately, the optimal conditions for *A. awamori* growth in almond hull extract were determined to be a C/N ratio of 15, an inoculum level of 10^3 spores/mL, without pH control, and an agitation rate of 150 rpm over a period of five days in a bioreactor with aeration at 1 vvm to control dissolved oxygen above 25%. Under these conditions, the biomass yield was around 0.85 g VSS/g sugar, with an average pellet size of 3.75 mm.

4.2 Introduction

Filamentous fungi play an important role in food and pharmaceutical industries and waste management. The growth performance of these complex organisms and their productivity are

highly related to multiple cultivation conditions and strains. The morphology of fungi is a key parameter in industry production, which could affect the biomass and fungal metabolic products production and could be affected by cultivation conditions. In submerged fermentation, three types of morphology can exist: big mycelium clump, pellets and free mycelium. In many cases, pellets are preferred due to the faster nutrients transfer, lower broth viscosity, better fluidity than free mycelium, and easiness of harvesting (Espinosa-Ortiz et al., 2016). The major factors which can influence fungal growth performance and pellet formation include inoculum amount, aeration rate, pH, nutrients concentration, mixing duration and rate, and temperature. Those factors have been studied on different strains for many years. Even the strains belong to the same species, individual strains can differ in their performance and responsiveness to different cultivation conditions. Therefore, designing and optimizing the cultivation conditions for the specific strain of *Aspergillus awamori* (*A. awamori*) has to be carefully considered.

Studying fungal growth and cultivation often starts in a small-scale setting, typically in laboratory flasks, before scaling up to bioreactors. Most of the growth parameters are studied in flasks to save time and cost, such as inoculum level, nutrients requirements and temperatures. The scale up process is not always straightforward and often requires additional optimization. The conditions that were optimized in flasks may not directly translate to the bioreactor due to different factors, such as aeration, agitation methods and configurations. Therefore, some conditions could be optimized in bioreactor scale, such as agitation. Due to the online pH monitoring of bioreactor, adjusting pH is more feasible in bioreactor than in flask.

The objectives of this study were to: (1) Determine the effects of cultivation parameters, including inoculum level, aeration, nitrogen source and carbon to nitrogen ratios, on fungal pellets

growth in flasks/glass bottles; (2) Find the suitable bioreactor configurations for fungal pellets formation; (3) Scale up, evaluate, and optimize the fungal growth in bioreactor.

4.3 Materials and Methods

4.3.1 Inoculum preparation

Freeze-dried fungal strain *Aspergillus awamori* (ATCC 22342) packed in an ampoule was obtained from the American Type Culture Collection (ATCC). The freeze-dried fungi were activated by applying 1 mL sterile deionized water (DI water) into the ampoule and stirring to hydrate and suspend the fungi. The suspension was then transferred to a sterile 15 mL falcon tube containing 5 mL sterile DI water. The falcon tube was let to sit at room temperature (around 25℃) undisturbed for three hours to allow rehydrating and stabilizing. Afterward, 100 µL suspension was added to a petri dish containing potato dextrose agar (PDA) and spread evenly by a sterile inoculum spreader. Several plates were prepared and incubated at 30℃ for four days and then stored in a refrigerator at 4℃.

In preparation for inoculation, spores were transferred to a new PDA plate and incubated at 30 ℃ for four days. After four days, spores were suspended in sterile DI water. The spore concentration of the resulting solution was then determined using a hemocytometer counting chamber with appropriate dilution. The fresh spore solution was used immediately as inoculum for the fungal cultivation. The volume of spore solution added to cultivation media in flask, glass bottle or bioreactor was calculated using Eqn. 4.1:

$$V_1 = \frac{C_2 \times V_2}{C_1} \qquad \text{(Eqn. 4.1)}$$

Where V_1 is the volume of spore solution needed (mL); C_1 is the spores concentration of spore solution (spores/mL); C_2 is the desired spores concentration to start fungal cultivation (spores/mL); and V_2 is the working volume of the flask or bioreactor (mL).

PDA (ATCC medium 336) plates were prepared by adding 24 g potato dextrose broth powder (Difco^{TM}) and 15 g agar into 1 L DI water. The media was sterilized by autoclaving at 121℃ for 30 min. After autoclaving, the media was cooled to 40-45℃ and then 20 mL of the media was poured into each petri dish for solidification. The prepared petri dishes were sealed by parafilm and stored at cool temperature for the future experiments.

4.3.2 Effect of inoculum level and aeration on fungal growth

Due to filamentous fungal morphology and growth could be affected by cultivation conditions. Aeration and inoculum levels were studied for their influences on pellet size and biomass production. Two-factor factorial experiments were conducted: two levels of aeration: with and without forced aeration and four levels of inoculated spores concentration (spores/mL): 10^3, 10^4, 10^5 and 2×10^3. All experiments were conducted in 250 mL glass bottles with 150 mL working volume. Two holes were pre-punched on each cap. For the experiments with forced aeration, one hole was connected to the 0.22 μm syringe filter and connected to an air pump and the other one is for venting. The gas flow rate was controlled at 0.67 vvm (air volume per working volume per minute) by gas flow meters. For the experiments without forced aeration, one hole was connected to a 0.22 μm syringe filter (MilliporeSigma), the other hole was to allow air exchange. The bottles were shaken in a shaker (Benchmark Scientific Incu-Shaker 10L) to help circulate the air through the hole and provide oxygen to the fungi in the bottles. As fixed conditions, sterile potato dextrose broth (ATCC medium 336) with initial pH 5 was applied for all experiments. All the glass bottles

were incubated at 30℃ and shaken at 200 rpm for three days. The experimental set-up is shown in Figure 4.1. All experiments were carried out in duplicate.

The fungal biomass was quantified as volatile suspended solid (VSS) that was analyzed according to the standard methods (APAH et al., 2017). Twenty pellets were randomly selected, and their diameters were measured by caliper.

Figure 4. 1. Experimental set-up with/without forced aeration

4.3.3 Nitrogen source

Different nitrogen sources on *A. awamori* growth were compared. The two inorganic nitrogen sources: $NaNO_3$ and NH_4Cl, and two organic nitrogen sources: yeast extract and peptone were compared. Sugars and all the other nutrients were added according to the Czapek's media (ATCC medium 312). The amount of nitrogen source was added to control carbon to nitrogen ratio

(C/N ratio) at 30. The mass-based nitrogen content in $NaNO_3$ and NH_4Cl was calculated to be 16.5% and 26.2%, respectively. The nitrogen content in yeast extract (Spectrum Chemical Mgf) and peptone (Fisher Bioreagents) were measured by Hach kits. No nitrogen was added in the control group. The detailed compositions of the media were listed in Table 4.1, which is modified from Czapek's media.

Table 4. 1. Medium composition used in the nitrogen source selection experiments

Nutrient	Glucose	K_2HPO_4	$MgSO_4 \cdot 7H_2O$	KCl	$FeSO_4 \cdot 7H_2O$	Nitrogen
Concentration (g/L)	20	1.0	0.5	0.5	0.01	0.267

All experiments were conducted in 250 mL flasks (Pyrex narrow mouth Erlenmeyer flask) with 100 mL working volume and shaken at 200 rpm (Drawell DW-SI-211B). Plastic foam stoppers (Jaece Industries Indenti-plug™) were capped on each flask to prevent contamination and support air exchange. 10^3 spores/mL spores were inoculated into each flask. After six days of cultivation, biomass (VSS) was harvested and measured. The remaining sugar (glucose) concentrations in the media were analyzed with high-performance liquid chromatography (HPLC). Biomass yield based on the consumed sugar was calculated with Eqn. 4.2:

$$\text{Biomass yield \% (gVSS/g sugar)} = \frac{M}{V*(C_0 - C_f)} \times 100\% \qquad \text{(Eqn. 4.2)}$$

Where M is the total biomass (VSS) measured after cultivation, g; V is the working volume, L; C_0 is the initial glucose concentration, g/L; C_f is the measured final glucose concentration, g/L.

4.3.4 Effect of C/N ratio

The effect of different C/N ratios of 15, 30 and 45 on fungal growth perfomace in almond hull extratct was studied. The almond hull extract was prepared following the optimum sugar extraction conditions found in Chapter 3, which was the extraction time of 86.6 minutes, temperature of 77.4°C, and a liquid to solid ratio of 14. All the total suspended solids (TSS) in the extract was removed by vacuum filtration with standard Whatman filter paper. Ten milliliter of the clear nutrients was sampled for sugar, total organic carbon (TOC) and total nitrogen (TN) analysis. The rest of the extract were refrigerated at 4℃ before use. Total sugars were analyzed by HPLC. Total TOC and TN in both almond hull extract and yeast extract powder were analyzed by using Hach test kits. Total sugar concentration in the extract were diluted to 20 g/L with DI water. For the control, no extra nitrogen sources were added. Yeast extarct was added 1 g/L to all the other treatments. NH_4Cl was amended to adjust the initial C/N ratios to target values. The C/N ratio was defined as (Eqn. 4.3):

$$\text{C/N ratio} = \frac{TOC_{almond\ hull\ extract} + TOC_{yeast\ extract}}{TN_{almond\ hull\ extract} + TN_{yeast\ extract} + TN_{NH_4Cl}} \quad \text{(Eqn. 4.3)}$$

Based on Eqn. 4.3, the amount of NH_4Cl was calculated and added to each treatment. The initial pH of each media was adjusted to 5.0 with sodium hydroxide. The biomass concentraion, yield, sugar consumption and pellet size were analyzed after cultivation. The composition of biomass, including crude protein, fat, fiber and trace elements were analyzed and compared. The characteristics of fungal morphology change, including surface and cross section were observed by scanning electron microscope imaging.

4.3.5 Scale up fungal pellets cultivation in bioreactor

4.3.5.1 Pellets formation testing in bioreactor

The Eppendorf Bioflo® 120 with a 2 L borosilicate glass vessel was used to scale up fungal pellets production. Methods for the bioreactor scale experiments are similar to the previous experiments in shaken flasks. Each batch was monitored by BioCommand® Batch Control software connected to a control station. The bioreactor system is shown in Figure 4.2, and the detailed configurations are listed in Table 4.2. Temperature was monitored and controlled at 30℃ by a heating blanket covered outside the vessel and a recirculating chiller connecting a stainless-steel circular tubing inside the vessel. Compressed air was connected to an air regulator with prefilter to control the pressure around 10 pounds per square gauge (psig) before connected to the control station. A ring sparger immerged at the bottom of the vessel was used for aeration. pH and dissolved oxygen (DO) probes were immerged in the media during cultivation. DO and pH values were monitored and recorded automatically by BioCommand® Batch Control software. Agitation was accomplished by a direct drive motor with 2 Rushton-type impellers.

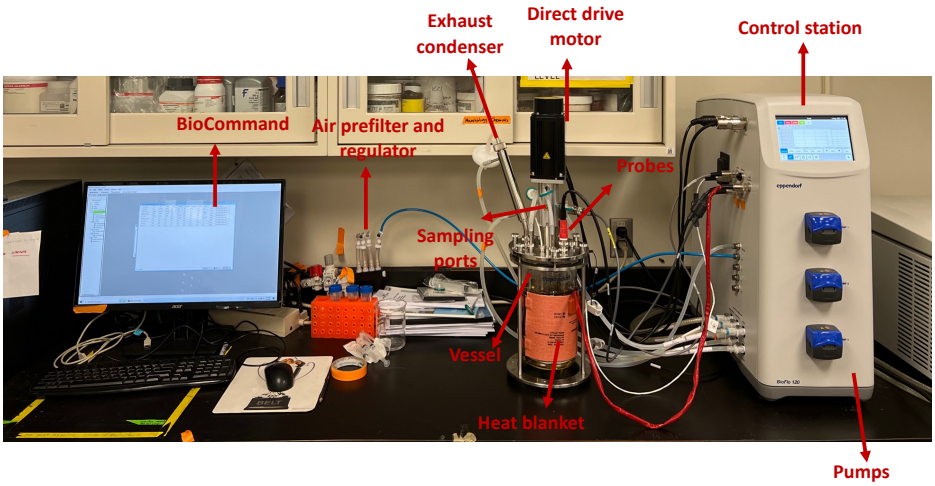

Figure 4. 2. Components of Bioflo® 120 system used in this research

Table 4. 2. Configurations of Bioflo® 120 hardware

Parameter	Configuration
Vessel	
Total volume	3L
Working volume	0.8-2.2 L
Size	Outer diameter: 20.3 cm; height: 54 cm
Material	Autoclavable borosilicate glass with baffle assembly (316 L stainless steel)
Temperature control	
Heating	Heat blanket
Cooling	Recirculating chiller, type WK 600 with closed cooling circuit
Impellers	
Direct drive	2 Rushton-type impellers
Gas supply	
Sparge	Ring sparger
Source	Compressed air prefiltered and regulated by air regulator kit to 10 psig
Sensors	
pH	Mettler Toledo® 405-DPAS-SC-K8S, gel filled, 225 mm
DO	Mettler Toledo® InPro® 6830, angled T-82, 220 mm,
Control station	
Agitation	25-1,200 rpm
Temperature	0 - 70℃
Gas flow	0 – 20 standard liters per minute (SLPM) flow range
Software	
BioCommand® Batch Control	BioCommand Revision 4.01.0006 Version

Because the configuration of bioreactor is very different from flask and fungal pellet formation is sensitive to the hydrodynamic conditions in a bioreactor, fungal cultivation was tested first in the bioreactor with default configurations as manufactured. In this testing experiment, 10^3 spores/mL was inoculated in the potato dextrose broth (PDB) media with 1 vvm aeration rate and 150 rpm agitation for two days. Fungal morphology was observed after two days.

4.3.5.2 Effect of pH control on fungal growth

The *A. awamori*'s growth, with or without pH control, was compared in the 2 L bioreactor. Spores were inoculated into 2 L almond hull extract media (initial C/N ratio of 15) at the level of

10^3 spores/mL. Agitation speed was initially set at 250 rpm for the first day, then it was reduced to 150 rpm for the subsequent cultivation period. The experiment was conducted at a controlled temperature of 30℃, starting with an initial pH of 5. In the case of the pH-controlled study, NaOH was filtered and then manually introduced into the bioreactor through a dedicated port on the reactor plate twice per day. The pH adjustments were guided by real-time online pH monitoring. During the fungal cultivation, 10 mL well mixed samples were collected every day to determine the biomass and sugar concentration.

4.3.5.3 Effect of different agitation speeds on fungal performance

The *A. awamori*'s growth in almond hull extract under different agitation speed were studied. Three agitation speeds were tested, including 50, 150 and 250 rpm, with initial pH values of 5. The biomass growth and sugar consumption overtime were analyzed. The pellets size and fungal morphology were measured.

4.3.6 Analytical method

4.3.6.1 Fungal biomass measurement

Fungal biomass (VSS) cultivated in flasks was measured by pouring out all the fungal biomass and filtered through standard Whatman filter paper by vacuum filtration. Fungal biomass grew in bioreactor was monitored daily by collecting 10 mL well-mixed samples from the bioreactor and filtered by vacuum. TSS was analyzed by loss after drying at 105℃ to a constant weight, and VSS was obtained after calcination at 550℃ following the standard methods (APHA et al., 2017). As for the measurement of fungal biomass composition, the harvested wet pellets were dried by freeze drying and analyzed for their composition by UC Davis Analytical Lab following the standard methods listed in Table 4.3.

Table 4. 3. Standard methods for compositional analysis

Compound	Standard method
Protein	AOAC 990.03
Crude fat	AOAC 2003.05
Crude fiber	AOAC 978.10
Ash	AOAC 942.05
Ca, Fe, Zn, Mg, Mn	Meyer, 1992; Sah & Miller, 1992

4.3.6.2 Nutrients characterization

Individual sugars including glucose, fructose, sucrose and xylose were analyzed with Shimadzu HPLC equipped with a Biorad Aminex HP-87P column and a refractive index detector (RID). Milli Q water was used as the mobile phase with a flow rate of 0.5 mL/min. The oven temperature was controlled at 80 ℃ (Z. Wang et al., 2010). Total sugar concentration was calculated by summing up the concentrations of glucose, fructose, sucrose and xylose. TN concentration was measured spectrophotometrically (Hach, DR3900) by using Hach Test 'N Tube^{TM} (High Range) according to Hach Method 10072. Hach method 10128 was applied to analyze the TOC concentration. Citric acid was analyzed by Shimadzu HPLC with CBM-20A controller and SPD-20A photo diode array (PDA) detector. A Biorad Aminex HP-87H column operated with the mobile phase containing 0.045N H_2SO_4 and 6% acetonitrile (v/v) was used for the measurement. The flow rate was controlled at 0.3 mL/min and the oven temperature was kept at 55℃ (Kelebek et al., 2009). All the liquid samples analyzed by HPLC or Hach kits were filtered through 0.22 μm filters and diluted before analysis.

4.3.6.3 Scanning electron microscope imaging

The micro-scale structure and morphology of the cross section and surface of fungal pellets were imaged by Quattro S Environmental scanning electron microscope (ESEM, Thermo Fisher Scientific, United States) equipped with a Schottky FEG. Direct observation of non-conductive and hydrated samples without coating and drying was accomplished under low vacuum mode with a low vacuum detector (LVD). Pellets were randomly chosen after cultivation and kept hydrated in media before imaging. The pellets were cut gently and carefully by using a blade before imaging the cross section of the pellets.

4.3.7 Statistical analysis

All experiments were conducted with duplicates, and the mean value and standard deviation of each assay were calculated for the duplicates. All data were organized, processed and subjected to statistical analysis using Microsoft Excel (Redmond, WA) and GraphPad Prism software (San Diego, CA). The difference between treatments were statistically analyzed by using Analysis of Variance (ANOVA) and Tukey's range test, with a significance level set at 5%.

4.4 Results and discussion

4.4.1 Effect of inoculum level and aeration on fungal growth

Figures 4.3 and 4.4 show the effect of inoculum level and aeration on fungal growth. As can be seen that pellet size reduced, and biomass increased when inoculum levels increased. The effect of aeration on pellet size was more significantly different at higher inoculum levels. At the inoculum level of 10^3 spore/ml, forced aeration and non-aeration had no significant difference on pellet size (p value = 0.61), which were around 2.5 mm.

However, aeration had a greater positive effect on the biomass production than inoculum levels (Figure 4.5). Similar to inoculum levels, aeration led to smaller pellets which had larger specific aera allowing for more nutrients and gas transferred to the pellets. The reason for causing smaller pellets of aeration was due to the additional mixing introduced by aeration (Kelly et al., 2006), which accelerated the nutrients and gas mixing and maintained a more uniform distribution of nutrients and oxygen within the bottles, and could finally accelerate the biomass growth. As shown in Figure 4.4, at an inoculum level of 10^3 spores/mL with aeration, the biomass production was higher than at 10^4, 10^5, and similar to 2×10^5 spores/mL without aeration.

In terms of the color of the cultured pellets, white pellets were formed at inoculum levels of 10^3 and 10^4 spores/mL with forced aeration. Without forced aeration, yellow pellets were observed at the same inoculum levels (Figure 4.3). The yellow pigment, known as asperyellone (J. Yu et al., 1967), is a secondary metabolite typically produced for survival and adaptation to environmental conditions. In this experiment, the restricted aeration or the limited nutrients due to the higher biomass concentration might have triggered the secretion of this pigment. When it came to higher inoculum levels, a grey color was observed under both conditions, with and without aeration, which could be attributed to the sporulation of the pellets.

In order to obtain white pellets and avoid too small pellets (hard to mix and harvest) and too large pellets (not efficient), cultivating fungal pellets at the level of 10^3 or 10^4 spores/mL at proper mixing level is recommended.

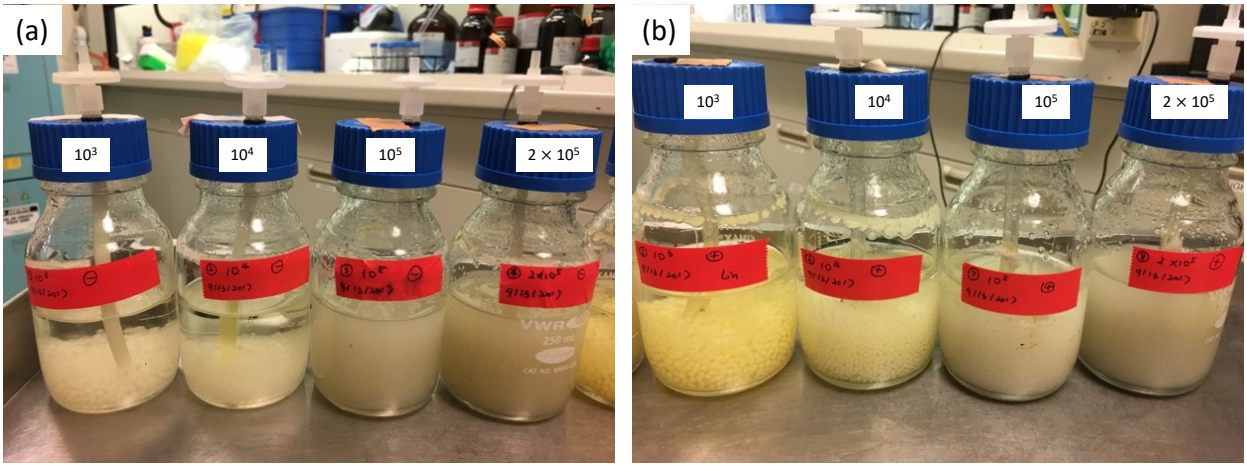

Figure 4. 3. Fungal pellets cultivated at different inoculum levels (shown by values marked on bottles) and aerations: (a) without forced aeration; and (b) with forced aeration

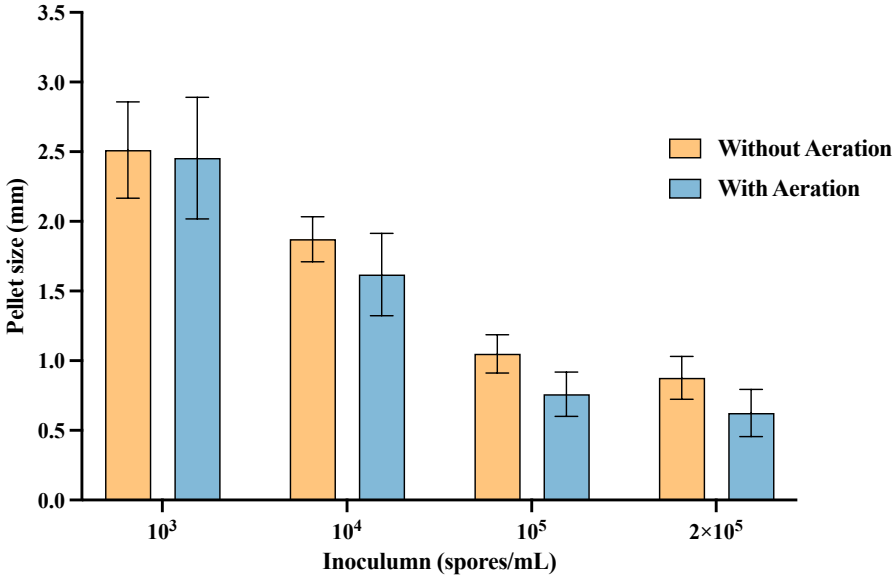

Figure 4. 4. Effects of inoculum level and aeration on fungal pellet size.

Y error bars are standard deviation.

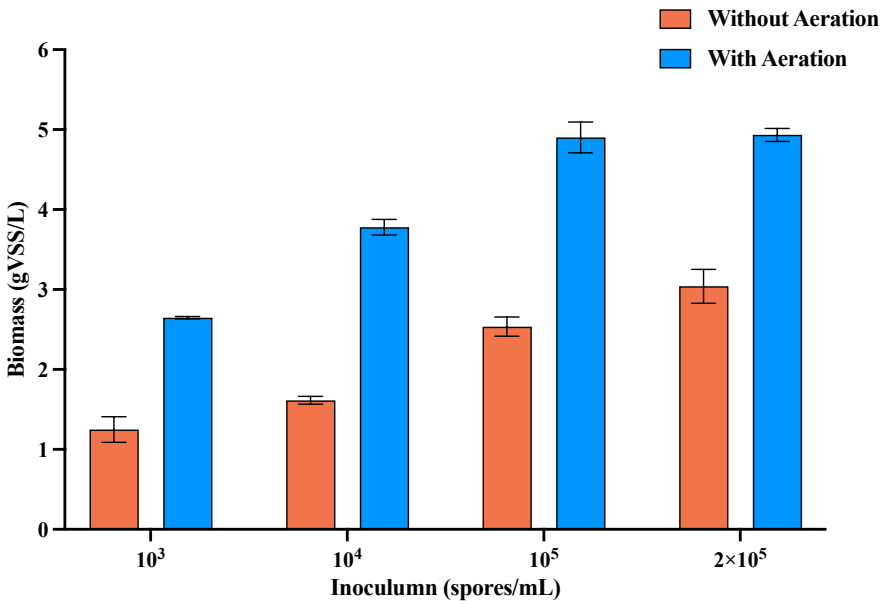

Figure 4. 5. Effects of inoculum level and aeration on biomass.

Y error bars are standard deviation.

4.4.2 Effect of nitrogen sources

The nitrogen content in yeast extract and peptone used were 5.0% and 13.4%, respectively. The detailed information of nitrogen sources used are listed in Table 4.4. The addition of different nitrogen sources to the growth medium was determined to control the nitrogen content of the media at 0.267 g/L.

Table 4. 4. Nitrogen sources used

Nitrogen source	Nitrogen content (%)	Addition to medium (g/L)
$NaNO_3$	16.5	1.62
NH_4Cl	26.2	1.02
Yeast extract	5.0	5.34
Peptone	13.4	1.99

As shown in Figure 4.6, no fungal pellets were formed without nitrogen source, the biomass concentration was only 0.203 g/L. Even though there were a lot of pellets formed in the flasks when fed with inorganic nitrogen sources, those pellets were ununiform, small, fluffy, loose and had black center. The biomass concentration cultivated in $NaNO_3$ and NH_4Cl were 0.445 g/L and 0.744 g/L, respectively. The differences were significantly (p value = 0.002) (Figure 4.7). More uniform and smooth pellets were formed when yeast extract and peptone were used as nitrogen sources, with final biomass concentration at 4.153 g/L and 3.3715 g/L respectively. In terms of biomass yield (Figure 4.8), NH_4Cl led to much higher biomass yield than $NaNO_4$. Similarly, yeast extract had higher biomass yield than peptone. Highest biomass yield was 27.14% when cultivated in yeast extract. In general, *A. awamori* grew better in organic nitrogen sources than in inorganic nitrogen sources. This probably due to the fact that both yeast extract and peptone contain amino acid, peptides, vitamins and essential elements. The difference is yeast extract is derived from the autolysis of baker's yeast cells, while peptone is derived from animal tissues by enzymatical hydrolysis. Yeast extract had lower protein content (31.3%) than yeast extract (83.8%), which means more vitamins and essential elements were added in the group of yeast extract and favored the fungal growth. From this study, organic nitrogen and growth factors are important for fungal growth. The price of yeast extract is higher than NH_4Cl, while the nitrogen content in yeast extract is lower than in NH_4Cl. In order to lower the production cost, a combination of NH_4Cl and yeast extract is recommended for fungal cultivation.

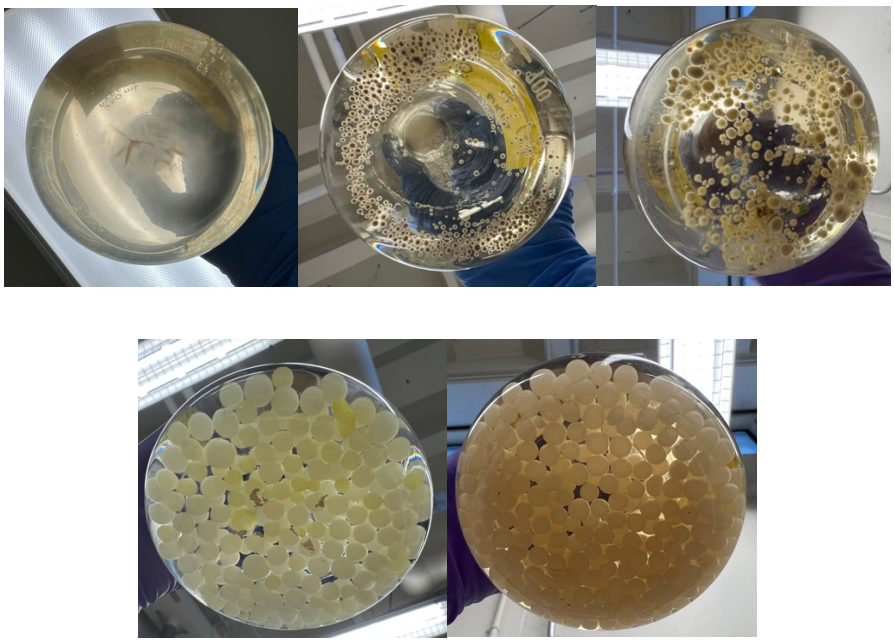

Figure 4. 6. Effect of nitrogen sources on fungal growth

(Order: Control, $NaNO_3$, NH_4Cl, peptone, yeast extract)

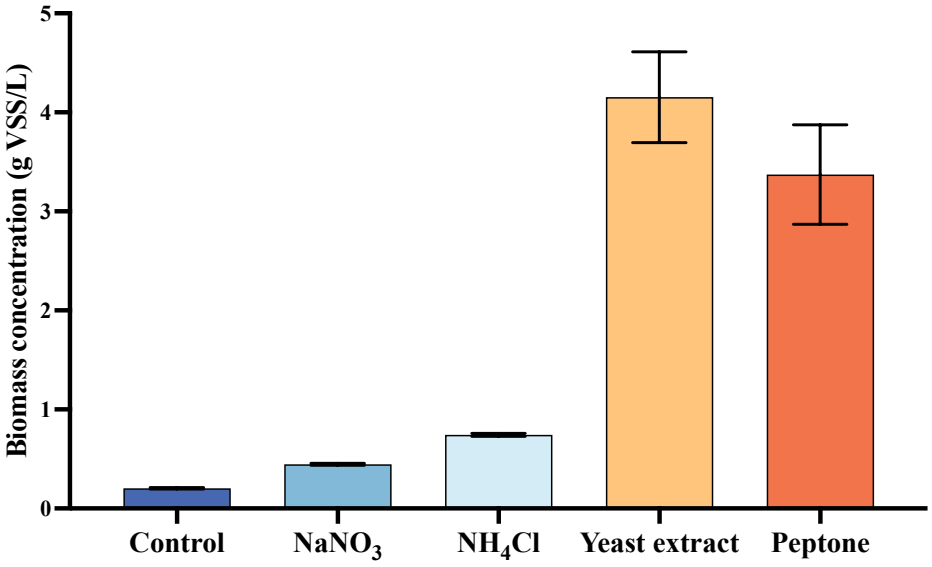

Figure 4. 7. Fungal biomass concentration obtained from different nitrogen sources.

Y error bars are standard deviation.

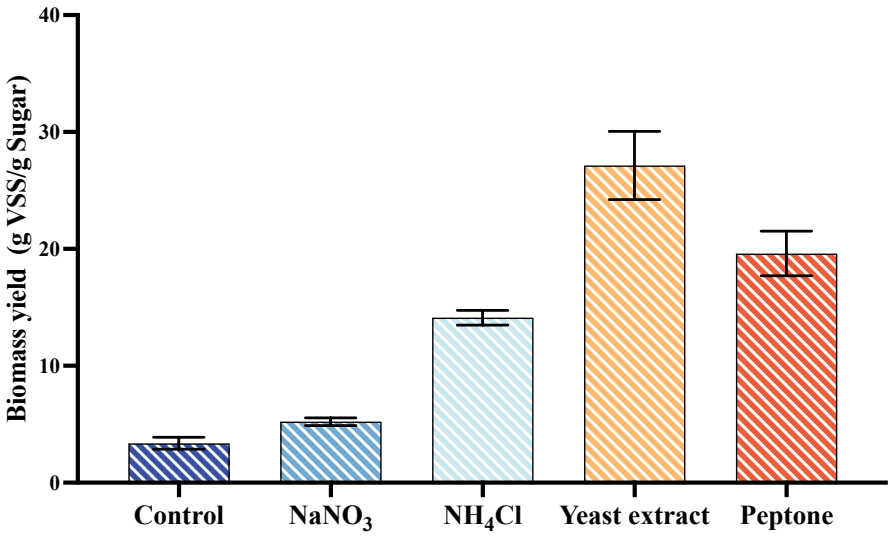

Figure 4. 8. Fungal biomass yield cultivated from different nitrogen sources.

Y error bars are standard deviation.

4.4.3 Effect of C/N ratio

TN and TOC contents in yeast extract were 5% and 24%, respectively. After adjusting the total sugar concentration in almond hull extract to 20 g/L, the measured TOC and TN concentrations in adjusted almond hull extract are 12.71 g/L and 0.083 g/L, respectively. Therefore, the C/N ratio in control (without extra nitrogen source) was 152. The detailed nutrients in all the other treatments are listed in Table 4.5.

Table 4. 5. Nutrients compositions of the media used

Carbon and nitrogen sources	Carbon source in media (gC/L)	Nitrogen source in media (gN/L)
Almond hull extract	12.71	0.083
Yeast extract	0.24	0.05
NH_4Cl	0	0.73 (C/N=15)
		0.30 (C/N=30)
		0.16 (C/N=45)

The fungal biomass (VSS) concentration (Figure 4.9) and yield (Figure 4.10) were measured and compared at different ratios. Highest biomass concentration (12.29 g/L) and yield (0.87 gVSS/g sugar) after 6 days cultivation was obtained with a C/N = 15. There was no significant difference (p value = 0.43) in the biomass concentration obtained at C/N of 30 and 45. It was reported by Cui et al. (1998) that the *A. awamori* biomass yield based on glucose or sucrose consumption was 0.78 g/g. The higher biomass yield found from this research could be due to the presence of other organic compounds which were able to be utilized by *A. awamori* in almond hull extracts. The total organic carbon concentration from 20 g/L sugars should be around 8 g/L, while the total organic carbon concentration in the initial media was 12.71 g/L. This means that there were 4.71 g/L more organic carbon from other organic compounds which could be utilized by fungi, such as organic acid, and phenolic compounds. The reason for not measuring the total organic carbon after fungal cultivation is there were some organic metabolites produced by A. *awamori.* It's hard to analyze the total organic carbon consumed by *A.awamori*. Sugar consumption is still a good reference, because sugars, especially glucose and sucrose are preferential substrates for most of the fungi.

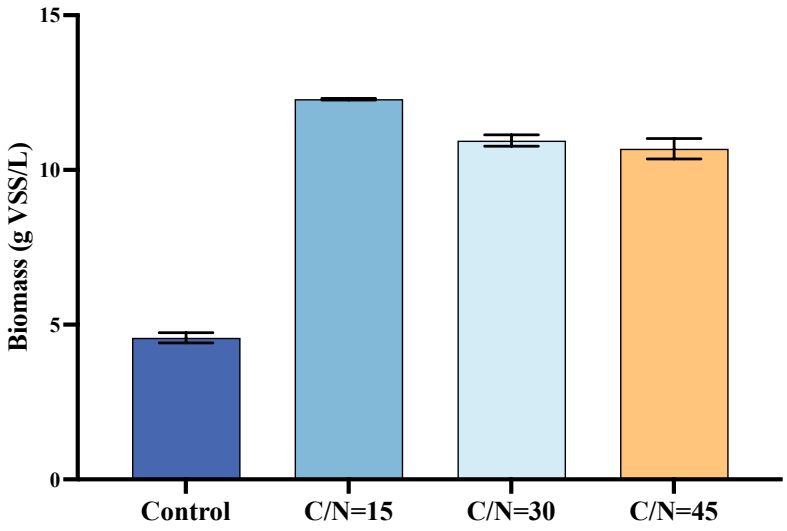

Figure 4. 9. Fungal biomass concentration obtained from different C/N ratios.

Y error bars are standard deviation.

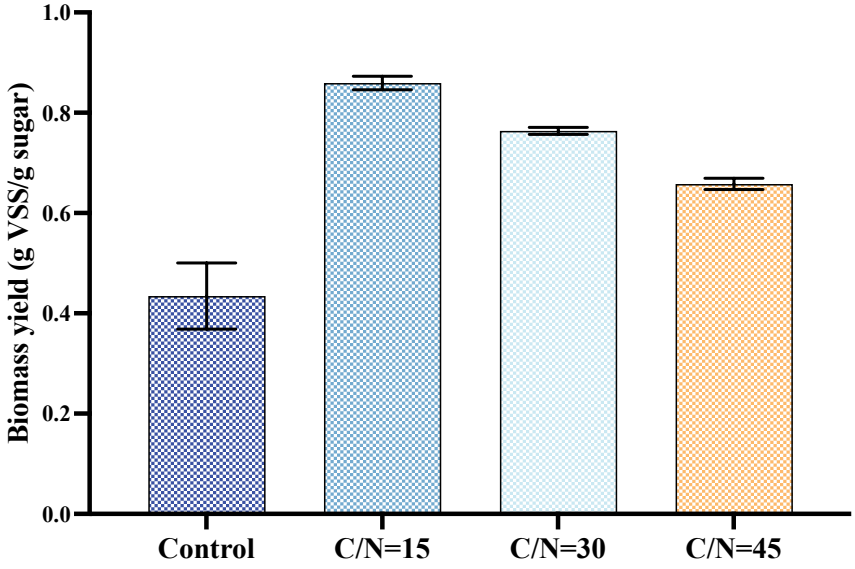

Figure 4. 10. Fungal biomass yield cultivated from different C/N ratios.

Y error bars are standard deviation.

Pellet formation in almond hull extract under controlled conditions is an important characteristic, which could influence the nutrients uptake, fungal growth and potential applications

of these pellets. As shown in Figure 4.11, *A. awamori* exhibited a similar average pellets size after six days cultivation in all treatments with extra nitrogen addition, which were around 6 mm. Smaller pellet size (3.13 mm) were formed in the control group. The average number of pellets in the control was around 6 pellets/mL. Less pellets were formed in all other three groups, which were 2 pellets/mL. All the total number of pellets were relatively stable during the fungal growth, indicating that there was no new pellets were formed in this flask cultivation conditions. Comparing the results of formed biomass concentration, pellets size and number of pellets indicating that more condensed pellets were formed in all nitrogen addition groups, especially in C/N=15 treatment.

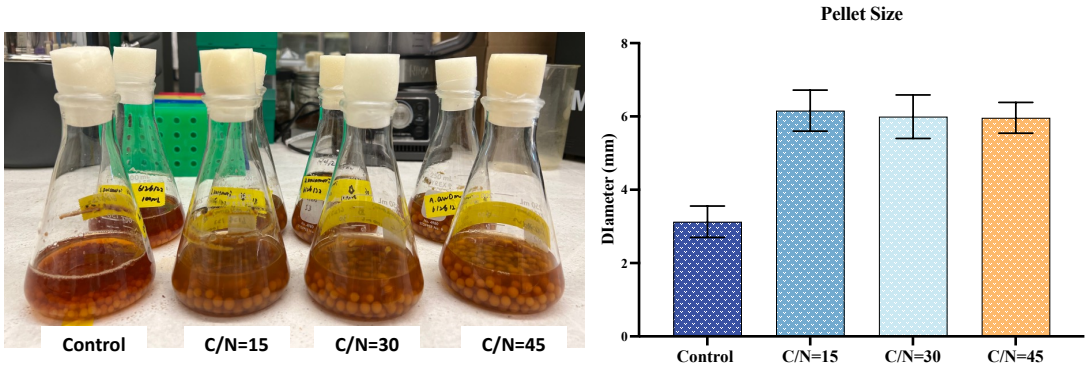

Figure 4. 11. Pellets growth at different carbon to nitrogen ratios. Y error bars are standard deviation.

Biomass growth curve, total and individual sugar consumption of fungal growth, and fungal pellets' size at C/N=15 are shown in Figure 4.12-4.14. Maximum fungal biomass was obtained at six days by utilizing glucose, sucrose and fructose in the media. The biomass concentration decreased after six days, even there were still 6.68 g/L sugars in the media. This decrease was due to the autolysis in the center of fungal pellets after the size getting larger while nutrients concentration in the media getting lower. This could also be the reason why the gross specific growth rate of fungal biomass was decreasing within six days. As shown in Figure 4.15,

the structure of a single large pellet is not homogeneous. The center of the pellets is the non-grown zone with limited nutrients mass transfer in the pellets. The outside shell is the growing zone, where nutrients are transferred into and utilized by fungi.

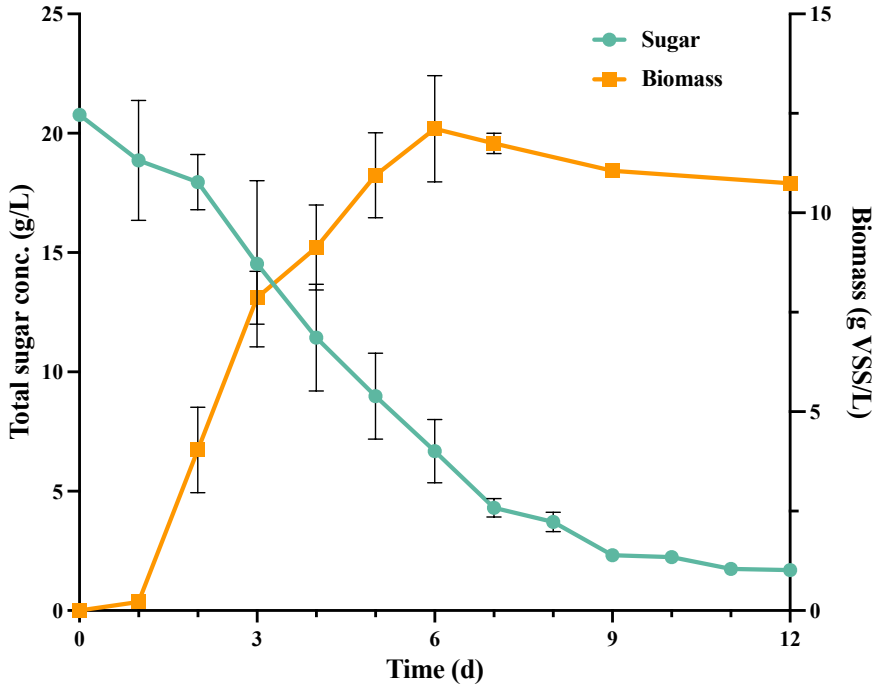

Figure 4. 12. Fungal biomass and total sugar changes during fungal cultivation at C/N ratio of 15. Y error bars are standard deviation.

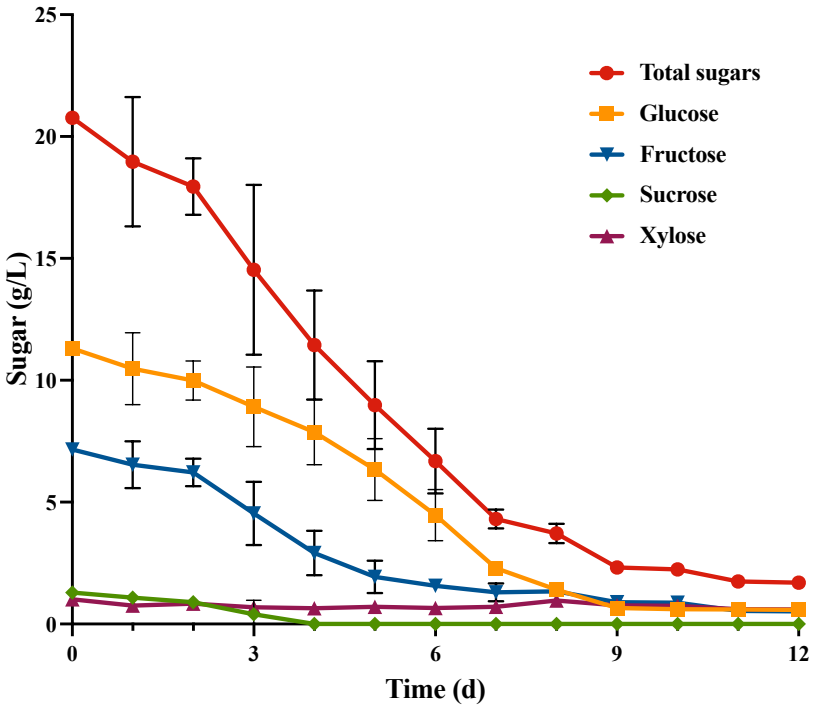

Figure 4. 13. Individual sugar changes during fungal cultivation at C/N ratio of 15. Y error bars are standard deviation.

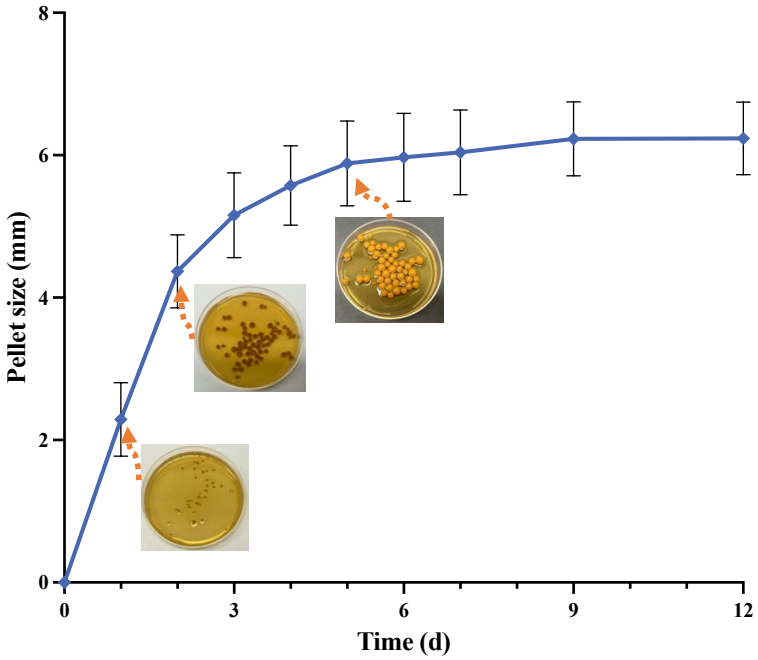

Figure 4. 14. The increase of fungal pellet size during fungal growth at C/N ratio of 15.

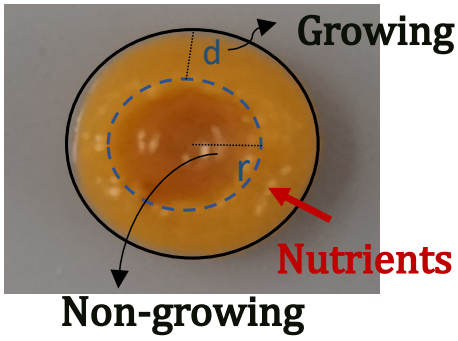

Figure 4. 15. Inhomogeneous structure of a single pellet.

The micro-scale structure of the mycelium inside (Figure 4.16) and outside (Figure 4.17) the pellets during different growth phase are observed and imaged by ESEM. A dense core with little internal structure or 'unsplit" hyphae and little bit cell debris were observed in the 2-day pellet. As growth proceeds, the interior of the pellet became even less dense, with clear void spaces appearing between the hyphae. The center became less dense due to the outwards growth of hyphae and also the autolysis of hyphae in the center (Cairns et al., 2019). More debris and fragments were observed in 5-day pellet. In the later growth phase, more fungal mycelium was degraded due to the nutrient limitations. During this process, the intracellular contents and debris from the degraded mycelium could be flushed out of the pellets leading to the formation of a 'bowel shape' inside the pellets (Figure 4.16e). At the same time, very thin thread-like structure was found inside of the 9-day pellet (Figure 4.16f).

Different from the inside structure of fungal pellets, the mycelium on the surface had direct intact to the nutrients in the media. As shown in Figure 4.17 a and b, the 2-day pellet's surface was densely covered by a network of fungal hyphae, with clear intertwining and branching. A mat-like surface was observed in pellets after five days of growth. One possible reason for this mat structure

was the fusion of hyphae, where the separate hypha strands fused to create a shared network. By forming this fused network, the nutrients and other resources could be shared within the fungi, and provide added structural stability to the fungal pellets, helping it to maintain its integrity during the growth (Glass et al., 2000). The obvious increase of the hardness of the pellets was observed when cultivating *A. awamori* in almond hull extract with extra nitrogen sources. This fused network can also facilitate the signal transmissions and communications between the fungi (Simonin et al., 2012). During the exponential phase of *A. awamori* growth with extra nitrogen sources, the more viscous media was observed comparing with the initial and final growth phase. Another possible reason for this observed mat-like structure was that the extracellular material, such as the compounds caused the increase of media viscosity, covered the surface of the fungal mycelium. The similar phenome was observed by Beauvais et al. (2007) when cultivated *Aspergillus fumigatus* under static aerial conditions. The fungal hyphae were glued together by extracellular matrix, which was composed of galactomannan, glucans, monosaccharides, polyols, melanin and proteins as they reported. However, no mat-like structure was found when cultivating *Aspergillus fumigatus* in shaking flask. Uneven and loose surface was observed in 9-day pellet. Instead of crossing or lying flat on the surface of the pellet, the hyphae grew outwards from the surface of the pellets to the media, which allowed them to access more nutrients from the media. This outward growth led to the uneven growth rates of different hyphae and unevenness of the surface.

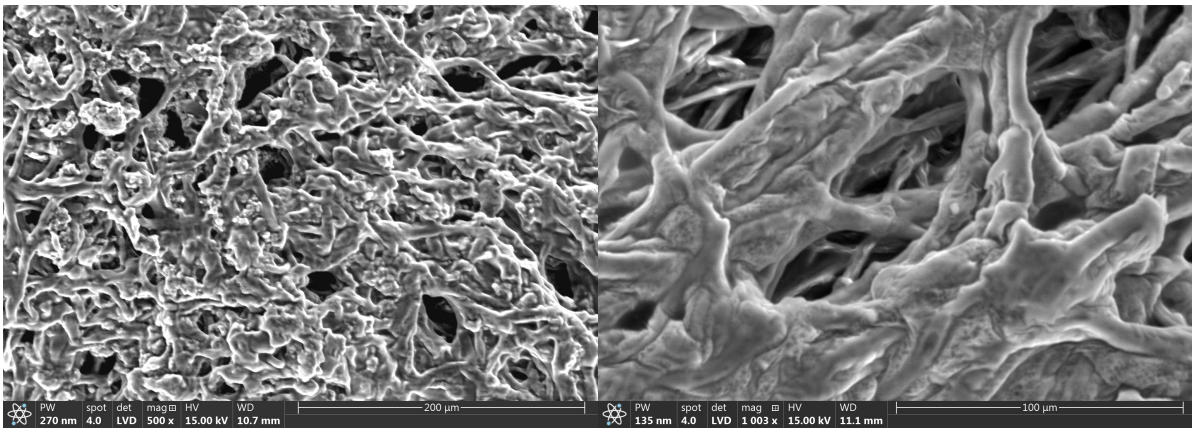

(a) **(b)**

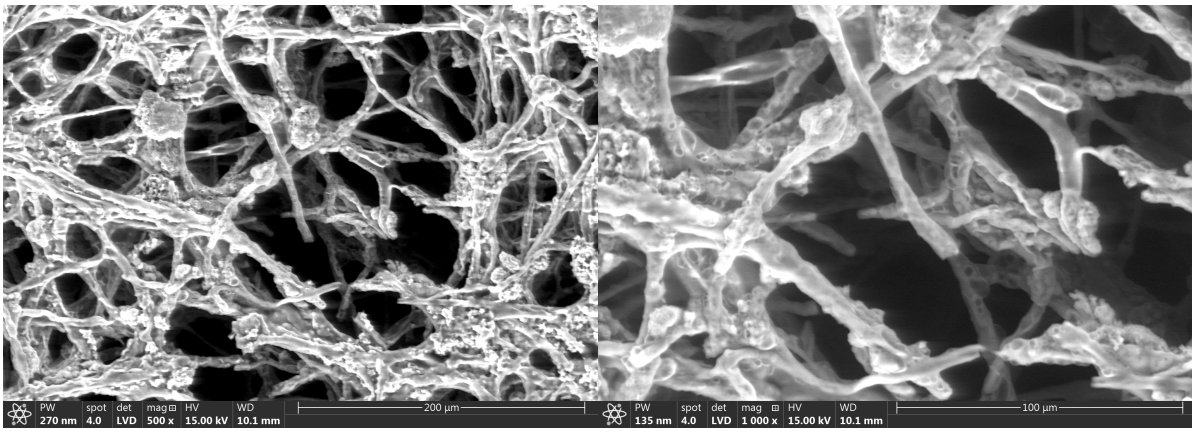

(c) **(d)**

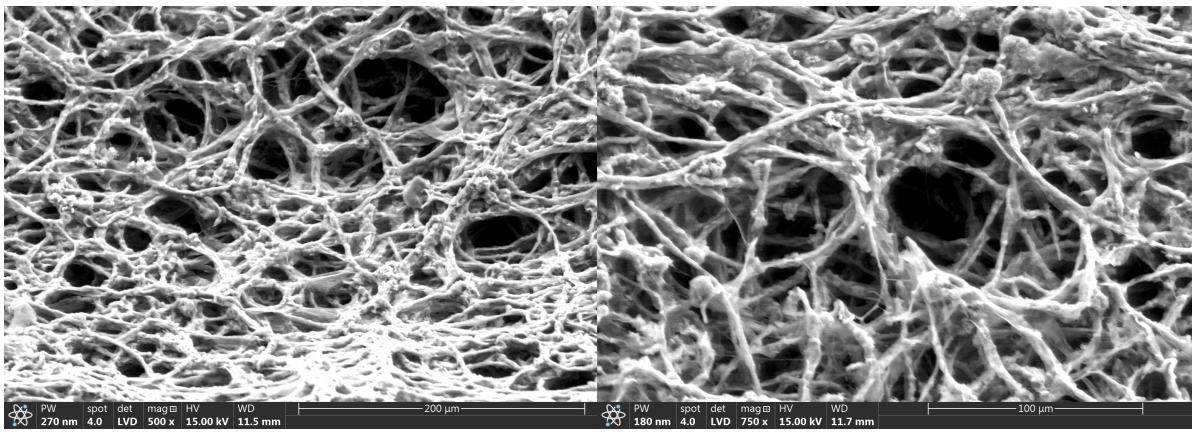

(e) **(f)**

Figure 4. 16. ESEM images of the cross sections of fungal pellets after cultivation of different time: a and b: two days; c and d: five days; e and f: nine days; Part of mycelium in the first column is enlarged in the second column.

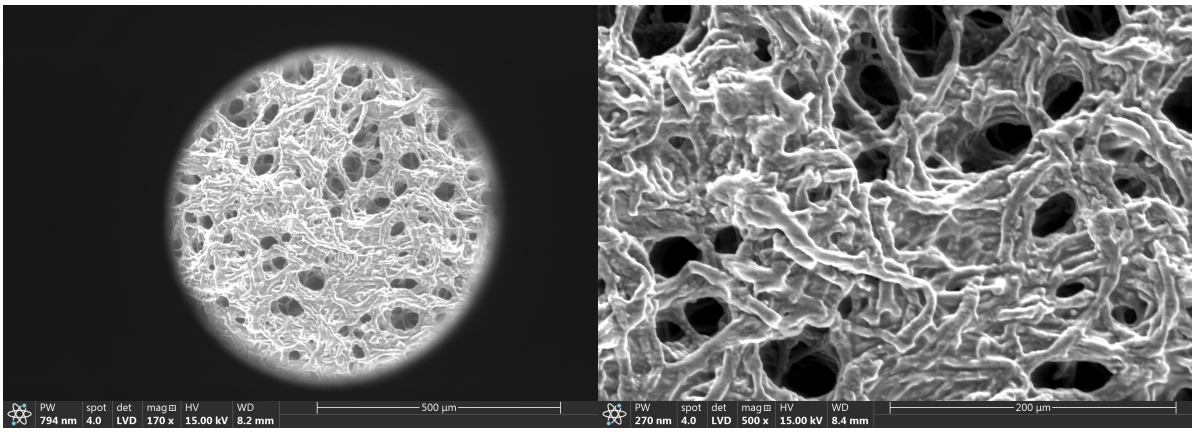

(a) **(b)**

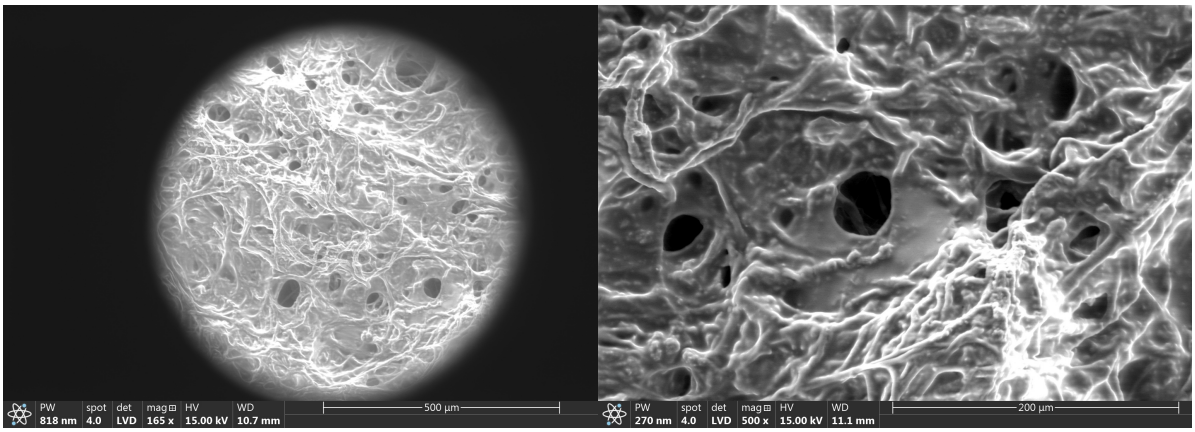

(c) **(d)**

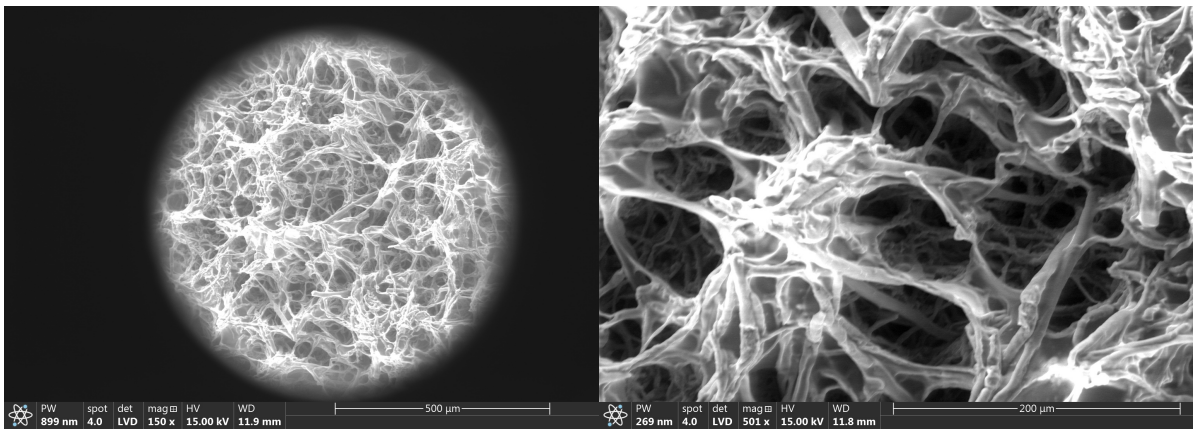

(e) **(f)**

Figure 4. 17.ESEM images of the surface of fungal pellets after cultivation of different time: a and b: two days; c and d: five days; e and f: nine days; Part of mycelium in the first column is enlarged in the second column.

The fungal biomass compositions cultivated from different C/N ratios are shown in Table 4.6. A positive relationship was found between the protein content and nitrogen concentration in the media. The highest protein content was 18.10 % when the initial C/N ratio was 15. TOC was fixed in all the treatment and extra nitrogen sources were added to adjust the initial C/N ratios. Low C/N ratio means high nitrogen sources available in the media. As nitrogen is required for the synthesis of ammino acids, the plentiful nitrogen sources would lead to synthesis of more amino acids. Different with protein content, a negative relationship between fat content and nitrogen concentration was found. Fat is served as a potent energy reserve. When there are abundant nutrients, particularly carbon sources in the media, fungi can convert the excess carbon into fat and store it for future use (Papanikolaou et al., 2007). When C/N ratio was low, more nitrogen and carbon were utilized for protein synthesis, led to limited carbon source for fat synthesis. Therefore, the lowest fat content, 2.28%, was found at the C/N ratio of 15. Fungal biomass cultivated at C/N ratio of 15 had the maximum total ash content. The predominant mineral in *A. awamori* was potassium, which accounted for almost 40% of the total amount of ash content. Comparing with edible mushrooms, all the Ca, Fe, Zn, Mg and Mn contents in *A. awamori* were higher than in *Pleurotus ostreatus*, *Pleurotus sajor-caju*, *Pleurotus florida* and *Calocybe indica* as reported by Alam et al. (2008). *A. awamori* cultivated from almond hull extract could be a good source of trace elements, with balanced protein and fiber content.

Table 4. 6. Composition of A. awamori cultivated at different C/N ratios (d.b.)

Compounds	Unit	C/N =15	C/N = 30	C/N = 45	Control (C/N=153)
Crude protein	%	18.10	12.90	11.90	9.70
Crude fat	%	2.28	2.84	3.15	3.70
Crude fiber	%	8.60	9.00	9.20	8.90
Ash	%	12.25	11.90	11.40	9.80
K	%	5.10	4.88	4.59	3.02
Ca	%	0.60	0.70	0.75	1.39
P	%	0.43	0.44	0.45	0.43
Mg	%	0.180	0.176	0.170	0.160
Zn	ppm	27.15	32.70	30.00	30.60
Fe	ppm	37.55	37.70	38.50	46.00
S	ppm	410	460	490	625
B	ppm	116.60	113.50	105.10	68.60
Mn	ppm	11.95	13.00	11.20	11.45
Cu	ppm	5.95	5.90	5.60	6.00

4.4.4 Initial testing of bioreactor for fungal pellets cultivation

Almost no fungal pellets were formed in the bioreactor under the tested conditions. Instead, the fungal mycelia were found to settle at the bioreactor's bottom or attach to its internal structures, especially the baffles, cooling coils, and the terminals of the pH and DO probes, as shown in Figure 4.18. This phenomenon could potentially be attributed to inadequate or improperly agitation within the bioreactor, thereby inhibiting the formation and movement of the fungal mycelia or pellets. To investigate this further, precultured fungal pellets from flasks were introduced into the bioreactor. The movement of these pellets was observed at the same agitation rate of 150 rpm and aeration rate of 1 vvm. Under these conditions, pellets were able to move in the bioreactor (Figure 4.19). However, some pellets were clogged in the gap between the baffle blades and the bioreactor vessel wall. Additionally, the movement of the fungal pellets upon colliding with the baffle blades diverged into two separate streams. The upward moving stream were well-mixed by both top and bottom mixing impellers. Conversely, pellets in the downward moving stream attempted to settle at the bottom, driven by gravitational pull and the collision effect with the baffle blade. Baffles are

key components within a vessel's mixing system. They are engineered to enhance the efficiency of mixing and prevent the tangential or swirling motion (Youssef, 2019). However, baffles were not beneficial for pellets formation. The flow pattern without baffles inside the bioreactor is more similar to the flow pattern in shaken flasks, which favored the uniform pellets formation. Therefore, baffles were removed from the bioreactor for further research.

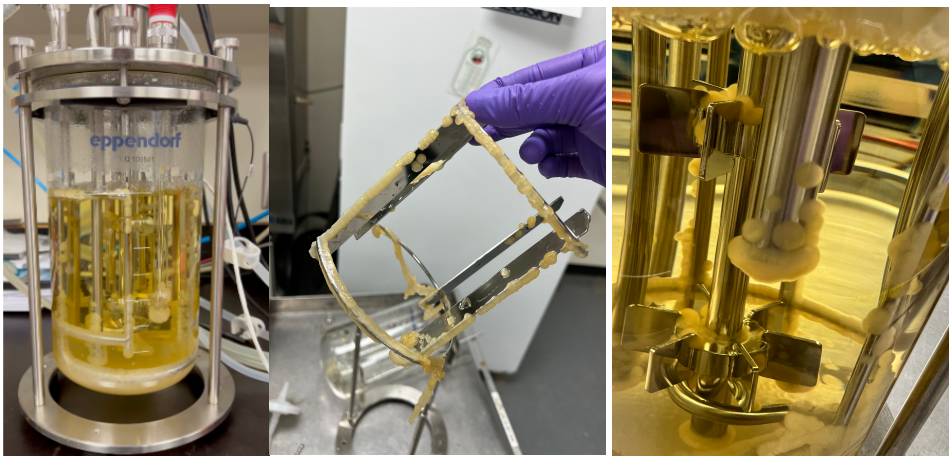

Figure 4. 18. Fungal pellet growth testing in bioreactor

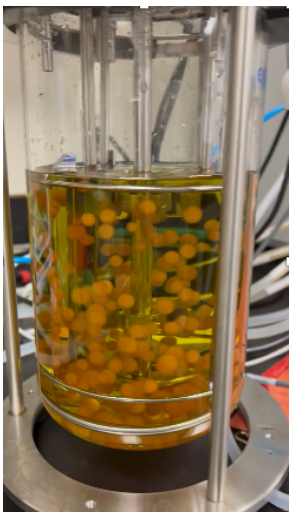

Figure 4. 19. Mixing intensity testing by precultured pellets

In addition to baffles, the cooling coils within the bioreactor were also deemed unnecessary and were removed. In this 2 L bioreactor, heat generation by the fungal growth is limited to increase the temperature, and ambient lab temperatures were always below 30°C (around 24 °C). Cooling was not necessary in this study.

To facilitate comprehensive mixing of spores in the bioreactor, an initial high agitation speed of 250 rpm was employed on the first day, and then switched back to the designed agitation speed. Based on these modifications, a subsequent batch of fungal cultivation was conducted and tested, which successfully yielded the fungal pellets.

4.4.5 Effect of pH control on fungal growth

The fungal performance was compared with fungal cultivation conducted at controlled pH conditions of five and uncontrolled pH conditions. Results showed that the pH dropped from 5.0 to 3.75 at the end of fungal cultivation (Figure 4.20) due to the production of organic acids. *A. awamori* reached maximum biomass concentration of 13.17 g/L at uncontrolled pH within five days, while it took seven days to achieve maximum biomass concentration of 9.13 g/ at controlled pH conditions (Figure 4.21). Therefore, the average cell growth rates were higher in uncontrolled pH conditions (2.63 g/L/d) than at controlled pH (1.30 g/L/d). In terms of the biomass yield, results showed uncontrolled pH led to higher biomass yield 0.85 g VSS/g sugar after five days than controlled pH, which was 0.50 g VSS/g sugar at seven days. This study suggested that *A. awamori* could potentially utilize the nutrients more efficiently for fungal growth under uncontrolled pH conditions. Similar finding was reported by Martin et al. (2003) for a genetically modified *A. awamori* strain.

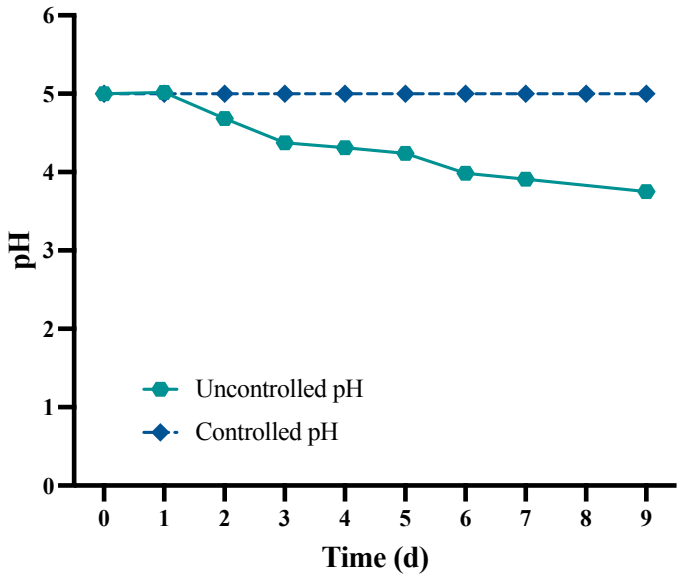

Figure 4. 20. pH values during fungal cultivation with controlled and uncontrolled pH.

Y error bars are standard deviation.

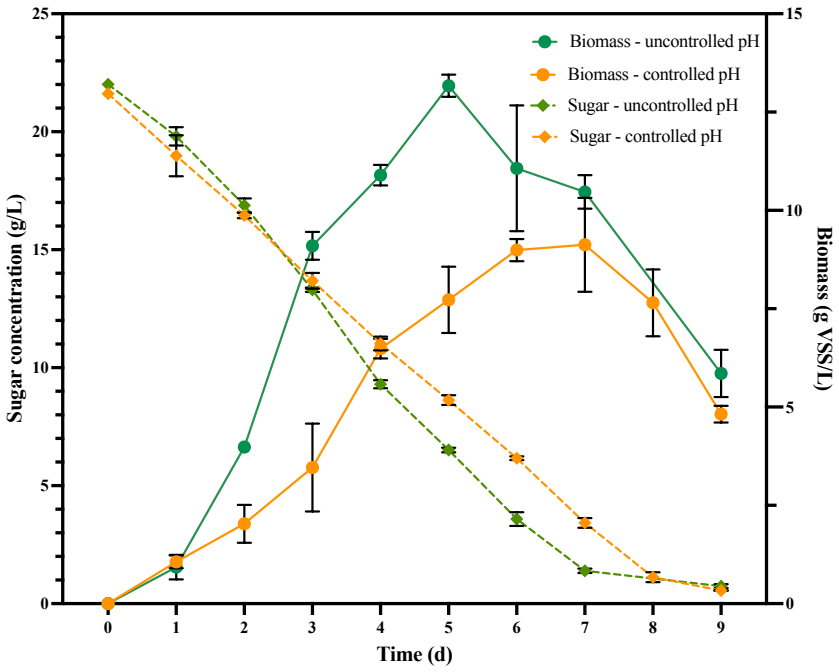

Figure 4. 21. Fungal biomass and sugar concentration change during fungal cultivation at controlled and uncontrolled pH conditions.

Y error bars are standard deviation.

4.4.6 Effect of agitation

Experiments were carried out to determine the effects of agitation on the fungal biomass growth and morphology. The changes of fungal biomass and sugar concentrations overtime at different agitation speeds are shown in Figure 4.22. The maximum biomass concentration of 13.17 g VSS/L was obtained at 150 rpm after five days of cultivation. Biomass cultivated at 50 rpm and 250 rpm had lower biomass concentration than at 150 rpm. A cultivation time of six days was needed at 50 rpm to reach the maximum biomass concentration of 5.62 g/L and took seven days at 250 rpm to reach 6.68 g/L biomass.

In terms of the morphology, almost all the fungi grew in pellet form when agitated at speeds of 50 and 150 rpm. However, free mycelium was noticed when the agitation speed increased to 250 rpm, comprising 26.4% of the total biomass in the bioreactor (Figure 4.23). The high agitation speed caused the fragmentation of fungal pellets, which subsequently formed the new small pellets or grew as free mycelium. When pellets are fragmented, the individual cells need to reestablish connection and restructure to form new pellets or grow as free mycelium. This restructuring process can temporarily divert energy and resources away from active cell division and biomass production, leading to a slower growth rate (Waldherr et al., 2023). Some of the cells were even damaged and were not able to regrow. Thus, the fragmentation and free mycelium growth may be the major reason for slow growth and low biomass yield at agitation speed of 250 rpm.

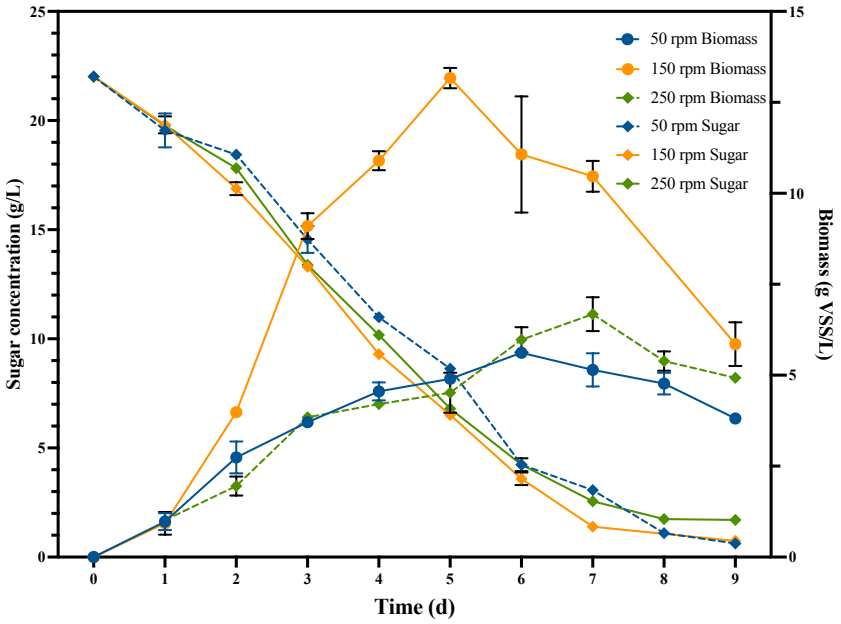

Figure 4. 22. Fungal biomass and sugar concentration change during fungal cultivation at different agitation speeds.

Y error bars are standard deviation.

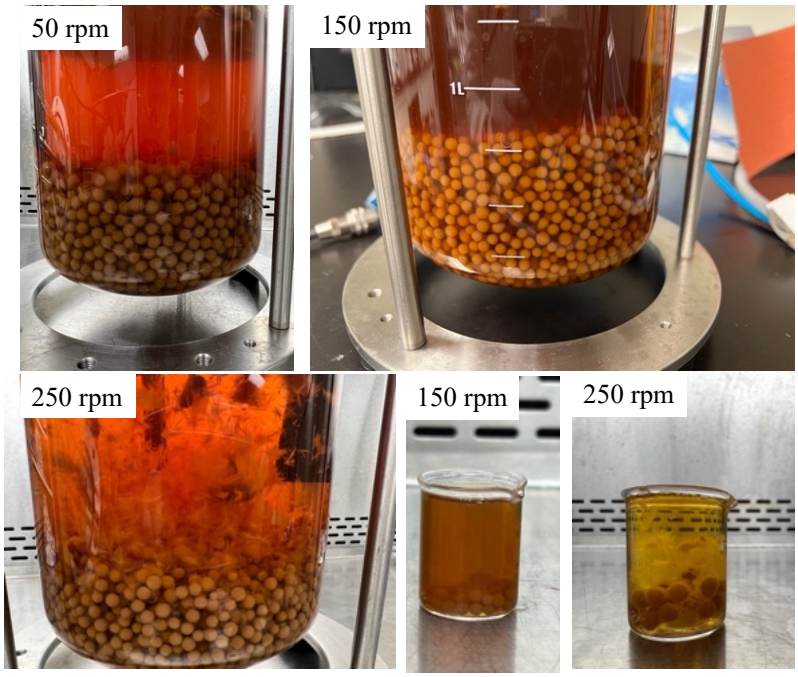

Figure 4. 23. Fungal growth in the bioreactor under different agitation speeds

The Box and Whiskers plot shows the size distribution of fungal pellets under different agitation speeds, when they reached their maximum biomass concentration during the cultivation (Figure 4.24). The average sizes for pellet cultivated at 50, 150 and 250 rpm were 5.06, 3.75 and 4.13 mm, respectively. More uniform and denser pellets were observed at 150 rpm. Tiny pellets and lose pellets were noticed at 250 rpm even though the average pellets size was slightly higher than at 150 rpm. Largest pellets were found at 50 rpm. The smaller specific surface aera available for nutrient uptake, coupled with the extensive internal autolysis, could accounted for the slower growth rate and lower biomass yield at this agitation speed. To conclude, 150 rpm led to the uniform fungal pellets growth with high biomass yield, which was suggested for *A. awamori* cultivation.

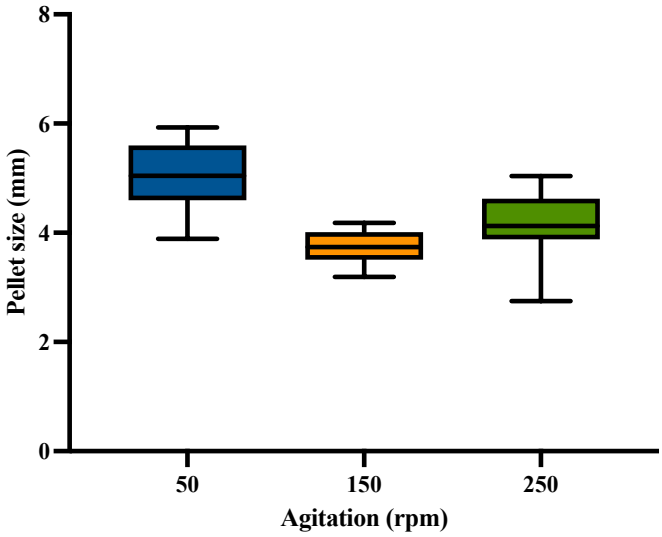

Figure 4. 24.Box and Whiskers plot for the size distribution of fungal pellets cultivated at different agitation speeds.

Y error bars are standard deviation.

4.5 Conclusions

This study extensively investigated the cultivation parameters for *Aspergillus awamori* pellets growth, including inoculum level, aeration, nitrogen source and C/N ratio in 250 mL glass

bottles or flasks. Both aeration and inoculum level had positive effects on fungal biomass. However, higher biomass concentration may lead to the secretion of yellow pigment by *A. awamori* due to the limited nutrients or restricted aeration. Higher inoculum levels led to the formation of grey pellets, which could be attributed to the sporulation of the pellets. An investigation of different nitrogen source was conducted, including two organic nitrogen sources (yeast extract and peptone) and two inorganic nitrogen sources (NH_4Cl and $NaNO_3$). It was found that organic nitrogen source favored *A. awamori* growth much better than inorganic nitrogen sources, due to presence of amino acid, peptides, vitamins and essential elements in organic nitrogen sources. Comparing the fungal performance cultivated in NH_4Cl and $NaNO_3$, higher biomass yield was achieved in NH_4Cl than in $NaNO_3$. In order to lower the raw material cost for fungal cultivation, a combination of yeast extract and NH_4Cl was recommended to adjust carbon to nitrogen ratio (C/N ratio) from this study. The optimal C/N ratio was determined by comparing the growth of the fungi in almond hull extract under control (C/N=153), and at ratios of 15, 30, and 45. The highest biomass concentration (12.29 g/L) was reached at a C/N ratio of 15 after six days cultivation. Inhomogeneous pellets were observed due to the autolysis in the center of pellets, which led to the decrease of fungal biomass concentration after six days. This phenomenon was confirmed by observing the micro-scale structure of the pellets using ESEM. The fungal composition at different C/N ratios were also analyzed and compared. It was found that a higher C/N ratio led to an increased protein content and reduced fat content. The maximum protein content (18.1%) and minimum fat content (2.28%) were found at C/N ratio of 15. Based on those studies, C/N ratio of 15 was recommend for *A. awamori* growth.

Subsequently, the fungal cultivation was scaled up to a 2L bioreactor, where configurations which could favor pellet formation were initially tested. Successful pellet formation was achieved

after the removal of baffles and cooling coils from the Biflo® 120 2L bioreactor. At the bioreactor scale, the effects of pH control and agitation speed were also explored, as these parameters can be more feasibly manipulated in a bioreactor than in a flask. Higher biomass concentration was obtained without pH control comparing with controlled pH. Maximum biomass was achieved at the agitation speed of 150 rpm. Higher agitation (250 rpm) led to the fragmentation of fungal pellets. While lower agitation (50 rpm) led to the formation of bigger pellets, which slowed down the fungal growth. Finally, the optimum conditions for *A. awamori* growth in almond hull extract in a bioreactor were determined. Under the optimum conditions, a biomass yield of 0.85 g VSS/g sugar and pellets with an average size of 3.75 mm were achieved.

Chapter 5 Enzymatic Hydrolysis of Almond Hull Fiber Residues for Fungal Cultivation

5.1 Abstract

Enzymatical hydrolysis and liquefaction of the residual almond hull solids (RASH) after sugar extraction were studied. The effect of three different enzymes (Cellic CTec2, Viscozyme L and Pectinex Ultra SPL) and their combinations on hydrolysis performance were investigated and compared. The optimum loadings of enzymes were identified. The ability of *Aspergillus awamori* (*A. awamori*) to grow on the resulting hydrolysate was evaluated. The most effective hydrolysis in terms of liquefaction and sugar yield was achieved through the combination of Cellic CTec2 and Viscozyme L. Using 200 uL/g RASH of Cellic CTec2 and 60 uL/g RASH of Viscozyme L resulted in a total sugar yield, total fiber conversion, and liquefaction efficiency of 41.36%, 86.01%, and 51.61%, respectively. Applying these optimal conditions at a large scale resulted in improved liquefaction efficiency, reaching 72.53%. While the sugar yield was similar to small scale hydrolysis. After cultivating *A. awamori* in hydrolysate for five days, uniform yellow fungal pellets were observed, resulting in a biomass yield of 0.8 g VSS/g sugar. This study suggests that RASH could be a promising source for fungal-based food production, thus optimizing almond hull utilization and increasing the yield of fungal biomass.

5.2 Introduction

Almond hulls, a significant byproduct of the almond processing industry, have potentials to been converted into high value products. As studied in previous chapters, around half of the nutrients in almond hulls could be extracted by using hot water. The major sugars in the almond hull extract were glucose, sucrose, fructose and xylose. All those sugars were found to be usable

by *A. awamori* together with other nutrients in the almond hull extracts. While the sugar extraction process and sugar utilization have been extensively studied, there remains a need to further explore the potential application of the residual solids after sugar extraction, which accounted for half of the initial almond hulls' dry weight.

The remaining solids after extraction mainly contain fibers, including cellulose, hemicellulose, pectin, and lignin. Traditionally, these residual high fiber materials could be utilized through solid-state fermentation by filamentous fungi, due to their enzyme production capabilities (Pal & Khanum, 2010; Shin et al., 2019; Umsza-Guez et al., 2011a). However, it has a challenge in obtaining pure clean fungal biomass after solid state fermentation as the produced fungal biomass are mixed with the solid feedstock. To produce clean, fungal-based food products that exclusively contain fungal biomass, submerged fermentation is preferred, due to the ease of separating fungal biomass from the liquid spent media. In order to implement this strategy, it's necessary to break down and liquefy the residual solids to liberate the sugars first and then utilize the hydrolysate for fungal cultivation. Processes for utilizing both almond hull extract and residual solids for fungal cultivation are shown in Figure 5.1. The proposed processes can help in maximizing the use of almond hulls and increase the yield of fungal biomass. They also contribute to a significant waste reduction and potentially brings additional economic advantages.

The main goal of this research was to study the enzymic hydrolysis of almond hulls residuals after sugar extraction. The release addition sugars from residual almond hulls could be used for fungal cultivation. The specific objectives were to:(1) characterize residual almond hull solid (RAHS**)** after water extraction, select appropriate enzyme(s) and determine the enzyme(s) loadings to hydrolyze RAHS; (2) hydrolyze RAHS at large scale at optimum enzymatical conditions; (3) evaluate the growth performance of *A. awamori* in the hydrolysate.

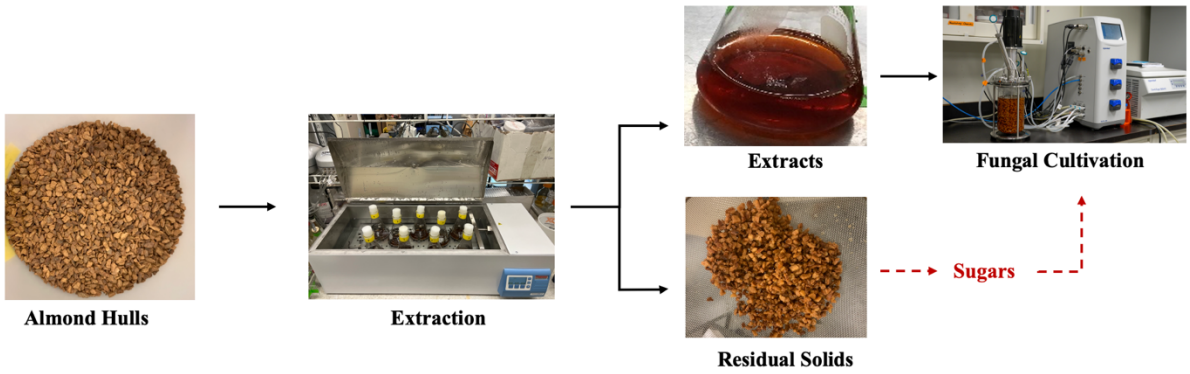

Figure 5. 1. General process of utilizing almond hulls for fungal cultivation.

5.3 Materials and Methods

5.3.1 Residual almond hull solids preparation and characterization

The RAHS after sugar extraction at optimum conditions from Chapter 2 was collected and frozen at -20℃ until used in the hydrolysis experiments (Figure 5.2). The contents of neutral detergent fiber (NDF), acid detergent fiber (ADF) and lignin were analyzed by Denele lab. ADF and NDF contents were determined using the ANKOM^{TM} detergent fiber analyzer (Ankom Model 220; Ankom Technology, Macedon, NY, USA) following the ANKOM Technology Method 5 and 6, respectively. Cellulose content was calculated as the difference between ADF and lignin. Hemicellulose was calculated as the difference between NDF and ADF. Pectin content was determined by measuring the amount of galacturonic acid produced after digesting the samples in buffered solution with pectinase using modified methods from Li et al. (2023). Galacturonic acid was measured with HPLC.

Figure 5. 2. Residual almond hull solids after sugar extraction

5.3.2 Enzyme selection and reaction time determination for enzymatic hydrolysis

Three different commercial enzymes were purchased from Sigma-Aldrich. One is Cellic CTec2 (C enzyme), which contains cellulase and endo-1,4-β -glucansase and is normally used as a cellulase product (Y. Chen, 2020). The other two enzymes are normally used as pectinase, Viscozyme L (V enzyme, contains pectinase, β -glucansase, hemicellulase and xylanase) and Pectinex Ultra SPL (P enzyme, contains pectinase, β -glucansase and hemicellulase) (Zicari, 2016). The effects of those individual or combined enzymes on RAHS hydrolysis were tested. Enzyme loadings were 0.03 mL/g and 0.1 mL/g of dried RAHS for pectinase and cellulase products, respectively. The enzymes loadings were selected based on the optimum loadings found by Zicari (2016) for sugar beets hydrolysis and adjusted based on RAHS compositions. The enzymes loadings for different treatments are listed in in Table 5.1.

Table 5. 1. Loadings of different enzyme mixtures for enzyme selection experiments

Trial ID	Cellic CTec2 (mL/g)	Pectinex Ultra SPL (mL/g)	Viscozyme L (mL/g)
Blk	0	0	0
C	0.1	0	0
P	0	0.03	0
V	0	0	0.03
PC	0.1	0.03	0
VC	0.1	0	0.03
PCV	0.1	0.015	0.015

All enzymatic hydrolysis were performed in 50 mL falcon tubes with a final working volume of 20 mL at 10% (mass/mass) total solids (TS) loading (Figure 5.3). All the falcon tubes were incubated in an incubator shaker at 50 ℃ with a shaking speed of 200 rpm. Samples were collected by scarifying two tubes from each treatment after 4, 8,12 and 24 hours. The sampled tubes from each treatment were centrifuged at 5000 rpm for 30 min. The mass of the supernatants was recorded after being decanted into tared 15 mL falcon tubes. The collected supernatants were heated at 99℃ for 10 min in water bath to deactivate enzymes activity (Zicari, 2016). Then the supernatants were frozen at -20℃ before used for sugar analysis by high-performance liquid chromatography (HPLC) as described below. The liquid in solid phase was determined by the reduction of mass of residual solids after enzymatic hydrolysis before and after being dried in an oven at 105℃ overnight (APHA et al., 2017).

The liquefaction efficiency was calculated by dividing the mass of supernatant after centrifugation by the initial total mass as expressed in Eqn.5.1

$$Liquefaction\ (\%) = \frac{mass\ of\ supernantant\ after\ centrifugation\ (g)}{initial\ total\ mass\ (g)} \times 100\% \quad \text{(Eqn.5.1)}$$

Total sugar yield calculated by the total mass of soluble sugars in the liquid divided by the initial dry matter of RAHS as shown in Eqn.5.2. In this calculation, the sugar concentration in the liquid in solid phase was assumed to be the same as in the supernatant. The density of supernatant was assumed to be 1 g/mL.

$$Total\ sugar\ yield\ (\%) = \frac{sugar\ concentration\ in\ supernantant\ \left(\frac{g}{L}\right) \times (volume\ of\ supernantant + volume\ of\ liquid\ in\ solid\ after\ hydrolysis)(mL)}{dry\ matter\ of\ RAHS\ (g) \times 1000} \times 100\% \quad \text{(Eqn.5.2)}$$

Recoverable sugar yield was defined as the sugar yield in supernatant as calculate by Eqn.5.3:

$$Recoverable\ sugar\ yield\ (\%) = \frac{sugar\ concentration\ in\ supernanant\ \left(\frac{g}{L}\right) \times volume\ of\ supernantant\ (mL)}{dry\ matter\ of\ RAHS\ (g) \times 1000} \times 100\% \quad \text{(Eqn.5.3)}$$

Soluble sugar concentrations, including glucose, sucrose, xylose, arabinose, galactose, fructose and mannose were analyzed with HPLC (Shimadzu SPD-M20A) that had CBM-20A controller, RID-10A refractive index detector, using methods modified from (Zicari, 2016). An Aminex HPX-87P column was operated with Milli Q water as mobile phase (0.5 mL/min, 80℃). Glucose, sucrose, xylose, arabinose and galactose eluted individually, and fructose and mannose co-eluted and were quantified as a cumulative peak. Galacturonic acid was quantified by using SPD-20A phot diode array (PDA) detector at 205 nm and an Aminex HPX-87H column. Sulfuric acid (0.05 mM) was used as the mobile phase at a flow rate of 0.5 mL/min. The oven temperature was controlled at 60℃. The best mixture of enzymes and reaction time for enzymatic hydrolysis

were selected by comparing the liquefaction efficiency, total sugar yield and total recoverable sugar yield.

5.3.3 Determination of enzyme loadings

Experiments were designed to test enzymatic hydrolysis at different enzyme loadings. The two enzymes used in this section were selected from previous section 5.3.2, which were Cellic CTec2 and Viscozyme L. Cellic CTec2 loadings was tested at five levels, 0.05, 0.1, 0.15,0.2 and 0.25 mL/g dried RAHS. Viscozyme L was also tested at five different loadings, 0.02, 0.03, 0.04, 0.05 and 0.06 mL/g dried RAHS. A two-factor factorial design was used, and samples were tested in duplicates. Blank samples with RAHS only. The experiments were conducted in 50 mL falcon tubes as described in previous section for 24 h. The liquefaction efficiency, sugar concentration, and sugar yield were analyzed after enzymatic hydrolysis.

5.3.4 Large scale enzymatic hydrolysis using optimum enzyme loadings

The large-scale enzymatic hydrolysis was carried out in 250 mL glass bottles with a final working volume of 200 mL at 10% TS loading (Figure 5.3). The optimum enzyme loadings found in the previous section (5.3.3) were applied in large scale enzymatic hydrolysis. All the other conditions used in large scale were the same as small scale conducted in 50 mL falcon tubes.

After hydrolysis, all the hydrolyzed samples from two hydrolysis glass bottles were transferred into one 500 mL centrifuge bottle. Finally, samples from six 250 mL glass bottles were combined into three 500 mL centrifuge bottles. The centrifuge bottles were centrifuged at 4℃ and 5000 rpm for 30 min. The hydrolysate obtained from large-scale enzymatic hydrolysis was subsequently heated at 99℃ for 10 minutes and the suspended solids were removed through vacuum filtration using standard filter paper. The purpose of the large-scale hydrolysis was to

produce enough supernatant for fungal cultivation. The sugar yield and liquefaction efficiency were analyzed and compared with small scale hydrolysis.

Figure 5. 3. Enzymatic hydrolysis of residual almond hull solids in incubator shaker. left: small scale (20 mL); right: large scale (200 mL)

5.3.5 Evaluate the growth performance of *A. awamori* in almond hull hydrolysate

The hydrolysate from large-scale hydrolysis was diluted to a sugar concentration of 20 g/L using deionized water (DI water). Yeast extract and ammonium chloride were added to achieve an initial carbon-to-nitrogen ratio of 15. The prepared medium was pasteurized at 80°C for three hours in water bath and then allowed to cool down to room temperature prior to fungal cultivation.

Spores that had been growing for four days were transferred from a potato dextrose agar (PDA) plate into 250 mL flasks containing 100 mL of the medium at a concentration of 10^3 spores/mL. The flasks were then placed in a shaker incubator set at 30°C and shaken at 200 rpm for five days. The biomass was harvested using vacuum filtration and filter paper. Total suspended solids (TSS) were analyzed by calculating the weight loss after drying at 105°C to a constant weight, while volatile suspended solids (VSS) were obtained after calcination at 550°C, following

standard methods (APAH et al., 2017). Sugar concentrations in the spent media were analyzed using HPLC.

5.4 Results and Discussion

5.4.1 Characteristics of residual almond hull solid

After sugar extraction, 50.50% (d.b.) of nutrients in initial almond hulls (AH) were extracted and separated, 49.5% (d.b) of initial AH were RAHS. 81.32% of sugars and ash in initial AH were extracted and went to the liquid extract by hot water. All the structural carbohydrates were remained in RAHS. The detailed mass balance of each compound before and after sugar extraction are shown in Table 5.2.

The moisture content of RAHS after sugar extraction was 17.88%, or 82.12% total solids (TS) content (Table 5.3). Ash content was 5.19% of the dry matter, indicating 94.81% of the total solids are volatile solids (VS). Soluble sugars were 14.81% of the TS which were the residual sugar dissolved in the liquid absorbed by RAHS. Structural carbohydrate contents are also displayed in Table 5.3. The RAHS sample had a cellulose content of 15.86%, hemicellulose content of 9.40%, pectin content of 9.93%, and lignin content of 15.94%. The total amount of cellulose, hemicellulose and pectin which could be potentially hydrolyzed were 35.19%. The theoretical maximum sugar yield could be determined to be 54% (g sugar/g RAHS).

Table 5. 2. Mass balance of individual compound in almond hulls before and after extraction (%, d.b.)

Compounds	Before Extraction	After Extraction	
		Extracts	Residual Solids
Sugar	39.30	31.96	7.33
Cellulose + hemicellulose	12.50		12.50
Pectin	4.92		4.92
Lignin	7.89		7.89
Ash	13.76	11.19	2.57
Others	21.63	7.35	14.29
Total	**100**	**50.50**	**49.50**

Table 5. 3. Composition of residual almond hull solid (unit: %, dry basis)

Compound	Content (%)
Moisture *	17.88
Total solids*	82.12
Sugar	14.81
ADF	31.8
NDF	41.2
Cellulose	15.86
Hemicellulose	9.40
Pectin	9.93
Lignin	15.94
Ash	5.19

* Wet basis

5.4.2 Enzyme selection and hydrolysis time determination

The pH values of all the treatments at each time point are shown in Figure 5.4. The pH value of blank and Cellic CTec2 only treated groups were relatively stable during the hydrolysis, which were kept around 4.5. pH dropped quickly in all the groups treated with pectinase (Viscozyme L and Pectinex Ultra SPL), indicating galacturonic acid produced from pectin

hydrolysis was the main reason causing pH drop. The change of galacturonic acid concentration during hydrolysis is shown in Figure 5.5. Consistent with pH change, no galacturonic acid produced in blank and Cellic CTec2 only treated groups. Most of the galacturonic acid in pectinase treated groups were produced within the first four hours, leading to the fast pH decrease to lower than 4 during this time period. Among the other five groups treated with pectinase, Pectinex Ultra SPL only treated group had a relative higher pH and lower galacturonic acid.

According to Kim & Lee (2021) and information supplied by the manufacture, the optimum pH ranges for Pectinex Ultra SPL, Viscozyme L and Cellic CTec2 are 4-5, 3.3-5.5, and 5-5.5, respectively. The pH values in all pectinase treatments were in the range of 3.7- 4.6, which were within the optimum pH ranges of Viscozyme L and close to the optimum pH range of Pectinex Ultra SPL. As reported by the manufacture (Novozymes), the enzyme relative performance of Cellic CTec2 at pH 3.7-4.6 was around 50%-80% compared to the enzyme performance at optimum pH condition. Usually, 50 mM sodium acetate buffer is applied to maintain a pH level of 5 during enzymatic hydrolysis (Paz-Cedeno et al., 2022). Sodium acetate buffer is made from sodium acetate and acetic acid. However, Taniguchi et al. (1977) found that acetic acid could inhibit mycelial growth and sporulation of *Aspergillus niger* (*A.niger*). *Aspergillus awamori* can also be named as *A. niger var. awamori*, which means *A. awamori* is a specific variety of *A. niger* (Saleh et al., 2011). Since the hydrolysate would be used for *A. awamori* cultivation, addition of sodium acetate buffer was not considered to avoid inhibition of fungal growth.

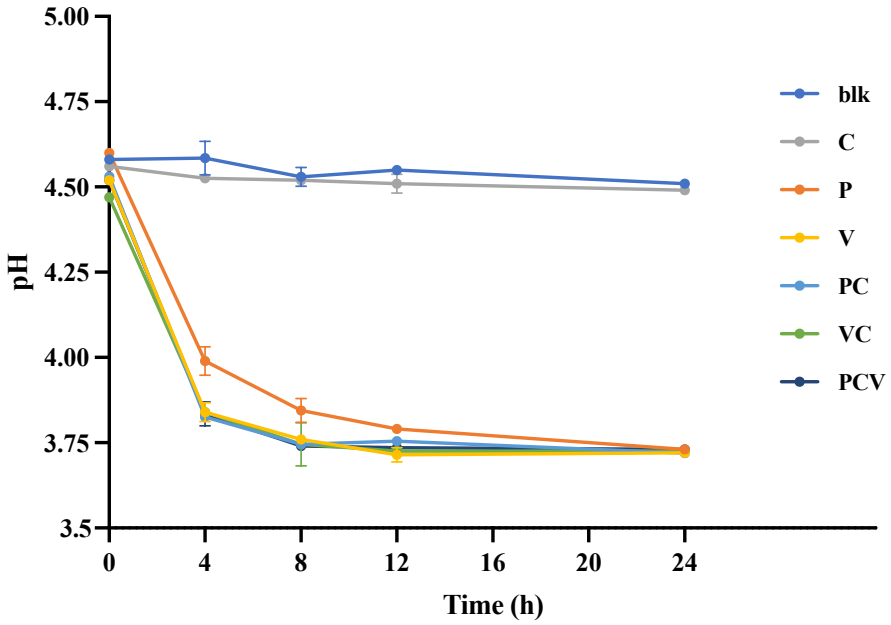

Figure 5. 4. pH change during RAHS hydrolysis by different enzymes.

Y error bars are standard deviation. (blk - no enzyme; C- Cellic CTec2 only; P-Pectinex Ultra SPL only; V- Viscozyme L only; PC- Pectinex Ultra SPL + Cellic CTec2; VC- Viscozyme L + Cellic CTec2; PCV: Pectinex Ultra SPL + Cellic CTec2 + Viscozyme L)

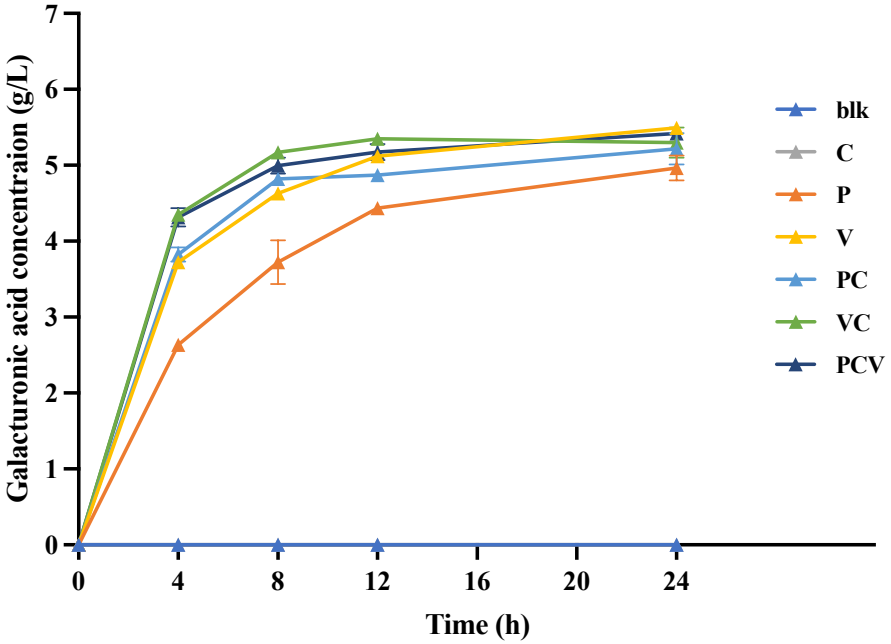

Figure 5. 5. The change of galacturonic acid concentration during RAHS hydrolysis with different enzymes.

Y error bars are standard deviation. (blk - no enzyme; C- Cellic CTec2 only; P-Pectinex Ultra SPL only; V- Viscozyme L only; PC- Pectinex Ultra SPL + Cellic CTec2; VC- Viscozyme L + Cellic CTec2; PCV: Pectinex Ultra SPL + Cellic CTec2 + Viscozyme L)

As shown in Figure 5.6, enzymatic hydrolysis resulted in significant liquefaction. Addition of pectinase (P or V enzymes) resulted in much higher liquefication efficiency than the cellulase (C) enzyme only. Furthermore, combining cellulase and pectinase (PC, VC and PCV) resulted in an increased liquefication efficiency than when using pectinase alone. This indicated that the addition of pectinase notably enhances liquefaction and cellulase addition also contributed to the liquefaction process. It has to be noted that the RAHS could quickly absorb most of the added water in the hydrolysis experiment at the beginning, which led to an initial decrease in liquefaction from 42.5% (initial unsaturated baseline) to 18.3% (initial saturated baseline). This change reflected the difference of liquefaction before and after the RASH became saturated. Among all the treatments, only the combination of PC, VC and PCV exceeded the initial unsaturated baseline after 4 hours hydrolysis. Samples hydrolyzed with P and V enzymes required 24 hours to exceed the initial unsaturated baseline. On the other hand, the recovered liquid in the C treatment was always less than the initial added liquid within 24 hours.

The liquification performance of P-only and V-only treatments suggested that V enzyme was more efficient in terms of liquefaction compared to the P enzyme. Regarding treatments that utilized both cellulase and pectinase, PCV showed a higher liquefication efficiency than PC (p value = 0.037). The liquefication in samples treatment by VC and PCV were similar (p value = 0.25), approximating 50%. In order to use less enzymes to achieve the same liquefication performance, using combination of V and C enzymes is recommended. Upon conducting a statistical analysis of the liquefaction treated by VC at all durations, significantly enhanced liquefaction efficiency was observed at 24 hours (p value = 0.033). This suggests 24 hours

treatment was required for hydrolysis in this case. Longer time was not suggested to avoid the sugar consumption by microbes.

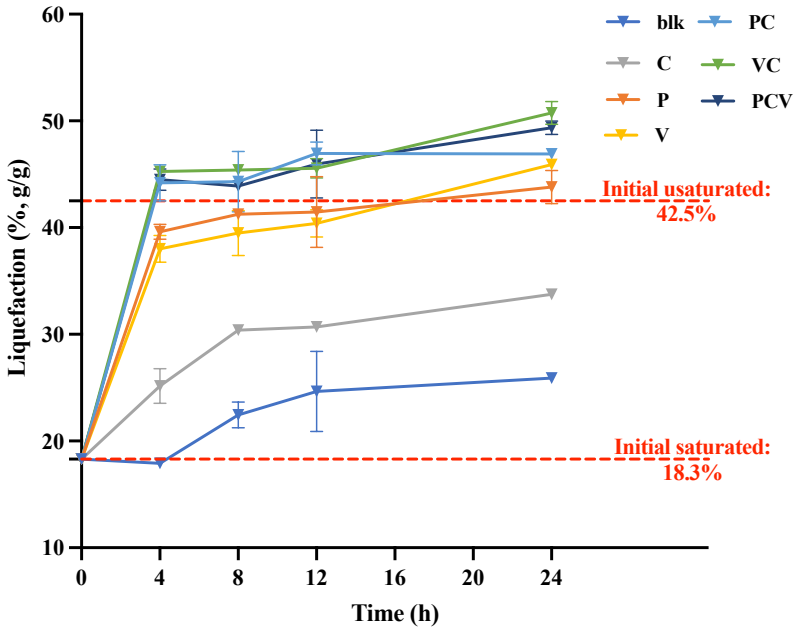

Figure 5. 6. Liquefaction extent during RAHS hydrolysis treated by different enzymes. Y error bars are standard deviation. (blk - no enzyme; C- Cellic CTec2 only; P-Pectinex Ultra SPL only; V- Viscozyme L only; PC- Pectinex Ultra SPL + Cellic CTec2; VC- Viscozyme L + Cellic CTec2; PCV: Pectinex Ultra SPL + Cellic CTec2 + Viscozyme L)

Sugar concentrations in the supernatant at different time points are depicted in Figure 5.7. Similar to liquefication, the combination of pectinase and cellulase achieved more effective than using either enzyme individually. The highest sugar concentration was achieved in both VC and PCV treatments, with no significant difference (p value = 0.29). The highest total sugar concentration was 39.87 g/L, which includes 19.93 g/L of residual sugars in the RAHS, left behind after the sugar extraction process.

Examining the specific sugar concentrations treated by different enzymes reveals that the release of glucose was primarily attributable to the C enzyme. Samples treated solely with the C

enzyme exhibited 20.06 g/L of glucose. The addition of P or V enzymes didn't significantly increase the glucose concentration when compared with the blank, or when comparing PC, VC, and PCV with C. This implies that P and C enzymes are predominantly pectinases. In addition to glucose, fructose + mannose were identified in the hydrolysate. Since fructose is an inherent sugar in almond hulls, most of the fructose may originate from the initial RAHS. Increased concentrations of fructose + mannose were detected in samples treated with P and V enzymes, particularly the V enzyme, which could be attributed to a trace amount of hemicellulase in these two enzymes. As expected, arabinose, galactose, and galacturonic acid were existed in the blank. The highest concentrations of arabinose and galactose were observed in samples treated with the V enzyme. This indicates that the interaction between pectinase and hemicellulose in the V enzyme released galactose, arabinose, and mannose from the pectin's side chain (Garna et al., 2004). Galacturonic acid was only produced in the samples treated with pectinase, especially those treated by V enzymes.

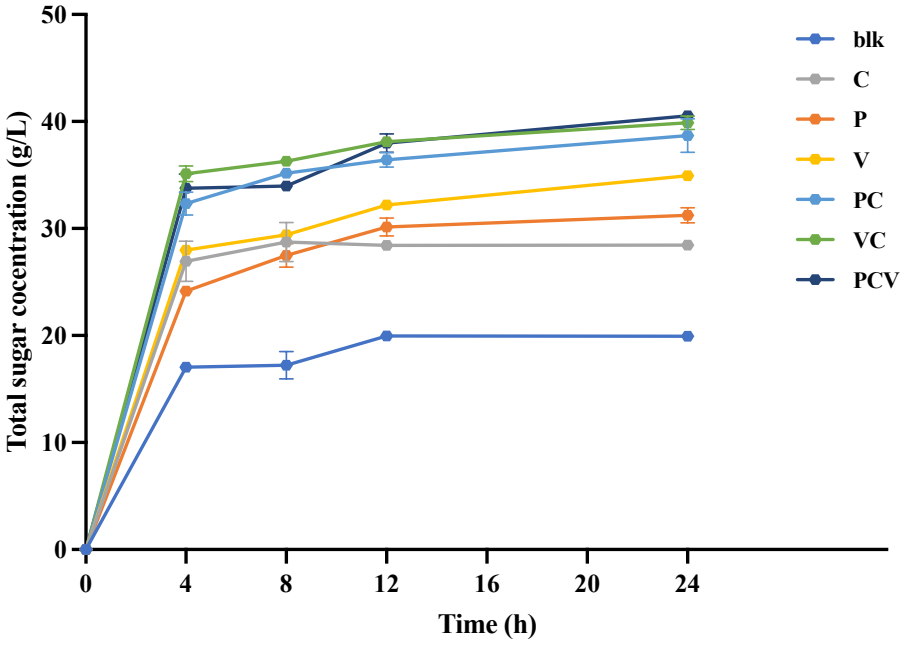

Figure 5. 7. Sugar concentration in the supernatant treated by different enzymes.

Y error bars are standard deviation.(blk - no enzyme; C- Cellic CTec2 only; P-Pectinex Ultra SPL only; V- Viscozyme L only; PC- Pectinex Ultra SPL + Cellic CTec2; VC- Viscozyme L + Cellic CTec2; PCV: Pectinex Ultra SPL + Cellic CTec2 + Viscozyme L)

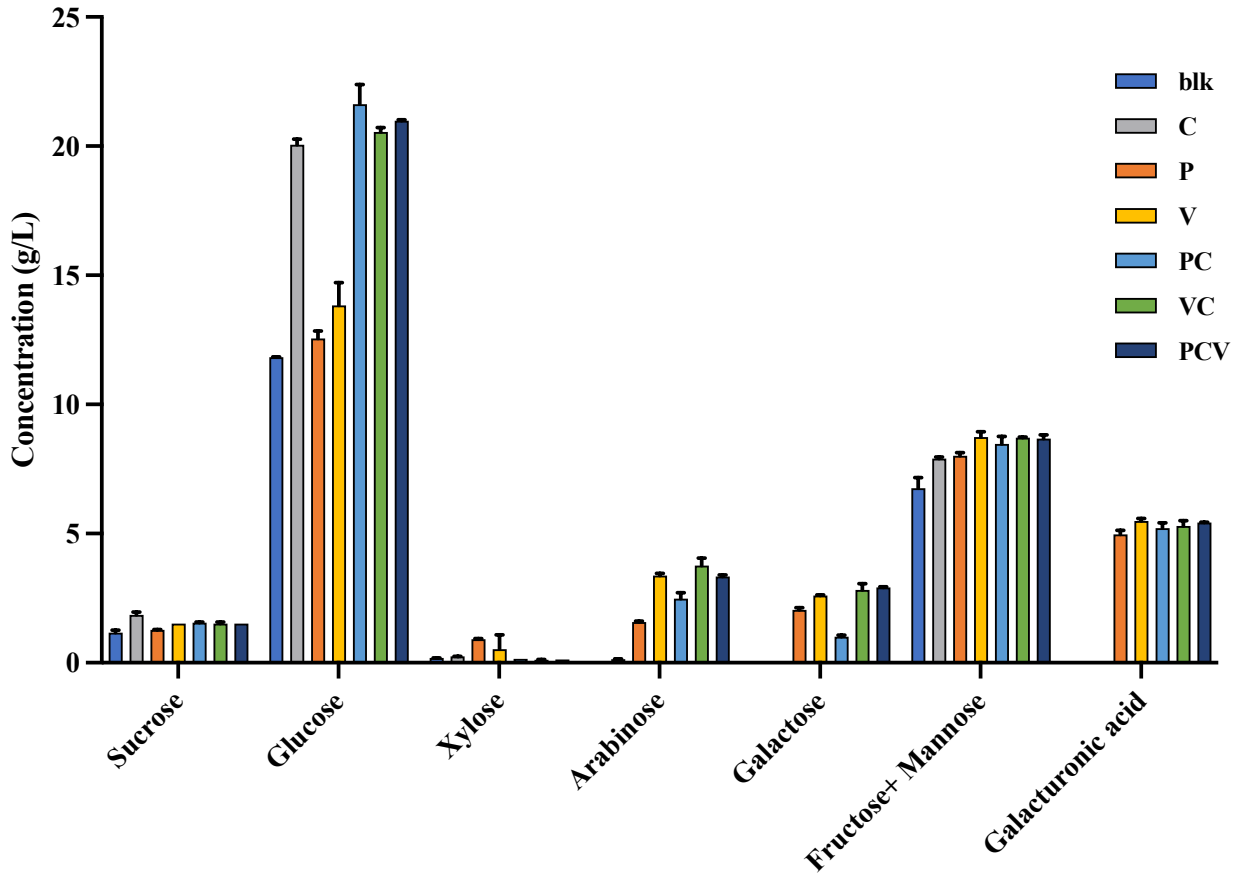

Figure 5. 8. Individual sugar concentrations after 24 hours hydrolysis.

Y error bars are standard deviation. (blk - no enzyme; C- Cellic CTec2 only; P-Pectinex Ultra SPL only; V- Viscozyme L only; PC- Pectinex Ultra SPL + Cellic CTec2; VC- Viscozyme L + Cellic CTec2; PCV: Pectinex Ultra SPL + Cellic CTec2 + Viscozyme L)

The recoverable sugar yield and total sugar yield are highly related to the liquefication and sugar concentrations, which are depicted in Figure 5.9 and Figure 5.10, respectively. As the samples treated by VC exhibited the highest total sugar concentration and liquefaction efficiency, the highest total and recoverable sugar yields were also found in the VC treatment after 24 hours.

Those were 36.80% and 20.15%, implying that 16.65% sugar were dissolved in the water in solid phase.

To conclude, the combination of V and C enzymes was the most effective compared to the other treatments and could be adopted in future experiments. After 24 hours of hydrolysis by VC, the pectin conversion was 66.56% (g/g pectin), the total conversion of hemicellulose and cellulose was 54.83% (g/g hemicellulose + cellulose), and the total fiber conversion was 58.14% (g/g hemicellulose+ cellulose + pectin). The distribution of individual sugars in the hydrolysate is illustrated in the provided Figure 5.11. Nearly half (47.12%) of the sugars were glucose, while the second most abundant group was fructose + mannose (19.90%). All those sugars could be utilized by *A. awamori*. Improved fiber conversion could potentially be attained by increasing the loadings of enzymes, which would be examined in the subsequent studies.

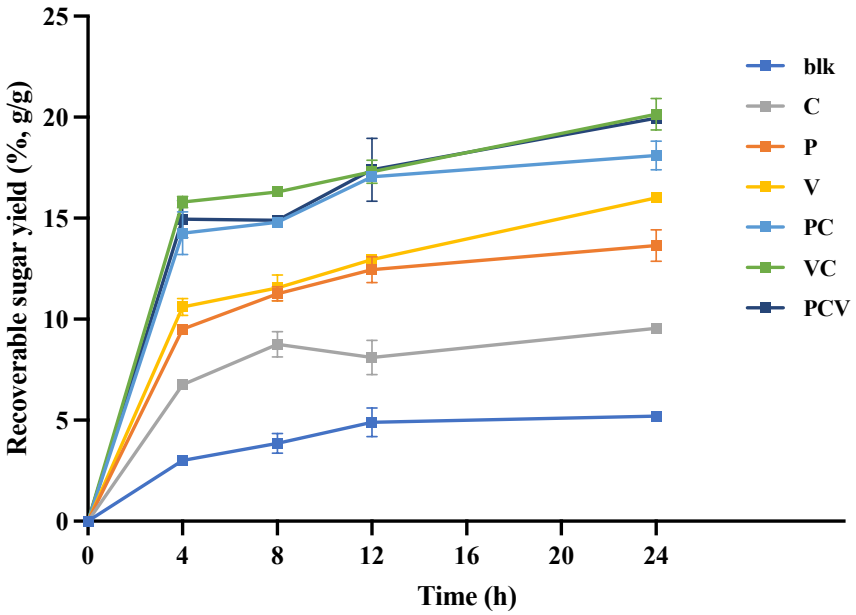

Figure 5. 9. Recoverable sugar yield from RAHS hydrolyzed by different enzymes.

Y error bars are standard deviation. (blk - no enzyme; C- Cellic CTec2 only; P-Pectinex Ultra SPL only; V- Viscozyme L only; PC- Pectinex Ultra SPL + Cellic CTec2; VC- Viscozyme L + Cellic CTec2; PCV: Pectinex Ultra SPL + Cellic CTec2 + Viscozyme L)

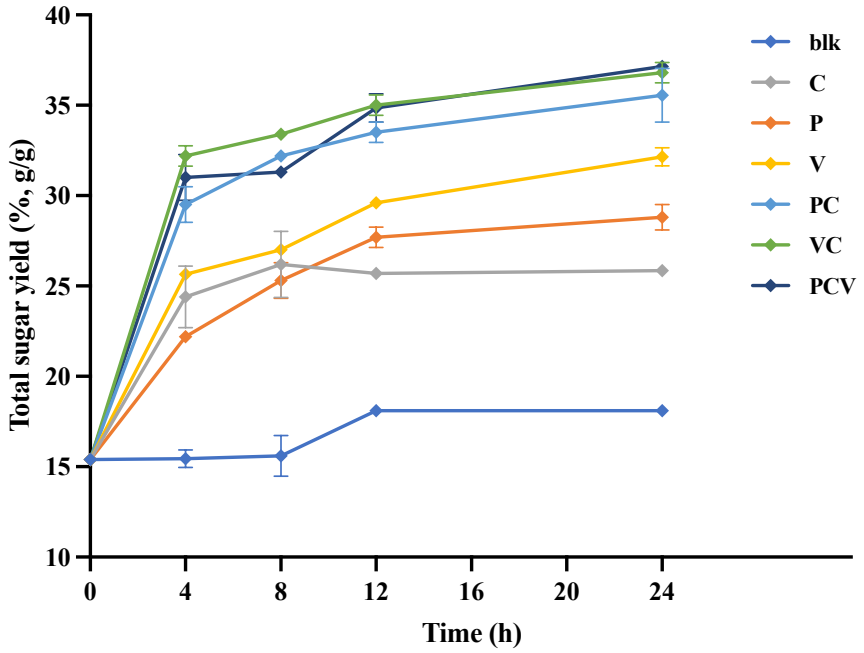

Figure 5. 10. Total sugar yield from RAHS hydrolyzed by different enzymes.

Y error bars are standard deviation. (blk - no enzyme; C- Cellic CTec2 only; P-Pectinex Ultra SPL only; V- Viscozyme L only; PC- Pectinex Ultra SPL + Cellic CTec2; VC- Viscozyme L + Cellic CTec2; PCV: Pectinex Ultra SPL + Cellic CTec2 + Viscozyme L)

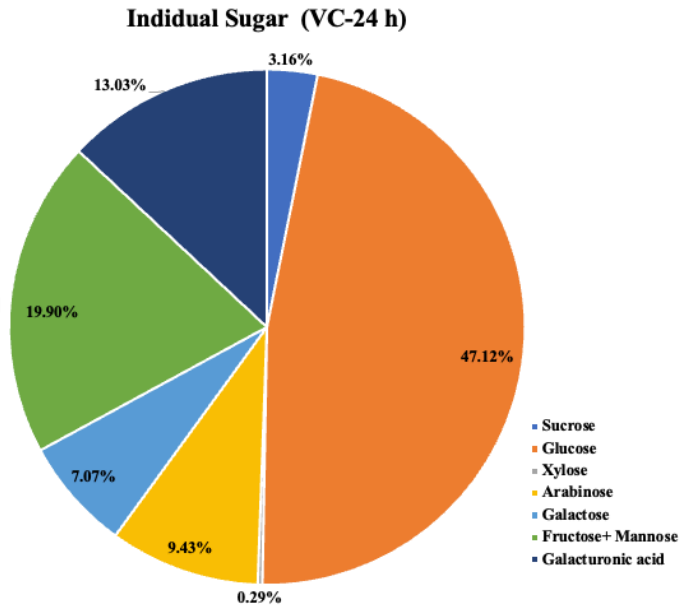

Figure 5. 11. Distribution of individual sugar yield in hydrolysate hydrolyzed by VC for 24 hours

(VC- Viscozyme L + Cellic CTec2)

5.4.3 Determination of enzyme loadings

The effects of different loadings of Cellic Ctec2 (C enzyme) and Viscozyme L (V enzyme) on RAHS hydrolysis were investigated. As depicted in Figure 5.12, a more noticeable increase in liquefaction was observed with rising loadings of C enzyme compared to increasing loadings of V enzyme. This may be attributed to the more significant variations in the quantities of C enzyme used (50 uL/g RAHS) compared to V enzyme (10 uL/g RAHS). Figure 5.13 provides a visual representation of the difference in liquefaction between varying loadings of V and C enzymes. Increase the loadings of C enzyme led to a more noticeable reduction in particle size, transforming larger particles into a more uniform slurry, and facilitating the release of more liquid. The highest level of liquefaction, 54.83%, was achieved when 250 uL/g of the C enzyme was combined with 40, 50, or 60 uL/g of the V enzyme. No significant difference (p value > 0.05) was found between the studied enzyme combinations. The lowest level of liquefaction, 42.44%, was observed when 50 uL/g of the C enzyme was mixed with 20 uL/g of the V enzyme. The difference in liquefaction between the highest and lowest levels was around 12%, which corresponded with a difference of 200 uL/g in C enzyme loading and 20 uL/g in V enzyme loading.

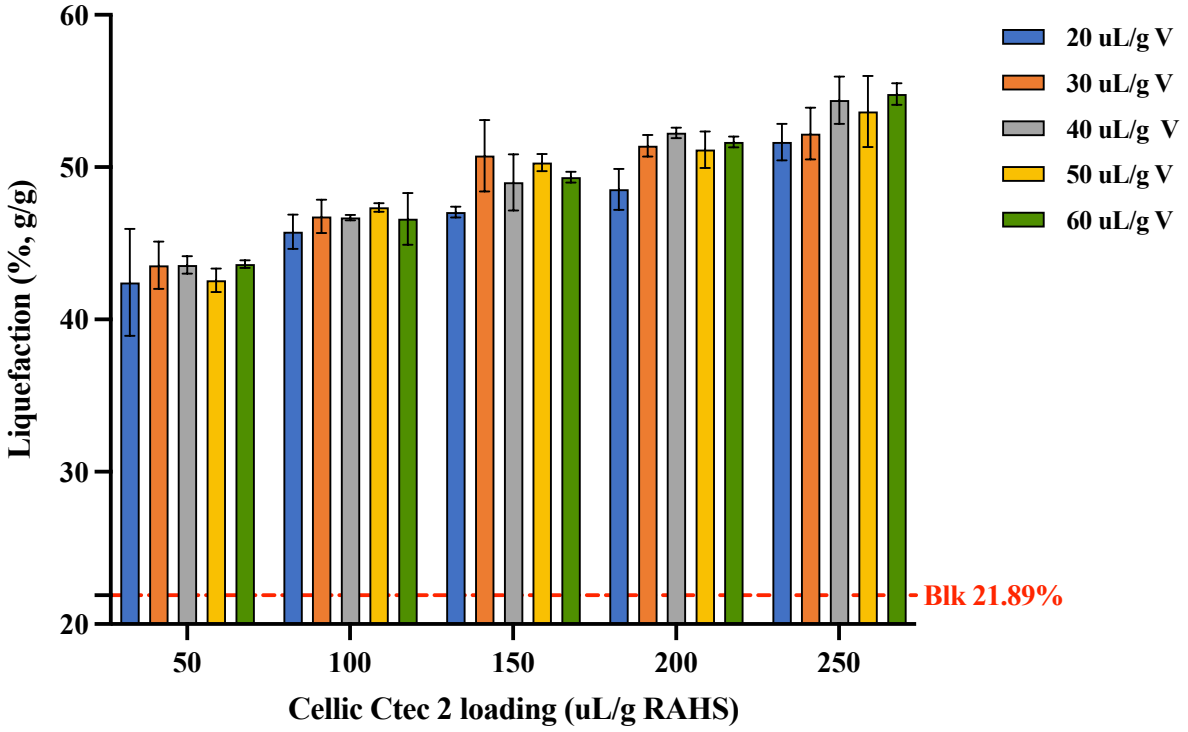

Figure 5. 12. Liquefaction of RAHS hydrolyzed by different enzyme loadings.

Y error bars are standard deviation.

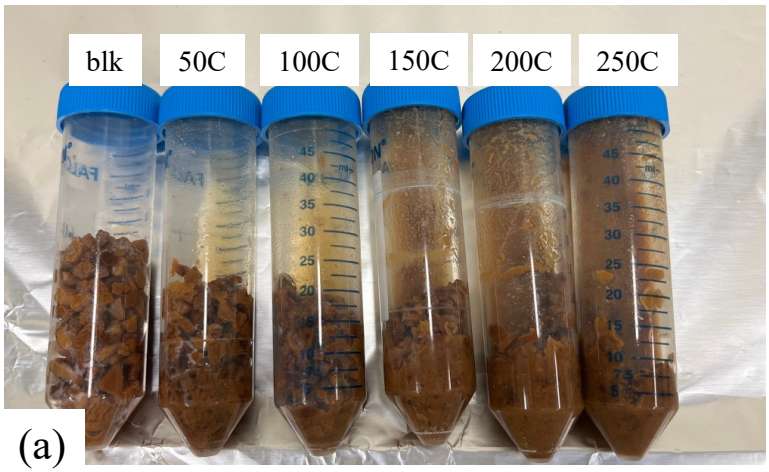

Viscozyme L: 20 uL/g

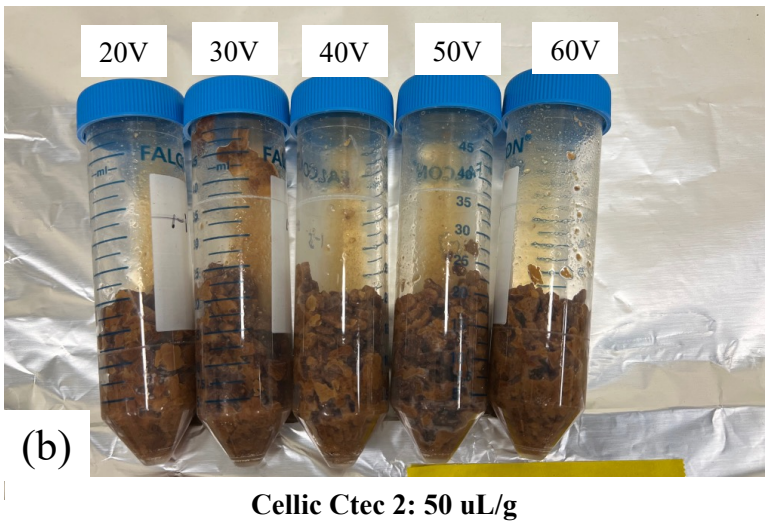

Figure 5. 13. Samples hydrolyzed by different enzyme loadings: (a) Viscozyme L loading fixed, Cellic Cetc 2 loading varied; (b) Cellic Cetc 2 loading fixed, Viscozyme L loading varied.

The recoverable and total sugar yields from RAHS, hydrolyzed by different enzyme loadings for 24 hours are depicted in Figure 5.14 and Figure 5.15. The recoverable and total sugar yields showed an increase with higher C enzyme loadings. The total sugar yields increased with the increase in V enzyme loadings due to the corresponding increase in galacturonic acid yield (from 4.73% to 5.90%, when V enzyme loadings were increased from 20 uL/g to 60 uL/g). However, the effect of C enzyme loadings on total galacturonic acid was not significant.

The highest total sugar yield was obtained with either 200 uL/g C mixed with 60 uL/g V or 250 uL/g C mixed with 50 uL/g V or higher V loadings, with no significant difference, achieving a total sugar yield around 47.21%. To use fewer total enzymes for hydrolysis, mixing 200 uL/g C with 60 uL/g V would be recommended for RAHS hydrolysis. Under these conditions, 88.11% of the total amount of cellulose and hemicellulose and 79.66% of pectin were hydrolyzed. The total fiber conversion was higher than 85%, specifically 86.01%. Under these optimal conditions, the recoverable sugar yield was around 26.43%, indicating that approximately 20% of the sugars were

dissolved in the water in the remaining solid. The measured total sugar concentration at this optimum condition was 56.40 g/L. In order to utilize the hydrolysate for fungal cultivation, the sugar concentration needs to be diluted to 20 g/L. The water planned for dilution could be used to wash the residual solids after hydrolysis first in order to extract more sugars and prevent excessive water usage.

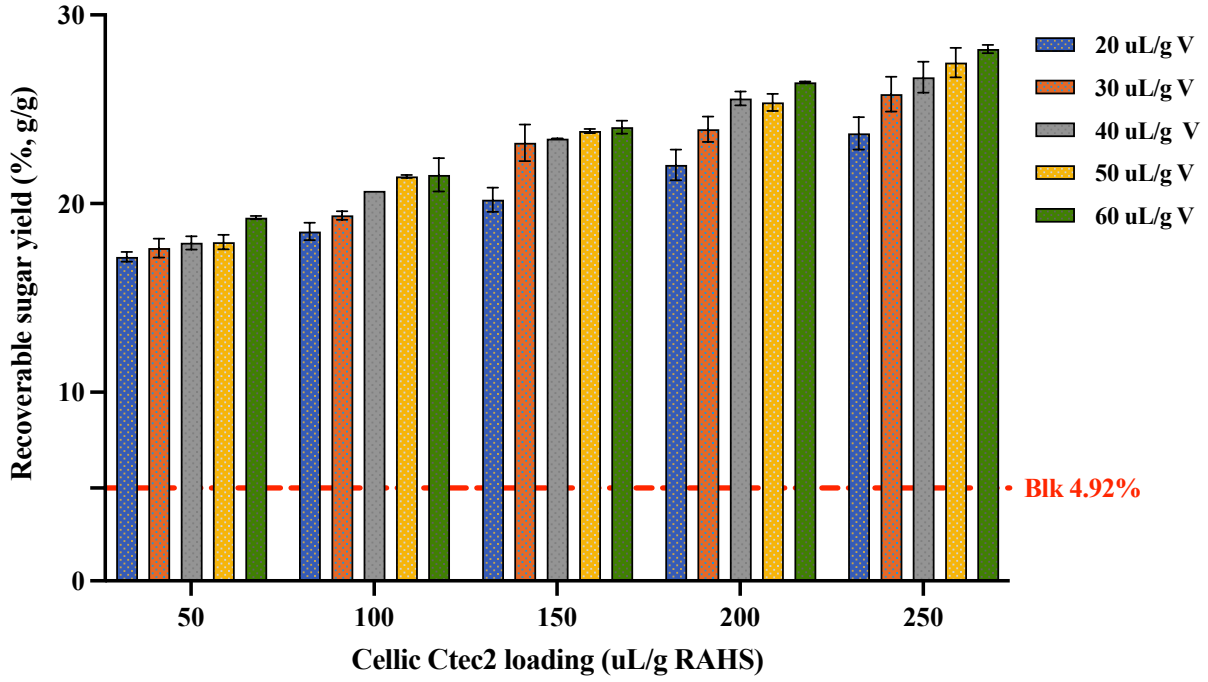

Figure 5. 14. Recoverable sugar yield from RAHS hydrolyzed by different enzyme loadings. Y error bars are standard deviation.

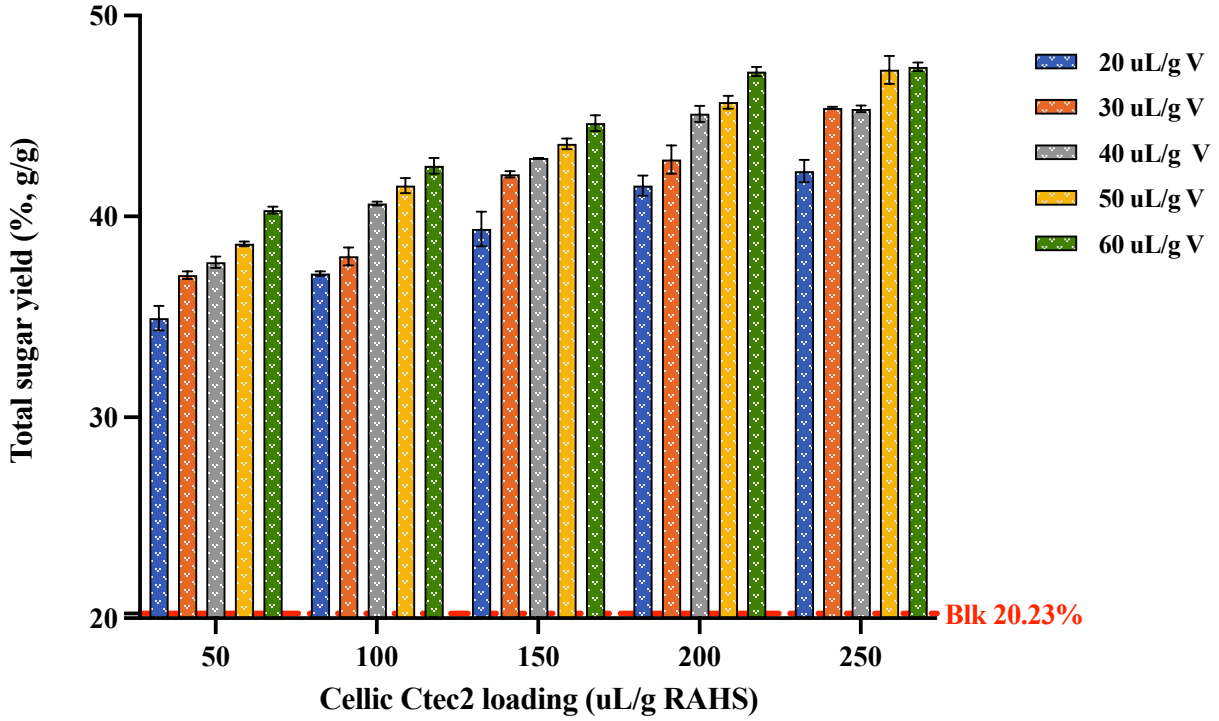

Figure 5. 15. Total sugar yield from RAHS hydrolyzed by different enzyme loadings. Y error bars are standard deviation.

The proportions of individual sugar yields under optimal conditions are depicted in Figure (5.16). Since the ratio of C to V enzymes loadings was the same as discussed in the previous section (5.3.2), which were in a 10:3 ratio, the proportions of individual sugar yields were similar. Glucose was the largest portion, accounting for 48.40% of the total sugar yield. The second-largest portion was the yield of fructose + mannose, which constituted 16.14% of the total sugar yield. In the previous section, fructose + mannose comprised 19.90% of the total sugar. This reduction could be due to the fact that most of the fructose originated from the initial RAHS; as more sugars are released during hydrolysis, the proportion of fructose diminishes. Galacturonic acid and arabinose

also constituted significant portions of the total yield. Understanding the composition of the hydrolysate is important in designing experiments for fungal cultivation.

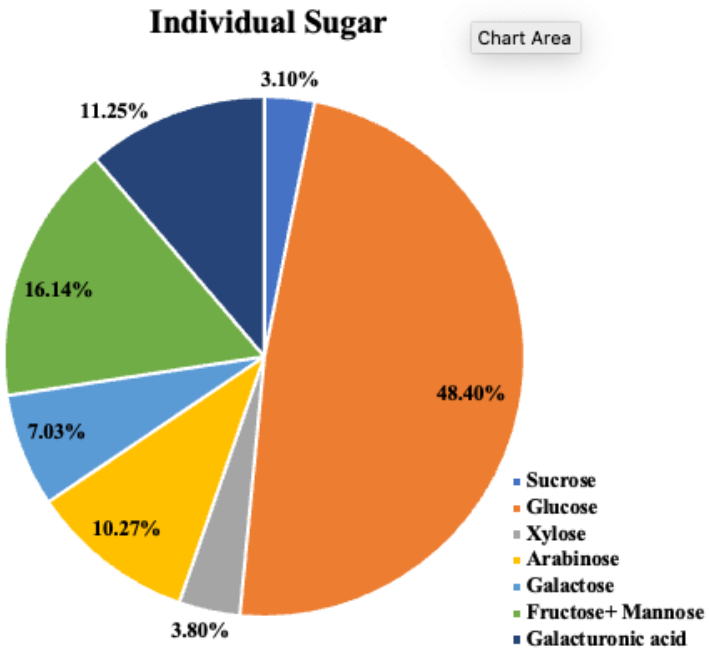

Figure 5. 16. Portions of individual sugar yield at optimum conditions (60 uL/g RAHS Viscozyme L, 200 uL/g RAHS Cellic Cetc2)

5.4.4 Large-scale enzyme hydrolysis

As determined from previous small-scale studies, a mixture of 200 uL/g RAHS of Cellic Cetc2 enzyme and 60 uL/g RAHS of Viscozyme L enzyme was used to hydrolyze RAHS on a large scale in 250 mL glass bottles. After hydrolyzing at 50°C for 24 hours, solid and liquid were separated and analyzed. Figure 5.17 depicts how large particles were hydrolyzed into homogeneous slurry-like solids. A noticeable change observed in the large-scale hydrolysis process compared to small-scale falcon tube hydrolysis was the better mixing and movement of the solid-liquid mixture in the bottle after hydrolysis due to the liquefaction. The initially solid-

dominated samples transitioned into a liquid-dominated phase after hydrolysis for 24 hours. Figure 5.17 (C) offers a more visual perspective, showing the samples after centrifugation. It's clear that the supernatant occupied the majority of the bottle, with only a small amount of solids settling at the bottom.

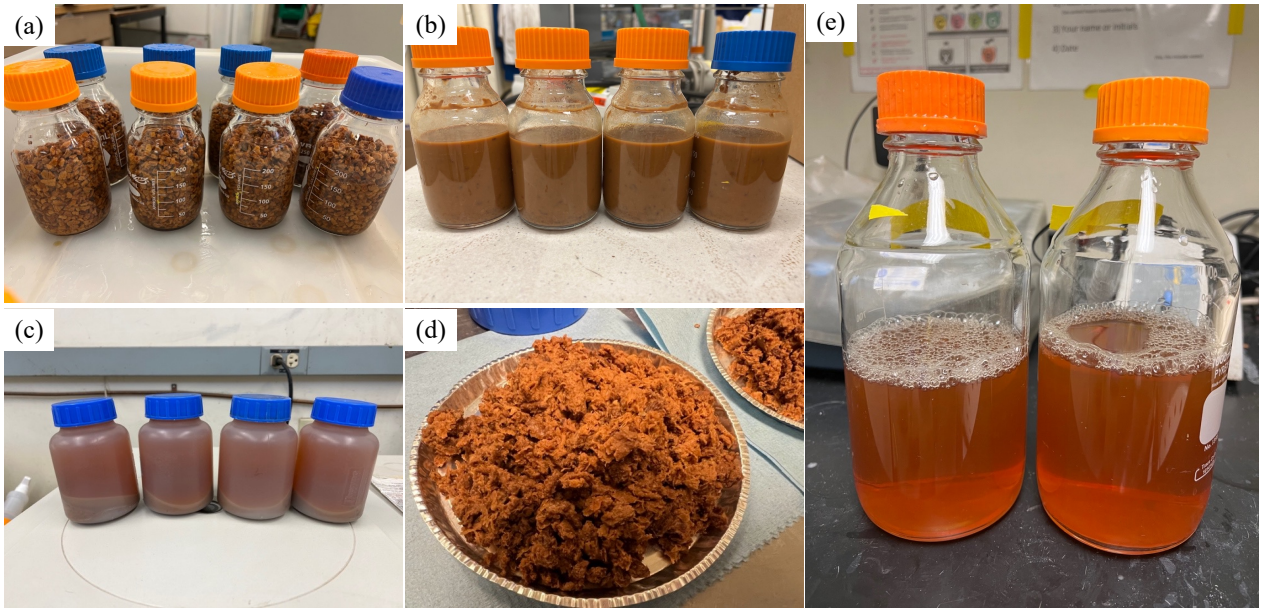

Figure 5. 17. Large scale enzyme hydrolysis of RAHS. (a) RAHS in 250 mL glass bottles before hydrolysis; (b) RAHS in 250 mL glass bottles after hydrolysis; (c) liquid and solid separation in 500 mL centrifuge bottles after centrifugation; (d) residual solids after hydrolysis; (e) hydrolysate after filtration.

After decanting and weighing the supernatant, a liquefaction efficiency of 72.53% was calculated. This large-scale liquefaction efficiency significantly exceeded that of the small scale, which was determined to be at 51.61%. However, the total sugar concentration in the supernatant from the large scale was lower than that of the small scale. Despite higher liquefaction efficiency, the total sugar yield didn't increase, but the recoverable sugar yield increased from 26.43% (small scale) to 38.61% (large scale). The detailed comparisons of small- and large-scale hydrolysis were tableted in Table 5.4. The higher liquefaction at the large scale wasn't due to increased fiber

conversion, as the total fiber conversion was comparable or even lower at the large scale (83.63%) compared to the small scale (86.01%). One potential explanation could be that the glass bottles provided better mixing than the falcon tubes. The conical shape of the falcon tubes might not be ideal for handling solids or solid-liquid mixtures. The narrow bottom could inhibit the movement and dispersion of solid particles, thereby making mixing less efficient. Conversely, the more effective mixing in glass bottles could facilitate better interaction between the enzymes and samples and potentially change the structure of the samples, leading to the release of more liquid.

To conclude, small-scale and large-scale hydrolysis proved comparable to one another when considering total sugar yield or fiber conversion. However, large-scale production using glass bottles showed a significant advantage in achieving higher liquefaction and recoverable sugar yield. This advantage enabled the recovery of more liquid from the original samples, potentially saving water usage in downstream processes. It might also save the cost to manage residual solid waste.

Table 5. 4. Comparison of small- and large- scale enzymatic hydrolysis of RASH

	Small Scale (20 g)	Large Scale (200 g)
Liquefaction (%, g/g)	51.61± 0.34	72.53± 0.56
Galacturonic acid concentrations (g/L)	6.40 ± 0.09	5.88 ± 0.17
Galacturonic acid yield (%, g/g RASH)	5.85 ± 0.09	5.58 ± 0.01
Total other sugar concentration (g/L)	50.00 ± 0.23	47.36 ± 3.53
Total other sugar yield (%, g/g RASH)	41.36 ± 0.14	41.05 ± 0.09
Total sugar yield (%, g/g RASH)	47.21± 0.23	46.03± 0.10
Recoverable sugar yield (%, g/g RASH)	26.43 ± 0.05	38.61± 0.30
Cellulose+ hemicellulose conversion (%)	88.11 ± 0.57	86.68 ± 0.35
Pectin conversion (%)	79.66 ± 1.20	75.87 ± 0.16
Total fiber conversion	86.01 ± 0.75	83.63 ± 0.30

5.4.5 Fungal growth in almond hull hydrolysate

A. awamori formed uniform pellets in almond hull hydrolysate and exhibited orange-yellow color (Figure 5.18). Unlike the cultivation in almond hull extract, which resulted in brown pellets, both of the pellets had similar color as the media. This observation suggests that most of the brown pigments were likely removed by water during the sugar extraction process.

After five days cultivation, 49.09 ± 2.38% of the initial sugars were consumed lead to a growth of 9.37 ± 0.05 g VSS/L biomass. The biomass yield was 0.80 ± 0.03 g VSS/g sugar. This study demonstrated that almond hull extract was a good source for fungal biomass cultivation, leading to good morphology and high biomass yield. Given the unique morphology of fungal pellets, it's important to harvest the fungal biomass before all the sugar is consumed. This is to prevent biomass loss due to autolysis that occurs at the center of the pellets.

As mentioned in previous section, the hydrolysate was generated from the optimum condition: using a mixture of 200 uL/g RAHS of Cellic Cetc2 enzyme and 60 uL/g RAHS of Viscozyme L enzyme. The total amount of glucose, fructose and mannose accounted for 64.54% of the total sugar, which were the preferred sugar sources for most of the fungi growth (Hamad et al., 2014), while galacturonic acid accounted for 11.25%. Even though *A. awamori* is known for pectinase production (Baladhandayutham & Thangavelu, 2011; Dey et al., 2014; Umsza-Guez et al., 2011b) and is capable of utilizing galacturonic acid, the 10% of galacturonic acid in almond hull hydrolysate did not get a chance to be consumed before fungal harvesting as glucose was consumed first. Given that the pectinase loading significantly influenced the yield of galacturonic acid in the hydrolysate and the high price of pectinase, a lower pectinase loading is suggested to reduce the galacturonic acid yield while maintaining a high yield of all other sugars. Based on this criterion, lowering Viscozyme L loadings from 60 uL/g to 40 uL/g RAHS and maintaining 200

uL/g RAHS of Cellic Cetc 2 enzyme was recommended, which led to total sugar (except for galacturonic acid) yield of 39.66% ± 0.37%. A detailed comparison of hydrolysis performance at this suggested enzyme loadings with the previous established optimum loadings at small scale are shown in Table 5.5. There was no significant difference in liquefaction (p value = 0.82) and recoverable sugar yield (p value = 0.82) between the optimal and suggested enzyme loadings. The total sugar yield and fiber conversion efficiency were lower with the suggested enzyme loadings, due to the reduced Viscozyme L loadings. Given the high cost of pectinase (around $16/kg) (Y. Chen, 2020), a slight reduction in sugar yield is acceptable when compared to the associated enzyme costs.

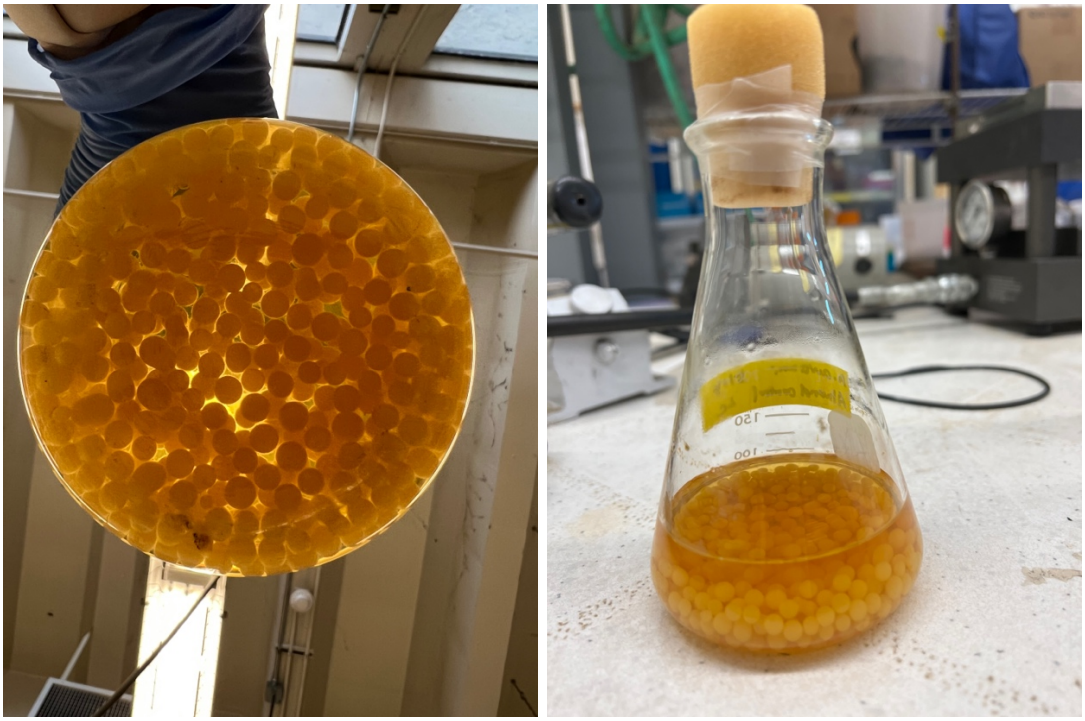

Figure 5. 18. A. awamori pellets grow in almond hull hydrolysate

Table 5. 5. Comparison of hydrolysis performance at optimum and suggested enzyme loadings

Enzyme loading per g RAHS	**Optimum** 200 uL C/g; 60 uL V/g	**Suggested** 200 uL C/g; 40 uL V/g
Liquefaction (%, g/g)	51.61± 0.34	51.48± 0.68
Galacturonic acid yield (%, g/g RASH)	5.85 ± 0.09	5.45 ± 0.02
Total other sugar yield (%, g/g RASH)	41.36 ± 0.14	39.66 ± 0.37
Total sugar yield (%, g/g RASH)	47.21± 0.23	45.11± 0.39
Recoverable sugar yield (%, g/g RASH)	26.43 ± 0.05	25.21 ± 0.54
Cellulose+ hemicellulose conversion (%)	88.11 ± 0.57	81.39 ± 1.48
Pectin conversion (%)	79.66 ± 1.20	74.18 ± 0.28
Total fiber conversion	86.01 ± 0.75	79.64 ± 1.14

5.5 Conclusions

The composition of residual solids after sugar extraction from almond hulls (RAHS) included 14.81% sugar, and a total of 35.19% cellulose, hemicellulose, and pectin. An optimal enzymatic combination of Cellic CTec2 and Viscozyme L, applied at 50℃ with a 200 rpm shaking speed in 50 mL falcon tubes, showed the most effective hydrolysis of RAHS. Both pectinase and cellulase enzymes demonstrated significant contribution to the liquefaction process. Specifically, pectinase played a crucial role in liquefaction, while cellulase was mainly responsible for glucose release.

There was a more significant increase in liquefaction with increasing cellulase loadings compared to increased pectinase loadings, potentially due to larger variations in cellulase quantities used. Utilizing 200 uL/g RASH of Cellic CTec2 and 60 uL/g RASH of Viscozyme L for a period of 24 hours yielded a total sugar yield of 41.36% (g/g RAHS), total fiber conversion of 86.01% (g/g fiber), and a liquefaction efficiency of 51.61%. These optimal conditions, when applied at a larger scale in 250 mL glass bottles, led to a higher liquefaction efficiency of 72.53%.

However, the sugar yield remained comparable between both scales. The sugars in the hydrolysate produced at the optimum conditions were analyzed. Around half (48.40%) of the sugar in the hydrolysate was glucose, followed by a combined of fructose + mannose, which accounted for 16.14% of total sugar composition.

After five days fungal cultivation in flasks, uniform yellow fungal pellets were formed, with a biomass yield of 0.8 g VSS/g sugar. Due to the high proportions of glucose and fructose in the hydrolysate and *A. awamori*'s preferential consumption of these sugars, the main sugar released by pectinase, galacturonic acid, was not utilized by the fungi at any stage of cultivation. Consequently, a reduction in pectinase loading levels is suggested to lower galacturonic acid yield while maintaining high yields of other sugars. The recommended enzyme loadings include 40 uL/g RAHS of Viscozyme L and 200 uL/g RAHS of Cellic CTec2, leading to a total sugar yield (excluding galacturonic acid) of 39.66%. Neither liquefaction nor recoverable sugar yield showed significant differences between the optimal and recommended enzyme loadings, making it more economical by lowering enzyme levels.

This study demonstrated that RASH could be a potential source for fungal-based food production. The processes developed in this study not only enhances sustainability but also increases the overall yield of fungal biomass from fungal biomass. Based on the results from this study, around 300 kg of fungal biomass can be produced from one tone of almond hulls. Consequently, the implications of this research could potentially bring benefits to both the almond and food industries.

Chapter 6 Techno-Economic Analysis of an Industrial-scale System for Producing Myco-foods from Almond Hulls

6.1 Abstract

Producing myco-foods from agricultural byproducts is a promising process from both economic and byproduct management points of view. A techno-economic analysis was conducted for an industrial-scale system for the production of *Aspergillus awamori* fungal biomass. Almond hulls, a byproduct from the almond processing industry, were utilized as the feedstocks, with an input of 50 MT/batch. SuperPro Designer software was used for processes simulation and economic assessment. Two different scenarios were evaluated: the first system was using sugar extract alone as a source of nutrients needed for fungi cultivation and the second was similar to the first system plus the nutrients produced from the enzymatic hydrolysis of residual almond hull solids after sugar extraction. A sensitivity was carried out for studying different parameters affecting the breakeven price of fungal biomass as almond hull price and facility processing capacity. The simulated systems produced approximately 2,971 MT/year fungal biomass from around 16,000 MT/year hulls (w.b.) without enzymatic hydrolysis, and around 4,653 MT/year fungal biomass with enzymatic hydrolysis with the same amount of almond hulls. The breakeven price of the fungal biomass from both systems ranged around $6 -7 per kg of fungal biomass (dry basis). The system excluding enzymatic hydrolysis exhibited a higher sensitivity to both almond hull price and facility scale. This study indicates that using almond hulls as feedstock could potentially myco-foods competitive in markets for proteins, probiotics, and other food categories, benefiting both the almond and food industries.

6.2 Introduction

The global food system is faced with the challenge of feeding a growing population while minimizing environmental impact (Matassa et al., 2016). One sustainable solution is to convert agricultural waste/byproducts into value-added products, such as myco-foods. Almond hulls, a byproduct of the almond industry, presented a high potential to be used for fungal biomass production. Their conversion into myco-foods through bioprocessing not only create a sustainable food source but also offers a byproduct management solution, creating a circular economy within the agricultural sector. However, implementing such a concept on an industrial scale requires a thorough understanding of the technical and economic aspects of the process. Techno-economic analysis provides an insightful tool for this purpose, evaluating the financial viability of the process while considering its technical complexities. This analysis combines the process modeling with economical evaluations to determine the feasibility of the proposed production system.

A key component of the techno-economic analysis conducted is the evaluation of the breakeven price. This is the minimum price at which products must be sold in the market to cover all costs associated with its production. This parameter is particularly significant as it provides an indicator of the product's potential competitiveness in the marketplace and the price range that the products can sustain. Uncertainties exist in various aspects of the production system. Sensitive analysis can explore the uncertainties and enhance the understanding on the system's financial feasibilities. This investigation involves varying certain factors, such as feedstock cost, other raw material cost, capital cost, and system scale (Z. Liu et al., 2016; Okolie et al., 2021; Song & Ozkan, 2010).

This study aimed at conducting a techno-economic analysis of an industrial-scale system for producing myco-foods from almond hulls and comparing the economic performances of

different model scenarios. The objectives of this research were to: (1) develop a process simulation model for an industrial scale fungal-based food production system; (2) create and investigate the alternative scenarios involving producing fungal-based from almond hull extracts or mixture of almond hull extract with residual almond hull solids (RAHS) hydrolysate; and (3) evaluate and compare the economic performance of selected scenarios using breakeven analysis and sensitivity analysis.

6.3 Materials and Methods

6.3.1 Process and model development

The simulation model of myco-foods production from almond hulls was developed using SuperPro Designer Software v12.0 (Intelligen Inc., USA). Almond hulls were utilized as the feedstock in the model. There is around 2.2 million metric ton (MT) of almond hulls generated in California each year from around 100 almond processors (Almond Board of California, 2022). The capacity of this simulated facility was able to process 50 MT of almond hulls (wet basis, w.b.) (around 3 truck loads) per batch, which is the amount of daily average almond hulls generated from one almond processor in California. The assumptions and estimations for designing this model were based on lab and bench scale experiments or communications with experienced people.

As shown in Figure 6.1, there were 11 essential unit operations involved in the flowsheet of the production system (Scenario 1), which are operated to convert almond hull nutrients into myco-foods. The unit operations involved in this system were: grinding, heating, extraction, screw pressing, extract mixing, microfiltration, media mixing, pasteurization, fungal cultivation, stationary screening and washing. As the general description of the process, almond hulls collected from almond processers were first gone through the grinding process to break down into small particles and be used for nutrients extraction by hot water. The solids after extraction were

squeezed by screw press to get more extract. Fine solids in almond hull extract were removed by microfiltration. Before utilizing the almond hull extract for fungal cultivation, water and extra nutrients were added to adjust initial sugar concentration to 20 g/L and C/N ratio to 15 and then pasteurized. After five days cultivation in a bioreactor, fungal pellets were harvested from the media by a stationary screening and washed to remove residual metabolites and nutrients obtained from the media. Finally, this process would produce wet clean fungal pellets with a moisture content of 95%.

Based on previous lab scale experiments (Chapter 5), 49.5% of the initial almond hulls was left over after extraction, which could be further utilized for fungal cultivation by enzymatic hydrolysis. Scenario 2 (Figure 6.2) included utilization of residual almond hull solids (RAHS) after extraction. Comparing with the base Scenario (Scenario 1), three more operations were involved in this process, which were enzyme hydrolysis, centrifugation and ultrafiltration. Approximately 70% of enzymes were recycled by ultrafiltration in Scenario 2 in order to reduce the raw material cost. The capacity of both scenarios was processing 50 MT (wet basis, w.b.) of almond hulls per batch.

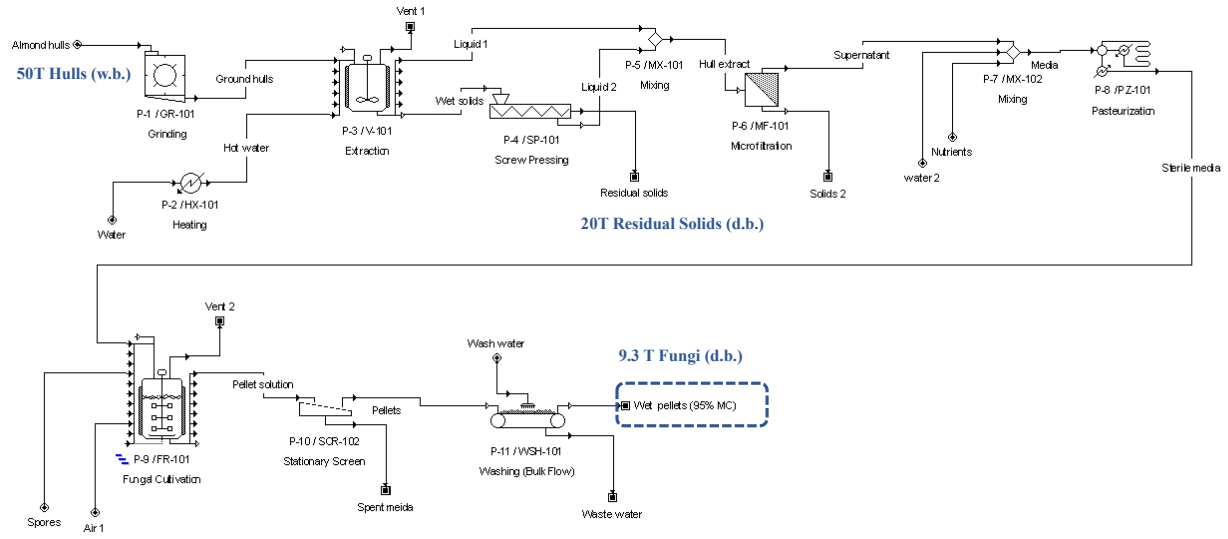

Figure 6. 1. A process flowsheet for myco-foods production from almond hulls (Scenario 1)

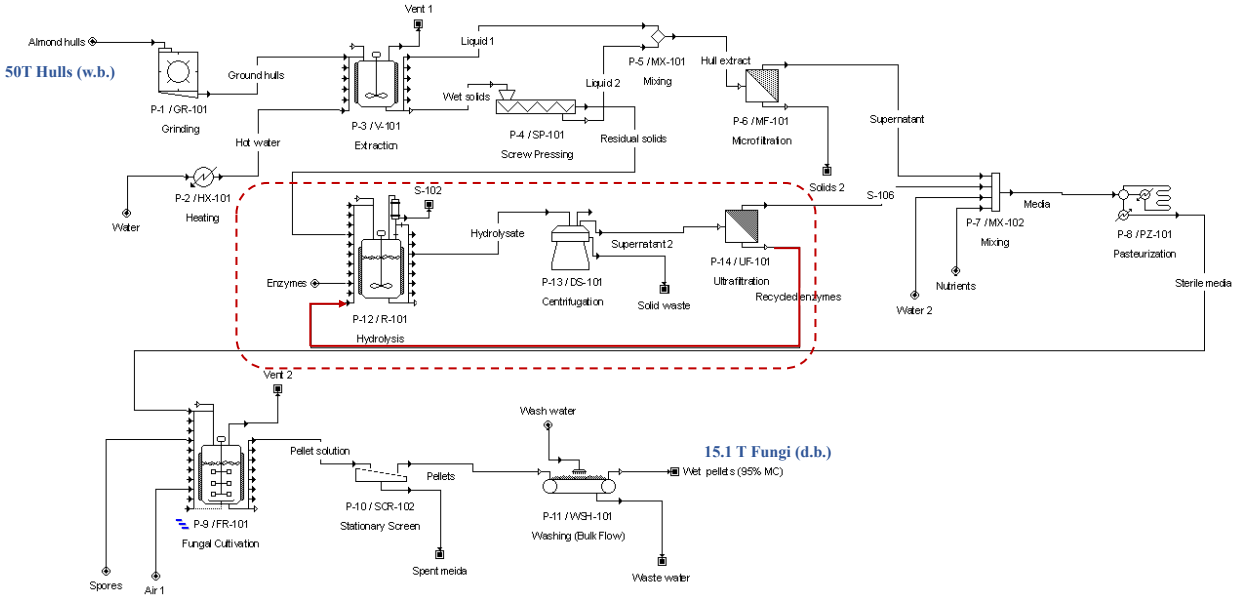

Figure 6. 2. A process flowsheet for myco-foods production from almond hulls with enzymatic hydrolysis of residual almond hull solids and enzyme recycle (Scenario 2)

6.3.2 Unit operations

6.3.2.1 Grinding

Grinding is the first operation for the whole process. The 50 MT/batch (w.b.) of hulls are firstly ground into small particles before extraction. A grinder with maximum throughput of 60 MT/h and a corresponding electric power input rating of 3 kW/MT/h is used in this simulated model. The grinder is set to work at around 80% of its maximum capacity, enabling it to process 50 MT hulls in an hour. Right after grinding, all the ground hulls are transferred to the following extraction process.

6.3.2.2 Heating, extraction and pressing

Water is preheated from room temperature (25℃) to 80℃ by a spiral heat exchanger, with a maximum heat transfer area of 150 m^2. Water (611.5 MT/batch) is heated in two hours using 134 m^2 of the heating aera. The preheated water is then transferred into the blending tank (V-101) and mixed with ground hulls, leading to the liquid to solid ratio of 14 as determined from lab scale experiment (Chapter 2). The tank had a maximum size of 850 m^3. This extraction process takes 90 min with a continuous agitation. After extraction process, liquid and solids are transferred out separately. The wet solids which have a moisture content around 90% are sequentially squeezed by a screw press, with an operating throughput of 69 MT/h, in order to get more liquid extract is used. Therefore, it takes three hours to press 207 MT of wet solids. After this screw pressing, around 104 MT of extract is mixed with the 453 MT extract from extraction tank forming the “Hull extract” stream as shown in both Figure 6.1 and 6.2. Meanwhile, there are 104 MT of residual solids left over, which has a moisture content of 80%.

After these unit operations, 18.7% water soluble nutrients and water are lost in solid phase and transferred out together with the insoluble solids from the “Residual solids” stream as a solid

waste in Scenario 1 or utilized for enzymatic hydrolysis in Scenario 2. The "Hull extract" stream was assumed to have 5% of solids, which has to be further removed. The steam contains 2.53% sugars, 1.70% other soluble nutrients, 0.07% solids and 95.7% water.

6.3.2.3 Microfiltration, mixing, and pasteurization

Solids in the almond hull extract are removed by membrane microfiltration with a maximum membrane aera of 1200 m^2. The duration of microfiltration is set to be four hours per batch for both scenarios, with a filtrate flux rate of 120 L/m^2-h. The Dft membrane is used with a replace frequency of once every 1000 hours. It is assumed that 100% solids are rejected, and 95% (v/v) liquid is recovered (filtrate/feed = 95%). The concentrates are disposed as an aqueous waste ("Waste" stream). The filtrate is then diluted with water to reach a sugar concentration of 20 g/L and mixed with yeast extract and ammonium chloride to adjust C/N ratio to 15. In the first scenario, 1.68 MT/batch ammonium chloride, 0.67 MT/batch yeast extract and 176 MT water are added to mix with 530 MT almond hull extract. In Scenario 2, due to 8.42 MT more sugars are obtained from hydrolyzing almond hull fibers, 2.78 MT/batch ammonium chloride, 1.11 MT/batch yeast extract and 435 MT water are added. The prepared media is then pasteurized at 80℃ for three hours using steam as the heating transfer agent with a 100% heat transfer efficiency. The throughput of the pasteurizers used in Scenarios 1 and 2 are 239 m^3/h (maximum = 250 m^3/h) and 373 m^3/h (maximum = 400 m^3/h), respectively. Chilled water is used to cool the pasteurized media to 30℃ for later fungal cultivation.

6.3.2.4 Fungal cultivation

Aspergillus awamori (*A. awamori*), as an edible fungal biomass, is cultivated on almond hull nutrients. In this process, fungal spores are inoculated into the sterile media. Forced aeration is provided at a constant rate of 1 volume per volume per minute (vvm) during the fungal

cultivation. Other conditions are also controlled during the cultivation: continuous agitation, temperature (30℃) and venting. The specific power for the fermenter is 1 kW/m^3 as used by Oraby et al. (2022). Each batch takes five days, ended with 75% sugar conversion and fungal biomass yield of 0.5 g/g nutrients, which are based on lab scale experiments. Fungal cultivation is the longest unit operation among the whole production process. To maximize the utilization of all the equipment, five identical stirred bioreactors (maximum volume is 900 m^3 for Scenario 1 and 1500 m^3 for Scenario 2, height/diameter = 4) are operated in a staggered batch mode. One bioreactor starts fungal cultivation each day, while another bioreactor is emptied for the next batch cultivation. All the upstream and downstream operations were kept working to prepare media for a new batch every day or process products from different bioreactors every day. An example of the equipment occupancy chart for Scenario 1 is shown in Figure 6.3. By this way, these simulated processes can produce around five-fold products each year comparing with no staggered batch mode. The amount of fungal biomass produced from each cultivation batch was 9.28 MT and 15.11 MT of from Scenario 1 and Scenario 2, respectively. The produced biomass is transferred out for downstream processing.

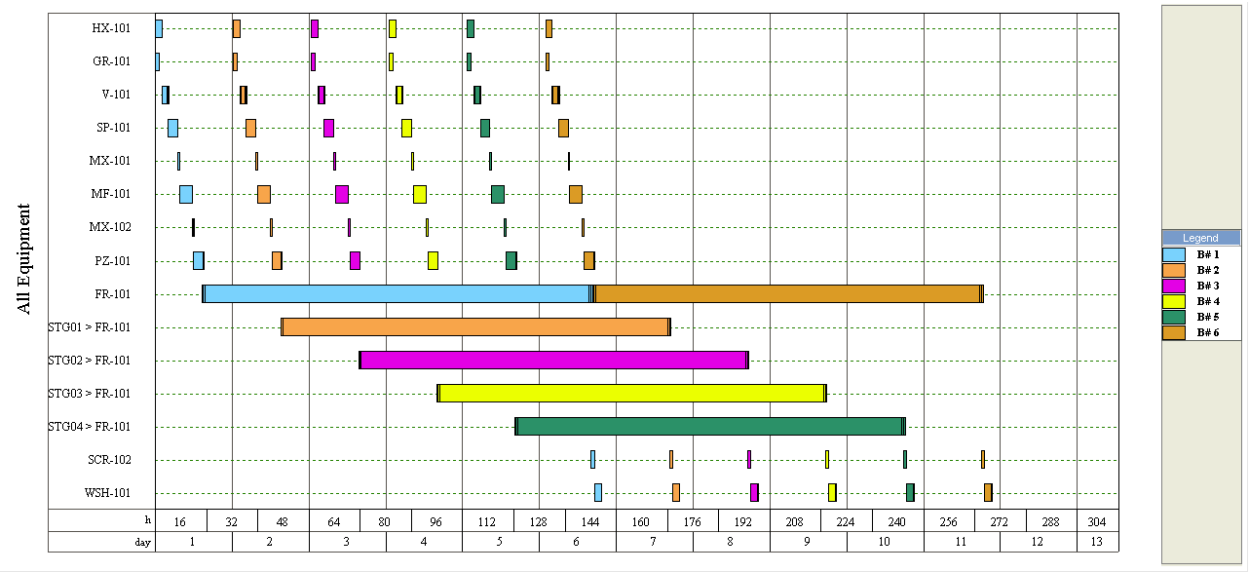

Figure 6. 3. An example of equipment occupancy chart in staggered batch production mode (Scenario 1)

6.3.2.5 Biomass harvesting and washing

A stationary screening is used to harvest fungal pellets from spent media. In Scenario 1, 707 MT/batch of fungal pellets and spent media are processed by a screen with a mesh size of 2 mm and throughput of 707 MT/h (maximum 850 MT/h) for one hour. In Scenario 2, 1,108 MT of fungal pellets and media are separated for one hour by a larger screen, which has the throughput of 1108 MT/h (maximum 1300 MT/h) and the same mesh size as Scenario 1. In both scenarios, 100% of the fungal pellets is assumed to be harvested by the screen and 75% of the spent media is left in pellets, which lead to a 95% moisture content of the harvest pellets.

Totally, 183 MT/batch of wet pellets from Scenario 1 and 288 MT/batch of wet pellets from Scenario 2 are transferred to the washing step. The amount of water used to wash out the spent media from the pellets is assumed to be the half of wet pellets' weight. It takes two hours to wash those pellets. Due to the more fungal pellets in Scenario 2, the larger washer with a higher throughput 144 MT/h is used than the one used in Scenario 1, which has a throughput of 91.5

MT/h. All the spent media and wash water are discharged as wastewater. Finally, 9.28 MT/batch and 15.11 MT /batch (dry matter) of clean fungal pellets are produced from Scenario 1 and Scenario 2, respectively, with a moisture content of 95%.

6.3.3 Additional unit operations involved in Scenario 2

Enzymatic hydrolysis, centrifugation and ultrafiltration units are added in Scenario 2 to utilize the solids after extraction process. As determined from lab scale experiments, cellulase and pectinase loadings for residual almond hull solids (RAHS) after extraction are 200 L/MT RAHS and 40 L/MT RAHS, respectively. Both enzymes are assumed to have a specific gravity of 1.2 kg/L (Zicari, 2016). Therefore, 4.80 MT of cellulase and 0.96 MT of pectinase are used for each batch. Meanwhile, 110 MT/batch of water is added to adjust the initial total solids loading of 10% (w/w). After hydrolyzing at 50℃ for 24 hours in a stirred bioreactor, which has a working volume of 257 m^3 (maximum volume = 280 m^3), the hydrolyzed feedstocks are transferred out and centrifuged in a Disk-Stack centrifuge for one hour. After centrifugation, 30% of both cellulase and pectinase are assumed to be mixed with the solid waste, and the rest 70% enzymes are in the supernatant.

An ultrafiltration unit is used to separate the 70% enzyme from the hydrolysate. In this unit operation, it's assumed that all the rest 70% enzymes are rejected (rejection factor =1) and permeate stream is 90% (v/v) of feed stream (concentration factor = 10). This process takes four hours with a filtrate flux of 80 $L/m^2/h$. Then, 3.36 MT cellulase and 0.67 MT of pectinase are recycled to the hydrolysis tank. By applying these three-unit operations, 8.42 MT/batch of more sugars are generated and will be utilized for fungal cultivation. After centrifugation, 74.60 MT/batch of residual solids is disposed as solid waste.

6.3.4 Economic evaluations

6.3.4.1 General economic evaluation parameters

Several financing assumptions and time valuation were made for economic analysis. All costs were adjusted to 2023, which was assumed as the first of year of the project. The project lifetime was 20 years, starting from the construction for six month and 3-month startup. Inflation rate was assumed to be 4%, which was the default value from SuperPro Designer. It was assumed that capital costs will be financed by 50% debt over a 20-year term with an interest rate of 9%.

6.3.4.2 Economic analysis

The economic analysis of these simulations focuses on two main components: capital cost and operating cost. The capital cost (DFC) comprises direct cost (DC), indirect cost (IC) and other cost (OC), all of them were calculated by multiplying the equipment purchase cost (EC) or IC with various factors. The estimation factors were obtained from SuperPro Designer's built-in database, which have been established and validated through the collaborative efforts of numerous experienced scientists and engineers. The utilized estimation factors are listed in Table 6.1.

Table 6. 1. Capital investment estimation factors

Cost item	Estimation factor
Direct cost (DC)	
Equipment cost (EC)	1 × EC
Unlisted equipment purchase cost	0.2 × EC
Piping	0.35 × EC
Instrumentation	0.40 × EC
Insulation	0.03 × EC
Electrical facilities	0.10 × EC
Buildings	0.45 × EC
Yard Improvement	0.15 × EC
Auxiliary facilities	0.40 × EC
Installation	0.5 × EC
Indirect cost (IC)	
Engineering	0.25 × DC

Construction	0.35 × DC
Other Cost (OC)	
Contractor's Fee	0.05 × (DC + IC)
Contingency	0.1 × (DC + IC)
Direct fixed capital cost (DFC)	DC + IC + OC

The annual operation cost (AOC) of this simulated project includes the raw materials, utilities, labor, consumables and waste treatment. The specific rates of each item are listed in Table 6.2. The price of almond hulls was calculated from the average price from 2020 to 2023. Labor costs included one supervisor at 2,080 labor-h/year (8 h/day, 5 day/week, 52 week/year) with a lumped rate of $70/h, and one QA analyst at 2,080 labor-h/year with a lumped rate of $60/h. There were four operators shifted at 2,080 labor-h/year with a lumped rate of $50/h to maintain the year-round operation of the facility.

Table 6. 2. Operation cost of model simulation

Item	Price	Unit	Source
Raw Materials			
Almond hull	0.2	$/kg	(Ceillia Parsons, 2022; USDA, 2023a)[a]
Yeast extract	0.48	$/kg	(Alibaba, 2023a)
NH_4Cl	0.16	$/kg	(Alibaba, 2023b)
Spores	4.0	$/kg	(Startercultures, 2023)
Cellulase	3.5	$/kg	(Y. Chen, 2020)
Pectinase	16	$/kg	(Y. Chen, 2020)
Water	0.0018	$/kg	(California Water Service, 2023)
Utilities			
Steam	12	$/MT	Default values from SuperPro Designer (2023)
Cooling water	0.05	$/MT	
Chilled water	0.4	$/MT	
Electricity	0.1	kW/h	
Labor			
Operator (4)	50	$/h	
QA Analyst	60	$/h	
Supervisor	70	$/h	
Consumables			
Filtration membranes	400	$/m^2	SuperPro (2023)
Maintenance			
Aqueous waste	0.002	$/kg	SuperPro (2023)
Solid waste	0.05	$/kg	Personal communication[b]
Emission	0.05	$/kg CO_2	SuperPro

[a]The price of almond hull was determined based on the average price of almond hull in the past four years, since 2020; [b]The rate of disposal solid waste for composting was determined from personal communications with scientists who collaborated with UC Davis Renewable Energy Anaerobic Digester (READ).

It was assumed that the capital costs would be spread out over a period of 20 years and would include an 9% nominal annual loan interest rate:

$$A = P\left[\frac{i(1+i)^n}{(1+i)^n-1}\right] \qquad \text{(Eqn. 6.1)}$$

Where A is the annual equivalent cost (\$/year), P is the present total fixed capital investment (\$), i is the annual interest rate (%), and n is the project lifetime (year). The breakeven price (BP, \$/kg) of fungal biomass (myco-foods) was calculated by setting the net annual worth (NAW, \$/year) as zero:

$$NAW = 0 = -(A + AOC) + BP \times PS \qquad \text{(Eqn. 6.2)}$$

Where AOC is the annual operation cost (\$/year); PS is the annual main product production and sales rate (kg/year), which is assumed constant over the project lifetime. The breakeven analysis was used to compare the studied two scenarios. In this way, the equipment was assumed to have a lifespan of 20 years and no salvage value was assumed for the assent beyond that point. Taxes were not considered in the model because this model is a breakeven analysis without profits or relevant taxable income. In other words, it is assumed that the internal rate of return is equal to zero.

6.3.4.3 Sensitivity analysis

A sensitivity analysis was carried out to understand the influence of certain key factors on the breakeven price of the fungal biomass. The almond hull price, which was identified as the major factor influencing the operation cost, was considered in the range 100 to 300 \$/MT that was the ranged price since 2020. The influence of the scale of the facility on breakeven price was also studied with a range from 25 MT/batch to 125 MT/batch. The different responses of breakeven price to the two factors were recalculated, compared, and plotted among the two scenarios. This information can help decision-makers to better understand the risks and uncertainties associated with this project.

6.4 Results and Discussion

6.4.1 Mass and energy flows in the model

The base model (Scenario 1) with 16,000 MT/year almond hull input resulted in fungal biomass production of 2,971 MT/year at 7,918 hours annual operation from 320 batches. Due to the longer recipe batch time and cycle time, less batches were able to run each year in Scenario 2. However, 4,653 MT/year of fungal biomass were produced from 308 batches in Scenario 2. The detailed information of the overall process for both scenarios are presented in Table 6.3. The majority mass of input and output stream are listed in Table 6.4.

Table 6. 3. Overall process data of Scenarios 1 and 2

	Scenario 1	**Scenario 2**
Annual operation time (h)/year	7,917.78	7,916.58
Annual main product (MP) production rate (MT MP/year)	2,970.51	4,653.36
Batch size (MT MP/batch)	9.28	15.11
Recipe batch time (h)	139.50	164.83
Recipe cycle time (h)	24.38	25.25
Number of batches per year	320	308

In Scenario 2, the input of almond hulls was less compared to Scenario 1, attributable to twelve fewer batches being operated each year, equating to a reduction of 660 MT of almond hulls utilized. The use of cellulase and pectinase enzymes to hydrolyzed RAHS resulted in a fungal biomass yield of 0.30 g/g almond hull. This was a significantly higher than the yield of 0.19 g/g almond hull from Scenario 1. This hydrolysis process also led to an increase in the use of NH_4Cl, yeast extract, spores, air, and water in Scenario 2. Importantly, Scenario 2 utilized the RAHS which

were otherwise disposed of as a solid waste in Scenario 1. As a result, the amount of solid waste in Scenario 2 was only 69.3% of that in Scenario 1. The solid waste from Scenario 2 consisted of unhydrolyzed solids with a moisture content of 80%.

Table 6. 4. The mass of model input- output streams

Input stream (MT/yr)	**Scenario 1**	**Scenario 2**	**Output stream (MT/yr)**	**Scenario 1**	**Scenario 2**
Almond hull	16,000	15,400	Fungal biomass	2,971	4,653
NH_4Cl	538.9	855.9	Solid waste	33,163	22,976
Yeast extract	214.7	341.0	Aqueous waste	225,542	336,635
Spores	0.004	0.007	Emissions	2,071,752	3,128,055
Air	2,071,016	3,126,947			
Water	299,894	430,337			
Pectinase	0	88.7			
Cellulase	0	443.6			

Table 6.5 presents the electricity and heat transfer reagents (steam, cooling water and chilled water) inputs to the facility for both scenarios. Fungal cultivation process was the highest individual electric process loads at 77.3 % and 76.8% of total demand in Scenario 1 and 2, respectively. This high demand was expected, considering five identical bioreactors operate continuously throughout the year. Scenario 2 required an additional 4,457 MW-h/year electricity due to the inclusion of three extra unit operations: hydrolysis, centrifugation, and ultrafiltration.

Hot steam was mainly used for preheating water, media pasteurization, and bioreactor sterilization. Both scenarios utilized the same amount of steam for preheating water for each batch during sugar extraction. However, due to the increased throughput of pasteurization and sterilization operations in Scenario 2, a higher quantity of steam was required. Likewise, Scenario 2 consumed more cooling water and chilled water for cooling the pasteurized media and fermenter

during fungal cultivation and to overcome the heat produced in this process to keep the temperature constant at 30℃.

Table 6. 5. Utilities consumption in Scenarios 1 and 2

	Scenario 1	**Scenario 2**
Electricity (MW-h/yr)	35,117	53,311
Steam (MT)	29,531	34,674
Cooling water (MT)	4,165,594	6290,487
Chilled water (MT)	1,741,419	2,131,609

6.4.2 Economic evaluations

6.4.2.1 Capital investment

As described in the previous Materials and Methods section, the total capital investment of the simulated project consisted of direct, indirect and other costs, which were calculated based on the equipment cost. The detailed throughput of the major equipment used in both scenarios are shown in Table 6.6. Most equipment costs were derived from the default values in the SuperPro built-in database, and these were verified with values from various literatures. The costs associated with the blending tank, centrifuge, and reactor were sourced from a study by Wang et al. (2021) and the cost for screw press was based on the study from Kontovas et al. (2022), where equipment of comparable capacities was employed. The cost of fermenter was estimated based on a study from Koulouris (2023), which involved the use of a similar fermenter to produce food-grade products. In the simulated model, five identical fermenters were used due to the implementation of a staggered mode. For all other types of equipment, only one unit was utilized.

Table 6. 6. Equipment with sizing and purchase cost information used in Scenarios 1 and 2

Equipment	Label	Scenario 1		Scenario 2	
		Throughput (True/Max)	Price ($/unit)	Throughput (True/Max)	Price ($/unit)
Grinder	GR-101	50/60 MT/h	296,000	50/60 MT/h	296,000
Blending tank	V-101	745/850 m^3	430,000	745/850 m^3	430,000
Heat exchanger	HX-101	124/150 m^2	65,000	124/150 m^2	65,000
Screw Press	SP-101	69/75 MT/h	1,323,000	69/75 MT/h	1,323,000
Microfilter	MF101	1056/1200 m^2	671,000	1056/1200 m^2	671,000
Pasteurizer	PZ-101	239/250 m^3/h	296,000	373/400 m^3/h	392,000
Fermenter*	FR-101	796/900 m^3	1,000,000	1335/1500 m^3	1,300,000
Screen	SCR-101	707/900 MT/h	22,000	1108/1300 MT/h	35,000
Washer	WSH- 101	91/100 MT/h	100,000	144/165 MT/h	150,000
Reactor	R-101			257/280 m^3	130,000
Centrifuge	DS-101			232/250 m^3/h	265,000
Ultrafilter	UF-101			442/480 m^2	285,000

* There were 5 identical fermenters used in the process, the throughputs and prices listed were for one fermenter.

The capital investment, including equipment cost, direct fixed cost and total capital cost are shown in Figure 6.4. In Scenario 1, the estimated cost for equipment purchases is approximately $10.25 million. The fermenters represent the most significant expense, accounting for about 48.78% of the total cost. This high percentage is associated with the five staggered fungal cultivation fermenters. Similarly, in Scenario 2, the fermenters make up 49.32% of the total purchase cost of $13.18 million, which is higher due to the more expensive unit price in this

scenario. However, in Scenario 2, the three pieces of equipment used for the utilization of RAHS make up only 5.16% of the total cost.

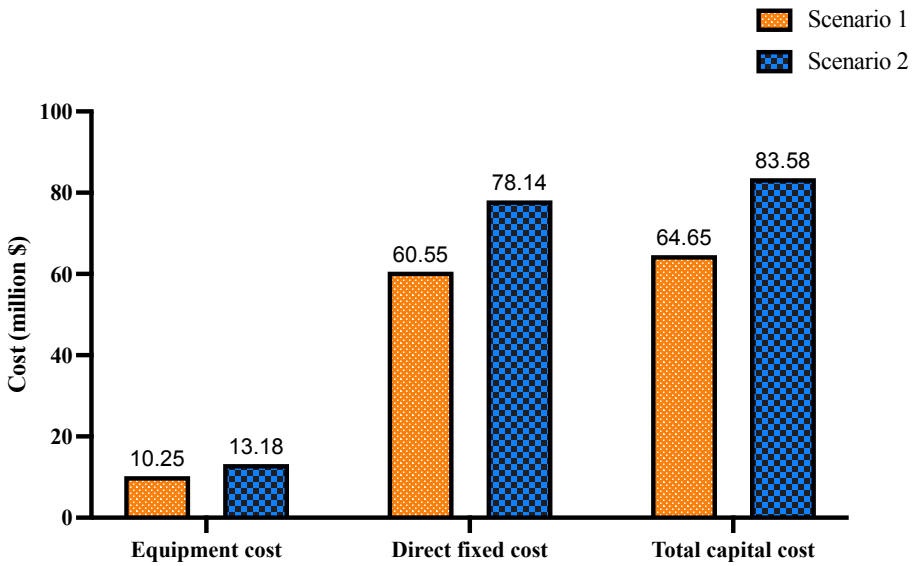

Figure 6. 4. Plant total capital investment of Scenarios 1 and 2

6.4.2.2 Operation cost

The operation cost is the total of all "on-going" expenses involved in running the business, mainly including the raw materials, labor, consumables, utilities, waste management, etc. The annual operation costs of both scenarios are depicted in Figure 6.5, with Scenario 2 incurring an additional $6.08 million in operating costs compared to Scenario 1. Figure 6.6 shows the breakdown of operation cost for both scenarios, with the primary differences between Scenarios 1 and 2 arising from the costs of raw materials and utilities. In Scenario 1, utilities cost represents the largest share of the total operating cost, contributing to 32.53% of the overall operation cost, closely followed by raw material cost at 26.53%. For Scenario 2, the top two contributors to the total operating cost are raw material cost (34.12%) and utilities cost (33.11%).

The distributions of utilities costs and raw materials costs for both scenarios are illustrated in Figure 6.7 and Figure 6.8, respectively. Electricity represents the most expensive utilities cost

in both scenarios, contributing to 73.61% and 77.10% of the total utilities cost in Scenarios 1 and 2 respectively. Most of this electricity is consumed by the fungal cultivation fermenters, mainly for continuous aeration and agitation. The second-highest cost in both scenarios is the chilled water, which accounts for 14.60% and 12.33% in Scenarios 1 and 2 respectively. Most of this chilled water is employed to cool the pasteurized media from 80℃ down to 30℃. Owing to the higher costs of electricity and chilled water in Scenario 2, the total utilities cost is higher in Scenario 2 than in Scenario 1, with costs $6.91 million and $4.71 million, respectively.

Figure 6.8 illustrates that the most expensive portion of raw material costs in both scenarios, particularly in Scenario 1, is attributed to almond hulls. These account for 81.48% of the raw material cost in Scenario 1 and 43.22% in Scenario 2. Despite similar total costs of almond hulls in both scenarios ($3.2 million in Scenario 1 and $3.08 million in Scenario 2), the proportion of the cost of almond hulls to the total raw material cost varies significantly between the two scenarios. This difference is mainly due to the high enzyme costs in Scenario 2, which diluted the relative share of almond hulls. The total enzyme cost, including cellulase and pectinase, amounts to $2.97 million (with cellulase contributing $1.55 million and pectinase contributing $1.42 million). This represents 41.69% of the total raw material cost (or 14.22% of the AOC) in Scenario 2. As mentioned in the Materials and Methods section, 70% of the enzymes are recycled. Therefore, the enzyme cost discussed here is the expense of purchasing 100% fresh enzymes for the first batch and 30% fresh enzymes for the following batches. The enzyme cost could be significantly higher without the recycling of enzymes. Water cost is another relatively high expense in both Scenarios 1 and 2, contributing to 13.7% and 10.87% of the total raw material costs in each scenario, respectively. The considerable amount of water used is mainly for the extraction process, dilution of almond hull extract for fungal cultivation, and rinsing out residual spent media from fungal

pellets after harvesting in both scenarios, as well as adjusting the initial total solids (TS) loading for hydrolysis in Scenario 2.

Labor costs are the same in both scenarios, as an identical number of operators, manager, and QC/QA analyst are assigned to the facilities. In Scenario 1, the waste management cost amounts to $2.32 million, higher than Scenario 2's cost of $2.16 million. This is attributed to the fact that the RAHS, which was discarded as solid waste in Scenario 1, was utilized and hydrolyzed in Scenario 2, resulting in less solid waste treatment. A slight increase in consumables cost in Scenario 2 arises from the use of a membrane for ultrafiltration for enzyme recycling. The facility-dependent cost represents additional expenses tied to the facility's use and is calculated based on the total costs associated with equipment maintenance, depreciation of fixed capital costs, and various miscellaneous costs. This cost, amounting to $2.42 million in Scenario 1 and $3.13 million in Scenario 2, accounts for 16.35% and 14.97% of the total operating costs in their respective scenarios.

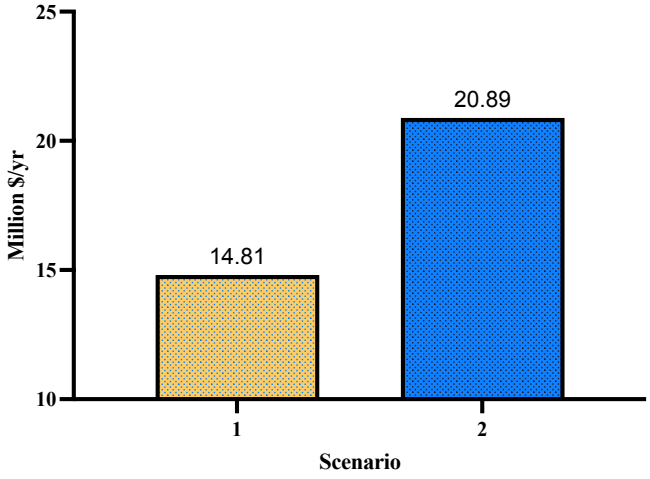

Figure 6. 5. Annual operation cost of Scenarios 1 and 2

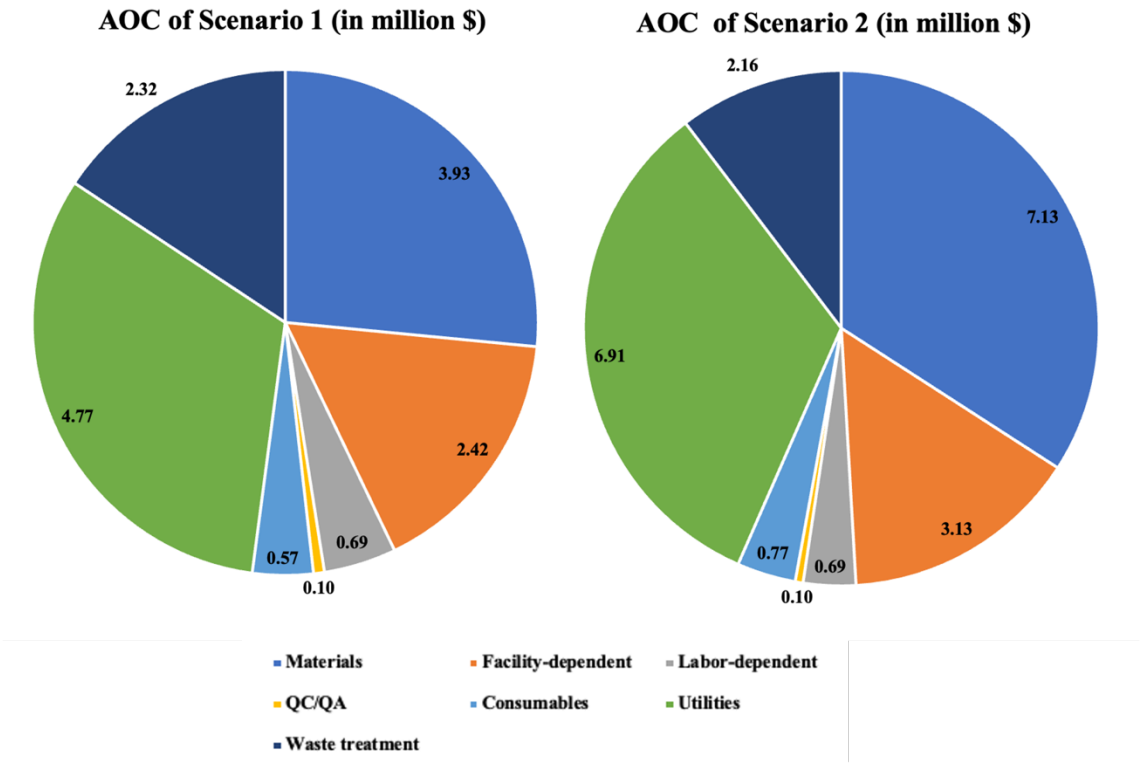

Figure 6. 6. Breakdown of annual operation cost of Scenarios 1 and 2

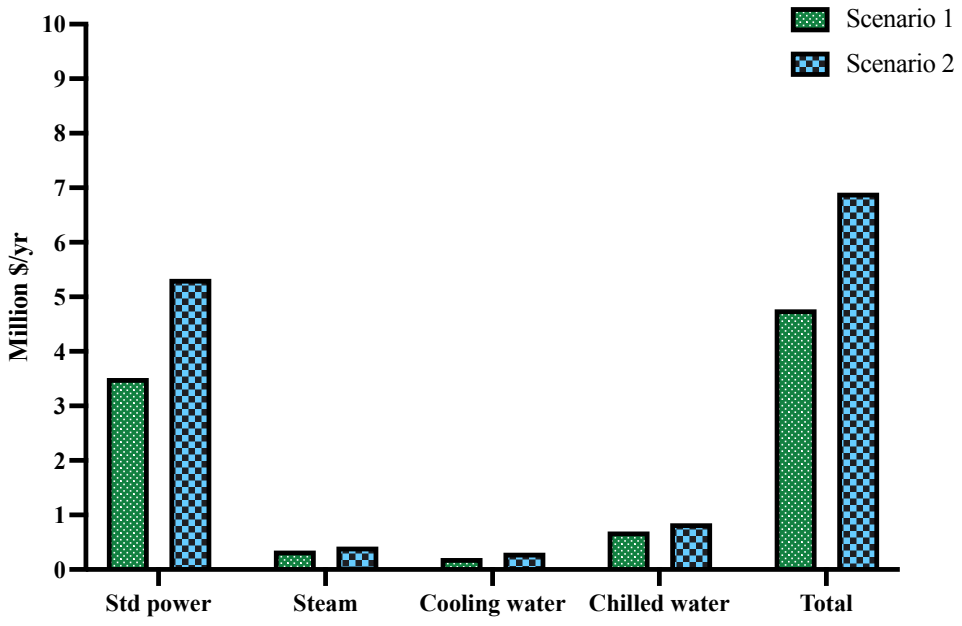

Figure 6. 7. Breakdown of utilities costs of Scenarios 1 and 2

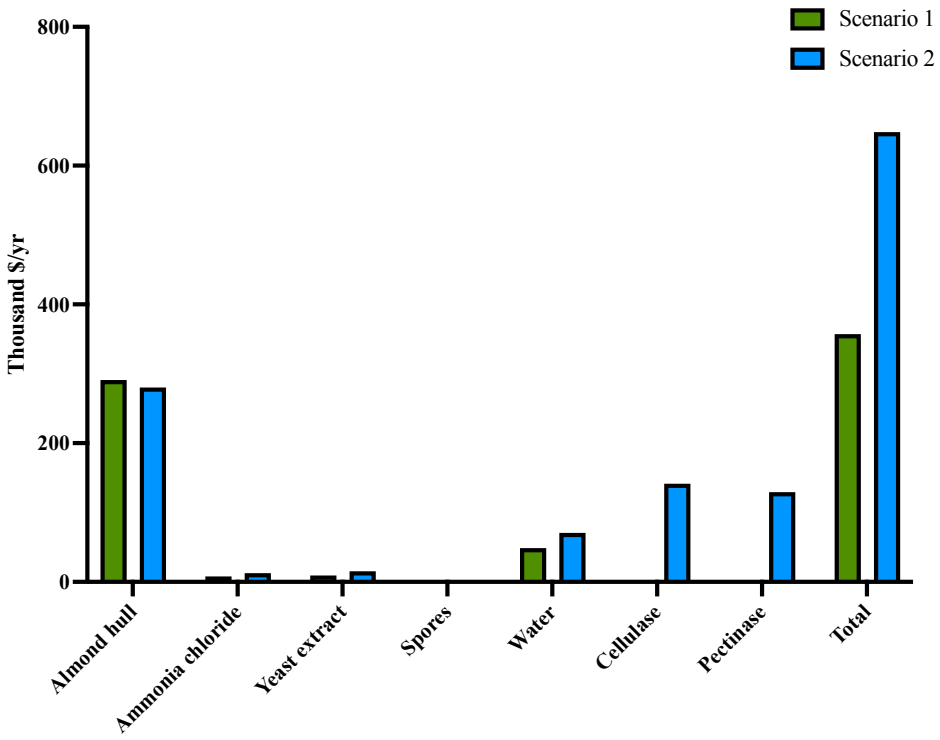

Figure 6. 8.Breakdown of raw material costs if Scenario 1 and 2

6.4.2.3 Breakeven price and sensitivity analysis

The breakeven price is the minimum price at which the fungal biomass must be sold to cover the total cost (including annualized capital cost and operation cost), which make the net present worth equal zero. Calculating the breakeven price is crucial for business planning, decision making, and profitability analysis. As mentioned in Materials and Methods section, the breakeven prices of the dried fungal biomass were calculated from Eqn. 6.2, and the values are shown in Figure 6.9. Scenario 1 had a higher breakeven price ($6.91/kg) than Scenario 2 ($6.07/kg). Although Scenario 2 had higher capital investment and operation cost than Scenario 1, it's still more economically favorable because the annual main product yield is about 1,683 MT/year, due to more sugars utilized from the almond hulls by enzymatic hydrolysis.

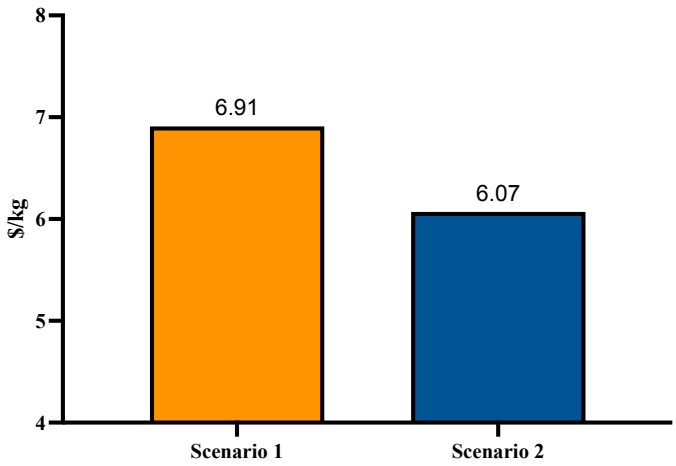

Figure 6. 9.Breakeven prices of fungal biomass (d.b.) produced from Scenario 1 and 2

As mentioned in previous section, the cost of raw materials, particularly almond hulls, makes up a significant portion of operational costs. The price of almond hulls fluctuates every year in California. Therefore, a sensitivity analysis was performed by varying the almond hull price from the lowest to the highest recorded in the past four years, starting from 2020. This price range spanned approximately $100/MT to $300/MT, or -50% to +50% of the almond hull price ($200/MT as baseline) used in the economic analysis. The facility's capacity to process 50 MT/batch of hulls was fixed in this sensitivity analysis, which considered varying hull prices. The impact of these price fluctuations on the breakeven prices for fungal biomass production can be observed in Figure 6.10, Scenario 1 is more sensitive to changes in almond hull prices than Scenario 2 due to a larger share of almond hull costs in the operational cost of Scenario 1. As hull prices change from -50% to +50% of the baseline hull prices, the breakeven biomass prices shift from -7.79% to + 7.79% of the baseline breakeven price (6.91$/kg) in Scenario 1, and from -5.45% to + 5.45% of the baseline breakeven price (6.07$/kg) in Scenario 2. Consequently, the breakeven biomass price ranges from 6.37 $/kg to 7.45$/kg in Scenario 1, and from 5.74$/kg to 6.40 $/kg in Scenario 2. This price is much lower than meat, such as pork and beef, which have a price ranged

from $14 /kg to $22/kg (w.b) (USDA, 2023b). The moisture content in meat is over 55% (USDA, 2023d). Besides competing with meat, this fungal biomass price is also lower than dried tapioca pearls, which is around $15/kg (Alibaba, 2023c).

The processing capacity of the plant is another factor to consider, as it could be influenced by the capital investment, market demand for the products, and the availability of almond hulls, etc. Therefore, the sensitivity analysis of the breakeven price for fungal biomass at varying plant capacities was conducted. The facility capacities varied from processing 25 MT/batch to 125 MT/batch of almond hulls, representing a relative change from -50% to +150% of the baseline (50 MT/batch), with the almond hull price held constant at $200/MT. The capital scaling factor for this myco-foods production plant at different scales was set at 0.6 based on the rule of six-tenths (Tribe & Alpine, 1986), and is in agreement with the range commonly used for scaling factors (T. Barzee, 2020). The operational cost scaling factor was calculated proportionally to the baseline operational cost. These scaling factors were assumed to remain constant across all processing scales. Figure 6.10 illustrates that Scenario 1 is more sensitive to changes in capacity than Scenario 2. Unlike the effect of hull prices, the sensitivity to capacity is non-linear due to the application of scaling factors. As the capacity shifts from -50% to +150%, the breakeven price fluctuates from +8.90% to -8.54% in Scenario 1 and +8.34% to -8.01% in Scenario 2. In both scenarios, the breakeven prices are more sensitive at smaller scales.

This sensitivity analysis effectively helps to explore and comprehend the uncertainty involved in the operational dynamics of the plant by examining the impact of key factors, almond hull price and facility capacity, on the model's outcome. By altering these factors within a reasonable range, we can observe how changes in these factors affect the breakeven price of the fungal biomass. This provides valuable insight into how the plant's profitability may fluctuate

under different circumstances and aids in making informed business decisions. It also highlights the elements that the business is most sensitive to and helps in understanding where risk management efforts or strategies for cost optimization could be most effective (Y. Chen, 2020; K. Wang et al., 2021).

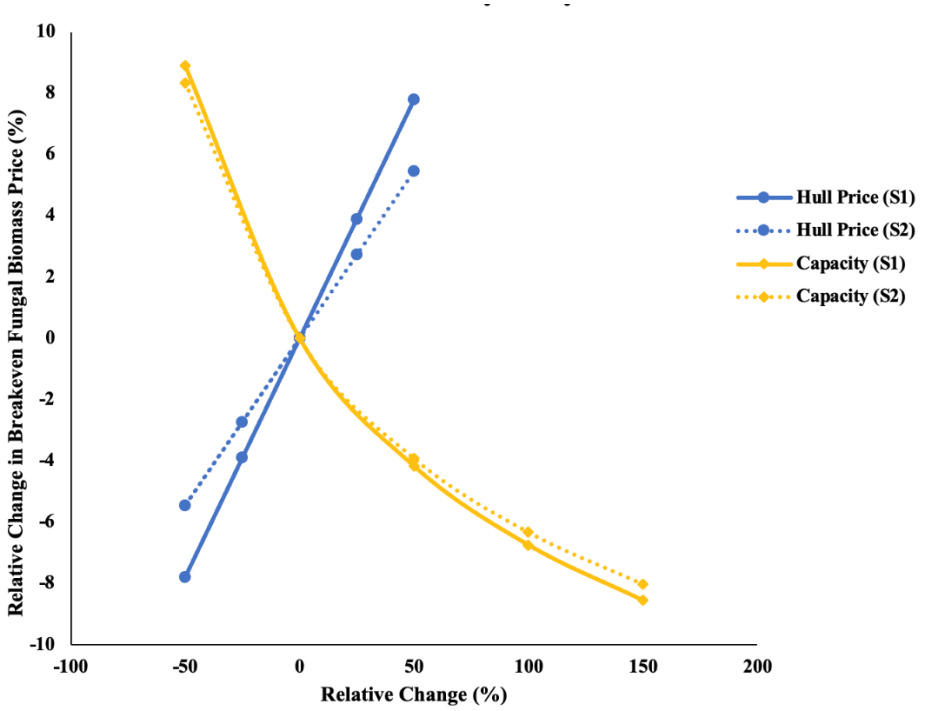

Figure 6. 10. Sensitivity analysis of breakeven sale price of fungal biomass under varying almond hull prices and plant capacities

6.5 Conclusions

Two scenarios with different unit operations were developed and compared in terms of materials and energy flow, capital investment, annual operation cost, breakeven fungal biomass price, and sensitivity analysis. Scenario 2 involves additional unit operations to hydrolyze RAHS into sugars for fungal biomass cultivation and employs equipment with greater throughputs from pasteurization to washing processes. As a result, Scenario 2 has a higher capital investment, utilities cost, and most raw material cost (excluding almond hulls) when compared to Scenario 1.

However, due to the utilization of RAHS, which were discarded as solid waste in Scenario 1, the total waste treatment cost in Scenario 2 is lower. The model simulation revealed production levels of approximately 2971 MT/year of fungal biomass from around 16,000 MT/year hulls without enzymatic hydrolysis (Scenario 1) and around 4,653 MT/year of fungal biomass with enzymatic hydrolysis (Scenario 2). The breakeven price for both scenarios was within the range of $6 - $7 per kg of fungal biomass (dry basis). A sensitivity analysis was conducted for the breakeven price of fungal biomass with respect to almond hull price and facility size for both scenarios, with Scenario 1 showing higher sensitivity to both of factors. In both scenarios, the breakeven price of fungal biomass is more sensitive to the capacity at small scale (lower than 50 MT/batch). While the breakeven price is more sensitive to almond hull price at larger scale. The low breakeven price for fungal biomass makes myco-foods economically competitive with existing food products on the market. This study demonstrates the promising economic potential of converting almond hulls into myco-foods through industrial scale processes.

Chapter 7 Development and Evaluation of Myco-food Products

7.1 Abstract

The potential of using *Aspergillus awamori* (*A. awamori*) pellets to develop different products (myco-foods) was explored. Techniques were studied to change pellet color using both artificial food dyes and natural colored media derived from agricultural and industrial byproducts. Pellets' colors obtained from natural colored media were more stable after one-month storage. A method was developed to create multilayered color pellets successfully by deactivating pre-cultured pellets and then growing new spores on them. Additionally, the texture of pellets was improved by coating them with potato dextrose agar (PDA) and re-growing them to form condensed mycelium inside fungal pellets. The potential for developing *A. awamori* biomass into dried products was also evaluated. The biomass could potentially be processed into protein/fiber powder-based products through freeze drying or transformed into crispy, snack-like myco chips through hot air drying. Lighter color was obtained after freeze drying, while hot air drying led to darker color of the fungal biomass. No mycotoxins were detected in the *A. awamori*-based foods, and the foods showed significant health benefits in a mouse study. The spent media collected after pellet production contained enzymes, suggesting the potential for its utilization in the development of beverages. The findings from this study provided important information of the potential of developing *A. awamori* biomass into novel functional food.

7.2 Introduction

Developing a new fungal-based food (myco-foods) must consider and evaluate multiple factors to ensure its appearance, safety, taste, nutritional value, and marketability. Depending on the intended use and potential benefits, consumers may ingest live microbial cultures as probiotics,

or deactivated microbes for nutritional supplementation. Probiotics can promote a healthy gut microbiome by maintaining or restoring the balance of beneficial microbes in the digestive system (Sanders, 2011). Even when inactivated, microbes can still deliver nutritional benefits, such as vitamins, minerals, proteins, and fiber. Therefore, the conditions must be evaluated to keep the microbes active or deactivated.

Making the products visually appealing, such as color, is a significant aspect of product development. The use of natural colored media, derived from agricultural byproducts, offers a sustainable and environmentally friendly alternative to artificial dyes. Natural colored media are generally non-toxic, biodegradable, and can potentially enhance the nutritional profile of food by adding antioxidants and other beneficial compounds. The use of such dyes can create visually attracting foods with unique colors and flavors, enhancing their marketability. In addition to color, enhancing the texture of the developed food can also increase the appeal of myco-foods. However, the safety and health benefits of myco-food must always remain a priority.

This study aimed on developing fungal-based novel food product at lab scale and providing a preliminary evaluation, focusing on key factors such as deactivation conditions, color enhancement, toxins evaluation, texture improvement, and potential health benefits. By conducting the product development and assessment at the laboratory, it will be possible to establish a solid foundation for further optimization and scale-up of the production process. The specific objectives were to: (1) study the conditions necessary to deactivate fungal pellets; (2) change the color of fungal pellets using both artificial and natural colored media and evaluate their stability over time; (3) develop dried fungal products by freeze drying and hot air drying and evaluate their texture; and (4) evaluate the safety and health benefits of *A. awamori* products.

7.3 Materials and Methods

7.3.1 Evaluate the effect of temperature on biological stability of fungal pellets

Fungal mycelium is sensitive to environmental temperature. Temperature and time are key parameters that need to be controlled during the production process. To study the effects of temperature and time on biological activity of fungal mycelium, heat treatment was carried out at different temperatures (40-70 °C) and holding times (1-10 min). Sterile fungal pellets were soaked in preheated sterile deionized (DI water) and heat treated for different holding time in sterile 15 mL centrifuge tubes in water bath. After heat treatment, pellets were transferred to potato dextrose agar (PDA) plates in biosafety cabinet and incubated at 30℃ for five days to see if biological activity remained in the heat-treated pellets. Active fungal mycelium could produce black spores and yellow pigment, while deactivated mycelium was not changed. The yellow pigment, which is specifically produced by *A. awamori*, is an indicator for the growth of *A. awamori.*

7.3.2 Produce fungal pellets with different color and evaluate color stability

The feasibility of producing two types of fungal pellets was tested: single-layer pellets, featuring a uniform color throughout; and multi-layered pellets, exhibiting multiple colors within a single pellet. To achieve this, artificial food colorings and natural colored media extracted from agricultural byproducts, vegetables and fruits were used. Instead of directly applying food colorings or natural colored media to color the fungal pellets, those coloring agents were introduced into the growth media. The purpose of this approach was to investigate whether the fungal pellets could firmly adsorb the color from the media or interact with those pigments, resulting in stable and evenly distributed colors. Additionally, the color stability of the colored pellets during storage in refrigerator and deactivation by heat were assessed by measuring the color change before and after storage or deactivation with the colorimeter. The purpose of this

examination was to ascertain if the color could maintain their stability under a range of conditions typically experienced during food processing and storage.

7.3.2.1 Precultured pellets preparation

Small white *A. awamori* pellets were prepared by inoculating 4-day spores into flasks containing 100 mL sterile potato dextrose broth (PDB) at the level of 10^3 spores/mL. The flasks were shaking at 200 rpm and incubated at 30℃ for two days.

7.3.2.2 Media preparation from artificial food color

Four different commercial food color liquid samples (Ktdorns, ChuangLanTu Technology) were used, including sunset yellow, fruit green, sunset red and grape violet. Each food color was a mixture of two artificial color additives coded with E numbers which serve as a European classification system standardize and simplify labelling across the region. The specific combination of each food color is listed in Table 7.1. Each color was passed through a 0.22μm filter to sterilize the color reagent and then 100 μL was added to individual flasks containing 100 mL of sterile PDB (Figure 7.1).

Table 7. 1. Details of food colors used

Food color	Compositions	Chemical name	Color
Sunset yellow	E102	Tartrazine	Yellow
	E110	Sunset Yellow FCF or Orange Yellow S	Yellow orange
Fruit green	E102	Tartrazine	Yellow
	E133	Brilliant Blue FCF or FD&C Blue No.1	Blue
Sunset red	E110	Sunset Yellow FCF or Orange Yellow S	Yellow orange
	E124	Ponceau 4R, Cochineal Red A, or Brilliant Scarlet	Red
Grape violet	E123	Amaranth	Reddish-rose
	E133	Brilliant Blue FCF or FD&C Blue No.1	Blue

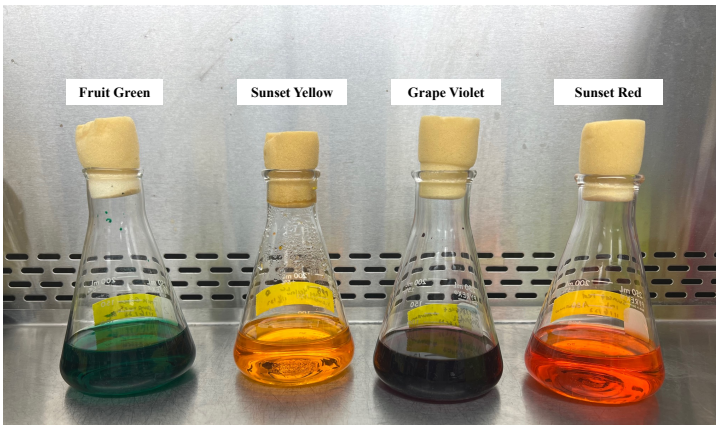

Figure 7. 1. PDB mixed with different artificial food color

7.3.2.3 Media preparation from natural colored media

Natural colored media were prepared from five agricultural/food industry processing materials, including almond hulls, walnut hulls, ground coffee, pomegranate peel and delactosed permeate, one vegetable (red beet) and one juice (carrot juice). Some characteristics of the materials used for preparing natural colored media are listed in Table 7.2; and pictures of those materials are shown in Figure 7.2. Fresh and liquid feedstocks, including walnut hulls,

pomegranate peels, delactosed permeate, red beets and carrot juice were kept in freezer before use. Dried feedstocks, including almond hulls and ground coffee, were stored in an ambient environment (around 24℃).

Table 7. 2. Characteristics of the materials used as sources for natural colored media

Feedstocks	Variety/Brand	Pigment	Color	Status	Collection place
Almond hulls	Independence	Tannins	Brown	Dried	West Valley Hulling Company (Firebaugh, CA)
Ground coffee	Starbucks	Melanoidins	Dark brown	Dried	Safeway Inc. (Davis, CA)
Walnut hulls	Howard	Juglone	Black	Fresh	Mariani Nut Co. (Winters, CA)
Pomegranate peel	Wonderful	Anthocyanins	Red (acid condition)	Fresh	SunnyGem LLC (Buttonwillow, CA)
Red beet	-	Betalain	Red-purple	Fresh	Safeway Inc. (Davis, CA)
Delactosed permeate	-	Protein or other compounds	White or slightly yellow	Liquid	Hilmar Cheese Co. (Hilmar, CA)
Carrot juice	Bolthouse Farms	Carotenoids (Mainly beta-carotene)	Orange	Liquid	Safeway Inc. (Davis, CA)

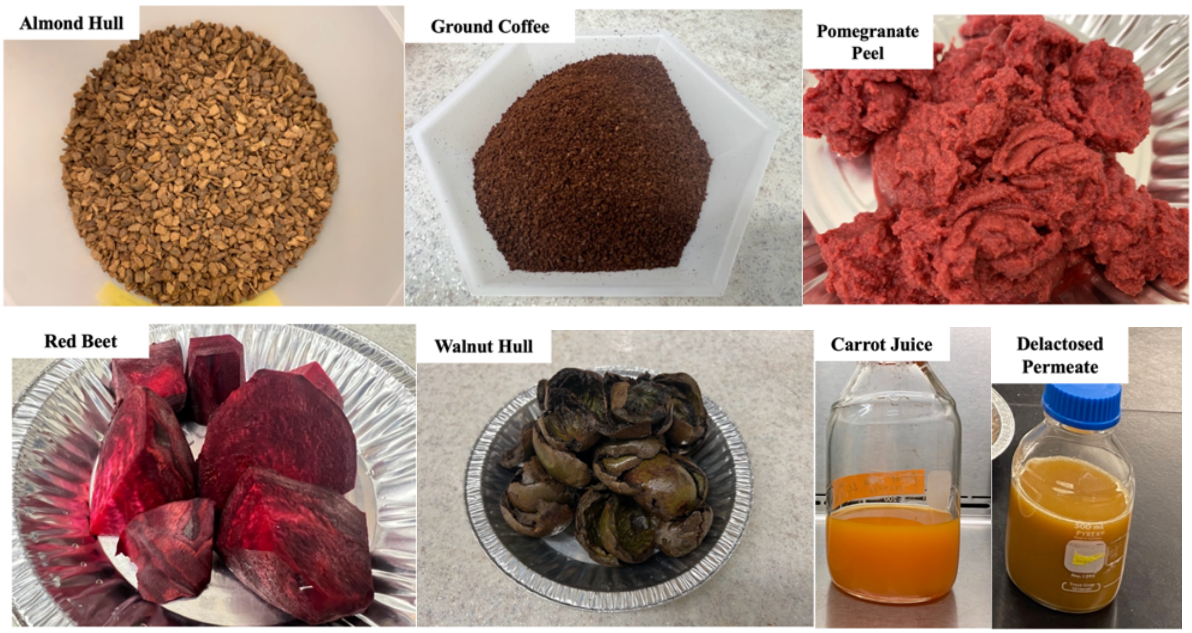

Figure 7. 2. Materials used for coloring media preparation

The moisture content (MC), total solids (TS) volatile solid (VS) of those materials were analyzed, except for delactosed permeate and carrot juice. The sugar content in all materials were also analyzed by high-performance liquid chromatography (HPLC).

Seven media from juice, vegetable, agricultural byproducts were prepared as follows: (1) walnut hulls, pomegranate peels and red beet were thawed at room temperature first. Nutrients extraction was done by mixing those feedstocks with DI water at 7% TS loading and then ground by food processor for one min. After grinding, cheese cloth was applied to separate solids from liquid. (2) Almond hull and ground coffee extracts were prepared by soaking them in hot water (80℃) at 7% TS loading and shaking at 120 rpm for 90 min. Solids were separated from liquid by cheese cloth. Suspended solids in all the extracts, including carrot juice and delactosed permeate, were removed by using vacuum filtration with standard glass fiber filter paper to obtain clear solutions. In order to achieve 20 g/L total sugar concentration in all extracts for fungal cultivation,

14 g/L glucose were added into walnut hull extract and 20 g/L of glucose was added into ground coffee extract. Delactosed permeate and carrot juice were diluted by using DI water with dilution factors of 7.5 and 2.5, respectively. The pH of all the media were adjusted to 5 by using sodium hydroxide and sulfuric acid.

Before fungal cultivation, those media had to be sterilized. Therefore, the color stability of those media after pasteurization were tested by heating them to 80℃ for three hours. The color of both pomegranate peel and red beet changed after heating as shown in Figure 7.3. Therefore, pomegranate peel and red beet media were sterilized by filtering through sterile filters with pore size of 0.22 µm. The remaining five media, almond hull, walnut hull, ground coffee, delactosed permeate and carrot juice, underwent pasteurization by heating. For each medium, 100 mL were transferred into sterile flasks for fungal cultivation. For each treatment, there were two replicates.

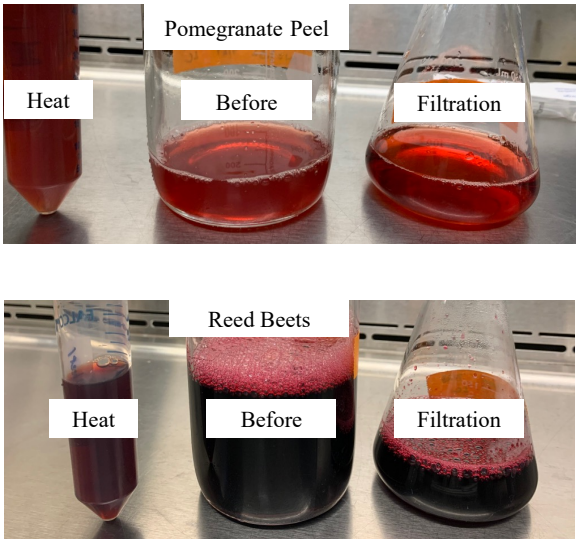

Figure 7. 3. Comparison of color change of pomegranate peel and red beet media before and after heating or filtration

7.3.2.4 Colorful pellets production

Single-layer pellets

White small pellets from pre-cultivation were harvested, and a random sample of 60 pellets was selected and transferred into flasks containing prepared media with different colors. These flasks were incubated at 30℃ and shaking at 200 rpm for three days. The color after cultivation was measured by colorimeter. The biomass concentration cultivated in the natural colored media was quantified, and pellet sizes were determined by measuring the average diameter of 30 randomly chosen pellets. The density of individual fungal pellet was defined as dry mass per wet volume and was calculated as (Hille et al., 2009):

$$\text{Density (g/L)} = \frac{M_{final\ biomass}/n}{\frac{4}{3}*\pi*(\frac{D}{2})^3} \times 10^6 \quad \text{(Eqn.7.1)}$$

Where n is the total number of pellets in the flask, assuming no new pellets formed. Therefore, n = 60; D is the average pellets diameter (mm).

Multi-layered pellets

Multi-layered pellets were created by first deactivating single-layer pellets trough heat treatment using the conditions found from section 7.3.1, followed by re-inoculating fresh spores into new colored media containing the deactivated pellets. After cultivating for three days, two distinct types of pellets would be formed. One type was the multilayered pellets which developed as a result of spores adhering to original deactivated pellets and subsequently growing mycelium around them, resulting in larger pellets. The other type was single-layer pellets, which originated from free spores in the media or fragments of fungal mycelium. Therefore, those two types of pellets were separated and harvested by coarse screening. The newly formed single-layer pellets would be re-utilized. Those steps could be repeated to produce pellets with more layers of color. Figure 7.4 shows the processes to produce single layer and muti-layered pellets.

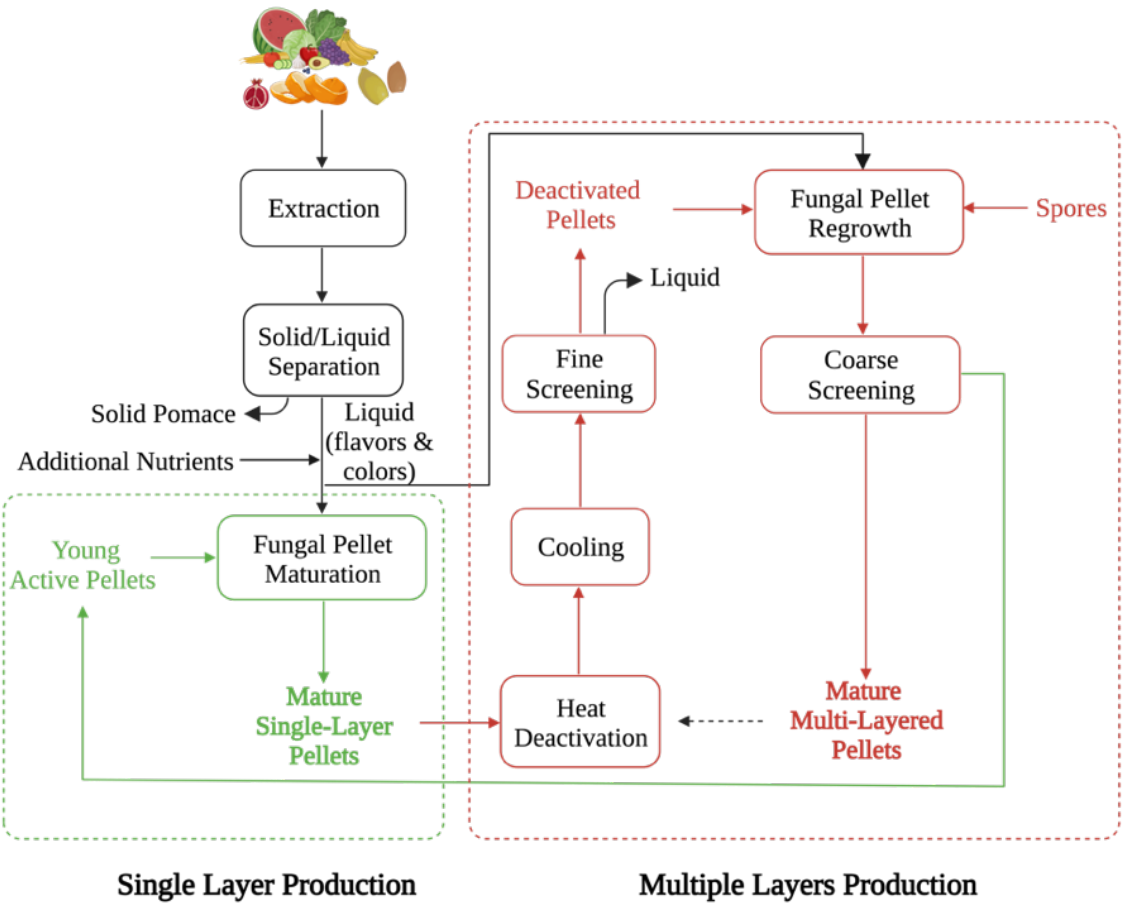

Figure 7. 4. Process of single-layer and multi-layered pellets production

7.3.3 Improve the texture of fungal pellets by using agar coating

Precultured pellets were produced in 120 mL PDB for two days at an inoculum level of 10^4 spores /mL in flasks. The flasks were agitated at 150 rpm at 30 ℃ on a shaking incubator (Benchmark Incu-Shaker™ Mini, 19mm orbit). One flask of fungal pellets was cultivated for five days without agar coating. These pellets were referred to as "simple pellets". Another flask of fungal pellets was cultivated for two days and then the pellets were subjected to an agar coating process followed by three more days of cultivation. The fungal pellets obtained from this process are referred to as "complexed pellets". For complexed pellet samples, the fungal pellets obtained after two days of initial growth were transferred into a warm (50℃) and sterilized potato dextrose

agar solution (containing 15g/L agar) for 5 seconds, removed from the liquid and then cooled to room temperature (20-25℃). The pellets were then placed into a 250 mL flask containing 120 mL of sterilized PDB and agitated at 150 rpm at 30 ℃ on a shaking incubator for three more days. After cultivation, the texture of simple and complexed pellets were analyzed using a Texture Analyzer (model TA.XT.Plus).

7.3.4 Wet myco-food (mycoBoba) evaluation

7.3.4.1 Color stability

The color stability of both active and deactivated colorful pellets was tested by immersing the pellets in DI water at a ratio of 1:10 (w/w). The submerged pellets were then stored in a refrigerator at 4℃, under dark conditions, for a period of one month. After one-month storage period, the color of the pellets was measured.

7.3.4.2 Nutrition evaluation

The nutrition value of fresh multilayered pellets was analyzed by Medallion Labs (Minneapolis, USA) following the standard methods. The potential enzyme activities in the media after fungal cultivation were also analyzed. All the methods utilized by Medallion Labs were listed in Table 7.3.

Table 7. 3. Standard methods used by Medallion Labs for analyzing pellets nutrition values and enzyme activities in spent media

Pellets		**Spent media**	
Analysis	Methods	Analysis	Methods
Cholesterol	AOAC 976.26	Alpha-Amylase activity	AOAC 2002.01
Fat	AOAC 996.06	Protease activity	Megazyme S-AZCAS 12/2007
Fiber	AOAC 2011.25	Lipase activity	BioAssay Systems Lipase Assay Kit (DLPs-100)
Metals	AOAC 975.03, 985.01, 984.27, 2011.14		
Protein	AACC 46-30; AOAC 992.15		
Sugars	AOAC 977.20		

7.3.4.3 Mycotoxins evaluation

The mycotoxin screening of pellet samples and media after fungal cultivation were conducted by California Animal Health & Food Safety Laboratory at UC Davis (California, USA) using the fungi/mold toxicities screening methods they developed. The mycotoxins assessed including Aflatoxin B1, Deoxynivalenol (DON), T-2 toxin, Ochratoxin-A, Fumonisin-B1 and Zearalenone which are the common toxins produced by fungi.

7.3.5 Dried myco-foods production and evaluation

7.3.5.1 Color change by using different drying methods

The effects of freeze- and hot air-drying methods on the color of pellets cultivated from different natural colored media, including almond hull, coffee, walnut hull, pomegranate peel, red

beet, delactosed permeate and carrot juice were compared. Hot air drying was carried out by placing 10 grams of wet pellets on aluminum tins with an initial thickness of approximately 1 cm. These were then dried at 60℃ with an air speed of 2 m/s for a duration of nine hours. Freeze-drying was performed by pre-freezing 10 grams of wet pellets in 50 mL falcon tubes. Three uncapped 50 mL falcon tubes were then placed in a 1.2 L Labconco Complete Fast-Freeze Flask, which was connected to a Labconco freeze dryer. The drying conditions were maintained at a temperature of - 45℃ and a vacuum pressure of 0.12 mBar for one day. The color of the surface of dried fungi was analyzed after drying.

7.3.5.2 Crispness of dried fungal biomass

A large quantity of pellets cultivated from almond hull extract was tested to analyze the crispness of ‘myco chips’ after hot air drying. It was conducted by spreading 200 g of wet fungal pellets over an aluminum tin with an initial thickness about 1 cm. Hot air at 60℃ was then blown across the surface of the biomass at a speed of 2 m/s using a hot air dryer as shown in Figure 7.5. After drying, the large dried piece was cut into small pieces (6×3cm) for crispness analysis with 10 replicates.

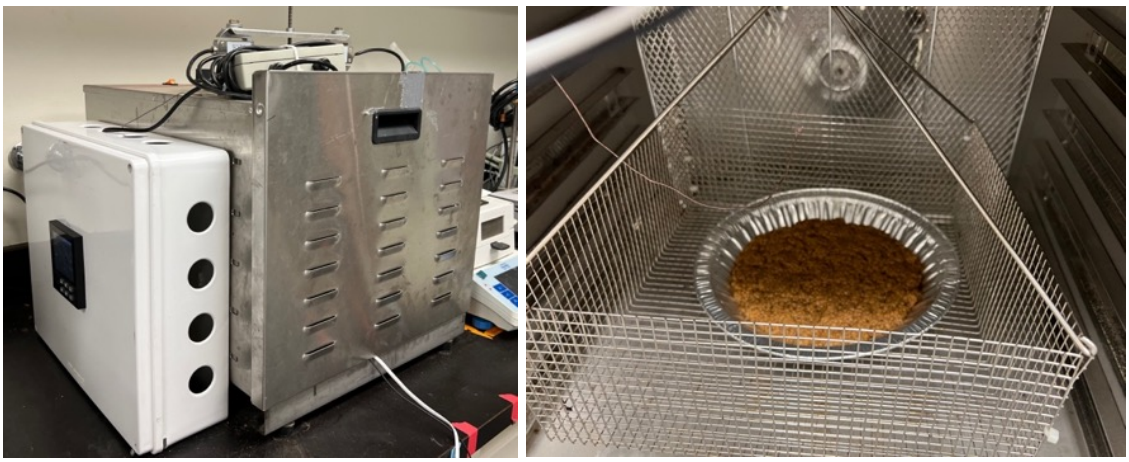

Figure 7. 5. “Myco chips” dried by hot air at 60℃

7.3.5.3 Health evaluation by mouse study

The effects of feeding hot air dried *A. awamori* fungal biomass (myco chips) on mice were investigated and conducted by the researchers at USDA ARS Western Regional Research Center. Thirty black mice were randomly divided into three groups (n = 10 each) with each group fed either high-fat (HF) diet, low-fat (LF) diet or HF diet supplemented with 5% fungal biomass. During the four weeks of feeding, fresh food was provided to mice weekly and their body weight were recorded weekly. After four weeks, mice were sacrificed following the procedure in (H. Kim et al., 2014). Blood was collected for plasma cholesterol analysis, and the adipose tissues were excised and weighed. More details will be reported by the USDA researchers.

7.3.6 Analytical measurements

7.3.6.1 HPLC sugar analysis

Lactose concentration was analyzed by using a HPLC equipped with CBM-20 A controller, PDA and RID detectors following the standard methods (Sluiter et al., 2006). A Biorad Aminex HPX-87H column was used with 5 mM sulfuric acid as mobile phase (flow rate, 0.6 mL/min). Oven temperature was controlled at 60℃.

Glucose, sucrose, fructose, galactose, arabinose, xylose and mannose were analyzed by using the HPLC that was equipped with a Biorad Aminex HPX-87P column with Milli Q water (18MΩ) mobile phase. The flow rate was set at 0.6 mL/min and oven temperature was controlled at 80℃. Glucose, sucrose, galactose, arabinose and xylose were quantified as individual peaks. Fructose and mannose were measured as a cumulative peak (Zicari, 2016).

7.3.6.2 Color measurement

The Minolta Chroma Meter CR-400 (Minolta Crop, Japan) was used to measure the color of fungal surface. The color meter utilizes the CIELAB system to measure the L*, a* and b* values from the samples. L* represents the lightness of a color, with 0 being pure black and 100 being pure white; a* represents the greenness (negative) to redness (positive); and b* represents blueness (negative) to yellowness (positive) (Weatherall & Coombs, 1992). The mean L*, a* and b* values were calculated for each sample. The overall color change (ΔE) was determined by comparing the L*, a* and b* values after specific treatments as calculated by Eqn.7.2 (Chen et al., 2018):

$$\Delta E = \sqrt{(L_0 - L)^2 + (a_0 - a)^2 + (b_0 - b)^2} \qquad \text{(Eqn.7.2)}$$

7.3.6.3 Texture analysis

Texture Profile Analysis (TPA) of fungal pellets was performed using a Texture Analyzer (model TA.XT.Plus). The TPA was carried out with two compression cycles using a TA-4 probe. Trigger force was 5g. Pretest, test and post-test speeds of the probe were 1 mm/s. One pellet was placed on the testing plate of the instrument and compressed to 50% of its initial height for both cycles. Twelve pellets from each preparation were tested. Hardness, resilience, and chewiness were calculated from the force time curve obtained following the published methods of Wee et al. (2018).

The crispness of hot air dried myco chips was evaluated through a puncture test following the methods used by (J. Chen et al., 2018b). A TA-5 cylinder penetrometer (2 mm diameter) was used for this assessment. The parameters included a pretest and teste speed of 5 mm/s, a post-test speed of 10 mm/s, and a trigger force of 20 g. The maximum force and the slope of the force curve from the initiation of the compression to the point of factorability (the first peak of force) were

collected. Ten replicates were performed for the crispness analysis. The average and standard deviation were reported.

7.3.6.4 Scanning electron microscope imaging

The structure and morphology of the cross section of complexed fungal pellets was imaged by Quattro S Environmental scanning electron microscope (ESEM, Thermo Fisher Scientific, United States) equipped with a Schottky FEG. Direct observation of non-conductive and hydrated samples without coating and drying was accomplished under low vacuum mode with a low vacuum detector (LVD). Pellets were randomly chosen after cultivation and kept hydrated in media before imaging. The pellets were cut gently and carefully by a blade before imaging the cross section of the pellets.

7.4 Results and Discussion

7.4.1 Fungal pellets deactivation with heat

The first experiments, which were preliminary screening, were done by testing fungal activity after been heat treated at 40, 50, 60 and 70℃ for 5 and 10 min. The results are shown in Table 7.4. The examples of active and deactivated fungal pellets' growth on PDA after five days are shown in Figure 7.6. Active pellets produced spores and yellow pigment while deactivated pellets did not. No fungal pellets growth was found after heat treatment at 60 ℃ and 70℃. They were still active after treatment at 40 ℃ and 50℃.

Table 7. 4. Preliminary fungal pellets deactivation test results

T (°C)	70		60		50		40	
Time (min)	5	10	5	10	5	10	5	10
Activity	×	×	×	×	✓	✓	✓	✓

×: deactive after heat treatment; ✓: active after heat treatment

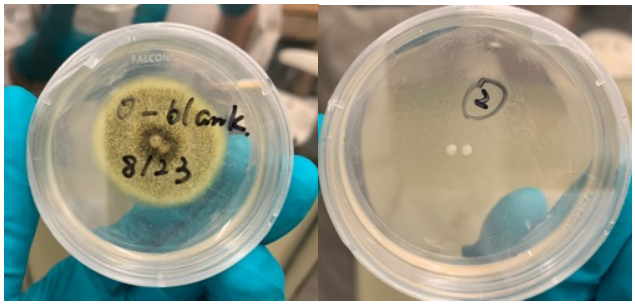

Figure 7. 6. Example of active (left) and deactivated (right) fungal pellets

Based on these preliminary experimental results, a more detailed screening process was carried out to determine the most efficient and effective conditions for deactivating fungal pellets in order to minimize the time and energy consumption. Fungal pellets were heated at 55℃ and 60℃ for 1, 2, 3, 4 and 5 min. The fungal activities after heat treatment were summarized in Table 7.5. Temperatures of at least 55°C for 3 min or 60°C for 2 min were needed to deactivate the fungal pellets.

Table 7. 5. Effects of temperature on fungal pellets activity

T (°C)	55					60				
Time (min)	1	2	3	4	5	1	2	3	4	5
Activity	✓	✓	×	×	×	✓	×	×	×	×

×: deactivated after heat treatment; ✓: active after heat treatment

7.4.2 Pellets produced from artificial food color and color stability

The fungal pellets cultivated from four different colors are shown in Figure 7.7. The color those fresh colored pellets and their stability after one-month storage in fridge (4℃) are shown in Table 7.6. A similar color stability analysis was performed on deactivated pellets, deactivated by 55°C for three minutes.

In both active and deactivated states, the pellets exhibited an increase in brightness (L* value) while their redness (a* value) decreased. However, the overall color change (ΔE) was higher in the deactivated pellets than in the active ones, except for sunset red. This indicates that the active mycelium plays a role in biosorption. However, the ability of fungal pellets to maintain the biosorption could be low at 4℃ due to the low metabolic activity, since most of the biosorption of dyes were conducted at higher temperature than 4℃ (Abd El-Rahim et al., 2009; Kaushik et al., 2014; S. Li et al., 2019).

Normally, color change in food products can result from processes such as photodegradation or oxidation. However, commercial dyes are specifically designed to resist photodegradation and oxidation (Forgacs et al., 2004). Given that the pellet samples were stored under refrigerated conditions and shielded from light exposure, those two factors could be excluded. It is probable that desorption of pigments from the pellets is the primary factor causing color change in both active and deactivated states. This is supported by the fact that the color change for all fungal pellets exceeded a ΔE value of 10, except for the grape violet. The grape violet pellets exhibited the highest color stability, with redness decreasing and yellowness remaining consistent for both active and deactivated states. The difference of overall color change indicating that the affinity of fungal pellets to different pigments also played an important role.

An interesting observation was the enlargement and floating of all active pellets on the liquid surface, accompanied by an unpleasant odor. As all the synthetic dyes used were azo dyes and considering a previous report by Gou et al. (2009) that *Penicillium sp* could degrade all azo dyes under anaerobic conditions. It can be posited that *A. awamori* might have metabolized the azo dyes as a substrate. Despite the low metabolic activity of *A. awamori* at 4°C, noticeable changes could occur over a month-long storage period. This study implies that artificial color-dyed pellets may not be suitable for prolonged storage in a refrigerator.

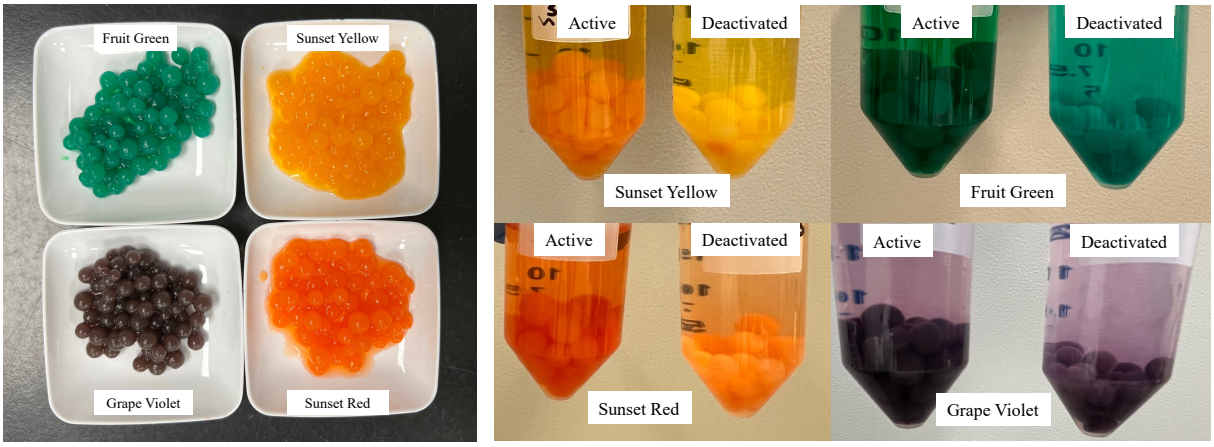

Figure 7. 7. Colorful pellets made from artificial food color. Left: harvested active fresh pellets; Right: comparison of active and deactivated pellets

Table 7. 6. Color stability of active pellets cultivated from artificial food color

		L^*	a^*	b^*	ΔE
Pre-cultured		49.78 ± 0.94	-0.20 ± 0.05	14.92 ± 0.97	
Sunset yellow	fresh	45.87 ± 2.04	23.11 ± 2.63	29.06 ± 1.71	
	1 month	53.32 ± 2.03	12.22 ± 2.23	33.87 ± 1.23	14.14 ± 2.66*
Fruit green	fresh	32.20 ± 2.06	-29.24 ± 2.95	1.32 ± 0.42	
	1 month	40.00 ± 1.48	-34.01 ± 1.22	-3.63 ± 0.46	10.49 ± 1.32
Sunset red	fresh	38.94 ± 2.15	21.50 ± 2.28	18.69 ± 0.85	
	1 month	58.81 ± 0.81	9.94 ± 0.50	18.39 ± 1.05	23.02 ± 0.75*
Grape violet	fresh	30.57 ± 2.13	3.07 ± 0.30	0.54 ± 0.06	
	1 month	34.84 ± 3.21	0.01 ± 0.60	0.54 ± 0.06	6.16 ± 1.64*

* Compared with fresh active pellets

Table 7. 7. Color stability of deactivated pellets cultivated from artificial food color

		L^*	a^*	b^*	ΔE
Sunset yellow	fresh	37.94 ± 1.54	9.41 ± 1.74	18.75 ± 2.77	
	1 month	56.50 ± 3.64	3.38 ± 0.34	15.94 ± 0.73	19.78 ± 3.35*
Fruit green	fresh	34.21 ± 0.54	-29.70 ± 1.82	-1.68 ± 0.20	
	1 month	45.53 ± 1.26	-35.99 ± 1.67	-7.13 ± 0.34	12.54 ± 1.76*
Sunset red	fresh	35.36 ± 0.75	12.53 ± 0.67	13.63 ± 0.72	
	1 month	52.46 ± 2.54	5.14 ± 0.25	12.31 ± 0.47	18.72 ± 2.26*
Grape violet	fresh	26.03 ± 0.17	2.05 ± 0.38	-0.20 ± 0.15	
	1 month	32.17 ± 0.82	-2.01 ± 0.54	-0.87 ± 0.42	7.42 ± 0.82*

* Compared with fresh deactivated pellets

7.4.3 Pellets production from natural colored media

7.4.3.1 Characteristics of initial feedstock

The feasibility of producing colorful pellets with natural colored media was also tested by cultivating fungal pellets in media made from five agricultural byproducts, including almond hulls, walnut hulls, ground coffee, pomegranate peel and delactosed permeate, one vegetable (red beet) and one juice (carrot juice). The characteristics of these materials including TS, MC, VS and sugar contents are shown in Table 7.8. Most of these feedstocks had enough sugar for fungal cultivation, except for ground coffee and walnut hull. As mentioned in Materials and Method section, glucose was added to walnut hulls and ground coffee extract for fungal cultivation.

Table 7. 8. Characteristics of initial feedstocks

Feedstock	TS% (w.b)	MC% (w.b)	VS% (d.b.)	Sugar % (d.b.)
Almond hull	88.4 ± 0.3	11.6 ± 0.3	82.8 ± 0.8	38.7 ± 0.6
Ground coffee	95.7 ± 0.0	4.3 ± 0.0	95.3 ± 0.1	0.0 ± 0.0
Walnut hull	14.0 ± 0.1	86.0 ± 0.1	84.8 ± 0.7	7.9 ± 0.1
Pomegranate peel	22.1 ± 0.1	77.9 ± 0.1	96.1 ± 0.1	52.1 ± 0.3
Red beet	8.1 ± 0.3	91.9 ± 0.3	86.2 ± 0.8	60.1 ± 0.1
Delactosed permeate				151.5 ± 3.2*
Carrot juice				50.9 ± 0.5*

* unit : g/L

7.4.3.2 Characteristics of pellets produced from natural colored media

After three days cultivation from precultured pellets, the fungal pellets were harvested and analyzed for biomass and pellet size. It was observed that these media favored the growth of the pellets to varying degrees. The average pellet size and biomass measurements are depicted in

Figure 7.8 and 7.9 respectively. Fungal pellet sizes were significantly increased compared to the pre-cultured pellets.

Typically, traditional tapioca pearls range between 5 mm and 10 mm in diameter (Wikipeida, 2023). All the fungal pellets cultivated were in this range, with the largest average size of 8.38 mm obtained from carrot juice, and the smallest average size of 5.21 mm from red beet. This suggested that pellets cultivated in carrot juice, suggesting that the nutrients in carrot juice most effectively facilitated pellet growth among the tested media. This might be attributed to the high vitamin content in carrot juice, which can act as growth factors for the fungal biomass. While the pellets cultivated from walnut hulls also displayed a large size, their biomass concentration was lower compared to that of the carrot juice, resulting in a looser pellet structure, hence, a lower density as depicted in Figure 7.10.

By correlating Figure 7.8 and 7.9, no distinct positive or negative relationship was found between pellet size and biomass concentration. This led to different specific biomass densities for pellets cultivated in different media, despite the total number of pellets in each flask being identical. These observations suggest that the nutrients present in the media can significantly influence the characteristics of the pellets. This study tested the effects of raw materials media on fungal pellets characteristics, extra nutrients could be added in the future study to produce fungal pellets with desired characteristics.

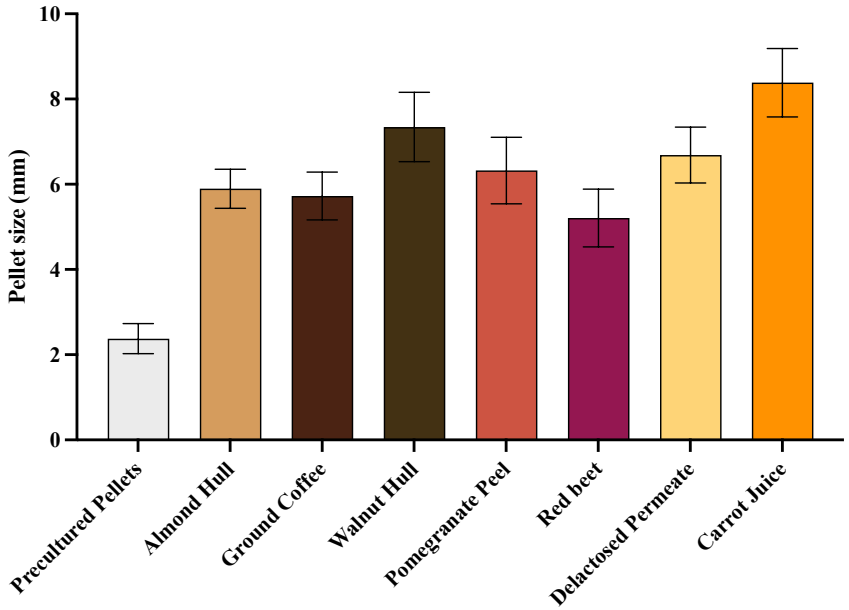

Figure 7. 8. Average size of fungal pellets cultivated from different natural media.

Y error bars are standard deviation.

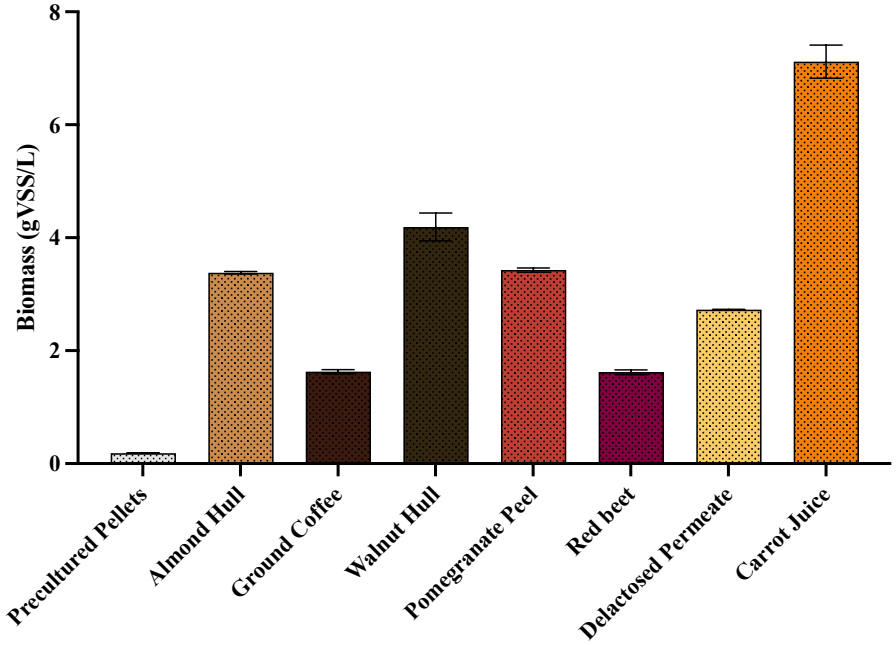

Figure 7. 9. Fungal biomass cocentraion cultivated from different natural media.

Y error bars are standard deviations.

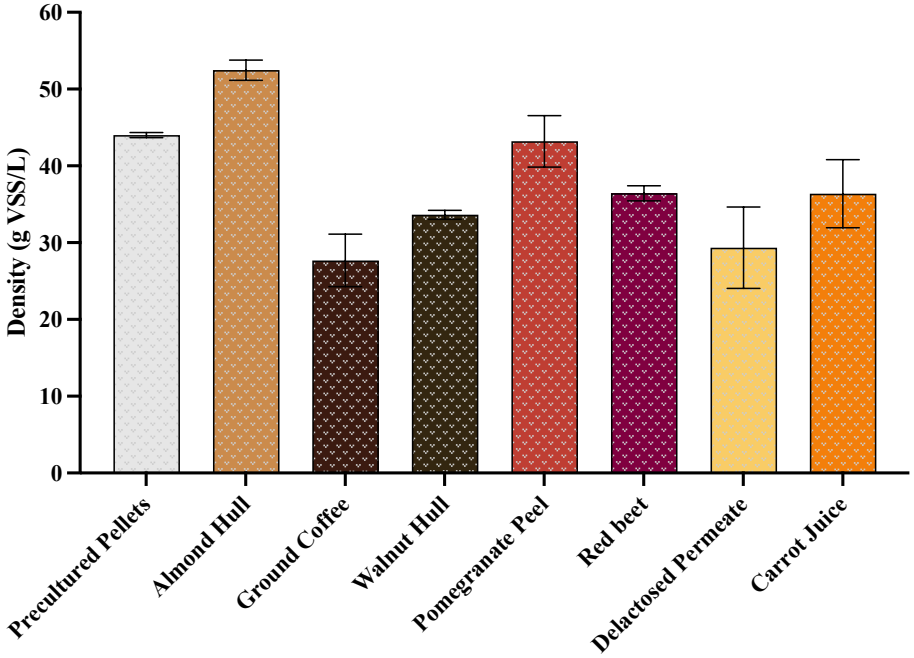

Figure 7. 10. Specific biomass density of fungal pellets cultivated from different natural media. Y error bars are standard deviations.

7.4.3.3 Color stability of pellets produced from natural colored media

After three days cultivation of precultured white pellets in different natural colored media, the pellets exhibited similar colors to their respective media colors (Figure 7.11). A particularly obvious color change was observed in the pellets and the media from pomegranate peel, with a shift from initial pinkish-red color to a more brownish color. Even though the media became more acidic after cultivation due to the production of organic acids, the anthocyanin pigments in pomegranate peel can exhibit a red color and has greater stability under acidic condition`s (Wahyuningsih et al., 2017). Therefore, the color change could likely be attributed to oxidation of anthocyanin, which was accomplished by the continuous air exchange in shaken flasks or the

action of enzymes like polyphenol oxidase that oxidize phenolic compounds to quinones and then polymerize to form brown pigments (Kader et al., 1997).

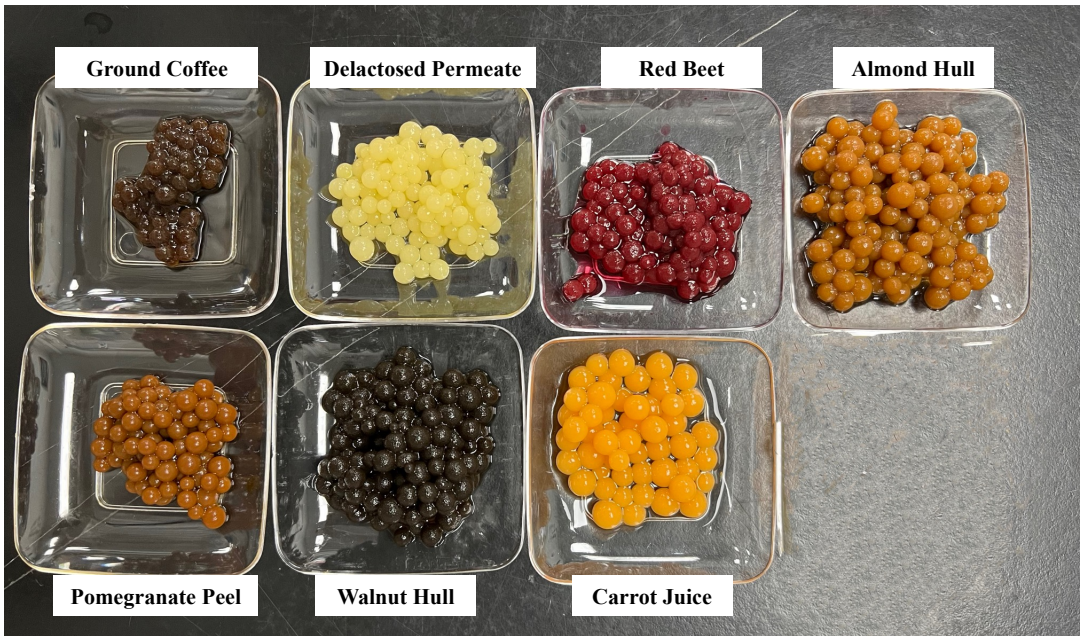

Figure 7. 11. Colorful pellets cultivated from natural media

The stability of both active and deactivated pellets over one-month period storage at 4℃ are shown in Table 7.9 and 7.10. Almond hull extract, ground coffee, walnut hull, carrot juice, and delactosed permeate were pasteurized at 80℃ before fungal cultivation, therefore the deactivation temperature (55℃) couldn't be a reason to cause the color change after heat deactivation. Among those five media, almond hull pellets were the most stable ones, with almost no color change after deactivation. There was only a slightly color change after one month storage, where ΔE were 3.45 and 3.02 of active and deactivated pellets, respectively. Combining with the high specific biomass density as shown in Figure 7.10, almond hull can be recommended for the production of fungal pellets with a one-month shelf life in both active and deactivated forms.

Carrot pellets also demonstrated stable, maintaining color consistency after heat deactivation. Given that the carotenoids in carrot juice can tolerate temperatures up to 100 ℃ (Dutra-de-Oliveira et al., 1998), the stability of color before and after heat deactivation indicated that fungal mycelium's activity had a minor impact on the carotenoid adherence to the fungal pellets. The color change after one-month storage for active and deactivated pellets was 6.8 and 8.6, respectively. This suggests that fading of the carotenoids, rather than desorption, might be the primary cause of color change. Fungal pellets cultivated from walnut hull, pomegranate peel, and coffee remained relatively stable; all except for coffee displayed a lightening of color after heat deactivation. The color of deactivated pellets from these media remained stable ($\Delta E < 5$) after one month of storage. The color of active pomegranate peel also remained stable after this period. This can be attributed to the oxidation of anthocyanin pigments in the pomegranate peel during the fungal cultivation process, which left minimal scope for further oxidation during the storage period and heat deactivation. A high overall color change of 13.19, primarily attributed to increased brightness, was observed in active pellets cultivated from delactosed permeate. This is likely due to the utilization of a protein source absorbed by the fungi, which led to slow growth of the fungal pellets over the one-month storage period. The stable color ($\Delta E = 3.83$) of deactivated pellets after storage excluded the possibility of color fading. Neither the active nor deactivated pellets from red beets maintained a stable color after storage.

Compared to the stability of artificial food color, these natural colored media proved more stable, as most of the overall color change were less than 10, particularly in deactivated pellets, where most had values lower than 5. This suggests that almond hull, ground coffee, walnut hull, and carrot juice can be used to produce both active and deactivated pellet products. Delactosed permeate can be utilized for the production of deactivated pellet products, or potentially for the

production of active pellet products by removing protein first. The color of pomegranate peel pellets was stable, although the expected pinkish-red color was not exhibited due to oxidation during the fungal cultivation process. Whether or not pomegranate peel should be considered for pellet production depends on the desired color and overall purpose of the final product.

Table 7. 9. Color stability of active pellets cultivated with natural colored media

		L^*	a^*	b^*	ΔE
Pre-cultured		49.78 ± 0.94	-0.20 ± 0.05	14.92 ± 0.97	
Almond hull	fresh	36.95 ± 2.60	13.62 ± 4.03	15.73 ± 2.32	
	1 month	37.18 ± 1.06	11.87 ± 2.04	16.92 ± 1.96	3.45 ± 0.97*
Coffee	fresh	37.03 ± 2.31	6.94 ± 1.67	2.76 ± 0.56	
	1 month	29.37 ± 1.52	4.18 ± 0.60	3.19 ± 1.44	8.29 ± 1.51*
Walnut hull	fresh	28.75 ± 2.19	0.81 ± 0.24	-0.48 ± 0.24	
	1 month	35.19 ± 2.06	3.93 ± 0.96	2.29 ± 0.84	7.81 ± 1.85*
Pomegranate peel	fresh	35.91 ± 2.58	7.12 ± 1.13	3.08 ± 0.81	
	1 month	31.97 ± 1.61	6.60 ± 1.01	4.34 ± 0.90	4.48 ± 1.22*
Red beet	fresh	42.34 ± 2.20	10.17 ± 1.41	3.21 ± 0.95	
	1 month	32.23 ± 1.30	7.45 ± 0.68	7.54 ± 0.71	11.37 ± 1.25*
Delactosed permeate	fresh	46.27 ± 5.50	0.52 ± 0.23	7.86 ± 2.04	
	1 month	59.42 ± 1.82	0.31 ± 0.21	8.75 ± 0.43	13.19 ± 1.82*
Carrot juice	fresh	44.24 ± 1.22	9.52 ± 0.95	23.08 ± 1.32	
	1 month	49.74 ± 1.63	11.44 ± 0.68	26.46 ± 0.92	6.80 ± 1.72*

* Compared with fresh active pellets

Table 7. 10. Color stability of deactivated pellets cultivated with natural colored media

		L^*	a^*	b^*	ΔE
Almond hull	fresh	36.58 ± 2.46	13.03 ± 4.71	15.98 ± 3.66	
	1 month	37.19 ± 1.77	14.41 ± 1.81	15.42 ± 1.71	3.02 ± 1.46*
Coffee	fresh	30.86 ± 2.43	5.12 ± 0.73	2.55 ± 0.97	
	1 month	31.71 ± 3.68	5.15 ± 1.42	2.22 ± 0.74	3.67 ± 1.44*
Walnut hull	fresh	34.02 ± 3.37	1.20 ± 0.93	1.12 ± 0.66	
	1 month	33.35 ± 1.97	4.37 ± 0.92	1.69 ± 0.79	3.85 ± 0.98*
Pomegranate peel	fresh	38.28 ± 3.67	11.75 ± 3.59	5.68 ± 1.05	
	1 month	35.79 ± 3.53	10.36 ± 2.83	5.81 ± 0.72	4.82 ± 2.04*
Red beet	fresh	30.58 ± 1.24	11.26 ± 1.97	2.30 ± 0.99	
	1 month	35.21 ± 2.31	9.83 ± 2.06	11.34 ± 1.56	10.59 ± 2.00*
Delactosed permeate	fresh	55.43 ± 3.48	0.53 ± 0.37	9.25 ± 0.89	
	1 month	57.85 ± 3.47	0.95 ± 0.43	8.89 ± 0.97	3.83 ± 1.88*
Carrot juice	fresh	45.62 ± 0.90	9.87 ± 0.36	23.48 ± 1.23	
	1 month	50.73 ± 0.96	14.21 ± 1.43	28.74 ± 1.50	8.60 ± 1.94*

* Compared with fresh deactivated pellets

7.4.4 Multilayered pellets produced from natural colored media

Based on previous studies, carrot juice was picked as an example feedstock for multilayered pellets production. The production of multilayered pellets was accomplished through a series of steps. Firstly, orange fungal pellets cultivated from pre-cultured pellets and carrot juice were heat-deactivated and then re-inoculated with spores in PDB. This allowed new fungal spores to attach to the surface of the deactivated carrot juice pellets and form fresh white mycelium on

the surface within three days (Figure 7.12a). Because *A. awamori* produces a yellow pigment known as aurasperone (J. Yu et al., 1967), this fresh mycelium could turn into yellow color after three days (Figure 7.12b). Further deactivation of these double layered yellow pellets and re-inoculation of new spores into PDB led to the formation of egg-like, multilayered pellets. These had a carrot color at the core, a yellow aurasperone layer in the middle, and an outer shell formed by new white mycelium (Figure 7.12c).

This study not only demonstrated the color stability of each pigment (either from natural feedstock or produced from fungi themselves) in both active and deactivated pellets but also showcased that the growth of new mycelium occurs on the surface of the pellets, rather than permeating the entire structure. These characteristics enable the production of multilayered pellets with distinct colors in each layer, rather than pellets with a uniform color throughout. By utilizing the inherent growth characteristics of fungi, this study offered a novel method to create visually appealing, pellet-based products that could potentially be attractive on the market. It's recommended to use natural feedstock instead of artificial food color based on color stability and nutritional value.

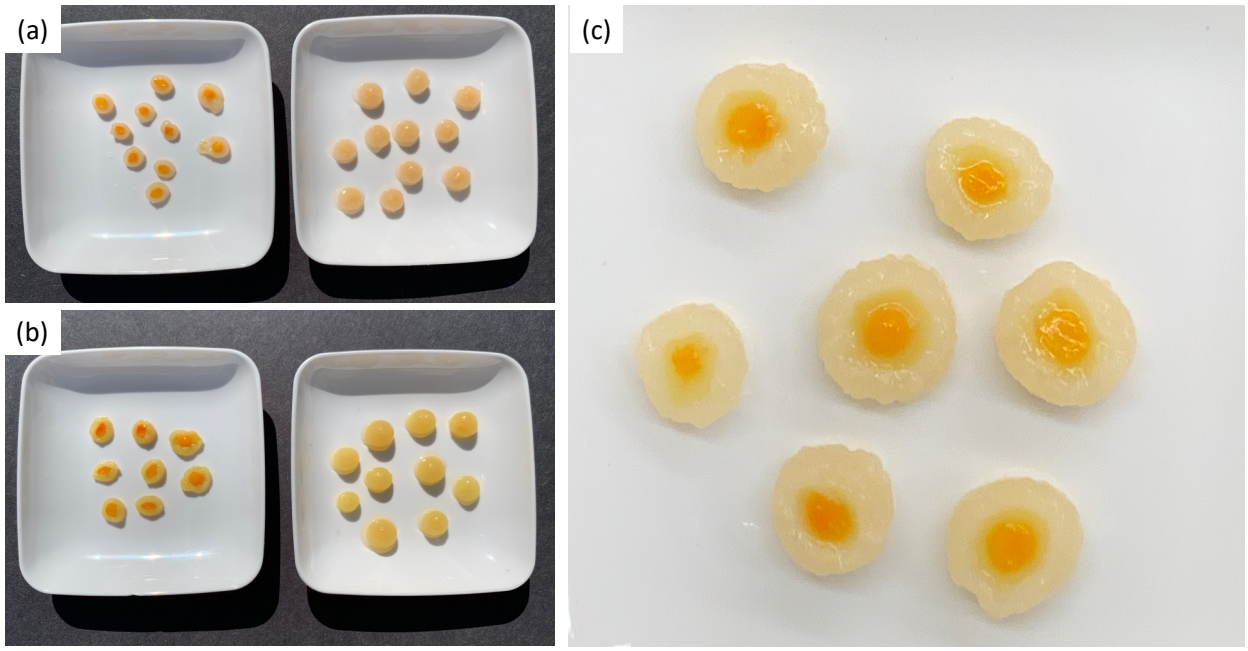

Figure 7. 12. Multilayered pellets cultivated from carrot juice and potato dextrose broth.

7.4.4.1 Nutrition value of two-layered pellets and spent media

In addition to color, it's essential to assess the nutritional value of the pellets. In this evaluation, the two-layered pellets displayed in Figure 7.12a were analyzed as representative samples and their nutritional values are shown in Table 7.11. One of our target products was alternative boba, named as “mycoBoba”. Therefore, its nutritional profile was compared with that of traditional tapioca pearls. As shown in Table 7.11, mycoBoba has a higher protein and dietary fiber contents than tapioca pearls. It also has a lower fat content, at 3.5% of dry matter, with no detectable trans-fat. The fat in mycoBoba comprises predominantly of palmitic, stearic, oleic, and linoleic fatty acids, accounting for 22.3%, 11.1%, 33.3%, and 33.3% of the total fatty acid content, respectively.

The caloric content of dried mycoBoba and tapioca pearls were 360 and 400 kcal/100g, respectively. It's important to note that these products are typically consumed in wet form,

immersed in a beverage. Thus, a fairer comparison would consider the nutritional profile of the products in their consumed form. MycoBoba contained 97% moisture, while cooked tapioca boba contain about 45% moisture (N.-N. Zhang et al., 2022). Consequently, the total calories in mycoBoba are significantly lower than in tapioca boba when consumed, at just 10 kcal/100g in mycoBoba compared to 220 kcal/100g of tapioca boba. Moreover, mycoBoba had a higher protein content than tapioca boba, along with higher contents of essential minerals like calcium, potassium, and sodium. Although excessive sodium intake can contribute to high blood pressure (Filippini et al., 2021), the sodium content in mycoBoba was significantly lower than the 2.3 g daily limit suggested by the Dietary Guidelines for Americans (FDA, 2023). Both tapioca pearls and mycoBoba had low iron content, although it's slightly higher in the tapioca pearls.

Table 7. 11. Nutrient contents of mycoBoba compared with Tapioca pearl

	100 g dried		100 g wet[a]	
	MycoBoba	Tapioca pearl[b]	Myco Boba	Tapioca pearl
Calories (kcal)	360	400	10	220
Total Fat (g)	3.5	0.02	0.1	0.01
Saturated Fat (g)	1.1	0.006	0.03	0.003
Monounsaturated Fat (g)	1.1	0.006	0.03	0.003
Polyunsaturated Fat (g)	1.1	0.003	0.03	0.002
Trans Fat (g)	0	0	0	0
Total Carbohydrate (g)	60	99	1.7	54.5
Dietary Fiber (g)	21	1	0.6	0.6
Protein (g)	33	0.2	0.9	0.1
Calcium (mg)	81	22	2.3	
Sodium (mg)	432	1	12.3	0.6
Potassium (mg)	667	12	19	6.6
Iron (mg)	<1	1.7	<1	0.9
Vitamin D (mcg)	<0.1	0	<0.1	0

[a] moisture content of mycoBoba and tapioca pearls were 97.15% and 45%, respectively; [b] reference (USDA, 2023c)

The existence of three digestive enzymes, amylase, protease, and lipase in spent media were analyzed to see if the spent media has any potential to be developed into drinks. An impressive alpha-amylase activity level of 15.92 Ceralpha Units (CU) per gram was detected in the spent media (Table 7.12). This implies that, under ideal conditions, each gram of spent media has enough alpha amylase to catalyze the conversion of starch into maltose at a rate of

approximately 16 μmol per minute. A significant presence of alpha amylase is thus indicated in the media by this high activity level. However, the presence of lipase and protease fell below the detection limit. This was anticipated since the tested mycoBoba were cultivated in PDB, a medium rich in starch without lipids and proteins. Therefore, only alpha amylase, the enzyme responsible for starch hydrolysis, was detected. In our previous studies (Chapter 4), organic acids, such as citric acid were also detected in the media collected after *A. awamori* cultivation. The alpha-amylase detected further demonstrated the potential of developing this spent media into health drinks.

Table 7. 12. Enzymes in spent media

Enzyme	Results
Alpha-Amylase activity	15.92 CU*/g
Lipase Activity	< 2783.0 U/g
Protease Activity	< LOQ U/g

*CU- Ceralpha Units

7.4.4.2 Mycotoxin screening of two-layered pellets and spent media

Since the mycoBoba were made from fungi, despite the fact that it utilizes an edible fungus (*A. awamori*) recognized as Generally Recognized as Safe (GRAS), it is understandable that there might still be safety concerns on food products produced from fungi, particularly regarding potential fungal/mold mycotoxin production. The screening process evaluated the most common mycotoxins associated with fungi, which were Aflatoxin B1, Deoxynivalenol (DON), T-2 toxin, Ochratoxin-A, Fumonisin-B1, and Zearalenone. Among these six mycotoxins, Aflatoxin B1 and Ochratoxin-A are known to be produced by *Aspergillus* species. As shown in Table 7.13, none of these mycotoxins were detected in either the mycoBoba or the spent media after fungal cultivation.

This demonstrated the safety of *A. awamori*-based products, at least from a toxicological perspective.

Table 7. 13. Mycotoxin screening of mycoBoba and spent media

Analyte	Results		Units	Rep. Limit
	MycoBoba	'Drink'		
Aflatoxin B1	Not detected	Not detected	ppb	5.0
DON	Not detected	Not detected	ppm	0.50
T-2	Not detected	Not detected	ppm	1.0
Ochratoxin - A	Not detected	Not detected	ppb	80
Fumonisin – B1	Not detected	Not detected	ppm	5.0
Zearalenone	Not detected	Not detected	ppm	0.50

7.4.5 Texture of fungal pellets

The texture characteristics of simple (no coating) and complexed pellets (coated with PDA and allowed to regrow) were analyzed and compared. As shown in Figure 7.13, complexed pellets displayed significantly increased characteristics of hardness, chewiness and resilience. The micro-scale structure of mycelium inside the complexed pellets was investigated and imaged by ESEM. As depicted in Figure 7.14a, a thick layer within the pellets was observed in complexed pellets, which is attributable to the agar coating process. As mentioned in Materials and Methods section, the complexed pellets were produced by coating PDA on pre-cultured pellets and then allowing regrowth in PDB. The micro-scale structure of pellets, cultivated by regrowing pre-cultured pellets into fresh PDB without any coating, is shown in Figure 7.14d. A condensed mycelium layer was seen in these pellets, but distinct from the thick layer present in the complexed pellets.

In complexed pellets, the mycelium could obtain nutrients and grow in both solid (PDA) and liquid (PDB) phases, especially the mycelium on thick layer. As shown in Figure 7.14b, no agar was observed on the thick layer, which could be penetrated and covered by the fast-growing mycelium on this layer. Normally, the transfer of nutrients towards the inner parts of the pellets are limited, thereby restricting growth at the center of the pellets. However, due to the coating, a more condensed mycelium formed inside the coating layer, where the mycelium can obtain nutrients from the PDA for continued growth. As shown in Figure 7.14c, some of the mycelia were covered by or covered on the PDA. This thick layer could potentially contribute to the improved texture of complexed pellets. However, this improvement in texture is not simply a result of the added agar texture to the fungal pellets. It also utilizes the PDA as both a nutrient source and supporting material. This approach, combing with the growth characteristics of fungi, provides a hybrid 'solid-submerged' cultivation system for fungal growth. Taste tests of these complex pellets revealed no detectable agar mouth feel among all our testers (data is not reported), indicating the fungal mycelium was well-incorporated within the PDA, leading to a consistent and homogeneous sensory experience.

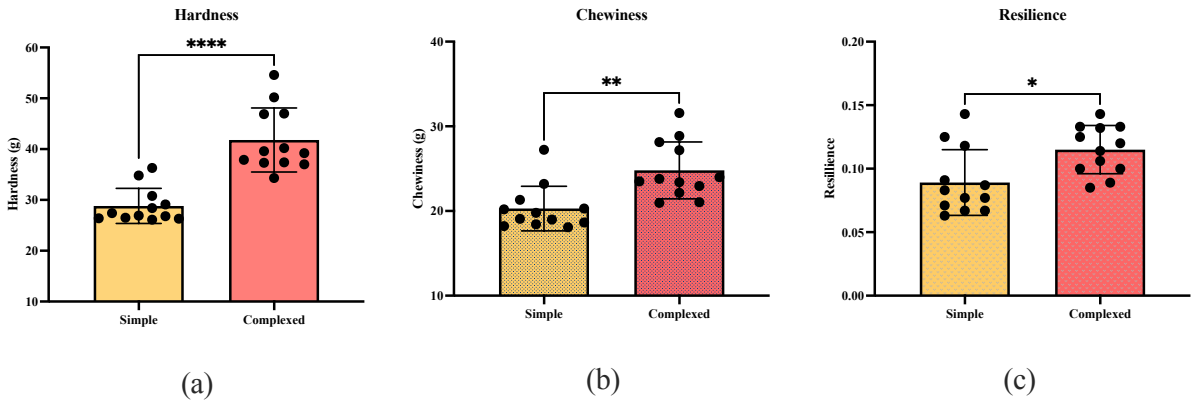

Figure 7. 13. Texture comparison of simple and complexed pellets (n =12).

Starred (*) marks demote statistically significance at the p< 0.05 level of two-tailed t-tests. Additional starts (e.g.**) indicate p << 0.05.

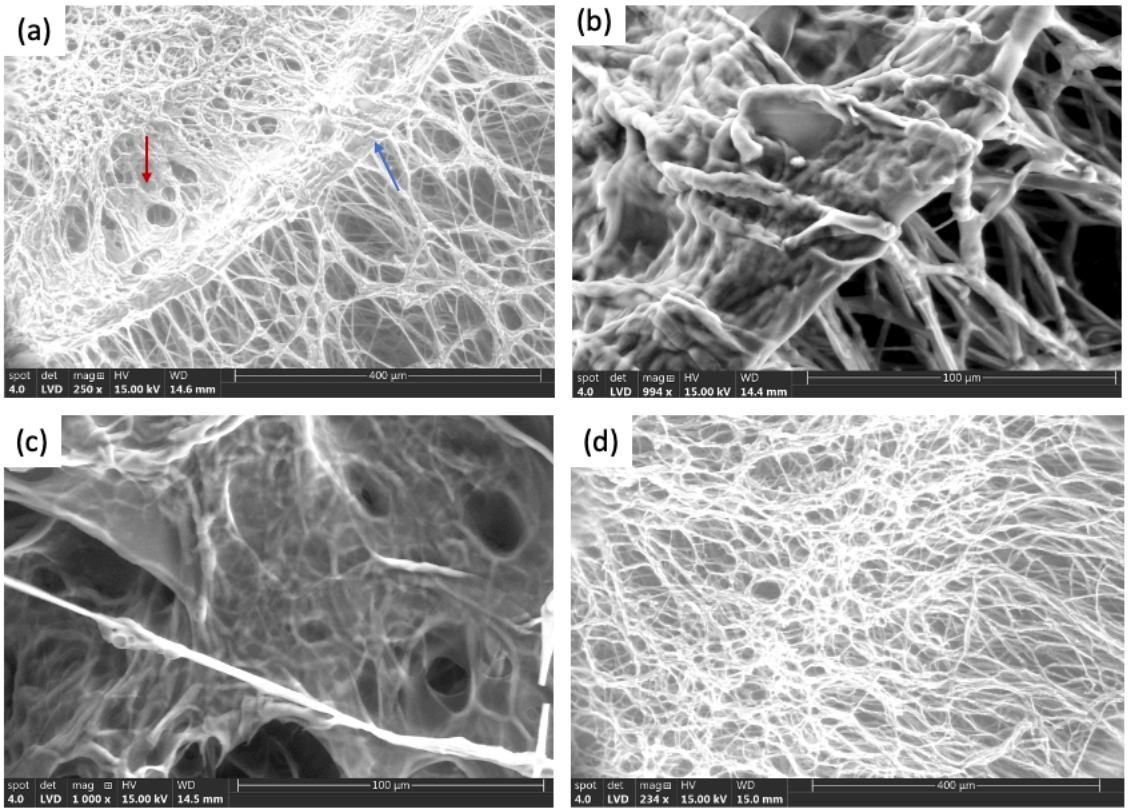

Figure 7. 14. ESEM imaging of fungal pellets: (a) thick layer inside complexed pellets; (b) fungal mycelium on the layer, blue arrow in a; (c) inside side the layer, red arrow in figure a; (d) layer inside uncoated pellets

7.4.6 Texture and color of dried pellets

The color values of the fungal biomass after both hot air and freeze dying, along with their initial wet color values are listed in Table 7.14. Almost all fungal pellets experienced a significant color change after both drying processes. Most hot air-dried pellets displayed a dark brown color (with the exception of carrot juice samples) (Figure 7.15a). This could potentially be due to the Maillard reaction or caramelization, both of which are heat-induced processes. In addition, the shrinkage of the samples after hot air could have compacted the biomass, led to the darker appearance. While the overall color change (ΔE) was lower in hot air drying compared to freeze drying. The high overall color change after freeze drying was mainly due to the increase of brightness (Figure 7.15b). For instance, the red beet sample exhibited a lighter purple color after freeze drying. However, it appeared to darken significantly when subjected to hot air drying observed by the naked eye. However, the total color change (ΔE) was higher in freeze drying compared to hot air drying. In this situation, it is essential to evaluate the acceptability of such color changes from diverse perspectives and for different applications, rather than only focusing on the numerical values of total color change.

Table 7. 14. The color of fungal pellets dried by hot air and freeze drying

		L^*	a^*	b^*	ΔE
Almond hull	fresh	36.95 ± 2.60	13.62 ± 4.03	15.73 ± 2.32	
	hot air drying	32.96 ± 3.50	5.37 ± 1.94	2.69 ± 1.42	$16.23 \pm 2.53^*$
	freeze drying	56.26 ± 2.18	11.90 ± 0.92	28.33 ± 1.17	$23.15 \pm 2.6^*$
Coffee	fresh	37.03 ± 2.31	6.94 ± 1.67	2.76 ± 0.56	

	hot air drying	33.01 ± 1.53	-0.94 ± 2.70	0.40 ± 0.92	9.31 ± 2.62*
	freeze drying	44.53 ± 0.58	9.31 ± 0.29	22.41 ± 0.40	21.18 ± 0.30*
Walnut hull	fresh	28.75 ± 2.19	0.81 ± 0.24	-0.48 ± 0.24	
	hot air drying	35.88 ± 1.72	-0.54 ± 0.59	1.47 ± 0.24	7.53 ± 1.77*
	freeze drying	38.05 ± 0.96	15.31 ± 0.75	17.06 ± 0.35	24.61 ± 0.58*
Pomegranate peel	fresh	35.91 ± 2.58	7.12 ± 1.13	3.08 ± 0.81	
	hot air drying	37.72 ± 00.58	2.50 ± 0.71	2.66 ± 0.74	5.05 ± 0.46*
	freeze drying	55.68 ± 1.02	16.20 ± 0.58	42.58 ± 1.18	45.11 ± 1.22*
Red beet	fresh	42.34 ± 2.20	10.17 ± 1.41	3.21 ± 0.95	
	hot air drying	26.55 ± 0.66	2.58 ± 0.22	-0.15 ± 1.25	17.87 ± 0.59*
	freeze drying	43.35 ± 1.25	30.18 ± 1.51	4.82 ± 0.33	20.14 ± 1.48*
Delactosed permeate	fresh	46.27 ± 5.50	0.52 ± 0.23	7.86 ± 2.04	
	hot air drying	43.79 ± 1.02	22.86 ± 1.70	31.99 ± 1.52	33.02 ± 1.60*
	freeze drying	73.83 ± 2.73	5.40 ± 0.66	28.76 ± 1.53	35.02 ± 1.63*
Carrot juice	fresh	44.24 ± 1.22	9.52 ± 0.95	23.08 ± 1.32	
	hot air drying	44.06 ± 1.00	26.37 ± 1.59	29.11 ± 1.04	17.96 ± 1.48v
	freeze drying	77.93 ± 1.13	6.27 ± 0.37	28.99 ± 0.45	34.37 ± 1.11*

* Compared with fresh activated pellets

Minor shrinkage was observed after freeze drying, while hot air drying resulted in significantly shrinkage, approximately 90%. During the freeze-drying process, frozen water is directly sublimated from solid to gas phase due to the reduced surrounding pressure. This direct transition, skipping the liquid phase, is less disruptive to the structure of the samples, thus preserving their original shape and size (Ratti, 2001). In contrast, hot air drying removes water through diffusion and fast evaporation due to heat and air flow, which can rupture cell walls and cause the pellets to shrink or collapse. Due to these water removal processes, the texture of samples after those two drying methods were very different. The samples after freeze drying were quite brittle. During freeze drying, the frozen water served as an internal support within the pellets. Once it was sublimated, it left behind a network of empty spaces and pores making the dried pellets more fragile (Figure 7.15c). Given this characteristic, freeze dried fungal biomass could be formulated into powdered products, such as protein and fiber powders. Meanwhile, hot air dried biomass is more suited for developing into chip-like products. Hence, the crispness of hot air dried samples was analyzed.

The thickness of the hot air dried fungal biomass shrank from the initial 10 mm to 1 mm (Figure 7.15d) with a final moisture content of 8.6%. In the puncture test, the initial slope was 2.4 kg/s and the maximum force of break was 0.04 kg. The initial slope value is positively correlated with crispness and the larger maximum force of break suggests less crispness (Pekke et al., 2013). Normally, the initial slope is recommended as a measure of crispness due to its lower variability compared to the maximum force of break (Pedreschi & Moyano, 2005). The crispness of "myco chip" analyzed was crispier than carrot chips (J. Chen et al., 2018b) dried by 60℃ hot air with a thickness less than 1 mm, which had an initial slope of 1.28 kg/s and 0.4 kg maximum force. This study suggests that fungal biomass dried by hot air has a great potential for the production of chips.

Figure 7. 15. Dried fungal biomass cultivated from natural materials by freeze drying or hot air drying. (a) hot air dried fungal biomass from natural materials; (b) freeze dried fungal biomass from natural materials; (c) freeze dried fungal biomass from almond hulls; (d) hot air-dried fungal biomass from almond hulls

7.4.7 Health evaluation by mouse study

After four weeks of mouse study, it was observed that the body weight of mice fed with *A. awamori* biomass was significantly lower compared to those fed with a high fat diet, and similar to those on the low fat diet. The lower body weight in mice consuming *A. awamori* might be linked to the high fiber content of the fungus, which is known to promote satiety and thus reduce overall

caloric intake. In addition, fibers are also known to affect the gut microbiota, which may have indirect effects on body weight management. The total plasma cholesterol levels of the mice fed with the fungal biomass also exhibited a notable decrease compared to those in the high fat group. This included a reduction in the levels of VLDL, LDL, and HDL cholesterol, indicating potential role of *A. awamori* in lipid metabolism. The average weight of adipose tissue was significantly lower in the group fed with *A. awamori* biomass compared to the high fat diet group, which further aligned with the lower body weight and suggested an overall decrease in body fat storage in mice consuming the *A. awamori* diet. These findings indicate that *A. awamori* biomass can have significant health benefits and have considerable potential as functional food. More detailed experimental set up, methodology, and the results from this mouse study will be released by USDA. The information listed here just show some key findings and conclusions from their study to demonstrate all the research done in this chapter was valuable. Ultimately, any improvements in texture and color must be linked with health benefits, as these are the foundational criteria for the development of novel products.

7.5 Conclusions

The color of fungal pellets was modified by cultivated them on artificial food colors and natural colored media derived from agricultural and food industry byproducts/waste for pellets cultivation. Both artificial dyes and natural colored media were successful in coloring the pellets. However, natural dyes proved more stable for long storage. Active pellets demonstrated the potential to degrade the pigment compounds over time during storage. Fungal pellets with multilayered colors were successfully created by deactivating pre-cultured color pellets and re-inoculating them with new spores. Texture of fungal pellets including hardness, chewiness and resilience were improved by coating precultured pellets with PDA and regrowing them in new

PDB. This process resulted in a thick layer of fungal mycelium inside the pellets, with the PDA serving as both a nutrient source and supporting material. Combined with the growth characteristics of fungi, this strategy provided a hybrid 'solid-submerged' cultivation system for fungal growth and finally the improved the texture of pellets.

The mycoBoba had significantly lower calories, higher protein content, and no detectable trans fats. Additionally, the medium collected after mycoBoba cultivation contained a good amount of alpha amylase, opening the possibility for its use in drinks. Hot air and freeze drying significantly altered the color of the fungal biomass. Freeze drying resulted in lighter colors while hot air drying led to darker colors. Freeze-dried fungal pellets retained their initial pellet shape but were very fragile, making them ideal candidates for development into protein and fiber powder-based products. On the other hand, hot air drying caused significant shrinkage (about 90%) of the fungal biomass. The resulting product demonstrated a crispness similar to carrot chips. Feeding mice with the pellets resulted in lower body weight, adipose weight, and cholesterol levels compared to a high fat diet. In conclusion, *A. awamori* biomass has great potential to be developed into different food products in both wet and dried forms, with adjustable color and texture properties. Moreover, these food products are not only safe but also offer significant health benefits.

REFERENCES

Abd El-Rahim, W. M., El-Ardy, O. A. M., & Mohammad, F. H. A. (2009). The effect of pH on bioremediation potential for the removal of direct violet textile dye by Aspergillus niger. *Desalination*, *249*(3), 1206–1211.

Abdelhady, D. H., El-Abasy, M. A., Abou-Asa, S. S. E., Elbialy, Z. I., Shukry, M., Hussein, A. H., Saleh, A. A., & El-Magd, M. A. (2017). The ameliorative effect of Aspergillus awamori on aflatoxin B1-induced hepatic damage in rabbits. *World Mycotoxin Journal*, *10*(4), 363–373.

Adapa, P., Tabil, L., & Schoenau, G. (2011). Grinding performance and physical properties of non-treated and steam exploded barley, canola, oat and wheat straw. *Biomass and Bioenergy*, *35*(1), 549–561.

Akpinar-Bayizit, A. (2014). Fungal lipids: the biochemistry of lipid accumulation. *International Journal of Chemical Engineering and Applications*, *5*(5), 409.

Alam, N., Amin, R., Khan, A., Ara, I., Shim, M. J., Lee, M. W., & Lee, T. S. (2008). Nutritional analysis of cultivated mushrooms in Bangladesh–Pleurotus ostreatus, Pleurotus sajor-caju, Pleurotus florida and Calocybe indica. *Mycobiology*, *36*(4), 228–232.

Alibaba. (2023a). *Yeast extract powder*. https://www.alibaba.com/product-detail/Water-Soluble-Yeast-Powder-Animal-Feed_1600573249450.html?spm=a2700.galleryofferlist.0.0.7c674e43a4qkPh

Alibaba. (2023b). *Ammonium chloride NH4CL 99.5% min*. mmonium chloride NH4CL 99.5% min

Alibaba. (2023c). *Tapioca Boba*. https://www.alibaba.com/product-detail/Boba-Tapioca-Boba-3kg_10000000347699.html?s=p

Alibes, X., Maestre, M. R., Munoz, F., Combellas, J., & Rodriguez, J. (1983). Nutritive value of almond hulls for sheep. *Animal Feed Science and Technology*, *8*(1), 63–67.

Almond Board of California. (2019). *Almonds Hulls in Chicken Feed? Capstone Project Explores Feasibility*. https://www.almonds.com/almond-industry/industry-news/almonds-hulls-chicken-feed-capstone-project-explores-feasibility#:~:text=Almond%20hulls%20contain%20free%20sugars,%25)%20on%20dry%20weight%20basis.

Almond Board of California. (2020). *Almond Varieties and Selections Evaluation of National and International Varieties or Selections Under Development*. chrome-extension://efaidnbmnnnibpcajpcglclefindmkaj/https://www.almonds.com/sites/default/files/2020-09/Almond%20Board%20of%20California%20Report%20%E2%80%93%20Almond%20Varieties%20and%20Selections.pdf

Almond Board of California. (2022). *Almond Almanac - 2022*. https://www.almonds.com/sites/default/files/2022-12/2022_Almanac.pdf

American Type Culture Collection. (2023). *Aspergillus awamori Nakazawa - 22342 | ATCC*. https://www.atcc.org/products/22342?matchtype=&network=g&device=c&adposition=&keyword=&gad=1&gclid=CjwKCAjw9pGjBhB-EiwAa5jl3B-Kp4gDpmANNggIFaOikASkbIhoGHLLFxfDL3yQXG0j0AEAbL2suRoC_L8QAvD_BwE

Andrews, E. M., Kassama, S., Smith, E. E., Brown, P. H., & Khalsa, S. D. S. (2021). A review of potassium-rich crop residues used as organic matter amendments in tree crop agroecosystems. *Agriculture*, *11*(7), 580.

Antecka, A., Bizukojc, M., & Ledakowicz, S. (2016). Modern morphological engineering techniques for improving productivity of filamentous fungi in submerged cultures. *World Journal of Microbiology and Biotechnology*, *32*, 1–9.

Anuradha, K., Padma, P. N., Venkateshwar, S., & Reddy, G. (2014). Effect of physical factors on pellet morphology of Aspergillus awamori MTCC 9166 and polygalacturonase production. *Biocatalysis and Agricultural Biotechnology*, *3*(4), 271–274.

APAH, Rice, E., Baird, R., & Eaton, A. (2017). *Standard Methods for the Examination of Water and Wastewater ed-23rd. Washington DC: American Public Health Association (APHA), American Water Works Association (AWWA) and Water Environment Federation (WEF)*.

APHA, AWWA, & WEF. (2017). 3120 B. Iductively Coupled Plasma (ICP) Method. *Standard Methods for the Examination of Water and Wastewater, American Public Health Association*, 1–5.

Archer, D. B., Connerton, I. F., & MacKenzie, D. A. (2008). Filamentous fungi for production of food additives and processing aids. *Food Biotechnology*, 99–147.

Asmus, J. (2016). *Nutritionist Perspective on Almond Hulls as a Feed Ingredient* -.

Athenaki, M., Gardeli, C., Diamantopoulou, P., Tchakouteu, S. S., Sarris, D., Philippoussis, A., & Papanikolaou, S. (2018). Lipids from yeasts and fungi: physiology, production and analytical considerations. *Journal of Applied Microbiology*, *124*(2), 336–367.

Baah Appiah-Nkansah, N., Li, J., Zhang, K., Zhang, M., & Wang, D. (2019). Study on mass transfer kinetics of sugar extraction from sweet sorghum biomass via diffusion process and ethanol yield using SSF. *Processes*, *7*(3), 137.

Babič, J., & Pavko, A. (2012). Enhanced enzyme production with the pelleted form of D. squalens in laboratory bioreactors using added natural lignin inducer. *Journal of Industrial Microbiology and Biotechnology*, *39*(3), 449–457.

Baladhandayutham, S., & Thangavelu, V. (2011). Optimization and kinetics of solid-state fermentative production of pectinase by Aspergillus awamori. *Int J ChemTech Res*, *3*(4), 1758–1764.

Barakat, A., Mayer-Laigle, C., Solhy, A., Arancon, R. A. D., De Vries, H., & Luque, R. (2014). Mechanical pretreatments of lignocellulosic biomass: towards facile and environmentally sound technologies for biofuels production. *Rsc Advances*, *4*(89), 48109–48127.

Barzee, T. (2020). *Processing and utilization of anaerobic digestate as biofertilizer for production of crops and microalgae*. University of California, Davis.

Barzee, T. J., El Mashad, H. M., Cao, L., Chio, A., Pan, Z., & Zhang, R. (2022). Cell-cultivated food production and processing: A review. *Food Bioengineering*, *1*(1), 4–25.

Bastos, R. G., & Ribeiro, H. C. (2020). Citric acid production by the solid-state cultivation consortium of and from sugarcane bagasse. *The Open Biotechnology Journal*, *14*(1).

Beauvais, A., Schmidt, C., Guadagnini, S., Roux, P., Perret, E., Henry, C., Paris, S., Mallet, A., Prévost, M., & Latgé, J. P. (2007). An extracellular matrix glues together the aerial-grown hyphae of Aspergillus fumigatus. *Cellular Microbiology*, *9*(6), 1588–1600.

Beniwal, V., & Chhokar, V. (2010). Statistical optimization of culture conditions for tannase production by Aspergillus awamori MTCC 9299 under submerged fermentation. *Asian J Biotechnol*, *2*(1), 46–52.

Cairns, T. C., Zheng, X., Zheng, P., Sun, J., & Meyer, V. (2019). Moulding the mould: understanding and reprogramming filamentous fungal growth and morphogenesis for next generation cell factories. *Biotechnology for Biofuels*, *12*(1), 1–18.

California Water Service. (2023). *California Water Service*. https://www.calwater.com/

Calixto, F. S., & Cañellas, J. (1982). Chemical composition of hulls of the sweet almond (Prunus amygdalus). *Journal of the Science of Food and Agriculture*, *33*(4), 336–339.

Cao, J., Zhang, H.-J., & Xu, C.-P. (2014). Culture characterization of exopolysaccharides with antioxidant activity produced by Pycnoporus sanguineus in stirred-tank and airlift reactors. *Journal of the Taiwan Institute of Chemical Engineers*, *45*(5), 2075–2080.

Ceillia Parsons. (2022). Almond Hull Prices are a Bright Spot for the Almond Industry. *West Coast Nut*. https://www.wcngg.com/2022/04/18/almond-hull-prices-are-a-bright-spot-for-the-almond-industry/#:~:text=Prices%20for%20hulls%20have%20nearly,%24170%2Dper%2Dton%20range.

Čertík, M., Adamechová, Z., & Laoteng, K. (2012). Microbial production of γ-linolenic acid: Submerged versus solid-state fermentations. *Food Science and Biotechnology*, *21*, 921–926.

Chan, L. G., Cohen, J. L., & de Moura Bell, J. M. L. N. (2018). Conversion of agricultural streams and food-processing by-products to value-added compounds using filamentous fungi. *Annual Review of Food Science and Technology*, *9*, 503–523.

Chen, J., Venkitasamy, C., Shen, Q., McHugh, T. H., Zhang, R., & Pan, Z. (2018a). Development of healthy crispy carrot snacks using sequential infrared blanching and hot air drying method. *LWT*, *97*, 469–475.

Chen, J., Venkitasamy, C., Shen, Q., McHugh, T. H., Zhang, R., & Pan, Z. (2018b). Development of healthy crispy carrot snacks using sequential infrared blanching and hot air drying method. *LWT*, *97*, 469–475.

Chen, Y. (2020). *Development of an Integrated Soluble Sugar and Biomethane Production System from Sugar Beets and Dairy Manure*. https://shorturl.at/jrMOP

Crank, J. (1979). *The mathematics of diffusion*. Oxford university press.

Cui, Y. Q., Van Der Lans, R. G. J. M., Giuseppin, M. L. F., & Luyben, K. C. A. M. (1998). Influence of fermentation conditions and scale on the submerged fermentation of Aspergillus awamori. *Enzyme and Microbial Technology*, *23*(1–2), 157–167. https://doi.org/10.1016/S0141-0229(98)00041-6

Danyluk, M. D., Brandl, M. T., & Harris, L. J. (2008). Migration of Salmonella Enteritidis phage type 30 through almond hulls and shells. *Journal of Food Protection*, *71*(2), 397–401.

DePeters, E. J., Swanson, K. L., Bill, H. M., Asmus, J., & Heguy, J. M. (2020a). Nutritional composition of almond hulls. *Applied Animal Science*, *36*(6), 761–770.

DePeters, E. J., Swanson, K. L., Bill, H. M., Asmus, J., & Heguy, J. M. (2020b). Nutritional composition of almond hulls. *Applied Animal Science*, *36*(6), 761–770.

Desnoues, E., Génard, M., Quilot-Turion, B., & Baldazzi, V. (2018). A kinetic model of sugar metabolism in peach fruit reveals a functional hypothesis of a markedly low fructose-to-glucose ratio phenotype. *The Plant Journal*, *94*(4), 685–698.

Dey, T. B., Adak, S., Bhattacharya, P., & Banerjee, R. (2014). Purification of polygalacturonase from Aspergillus awamori Nakazawa MTCC 6652 and its application in apple juice clarification. *LWT-Food Science and Technology*, *59*(1), 591–595.

Dutra-de-Oliveira, J. E., Fávaro, R. M. D., Junqueira-Franco, M. V. M., Carvalho, C. G., Jordão, A. A., & Vannucchi, H. (1998). Effect of heat treatment on the biological value of β-carotene added to soybean cooking oil in rats. *International Journal of Food Sciences and Nutrition*, *49*(3), 205–210.

ecovative. (2023). *ecovative*. https://www.ecovative.com/pages/food

El-Deep, M. H., Dawood, M. A. O., Assar, M. H., & Ahamad Paray, B. (2021). Aspergillus awamori positively impacts the growth performance, nutrient digestibility, antioxidative activity and immune responses of growing rabbits. *Veterinary Medicine and Science*, *7*(1), 226–235.

Eroshin, V. K., Satroutdinov, A. D., Dedyukhina, E. G., & Chistyakova, T. I. (2000). Arachidonic acid production by Mortierella alpina with growth-coupled lipid synthesis. *Process Biochemistry*, *35*(10), 1171–1175.

Espinosa-Ortiz, E. J., Rene, E. R., Pakshirajan, K., van Hullebusch, E. D., & Lens, P. N. L. (2016). Fungal pelleted reactors in wastewater treatment: Applications and perspectives. *Chemical Engineering Journal*, *283*, 553–571. https://doi.org/10.1016/j.cej.2015.07.068

FDA. (2023). *Sodium in Your Diet*. https://www.fda.gov/food/nutrition-education-resources-materials/sodium-your-diet

Fernandez-Bayo, J. D., Shea, E. A., Parr, A. E., Achmon, Y., Stapleton, J. J., VanderGheynst, J. S., Hodson, A. K., & Simmons, C. W. (2020). Almond processing residues as a source of organic acid biopesticides during biosolarization. *Waste Management*, *101*, 74–82.

Filippini, T., Malavolti, M., Whelton, P. K., Naska, A., Orsini, N., & Vinceti, M. (2021). Blood pressure effects of sodium reduction: dose–response meta-analysis of experimental studies. *Circulation*, *143*(16), 1542–1567.

Forgacs, E., Cserháti, T., & Oros, G. (2004). Removal of synthetic dyes from wastewaters: a review. *Environment International*, *30*(7), 953–971.

Garcia, B. R. (2021). *Hedgerow effects on pollinator abundance in San Joaquin valley organically managed almond orchards (Doctoral dissertation, California State Polytechnic University, Pomona)*. https://scholarworks.calstate.edu/downloads/3484zp00q

Garna, H., Mabon, N., Wathelet, B., & Paquot, M. (2004). New method for a two-step hydrolysis and chromatographic analysis of pectin neutral sugar chains. *Journal of Agricultural and Food Chemistry*, *52*(15), 4652–4659.

Gema, H., Kavadia, A., Dimou, D., Tsagou, V., Komaitis, M., & Aggelis, G. (2002). Production of γ-linolenic acid by Cunninghamella echinulata cultivated on glucose and orange peel. *Applied Microbiology and Biotechnology*, *58*, 303–307.

Glass, N. L., Jacobson, D. J., & Shiu, P. K. T. (2000). The genetics of hyphal fusion and vegetative incompatibility in filamentous ascomycete fungi. *Annual Review of Genetics*, *34*(1), 165–186.

Gou, M., Qu, Y., Zhou, J., Ma, F., & Tan, L. (2009). Azo dye decolorization by a new fungal isolate, Penicillium sp. QQ and fungal-bacterial cocultures. *Journal of Hazardous Materials*, *170*(1), 314–319.

Grand View Research. (2023). *Bubble Tea Market Size, Share & Trend Analysis Report* . Grand View Research. https://www.grandviewresearch.com/industry-analysis/bubble-tea-market

Hamad, H., Alma, M., ISMAEL, H., & GÖÇERİ, A. (2014). The effect of some sugars on the growth of Aspergillus niger. *KSÜ Doğa Bilimleri Dergisi*, *17*(4), 7–11.

Harris, L. J., & Ferguson, L. (2013). Improving the safety of almonds and pistachios. In *Improving the safety and quality of nuts* (pp. 350–378). Elsevier.

Hayashi, K., Kajiwara, Y., Futagami, T., Goto, M., & Takashita, H. (2021). Making traditional Japanese distilled liquor, shochu and awamori, and the contribution of white and black koji fungi. *Journal of Fungi*, *7*(7), 517.

Hille, A., Neu, T. R., Hempel, D. C., & Horn, H. (2009). Effective diffusivities and mass fluxes in fungal biopellets. *Biotechnology and Bioengineering*, *103*(6), 1202–1213.

Holtman, K. M., Offeman, R. D., Franqui-Villanueva, D., Bayati, A. K., & Orts, W. J. (2015). Countercurrent extraction of soluble sugars from almond hulls and assessment of the bioenergy potential. *Journal of Agricultural and Food Chemistry*, *63*(9), 2490–2498. https://doi.org/10.1021/jf5048332

Hong, S.-B., Lee, M., Kim, D.-H., Varga, J., Frisvad, J. C., Perrone, G., Gomi, K., Yamada, O., Machida, M., & Houbraken, J. (2013). Aspergillus luchuensis, an industrially important black Aspergillus in East Asia. *PloS One*, *8*(5), e63769.

Huang, G., & Lapsley, K. (2019). Almonds. In *Integrated Processing Technologies for Food and Agricultural By-Products* (pp. 373–390). Elsevier.

Huq, T., Khan, A., Brown, D., Dhayagude, N., He, Z., & Ni, Y. (2022). Sources, production and commercial applications of fungal chitosan: A review. *Journal of Bioresources and Bioproducts*.

Ibrahim, D., Weloosamy, H., & Lim, S.-H. (2015). Effect of agitation speed on the morphology of Aspergillus niger HFD5A-1 hyphae and its pectinase production in submerged fermentation. *World Journal of Biological Chemistry*, *6*(3), 265.

Isfahlan, A. J., Mahmoodzadeh, A., HASANZADEH, A., Heidari, R., & Jamei, R. (2010). Antioxidant and antiradical activities of phenolic extracts from Iranian almond (Prunus amygdalus L.) hulls and shells. *Turkish Journal of Biology*, *34*(2), 165–173.

Kader, F., Rovel, B., Girardin, M., & Metche, M. (1997). Mechanism of browning in fresh highbush blueberry fruit (Vaccinium corymbosum L). Role of blueberry polyphenol oxidase, chlorogenic acid and anthocyanins. *Journal of the Science of Food and Agriculture*, *74*(1), 31–34.

Kahlaoui, M., Borotto Dalla Vecchia, S., Giovine, F., Ben Haj Kbaier, H., Bouzouita, N., Barbosa Pereira, L., & Zeppa, G. (2019). Characterization of polyphenolic compounds extracted from different varieties of almond hulls (Prunus dulcis L.). *Antioxidants*, *8*(12), 647.

Kaushik, P., Mishra, A., Malik, A., & Pant, K. K. (2014). Biosorption of textile dye by Aspergillus lentulus pellets: process optimization and cyclic removal in aerated bioreactor. *Water, Air, & Soil Pollution*, *225*, 1–13.

Kelebek, H., Selli, S., Canbas, A., & Cabaroglu, T. (2009). HPLC determination of organic acids, sugars, phenolic compositions and antioxidant capacity of orange juice and orange wine made from a Turkish cv. Kozan. *Microchemical Journal*, *91*(2), 187–192.

Kelly, S., Grimm, L. H., Bendig, C., Hempel, D. C., & Krull, R. (2006). Effects of fluid dynamic induced shear stress on fungal growth and morphology. *Process Biochemistry*, *41*(10), 2113–2117.

Kim, H., Bartley, G. E., Arvik, T., Lipson, R., Nah, S.-Y., Seo, K., & Yokoyama, W. (2014). Dietary supplementation of chardonnay grape seed flour reduces plasma cholesterol concentration, hepatic steatosis, and abdominal fat content in high-fat diet-induced obese hamsters. *Journal of Agricultural and Food Chemistry*, *62*(8), 1919–1925.

Kim, K., Choi, B., Lee, I., Lee, H., Kwon, S., Oh, K., & Kim, A. Y. (2011). Bioproduction of mushroom mycelium of Agaricus bisporus by commercial submerged fermentation for the

production of meat analogue. *Journal of the Science of Food and Agriculture*, *91*(9), 1561–1568.

Kim, Y., & Lee, V. (2021). Enzyme-assisted Protein Extraction from Alfalfa Leaves. *2021 ASABE Annual International Virtual Meeting*, 1.

Kiran, E. U., Trzcinski, A. P., & Liu, Y. (2015). Enhancing the hydrolysis and methane production potential of mixed food waste by an effective enzymatic pretreatment. *Bioresource Technology*, *183*, 47–52.

Kontovas, S., Misailidis, N., & Petrides, D. (2022). *Levulinic Acid Production*.

Koulouris, A. (2023). Modeling of citric acid production using SuperPro Designer. In *Chemical Engineering Process Simulation* (pp. 221–252). Elsevier.

Lee, D. N., Hung, Y. S., Yang, T. S., Lin, J. H., & Weng, C. F. (2017). Aspergillus awamori-fermented mung bean seed coats enhance the antioxidant and immune responses of weaned pigs. *Journal of Animal Physiology and Animal Nutrition*, *101*(5), e342–e351.

Li, C., Zhang, B., Zhou, H., Wang, X., Pi, X., Wang, X., Mai, K., & He, G. (2019). Beneficial influences of dietary Aspergillus awamori fermented soybean meal on oxidative homoeostasis and inflammatory response in turbot (Scophthalmus maximus L.). *Fish & Shellfish Immunology*, *93*, 8–16.

Li, D., Hua, X., Luo, J., & Xu, Y. (2023). Quantitative determination of galacturonic acid in pectin and pectin products by combined pectinase hydrolysis and HPLC determination. *Food Additives & Contaminants: Part A*, 1–9.

Li, S., Huang, J., Mao, J., Zhang, L., He, C., Chen, G., Parkin, I. P., & Lai, Y. (2019). In vivo and in vitro efficient textile wastewater remediation by Aspergillus niger biosorbent. *Nanoscale Advances*, *1*(1), 168–176.

Li, W., & Bischel, H. N. (2022). Are resource recovery insects safe for feed and food? A screening approach for bioaccumulative trace organic contaminants. *Science of The Total Environment*, *837*, 155850.

Lin, P., Grimm, L. H., Wulkow, M., Hempel, D. C., & Krull, R. (2008). Population balance modeling of the conidial aggregation of Aspergillus niger. *Biotechnology and Bioengineering*, *99*(2), 341–350.

Liu, G., Zhao, X., Chen, C., Chi, Z., Zhang, Y., Cui, Q., Chi, Z., & Liu, Y. J. (2020). Robust production of pigment-free pullulan from lignocellulosic hydrolysate by a new fungus co-utilizing glucose and xylose. *Carbohydrate Polymers*, *241*, 116400. https://doi.org/10.1016/J.CARBPOL.2020.116400

Liu, X., & Kokare, C. (2023). Microbial enzymes of use in industry. In *Biotechnology of microbial enzymes* (pp. 405–444). Elsevier.

Liu, Z., Johnson, T. G., & Altman, I. (2016). The moderating role of biomass availability in biopower co-firing—A sensitivity analysis. *Journal of Cleaner Production*, *135*, 523–532.

López-Pérez, M., & Viniegra-González, G. (2016). Production of protein and metabolites by yeast grown in solid state fermentation: present status and perspectives. *Journal of Chemical Technology & Biotechnology*, *91*(5), 1224–1231.

Lu, H., Li, C., Tang, W., Wang, Z., Xia, J., Zhang, S., Zhuang, Y., Chu, J., & Noorman, H. (2015). Dependence of fungal characteristics on seed morphology and shear stress in bioreactors. *Bioprocess and Biosystems Engineering*, *38*(5), 917–928. https://doi.org/10.1007/S00449-014-1337-8/FIGURES/7

Martin, J. A., Murphy, R. A., & Power, R. F. G. (2003). Cloning and expression of fungal phytases in genetically modified strains of Aspergillus awamori. *Journal of Industrial Microbiology and Biotechnology*, *30*(9), 568–576.

Matassa, S., Boon, N., Pikaar, I., & Verstraete, W. (2016). Microbial protein: future sustainable food supply route with low environmental footprint. *Microbial Biotechnology*, *9*(5), 568–575.

Meati Foods. (2023). *Meati Food Homepage*. https://meati.com/

Melikoglu, M., Lin, C. S. K., & Webb, C. (2015). Solid state fermentation of waste bread pieces by Aspergillus awamori: Analysing the effects of airflow rate on enzyme production in packed bed bioreactors. *Food and Bioproducts Processing*, *95*, 63–75.

Metz, B., & Kossen, N. W. F. (1977). The growth of molds in the form of pellets–a literature review. *Biotechnology and Bioengineering*, *19*(6), 781–799.

Meyer, G. A. (1992). An overview of analysis by inductively coupled plasma-atomic emission spectrometry. *Inductively Coupled Plasma in Analytical Atomic Spectrometry, 2nd*.

Miller, G. L. (1959). Use of Dinitrosalicylic Acid Reagent for Determination of Reducing Sugar. *Analytical Chemistry*, *31*(3), 426–428. https://doi.org/10.1021/AC60147A030

Miner, L. P., Fernandez-Bayo, J., Putri, F., Niemeier, D., Bischel, H., & VanderGheynst, J. S. (2022). Predicting black soldier fly larvae biomass and methionine accumulation using a kinetic model for batch cultivation and improving system performance using semi-batch cultivation. *Bioprocess and Biosystems Engineering*, 1–12.

Mishra, B. K., & Arora, A. (2004). Optimization of a biological process for treating potato chips industry wastewater using a mixed culture of Aspergillus foetidus and Aspergillus niger. *Bioresource Technology*, *94*(1), 9–12.

Muniraj, I. K., Xiao, L., Hu, Z., Zhan, X., & Shi, J. (2013). Microbial lipid production from potato processing wastewater using oleaginous filamentous fungi Aspergillus oryzae. *Water Research*, *47*(10), 3477–3483.

Naher, L., Fatin, S. N., Sheikh, M. A. H., Azeez, L. A., Siddiquee, S., Zain, N. M., & Karim, S. M. R. (2021). Cellulase enzyme production from filamentous fungi Trichoderma reesei and Aspergillus awamori in submerged fermentation with rice straw. *Journal of Fungi*, *7*(10), 868.

Negi, S., & Banerjee, R. (2009). Characterization of amylase and protease produced by Aspergillus awamori in a single bioreactor. *Food Research International*, *42*(4), 443–448.

NHS. (2019). *What should my daily intake of calories be?* https://www.nhs.uk/common-health-questions/food-and-diet/what-should-my-daily-intake-of-calories-be/#:~:text=An%20ideal%20daily%20intake%20of,women%20and%202%2C500%20for%20men.

Norollahi, H., Kamalzadeh, A., & Karimi, A. (2005). Determination of chemical composition and digestibility of almond hull. *IV International Symposium on Pistachios and Almonds 726*, 591–594.

Offeman, R. D., Dao, G. T., Holtman, K. M., & Orts, W. J. (2015). Leaching behavior of water-soluble carbohydrates from almond hulls. *Industrial Crops and Products*, *65*, 488–495.

Offeman, R. D., Holtman, K. M., Covello, K. M., & Orts, W. J. (2014). Almond hulls as a biofuels feedstock: Variations in carbohydrates by variety and location in California. *Industrial Crops and Products*, *54*, 109–114. https://doi.org/10.1016/j.indcrop.2014.01.010

Okolie, J. A., Nanda, S., Dalai, A. K., & Kozinski, J. A. (2021). Techno-economic evaluation and sensitivity analysis of a conceptual design for supercritical water gasification of soybean straw to produce hydrogen. *Bioresource Technology*, *331*, 125005.

Onyeaka, H., Anumudu, C. K., Okpe, C., Okafor, A., Ihenetu, F., Miri, T., Odeyemi, O. A., & Anyogu, A. (2022). Single cell protein for foods and feeds: a review of trends. *The Open Microbiology Journal*, *16*(1).

Oraby, A., Rupp, S., & Zibek, S. (2022). Techno-Economic Analysis as a Driver for Optimisation of Cellobiose Lipid Fermentation and Purification. *Frontiers in Bioengineering and Biotechnology*, *10*.

Padma, P. N., Anuradha, K., Nagaraju, B., Kumar, V. S., & Reddy, G. (2012). Use of pectin rich fruit wastes for polygalacturonase production by Aspergillus awamori MTCC 9166 in solid state fermentation. *Journal of Bioprocessing and Biotechniques*, *2*(2).

Pal, A., & Khanum, F. (2010). Production and extraction optimization of xylanase from Aspergillus niger DFR-5 through solid-state-fermentation. *Bioresource Technology*, *101*(19), 7563–7569.

Palma, L., Ceballos, S. J., Johnson, P. C., Niemeier, D., Pitesky, M., & VanderGheynst, J. S. (2018). Cultivation of black soldier fly larvae on almond byproducts: impacts of aeration and moisture on larvae growth and composition. *Journal of the Science of Food and Agriculture*, *98*(15), 5893–5900.

Palma, L., Fernandez-Bayo, J., Niemeier, D., Pitesky, M., & VanderGheynst, J. S. (2019). Managing high fiber food waste for the cultivation of black soldier fly larvae. *NPJ Science of Food*, *3*(1), 15.

Palma, L., Fernández-Bayo, J., Putri, F., & VanderGheynst, J. S. (2020). Almond by-product composition impacts the rearing of black soldier fly larvae and quality of the spent substrate as a soil amendment. *Journal of the Science of Food and Agriculture*, *100*(12), 4618–4626.

Papagianni, M. (2004). Fungal morphology and metabolite production in submerged mycelial processes. *Biotechnology Advances*, *22*(3), 189–259.

Papagianni, M., & Moo-Young, M. (2002). Protease secretion in glucoamylase producer Aspergillus niger cultures: fungal morphology and inoculum effects. *Process Biochemistry*, *37*(11), 1271–1278.

Papanikolaou, S., Chevalot, I., Galiotou-Panayotou, M., Komaitis, M., Marc, I., & Aggelis, G. (2007). Industrial derivative of tallow: a promising renewable substrate for microbial lipid, single-cell protein and lipase production by Yarrowia lipolytica. *Electronic Journal of Biotechnology*, *10*(3), 425–435.

Pastrana, A. M., Shea, E. A., Fernandez-Bayo, J. D., Allison, B., Watson, D. C., Toniato, J., Gordon, T. R., & Simmons, C. W. (2022). Impact of biosolarization with almond hull and shell amendments for the control of Fusarium oxysporum f. sp. lactucae in a lettuce/tomato cropping system. *Crop Protection*, *156*, 105925.

Patel, A. K., Agrawal, R., Dong, C.-D., Chen, C.-W., Singhania, R. R., & Pandey, A. (2023). Filamentous fungal morphology in industrial aspects. In *Current Developments in Biotechnology and Bioengineering* (pp. 197–217). Elsevier.

Patterson, G. D., Orts, W. J., McManus, J. D., & Hsieh, Y.-L. (2022). Cellulose and Lignocellulose Nanofibrils and Amphiphilic and Wet-Resilient Aerogels with Concurrent Sugar Extraction from Almond Hulls. *ACS Agricultural Science & Technology*.

Paz-Cedeno, F. R., Carceller, J. M., Iborra, S., Donato, R. K., Rodriguez, A. F. R., Morales, M. A., Solorzano-Chavez, E. G., Roldán, I. U. M., de Paula, A. V., & Masarin, F. (2022). Stability of the Cellic CTec2 enzymatic preparation immobilized onto magnetic graphene oxide: Assessment of hydrolysis of pretreated sugarcane bagasse. *Industrial Crops and Products*, *183*, 114972.

Pedreschi, F., & Moyano, P. (2005). Effect of pre-drying on texture and oil uptake of potato chips. *LWT-Food Science and Technology*, *38*(6), 599–604.

Pekke, M. A., Pan, Z., Atungulu, G. G., Smith, G., & Thompson, J. F. (2013). Drying characteristics and quality of bananas under infrared radiation heating. *International Journal of Agricultural and Biological Engineering*, *6*(3), 58–70.

Pinelo, M., Rubilar, M., Sineiro, J., & Nunez, M. J. (2004). Extraction of antioxidant phenolics from almond hulls (Prunus amygdalus) and pine sawdust (Pinus pinaster). *Food Chemistry*, *85*(2), 267–273.

Prgomet, I., Gonçalves, B., Domínguez-Perles, R., Pascual-Seva, N., & Barros, A. I. (2017). Valorization challenges to almond residues: Phytochemical composition and functional application. *Molecules*, *22*(10), 1774.

Prime Roots. (2023). *Prime Roots is Made By Meat Eaters*. https://www.primeroots.com/pages/about-us

Purwanto, L. A., Ibrahim, D., & Sudrajat, H. (2009). Effect of agitation speed on morphological changes in Aspergillus niger hyphae during production of tannase. *World J Chem*, *4*(1), 34–38.

Ratti, C. (2001). Hot air and freeze-drying of high-value foods: a review. *Journal of Food Engineering*, *49*(4), 311–319.

Rivaldi, J. D., Carvalho, A. K. F., da Conceição, L. R. V, & de Castro, H. F. (2017). Assessing the potential of fatty acids produced by filamentous fungi as feedstock for biodiesel production. *Preparative Biochemistry and Biotechnology*, *47*(10), 970–976.

Rousta, N., Hellwig, C., Wainaina, S., Lukitawesa, L., Agnihotri, S., Rousta, K., & Taherzadeh, M. J. (2021). Filamentous fungus aspergillus oryzae for food: From submerged cultivation to fungal burgers and their sensory evaluation—A pilot study. *Foods*, *10*(11), 2774.

Rubilar, M., Pinelo, M., Shene, C., Sineiro, J., & Nuñez, M. J. (2007). Separation and HPLC-MS identification of phenolic antioxidants from agricultural residues: almond hulls and grape pomace. *Journal of Agricultural and Food Chemistry*, *55*(25), 10101–10109.

Saa, S. (2020). *Almond Varieties and Selections-Evaluation of National and International*.

Sáez, A., Aizen, M. A., Medici, S., Viel, M., Villalobos, E., & Negri, P. (2020). Bees increase crop yield in an alleged pollinator-independent almond variety. *Scientific Reports*, *10*(1), 3177.

Safarian, S., Azarmi, Y., Jahanban-Esfahlan, A., & Jahanban-Esfahlan, H. (2016). The beneficial effects of almond (Prunus amygdalus Batsch) hull on serum lipid profile and antioxidant capacity in male rats. *Turkish Journal of Medical Sciences*, *46*(4), 1223–1232.

Sah, R. N., & Miller, R. O. (1992). Spontaneous reaction for acid dissolution of biological tissues in closed vessels. *Analytical Chemistry*, *64*(2), 230–233.

Saleh, A. A., Eid, Y. Z., Ebeid, T. A., Kamizono, T., Ohtsuka, A., & Hayashi, K. (2011). Effects of feeding Aspergillus awamori and Aspergillus niger on growth performance and meat quality in broiler chickens. *The Journal of Poultry Science*, *48*(3), 201–206.

Saleh, A. A., Hayashi, K., Ijiri, D., & Ohtsuka, A. (2014). Beneficial effects of Aspergillus awamori in broiler nutrition. *World's Poultry Science Journal*, *70*(4), 857–864. https://doi.org/10.1017/S0043933914000907

Saleh, A. A., Ohtsuka, A., Yamamoto, M., & Hayashi, K. (2013). Aspergillus awamori feeding modifies lipid metabolism in rats. *BioMed Research International*, *2013*.

Sanders, M. E. (2011). Impact of probiotics on colonizing microbiota of the gut. *Journal of Clinical Gastroenterology*, *45*, S115–S119.

Saura-Calixto, F., Cañellas, J., & García-Raso, J. (1983). Contents of Detergent-Extracted Dietary Fibers and Composition of Hulls, Shells, and Teguments of Almonds (Prunus amygdalus). *Journal of Agricultural and Food Chemistry*, *31*(6), 1255–1259. https://doi.org/10.1021/jf00120a027

Schnell, T. D., Sofos, J. N., Morgan, J. B., Aaronson, M. J., Tatum, J. D., & Smith, G. C. (1997). Pesticide residues in beef tissues from cattle fed fruits, vegetables and their byproducts. *Journal of Muscle Foods*, *8*(2), 173–183.

Schweitzer, P. A. (1979). *Handbook of separation techniques for chemical engineers*.

Searchinger, T., Hanson, C., Ranganathan, J., Lipinski, B., Waite, R., Winterbottom, R., Dinshaw, A., Heimlich, R., Boval, M., & Chemineau, P. (2014). *Creating a sustainable food future. A menu of solutions to sustainably feed more than 9 billion people by 2050. World resources report 2013-14: interim findings*. World Resources Institute (WRI); World Bank Groupe-Banque Mondiale; United ….

Sechrist, E. A. (2022). *Investigating the Potential of Almond Hulls as a Feedstock for Fermented Cattle Feed*. UC Davis.

Seth, M., & Chand, S. (2000). Biosynthesis of tannase and hydrolysis of tannins to gallic acid by Aspergillus awamori—optimisation of process parameters. *Process Biochemistry*, *36*(1–2), 39–44.

Sfahlan, A. J., Mahmoodzadeh, A., Hasanzadeh, A., Heidari, R., & Jamei, R. (2009). Antioxidants and antiradicals in almond hull and shell (Amygdalus communis L.) as a function of genotype. *Food Chemistry*, *115*(2), 529–533.

Shin, H.-Y., Kim, S.-M., Lee, J. H., & Lim, S.-T. (2019). Solid-state fermentation of black rice bran with Aspergillus awamori and Aspergillus oryzae: Effects on phenolic acid composition and antioxidant activity of bran extracts. *Food Chemistry*, *272*, 235–241.

Sideli, G., DeJong, T., & Saa, S. (2020). Almond varieties and selections: Evaluation of national and international varieties or selections under development. *The Almond Board of California. Retrieved from Https://Www. Almonds. Com/Sites/Default/Files/2020-09/Almond% 20Board% 20of% 20California% 20Report*, *20*, E2.

Simonin, A., Palma-Guerrero, J., Fricker, M., & Glass, N. L. (2012). Physiological significance of network organization in fungi. *Eukaryotic Cell*, *11*(11), 1345–1352.

Sluiter, A., Hames, B., Ruiz, R., Scarlata, C., Sluiter, J., & Templeton, D. (2006). Determination of sugars, byproducts, and degradation products in liquid fraction process samples. *Golden: National Renewable Energy Laboratory*, *11*, 65–71.

Song, H., & Ozkan, U. S. (2010). Economic analysis of hydrogen production through a bio-ethanol steam reforming process: Sensitivity analyses and cost estimations. *International Journal of Hydrogen Energy*, *35*(1), 127–134.

Souza Filho, P. F., Nair, R. B., Andersson, D., Lennartsson, P. R., & Taherzadeh, M. J. (2018). Vegan-mycoprotein concentrate from pea-processing industry byproduct using edible filamentous fungi. *Fungal Biology and Biotechnology*, *5*(1), 1–10.

Souza Filho, P. F., Zamani, A., & Taherzadeh, M. J. (2017). Production of edible fungi from potato protein liquor (PPL) in airlift bioreactor. *Fermentation*, *3*(1), 12.

Souza Filho, P. F., Zamani, A., & Taherzadeh, M. J. (2019). Edible protein production by filamentous fungi using starch plant wastewater. *Waste and Biomass Valorization*, *10*, 2487–2496.

Startercultures. (2023). *A. luchuensis / A. awamori black koji*. https://startercultures.eu/product/fermentation/koji/a-luchuensis-a-awamori-noma-s-favorite/

Stoffel, F., de Oliveira Santana, W., Fontana, R. C., & Camassola, M. (2021). Use of Pleurotus albidus mycoprotein flour to produce cookies: Evaluation of nutritional enrichment and biological activity. *Innovative Food Science & Emerging Technologies*, *68*, 102642.

Strong, P. J., Self, R., Allikian, K., Szewczyk, E., Speight, R., O'Hara, I., & Harrison, M. D. (2022). Filamentous fungi for future functional food and feed. *Current Opinion in Biotechnology*, *76*, 102729.

Subramaniam, R., Dufreche, S., Zappi, M., & Bajpai, R. (2010). Microbial lipids from renewable resources: production and characterization. *Journal of Industrial Microbiology and Biotechnology*, *37*(12), 1271–1287.

Swanson, K. L., Bill, H. M., Asmus, J., Heguy, J. M., & DePeters, E. J. (2021). Feeding high amounts of almond hulls to lactating cows. *Journal of Dairy Science*, *104*(8), 8846–8856.

Taniguchi, K., Matsuda, K., Teramura, H., & Wake, K. (1977). Effect of acetic acid on growth of Aspergillus niger. *Journal of the Faculty of Science, Hokkaido University. Series 5, Botany*, *10*(4), 189–198.

Tomishima, H., Luo, K., & Mitchell, A. E. (2022). The almond (Prunus dulcis): Chemical properties, utilization, and valorization of coproducts. *Annual Review of Food Science and Technology*, *13*, 145–166.

Tribe, M. A., & Alpine, R. L. W. (1986). Scale economies and the "0.6 rule." *Engineering Costs and Production Economics*, *10*(4), 271–278.

Umsza-Guez, M. A., Díaz, A. B., Ory, I. de, Blandino, A., Gomes, E., & Caro, I. (2011a). Xylanase production by Aspergillus awamori under solid state fermentation conditions on tomato pomace. *Brazilian Journal of Microbiology*, *42*, 1585–1597.

Umsza-Guez, M. A., Díaz, A. B., Ory, I. de, Blandino, A., Gomes, E., & Caro, I. (2011b). Xylanase production by Aspergillus awamori under solid state fermentation conditions on tomato pomace. *Brazilian Journal of Microbiology*, *42*, 1585–1597.

U.S. Food & Drug. (2018). *Microorganisms & Microbial- Derived Ingredients Used in Food (Partial List)*. https://www.fda.gov/food/generally-recognized-safe-gras/microorganisms-microbial-derived-ingredients-used-food-partial-list

USDA. (2023a). *National Mill-Feeds and Miscellaneous Feedstuff Report*. https://www.ams.usda.gov/mnreports/ams_3512.pdf

USDA. (2023b). *Meat Price Spreads*. https://www.ers.usda.gov/data-products/meat-price-spreads/

USDA. (2023c). *Tapioca, pearl, dry*. https://fdc.nal.usda.gov/fdc-app.html#/food-details/169717/nutrients

USDA. (2023d). *Water in Meat & Poultry*.

van der Hoven, S. J., & Quade, J. (2002). Tracing spatial and temporal variations in the sources of calcium in pedogenic carbonates in a semiarid environment. *Geoderma*, *108*(3–4), 259–276.

Veiter, L., Rajamanickam, V., & Herwig, C. (2018). The filamentous fungal pellet—relationship between morphology and productivity. *Applied Microbiology and Biotechnology*, *102*(7), 2997–3006.

Wahyuningsih, S., Wulandari, L., Wartono, M. W., Munawaroh, H., & Ramelan, A. H. (2017). The effect of pH and color stability of anthocyanin on food colorant. *IOP Conference Series: Materials Science and Engineering*, *193*(1), 012047.

Waldherr, P., Bliatsiou, C., Böhm, L., & Kraume, M. (2023). Fragmentation of Aspergillus niger pellets in stirred tank bioreactors due to hydrodynamic stress. *Chemical Engineering Research and Design*.

Wang, J., Kong, F., & Kim, W. K. (2021). Effect of almond hulls on the performance, egg quality, nutrient digestibility, and body composition of laying hens. *Poultry Science*, *100*(9), 101286.

Wang, K., Hobby, A. M., Chen, Y., Chio, A., Jenkins, B. M., & Zhang, R. (2021). Techno-economic analysis on an industrial-scale production system of polyhydroxyalkanoates (PHA) from cheese by-products by halophiles. *Processes*, *10*(1), 17.

Wang, Z., Keshwani, D. R., Redding, A. P., & Cheng, J. J. (2010). Sodium hydroxide pretreatment and enzymatic hydrolysis of coastal Bermuda grass. *Bioresource Technology*, *101*(10), 3583–3585. https://doi.org/10.1016/J.BIORTECH.2009.12.097

Weatherall, I. L., & Coombs, B. D. (1992). Skin color measurements in terms of CIELAB color space values. *Journal of Investigative Dermatology*, *99*(4), 468–473.

Wee, M. S. M., Goh, A. T., Stieger, M., & Forde, C. G. (2018). Correlation of instrumental texture properties from textural profile analysis (TPA) with eating behaviours and macronutrient composition for a wide range of solid foods. *Food & Function*, *9*(10), 5301–5312.

Whittaker, J. A., Johnson, R. I., Finnigan, T. J. A., Avery, S. V, & Dyer, P. S. (2020). The biotechnology of Quorn mycoprotein: past, present and future challenges. *Grand Challenges in Fungal Biotechnology*, 59–79.

Wikipeida. (2023). *Tapioca pearl*. https://en.wikipedia.org/wiki/Tapioca_pearl

Winitsorn, A., Douglas, P. L., Douglas, S., Pongampai, S., & Teppaitoon, W. (2008). Modeling the extraction of valuable substances from natural plants using solid–liquid extraction. *Chemical Engineering Communications*, *195*(11), 1457–1464.

Youssef, A. (2019). *Paints Industry: Raw materials & unit operations & Equipment & Manufacturing & Quality tests*. August.

Yu, C. W. (2012). *Leaching pretreatments for improving biomass quality: feedstocks, solvents, and extraction modeling*. University of California, Davis.

Yu, J., Tamura, G., Takahashi, N., & Arima, K. (1967). Asperyellone, a new yellow pigment of Aspergillus awamori and Aspergillus niger: Part II. The chemical structure of asperyellone. *Agricultural and Biological Chemistry*, *31*(7), 831–836.

Zhang, J., & Zhang, J. (2016). The filamentous fungal pellet and forces driving its formation. *Critical Reviews in Biotechnology*, *36*(6), 1066–1077.

Zhang, N.-N., Yang, S., Kuang, Y.-Y., Shan, C.-S., Lu, Q.-Q., & Chen, Z.-G. (2022). Effects of different modified starches and gums on the physicochemical, functional, and microstructural properties of tapioca pearls. *International Journal of Biological Macromolecules*, *206*, 222–231.

Zhu, Y. (2007). Immobilized cell fermentation for production of chemicals and fuels. *Bioprocessing for Value-Added Products from Renewable Resources*, 373–396.

Zicari, S. M. (2016). *Enzymatic liquefaction of sugar beets as a feedstock for biofuel production*. University of California, Davis.